Continuous Chromatography of Biopharmaceuticals

Next Generation Process Development

Picanço Castanheira Da Silva, T.

DOI
10.4233/uuid:8fa9a391-46e0-41bc-abde-fb858409ca7f

Publication date
2024

Document Version
Final published version

Citation (APA)
Picanço Castanheira Da Silva, T. (2024). *Continuous Chromatography of Biopharmaceuticals: Next Generation Process Development*. [Dissertation (TU Delft), Delft University of Technology]. https://doi.org/10.4233/uuid:8fa9a391-46e0-41bc-abde-fb858409ca7f

Important note
To cite this publication, please use the final published version (if applicable).
Please check the document version above.

CONTINUOUS CHROMATOGRAPHY OF BIOPHARMACEUTICALS

NEXT GENERATION PROCESS DEVELOPMENT

Tiago Picanço Castanheira da Silva

Propositions

accompanying the dissertation

Continuous Chromatography of Biopharmaceuticals

Next Generation Process Development

by

Tiago PICANÇO CASTANHEIRA DA SILVA

1. Democracy is utopic.

2. Gender quotas promote meritocracy.

3. Virtual workspaces decrease productivity.

4. Free education ensures societal development.

5. In-person discussions progress science.

6. Participation in scientific conferences should be at the start of a PhD.

7. Structure prevents creativity and promotes frustration.

8. Mentors outperform supervisors.

9. Nothing outcompetes chromatography for monoclonal antibody purification (Chapters 2 & 6).

10. Microfluidics needs macro solutions (Chapter 3).

These Propositions are regarded as opposable and defendable, and have been approved by Prof. dr. ir. M. Ottens and by Prof. dr. ing. M. H. M. Eppink.

Continuous Chromatography of Biopharmaceuticals

Next Generation Process Development

Continuous Chromatography of Biopharmaceuticals

Next Generation Process Development

Dissertation

for the purpose of obtaining the degree of doctor at Delft University of Technology by
the authority of the Rector Magnificus Prof. dr. ir. T.H.J.J. van der Hagen,
Chair of the Board for Doctorates
to be defended publicly on
Friday 02nd of February 2024 at 10:00 o'clock.

by

Tiago PICANÇO CASTANHEIRA DA SILVA

Master of Science in Biological Engineering,

Instituto Superior Técnico, University of Lisbon, Portugal

born in Coimbra, Portugal

This dissertation has been approved by promotors.

Composition of the doctoral committee:

Rector Magnificus	Chairperson
Prof. dr. ir. M. Ottens	Delft University of Technology, promotor
Prof. dr. ing. M. H. M. Eppink	WUR / Byondis B.V., promotor

Independent members

Prof. dr. J. J. Hubbuch	Kalsruhe Institute of Technology, Germany
Prof. dr. ir. L. A. M. van der Wielen	Delft University of Technology
Prof. dr. ir. A. A. Kiss	Delft University of Technology
Prof. Dr. H. J. Noorman	Delft University of Technology
Dr. A. Azevedo	Instituto Superior Técnico, Portugal

The research described in this thesis was performed at the Department of Biotechnology, Delft University of Technology, The Netherlands, and at the Department of Downstream, Byondis B.V, Nijmegen, The Netherlands.

This research was funded by the European Union's Horizon 2020 research and innovation program under the Marie Skłodowska-Curie grant agreement No 812909 CODOBIO, within the Marie Skłodowska-Curie International Training Networks framework.

Printed by Proefschriftspecialist

Cover illustration and design: David Calderón Franco

ISBN: 978-94-6366-802-6

An electronic version of this dissertation is available at https://repository.tudelft.nl/

Table of Contents

Summary

The biopharmaceutical industry is moving from a batch to a continuous mode of manufacturing. This shift promises to reduce costs and manufacturing footprint while improving productivity and consistency of the product. This thesis implements miniaturized and automated high-throughput screening techniques alongside a mathematical chromatography model for the development of an integrated continuous chromatography process. The model is used for *in-silico* optimization of a capture and polishing step of a monoclonal antibody (mAb). The optimization focusses on chromatographic processes that would have to deal with higher titer solutions.

The transition to Integrated Continuous Biomanufacturing (ICB) is welcomed by industry and regulatory agencies, which are working together to accomplish this shift. Process development plays a crucial role in defining new processes or adapting existing processes to different modes of operation. High-Throughput Process Development (HTPD) has been used in the biopharmaceutical industry to accelerate and reduce costs of process development, by using miniaturized assays and performing computer-aided studies. However, the industry experiences gaps and sees opportunities for improvement in the HTPD tools that can help the transition to ICB. These gaps, together with a state-of-the-art of HTPD for ICB are presented in **Chapter 2**. Experts in the field identified microfluidics and modeling to be the most promising technologies to fill in the gaps in process development for ICB.

Subsequently, an overview on the state-of-the-art of automation and miniaturization for biopharmaceutical process development is given in **Chapter 3**. The focus is on different degrees of miniaturization and automation of the technologies for process development, for both Upstream and Downstream processing (USP and DSP, respectively). Liquid-Handling Stations (LHS) are the epitome of automation for process development, and have seen great adoption for the past decades. Examples of the use of this tool for USP and DSP process development are provided. A greater emphasis is placed on the often overlooked microfluidics and how it can also be used as a screening tool, and a SWOT analysis on LHS and microfluidics as potential process development tools is provided.

Further comparison between HTS tools for chromatographic process development is needed, since process development efforts for chromatography mostly rely on LHS-based experiments. Three methodologies are selected for this comparison: LHS, microfluidics, and Eppendorf tubes (**Chapter 4**). To achieve this, protein equilibrium adsorption isotherms are determined with each of the aforementioned methodologies. The microfluidics chip produced in-house provides a platform for resin screening that achieves liquid and resin volume reductions of 15- and up-to 200-fold, respectively.

Accurate resin volume determination is ensured with an image analysis software, and resin consumption is as high as 200 nl in the microfluidics system. After validating the HTS methodologies, a cost consideration study aims at fairly comparing the three methodologies for their chromatographic process development potential. Although at a lower Technology Readiness Level, microfluidics can be a viable alternative tool when the protein to be studied is very expensive or scarce (such as in early stages of process development), due to the high degree of miniaturization. Furthermore, it is discussed what would be the possible applications of the different methodologies in chromatographic process development.

The HTS methodologies developed paved the way for the implementation of a HTPD approach for the study and optimization of continuous chromatography (**Chapters 5** and **6**). A large database on the adsorption equilibrium isotherms of mAbs to different protein A (ProA) and Cation-Exchange (CEX) resins is generated from experiments with a LHS. This database is then used to further reduce resin candidates to be used in subsequent experiments. Four resin candidates are used to study the equilibrium adsorption isotherms of mAb to ProA ligands with a clarified cell culture supernatant (harvest). It is shown that pure mAb experiments reflect the same adsorption behavior as harvest experiments for all resin candidates, reducing the need to duplicate experiments in the future. The parameters determined are further used in a mechanistic Lumped Kinetic Model (LKM), used for the *in-silico* study of column chromatography (**Chapter 5**). The LKM uses a lumped overall mass transfer parameter that is linearly dependent on feed concentration, in line with mass transfer theory. The hybrid approach to HTPD emphasizes the importance of computational, experimental, and decision-making stages in chromatographic process development.

The LKM model described is further developed for the study of continuous chromatography. The continuous model is used for the *in-silico* optimization of a 3-Column Periodic Counter-current Chromatography (3C-PCC) capture and polishing step, for the purification of mAbs from high-titer solutions (**Chapter 6**). The model maximizes Productivity and Capacity Utilization (CU) keeping the yield high (99%) and having the flow rate and the percentage of breakthrough achieved in the interconnected phase as constraints. The shape of the breakthrough curve plays an important role in the optimization of continuous chromatography. The optimization results are validated for three different ProA resins, from which the best resin candidate is selected to continuously capture mAb from a harvest solution. The eluates of this operation are pooled and used as input for the continuous CEX step. The experimental results show very good agreement with model's predictions (lower than 7% deviation) and the proposed methodology helps to develop and optimize a continuous chromatography process in a short amount of time.

In summary, this thesis presents the exciting journey of process development for continuous chromatography, from conceptualization and selection of screening techniques until the end result of performing an optimized continuous chromatographic step for the successful capture and polishing of a mAb.

Samenvatting

De biofarmaceutische industrie bevindt zich midden in de transitie van batch productie naar continue productie. Deze verandering in de manier van produceren heeft de belofte in zich om productiekosten te verlagen en de milieu-impact te verkleinen, met een gelijktijdige verbetering van de productiviteit en productconsistentie. Dit proefschrift beschrijft de implementatie van geminiaturiseerde en geautomatiseerde experimentele technieken, genaamd "*high-throughput screening"* (HTS), dat tezamen met een mathematisch chromatografisch model gebruikt wordt voor de ontwikkeling van een geïntegreerd en continu chromatografisch zuiveringsproces. Het model wordt gebruikt in computer simulaties voor de optimalisatie van de zuivering van een monoklonaal antilichaam (mAb) in twee achtereenvolgende chromatografie stappen. Deze optimalisatie richt zich op chromatografische zuiveringsprocessen van geconcentreerde celkweek producten.

Deze transitie naar geïntegreerde continue productie van biologische materialen ("*Integrated Continuous Biomanufacturing*"- ICB) wordt door de biofarmaceutische industrie en regelgevende instanties gezamenlijk opgepakt. Procesontwikkeling speelt daarbij een belangrijke rol. Zowel bij het ontwerpen van geheel nieuwe processen als bij het aanpassen van bestaande processen aan verschillende manieren van productie. "*High-Throughput Process Development"* (HTPD) wordt in de biofarmaceutische industrie gebruikt om deze procesontwikkeling te versnellen en de daaraan gekoppelde kosten te verlagen. Dit gebeurd met een combinatie van (een veelvoud aan) geminiaturiseerde analyses en computersimulaties. De stand van zaken en mogelijke manieren voor verbetering van HTPD voor ICB wordt gepresenteerd in **Hoofdstuk 2**. Microfluïdica en uitbreiden van modellering technieken worden gepresenteerd als veelbelovende technologieën om hiaten in de huidige manier van procesontwikkeling voor ICB op te vullen.

Hoofdstuk 3 geeft vervolgens een overzicht van de stand van zaken op het gebied van automatisering en miniaturisatie voor biofarmaceutische procesontwikkeling. De nadruk ligt op verschillende gradaties van miniaturisering en automatisering van procesontwikkeling technologieën zowel voor celkweek/fermentatie ("*Upstream Processing"*) als productopwerking en zuivering ("*Downstream Processing"*) (USP en DSP respectievelijk). Een gerobotiseerd systeem voor het uitvoeren van een veelheid aan experimenten, de zgn. "*Liquid-Handling Station"* (LHS) is de belichaming van automatisering voor procesontwikkeling en uitvoerig gebruikt de afgelopen decennia. Voorbeelden van het gebruik van deze "*tool"* voor USP- en DSP-procesontwikkeling worden gegeven. Aandacht wordt besteed aan microfluïdica (chiptechnologie) als een

"*screeningtool*". Tevens wordt een SWOT-analyse ("*Strength Weakness Opportunity Threat*") gepresenteerd van LHS en microfluïdica als potentiële *tools* voor procesontwikkeling.

Het gebruik van verschillende HTS-*tools* voor chromatografische procesontwikkeling wordt vergeleken in **Hoofdstuk 4**. Drie methoden/manieren zijn geselecteerd voor deze vergelijking: de LHS, microchips en Eppendorf-testbuisjes. Eiwit adsorptie-isothermen worden bepaald met deze drie methoden. De in dit promotieonderzoek geproduceerde microchip verlaagt het gebruik van vloeistof en chromatografische adsorptiematerialen (hars) respectievelijk 15 en 200 maal. Nauwkeurige bepaling van het harsvolume (slechts 200 nl) gaat met behulp van beeldanalyse-software. Na validatie van de verschillende HTS-methoden volgt een analyse van de kosten om deze drie methoden op een eerlijke manier te vergelijken. De microchip blijkt een goed alternatief voor de bestudering van dure en/of schaarse eiwitten in het vroege stadium van procesontwikkeling. Als laatste wordt besproken wat de mogelijke toepassingen zouden kunnen zijn van de verschillende methoden in chromatografische procesontwikkeling.

De ontwikkelde HTS-methoden kunnen worden gebruikt in een HTPD gebaseerde optimalisatie van continue chromatografie (**Hoofdstukken 5** en **6**). Een grote *database* van mAb adsorptie isothermen van verschillende affiniteits- (*protein A – ProA*) en kationenuitwisselings- (*cation exchange – CEX*) harsen wordt gegenereerd via LHS experimenten. Deze *database* wordt vervolgens gebruikt om een keuze te maken voor enkele harsen voor gebruik in latere experimenten. Vier ProA harsen worden gebruikt om mAb adsorptie-isothermen te genereren met een geklaard celkweek supernatant (oogst). Zuivere mAb-oplossingen blijken hetzelfde adsorptiegedrag te vertonen als het onzuivere supernatant bij alle bestudeerde harsen. De gemeten adsorptieparameters worden gebruikt in een mechanistisch kinetisch model (*Lumped Kinetic Model – LKM*) in mathematische simulaties voor kolomchromatografie (**Hoofdstuk 5**). Het LKM gebruikt een samengevoegde massaoverdracht parameter die lineair afhankelijk blijkt van de productconcentratie in de ingaande vloeistofstroom tijdens chromatografie (in lijn met massaoverdracht theorie). Deze gepresenteerde hybride aanpak voor HTPD onderstreept het belang van computationele, experimentele en besluitvormingsfasen in chromatografische procesontwikkeling.

Het beschreven LKM-model wordt vervolgens gebruikt voor de ontwikkeling van een continue chromatografie proces. Een Periodieke Tegenstroom Chromatografie systeem bestaande uit 3-kolommen (*3 Column Counter-current Continuous Chromatography - 3C-PCC*) wordt geoptimaliseerd voor een 2 staps zuivering van mAbs uit oplossingen met een hoge titer (**Hoofdstuk 6**). Het model maximaliseert de productiviteit en capaciteitsbenutting (CB), bij een hoge opbrengst (99%), met de stroomsnelheid en het percentage doorbraak in de onderling verbonden fase tussen twee kolommen als randvoorwaarden. De vorm van de doorbraakcurve speelt een belangrijke rol in de

optimalisatie van continue chromatografie. De optimalisatieresultaten worden gevalideerd voor drie verschillende ProA-harsen, waaruit de beste hars wordt geselecteerd om continu mAb uit een oogstoplossing op te vangen. De eluaten van deze operatie worden samengevoegd en gebruikt als input voor de continue CEX-stap. De experimentele resultaten vertonen zeer goede overeenstemming met de modelvoorspellingen (minder dan 7% afwijking). De voorgestelde methodologie blijkt in staat om een continu chromatografie proces in korte tijd te ontwikkelen en te optimaliseren.

Samengevat presenteert dit proefschrift de spannende reis van procesontwikkeling voor continue chromatografie; van conceptualisering en selectie van screeningtechnieken tot het uiteindelijke resultaat van het uitvoeren van een geoptimaliseerd continue chromatografische proces voor de succesvolle zuivering van een mAb met twee gekoppelde chromatografische stappen.

Resumo

A indústria biofarmacêutica está a transitar o seu modo de produção de *batch* para contínuo, reduzindo custos e a pegada de fabricação, enquanto melhora a produtividade do processo e coerência do produto. Nesta tese, técnicas miniaturizadas e automatizadas de rastreio de alta capacidade (*High-throughput Screening – HTS*), juntamente com modelos matemáticos de cromatografia, são implementadas para o desenvolvimento de um processo de cromatografia integrado e em contínuo. O modelo é usado para a optimização *in-silico* dos processos cromatográficos de afinidade (primeira purificação – *capture*) e finais (*polishing*), para a purificação de anticorpos monoclonais (mAb) a partir de soluções com altos títulos de proteína.

A transição para Biomanufactura Contínua Integrada (BCI) é bem recebida tanto pela indústria como pelas agências reguladoras, que estão a trabalhar em conjunto para concretizar esta mudança. O desenvolvimento de processos tem um papel crucial na criação de novos processos ou na adaptação de processos existentes a diferentes modos de operação. O desenvolvimento de processos de alta capacidade (*High-Throughput Process Development – HTPD*) tem sido usado na indústria biofarmacêutica para reduzir custos e acelerar o desenvolvimento dos mesmos, recorrendo à miniaturização de ensaios e a estudos computacionais. No entanto, a indústria ainda reconhece várias lacunas e oportunidades para melhorar as existentes ferramentas de HTPD de forma a auxiliar a transição para BCI. Estas lacunas e a tecnologia de última geração de HTPD para BCI são discutidas em promenor no **Capítulo 2**. A microfluídica e a modelação computacional foram consideradas por vários especialistas em BCI como as tecnologias mais promissoras para colmatar estas lacunas no desenvolvimento de processos para BCI.

Posteriormente, um resumo da tecnologia de última geração de automatização e miniaturização para o desenvolvimento de processos biofarmacêuticos é apresentado no **Capítulo 3**, com ênfase nos diferentes graus de miniaturização e automatização das tecnologias para desenvolvimento de processos, tanto para os processos de *Upstream* (cultura celular/fermentação) como para *Downstream* (purificação) (USP e DSP, respectivamente). As estações de manuseamento de líquidos (*Liquid-Handling Stations - LHS*) são consideradas o apogeu de automatização no desenvolvimento de processos e têm sido amplamente utilizadas nas últimas décadas, com exemplos do uso desta ferramenta para USP e DSP discutidos neste capítulo. A microfluídica, habitualmente esquecida, também pode ser utilizada como ferramenta de rastreio, sendo discutida e comparada às LHS, recorrendo a uma análise SWOT (Forças – *Strengths,* Fraquezas – *Weaknesses,* Oportunidades – *Opportunities,* Ameaças – *Threats*).

Uma comparação mais detalhada entre as diferentes ferramentas de HTS para o desenvolvimento de processos cromatográficos é então necessária, visto que a maioria do desenvolvimento de processos para cromatografia é feito com LHS. Três metodologias foram seleccionadas para esta comparação: LHS, microfluídica, e tubos Eppendorf (**Capítulo 4**). Para esta comparação, isotérmicas de adsorção em equilíbrio de diferentes proteínas são determinadas com as diferentes metodologias. O *chip* de microfluídica, produzido na TU Delft, é utilizado como plataforma para o rastreio de resinas, permitindo a redução de líquido em 15 vezes e a redução de resina até 200 vezes. A determinação precisa do volume de resina é garantida com um *software* de análise de imagem, com o consumo de resina a representar um máximo de 200 nL com o chip microfluídico. Após a validação das metodologias de HTS, realiza-se um estudo relativo aos custos da utilização de cada metodologia para o desenvolvimento de processos cromatográficos, avaliando o seu potencial. Apesar de apresentar um nível de prontidão tecnológico inferior, a microfluídica pode ser uma alternativa viável quando a proteína a ser estudada é de preço elevado ou está disponível em pequenas quantidades (como é o caso das fases iniciais de desenvolvimento de processo), devido ao elevado nível de miniaturização. Além disso, as possíveis aplicações das diferentes metodologias para o desenvolvimento de processos cromatográficos são discutidas.

As metodologias de HTS abriram caminho à implementação do método HTPD para estudar e optimizar cromatografia em contínuo (**Capítulos 5** e **6**). Recorrendo a LHS, gerou-se uma extensa base de dados de isotérmicas de adsorção em equilíbrio de mAbs com diferentes resinas de proteína A (ProA) e troca catiónica (*Cation-Exchange – CEX*). Esta base de dados é então usada para reduzir o número de resinas a utilizar em futuras experiências. Quatro resinas são seleccionadas para estudar as isotérmicas de adsorção em equilíbrio de mAb a ligandos de ProA com uma solução de sobrenadante de cultura celular (*harvest*). A amostra pura de mAb apresenta o mesmo comportamento de adsorção que o sobrenadante para todas as resinas testadas, diminuindo a necessidade de duplicar experiências no futuro. Os parâmetros determinados são utilizados num Modelo Cinético Englobado (*Lumped Kinetic Model – LKM*), usado para o estudo de cromatografia *in-silico* (**Capítulo 5**). O LKM utiliza um parâmetro para a transferência de massa global que é linearmente dependente da concentração da amostra, e está de acordo com a teoria de transferência de massa. Esta abordagem híbrida com HTPD demonstra a importância das fases computacionais, experimentais, e de tomada de decisão no desenvolvimento de processos cromatográficos.

O LKM foi desenvolvido para estudar cromatografia em contínuo. O modelo em contínuo é usado na optimização *in-silico* de uma Cromatografia em Contracorrente Periódica de 3 colunas (*3-Column Counter-current Chromatography – 3C-PCC*) para os passos de *capture* e *polishing*, para a purificação de mAbs de soluções com título elevado

(**Capítulo 6**). O modelo maximiza a Produtividade e Capacidade Utilizada (CU) enquanto mantém um rendimento elevado (99%), tendo como condicionantes o caudal volumétrico e a percentagem de anticorpo que elui da coluna (percentagem de *breakthrough*) na fase de injecção interconectada. A forma da curva de *breakthrough* tem um papel vital na optimização de cromatografia em contínuo. Os resultados da optimização foram validados com três resinas de ProA, com a resina com melhor desempenho a ser seleccionada para a captura em contínuo de mAb a partir de uma solução de sobrenadante. As frações eluídas desta operação foram colectadas e agrupadas sendo posteriormente usadas num passo de CEX em contínuo. Os resultados mostram boa correlação com as previsões do modelo (desvio inferior a 7%) e a metodologia proposta auxilia a desenvolver e optimizar rápida e eficientemente um processo de cromatografia em contínuo.

Em suma, esta tese apresenta o caminho emocionante do desenvolvimento de um processo de cromatografia em contínuo, desde a conceptualização e selecção das técnicas de rastreio, até ao resultado final de execução de um passo optimizado de cromatografia em contínuo para a captura e *polishing* de um anticorpo monoclonal.

"In philosophy, or religion, or ethics, or politics, two and two might make five, but when one was designing a gun or an aeroplane they had to make four."

George Orwell – *1984*

Chapter 1

Introduction

1.1. Biopharmaceuticals and the mAb market

The definition of biopharmaceuticals has changed over the years and depends on the author. While some people use the "biopharmaceutical" term to describe all biosynthesized products (traditional pharmaceutical products produced biologically and products based on recombinant molecular-biology techniques), in this thesis the term "biopharmaceutical" will be used to describe products produced by molecular biology methods (*e.g.*, recombinant proteins, nucleic acid products, among others), as described by Walsh [1]. Biopharmaceuticals can be used to treat a plethora of conditions, ranging from different types of cancer, to different autoimmune diseases or diabetes [2]. Monoclonal antibodies (mAb) are therapeutic proteins that can be produced to target different diseases, with each mAb targeting different conditions, and are widely used to treat different types of cancer [3]. MAbs have seen an increase in sales over the past decade, reaching several billion dollars in sales and with increasing market every year [4, 5].

Patent expiry of mAbs has paved the way for the emergence of biosimilars. These are molecules that are very similar to the originator therapeutic (mAb, other recombinant protein, etc.), but are sold at a fraction of the price (as much as 70% reduction). Companies try to stay ahead of the curve by either finding different applications for their available drugs [4], or by developing new drugs from their available products, such as Antibody Drug Conjugates (ADC), which are new therapeutics that only recently saw their first approvals by FDA [3]. Nonetheless, biosimilars are an excellent alternative to the original mAb molecules, and have allowed the democratization of medicine, with more affordable products reaching a larger audience. Although biosimilars are sold at a fraction of the price, these are still expensive molecules and are often in the range of several thousands of euros per gram. This high price is directly related to the costs associated with the production process of such molecules.

Biosimilars are still falling short on their promise for widespread adoption, since the introduction of the first biosimilar in 2014 [2]. Predictions pointed to a much faster adoption of these therapeutics that would lead to a fast decrease in market share of the originator molecules. However, recent reports suggest that the market penetration, while still not as high as initially thought, is becoming faster and faster in recent years, both in the US and EU [5]. Biosimilars have been reported to save €5.7 billion in Europe in 2021

and $6.5 billion in the US in 2020 [5]. These savings look significant, however, it is important to put in perspective how much this represents in the total biopharmaceutical market and healthcare expenditure. Healthcare expenditure in EU was as high as €1 179 billion in 2021 [6], making these savings only 0.48% of the total EU healthcare expenditure. Even comparing to the health expenditure in the Netherlands, which was €126.2 billion in 2021 [7], the savings would only represent 4.52% of the total Dutch healthcare expenditure.

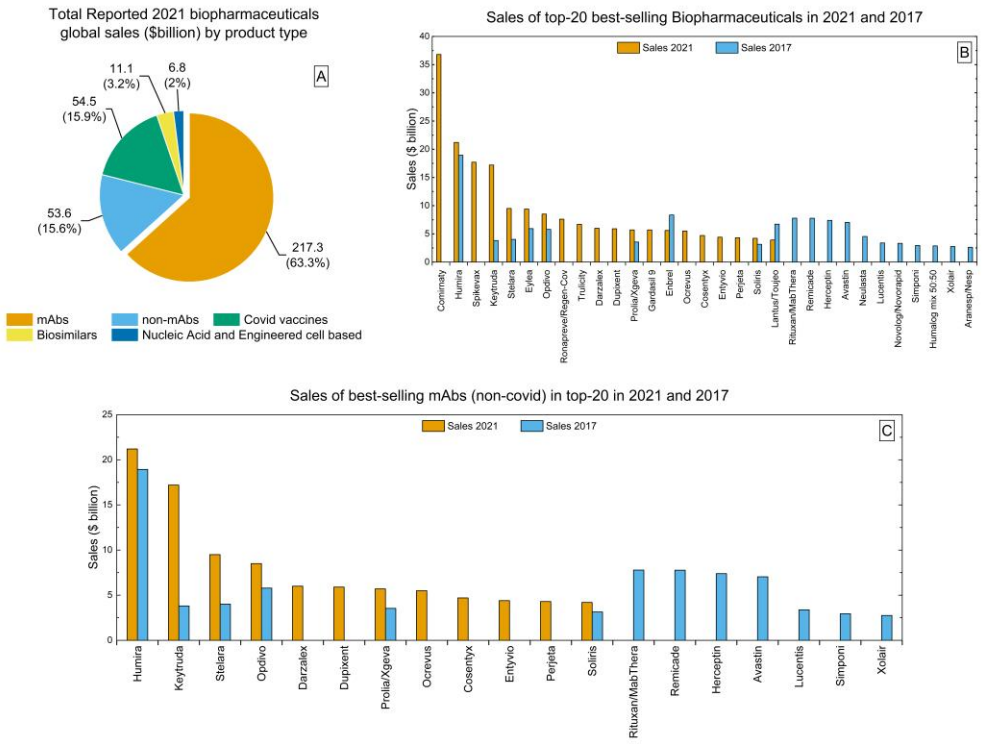

Figure 1.1 - Biopharmaceutical and mAb market analysis (2017 and 2021). A – Total reported 2021 biopharmaceutical global sales ($ billion) by product type; B – Sales of top-20 best-selling Biopharmaceuticals in 2021 and 2017; C – Sales of best-selling mAbs (non-covid) in top-20 in 2021 and 2017. Based on data from [5, 8].

Between January 2018 and June 2022, a total of 180 biopharmaceuticals entered the US and/or EU market, with more than half of the approvals pertaining to mAbs (97 approved mAbs in this period) [5]. This follows the trend where mAbs are the main biopharmaceutical approved every year for commercialization in EU and US markets.

The sales in the biopharmaceutical market have increased year after year, registering a total of 343.3 $billion in 2021 [5]. **Figure 1.1 A** shows the share that each product type had in the sales, with mAbs reporting 217.3 $billion, almost two-thirds of the total sales. This value is far superior even to the optimistic sales predictions by other authors, which

had projected mAb sales in 2021 to be at most of around 170 $billion [4]. **Figure 1.1 B** shows the top-20 best-selling biopharmaceuticals for the years of 2021 and 2017. The top-20 of 2021 was affected by the pandemic (Comirnaty, Spikevax, and Regen-Cov are all for treating Covid-19), but most of the products in both top-20 are mAbs (13 out of 20 for 2021 and 2017). **Figure 1.1 C** provides a better insight to this comparison if Covid products are not considered, since it is expected that pandemic years are outliers. In this figure, the non-Covid related therapeutic mAbs from the top-20 best-sellers of 2021 and 2017 are compared. The ones that remained in the top-20 from 2017 to 2021 all increased their sales, with Keytruda registering an impressive 451% increase in sales. **Figure 1.1** provides insight into the market of biopharmaceuticals and especially the role that mAbs have in this, showing that it is not only a growing market, but one that attracts enough attention and investment from companies and countries.

The selling price of biopharmaceuticals is dependent on a variety of factors. The production costs play a role in the selling price, but these only dictate what would be the minimum selling price of the molecules. This is, in general, a fairly good indication for biosimilars. However, when discussing this for proprietary molecules, more things need to be considered. Recent years have seen a decrease in drugs approved by billion dollar investment [2], highlighting the ferocity of the market. The selling price of the molecules is, therefore, a balance between what is invested by the companies and the profit goals. Besides the expenditure with R&D, there is also a significant investment needed for each stage of the clinical trials and the marketing of the products. Last, but not least, the revenues obtained from the new drugs need to compensate the money spent in the development of drugs that end up not being approved.

1.2. Production and Process Development

MAbs are recombinant proteins that are produced by cell culture, where cells are grown in suspension and (for the most part) secrete the desired product to the cell culture supernatant [9]. Even though there are plenty hosts that can be used for this effect, Chinese Hamster Ovary (CHO) cells are the most used host [5, 9, 10]. The production process of therapeutic proteins through any biological method is defined as Upstream Processing (USP). The development stages for USP include (but are not limited to) cell line engineering and cell culture media development [2]. There are also different modes of operation of the USP process: batch, fed-batch, and perfusion. Batch operation is characterized by a system where the inoculum and all components necessary to the operation are added at the beginning of the cell culture and the process is run until specific target values are achieved (only exception are gases, that are continuously added). Batch processes are the shortest of the three, with durations up to 7 days. Fed-batch operation is similar to batch, with the inoculum and essential components being

added in the beginning, but in this mode of operation there is gradual feed of fresh nutrients during the culture. This process has been shown to run for 14-25 days. This mode of operation has the ability to prolong the growth phase and has increased productivities. Perfusion is the only truly continuous process of the three. It is characterized by constant volume where there is a continuous feed of fresh culture medium and a continuous removal of the medium in the bioreactor. The cells in suspension are kept in the reactor by a cell retention device, which traps the cells and recirculates them back into the bioreactor and allows the collection of the culture media, that contains the product and other contaminants. This mode of operation is characterized by very long cell cultures, where 90 day cell cultures are common but there have also been reports of 6 months processes. Perfusion processes also allow to keep the metabolites level within an acceptable value for cells to keep thriving [2].

After the cell culture has reached its end, the bioreactors are harvested and the clarified cell culture supernatant (also known as harvest) is collected to be further processed (in the case of perfusion reactors, this is a continuous operation). The harvest has a plethora of components: our product of interest (*e.g.* mAbs), host cell proteins (HCPs), genetic material from the host, viruses, metabolites, etc. In order to administrate the mAbs to the patients, these need to be separated from all the other components in the harvest mixture (purified) and often concentrated. The sequence of unit operations used for this effect is known as Downstream Processing (DSP). For the CHO cell case, where mAbs are secreted to the supernatant, this starts by having a cell retention device, allowing us to retain the cells and keep the supernatant. The unit operations that follow differ from process to process. However, there are already platform DSP processes for the purification of mAbs, which use chromatographic steps in sequence [11]. Alternative processes to chromatography have also been proposed [12, 13], however with little adoption by industry. The first step is usually an affinity chromatography step with a protein A (ProA) ligand, which is highly specific for antibodies, with this step being often coined "Capture step". In this step, there is the removal of most of the impurities from the mixture, with purities after this step often surpassing 90% [2]. The following steps are usually a combination of Ion Exchange (IEX) steps (can be cation – CEX – or anion – AEX) and/or Hydrophobic Interaction Chromatography (HIC). The choice of the combination of the steps mainly depends on the molecules and the remaining impurities, which differ from process to process and also depends on the target molecule. These chromatography steps are often coined "Polishing steps", since the goal is to further polish an already highly pure sample. After the chromatographic steps there are commonly filtration steps for final formulation. DSP unit operations for the biopharmaceutical industry have often been processed in batch mode, mainly due to the discrete nature of chromatography, when operated in Bind and Elute mode.

MAb titers have changed drastically over the past three decades. The first processes had reported titers in the order of hundreds of milligrams per liter and nowadays it is common to have titers in the 5 g/L range, representing a 10-fold increase [14], with even some reported values in the order of tenths grams per liter. Initially, the main manufacturing costs associated with the production of mAbs were attributed to cell culture media, since the media components have a hefty price tag. However, with the tremendous increase in titers, the cost of these components per gram of product has increasingly reduced, shifting the cost pressure to DSP, with costs of DSP amounting up to 80% of the total production costs [15]. Of all unit operations in the DSP train, chromatography is the most expensive. This is due to the fact that there are often three chromatographic steps in sequence and the resin prices, with the ProA affinity ligand being responsible for a great portion of these costs.

Process development is an essential part of any biopharmaceutical company. There are different stages of process development, with early stages focusing on Research & Development (R&D) of the target molecule, which can range from trying to find or engineer a molecule for a specific target, to building a mutant library for the expression of the target molecule, among other things. Once the target has been identified, it is necessary to build a process that is able to produce it, and a process that can purify it. When the final process is achieved, there is still room for process development, with improvements in specific unit operations or support systems to manufacturing being possible throughout the lifetime of the process. Therefore, it is not possible to create or maintain a process for the manufacturing of a mAb without process development. While process development is an essential part of producing a mAb, it can also be a time and resource consuming effort. Furthermore, process development typically relied on purely experimental work to achieve its endeavors. Technological advances in the past 30 years paved the way for High-throughput Screening (HTS), which enabled the automation and miniaturization of experiments, generating results fast and reliably, at a fraction of the time and cost [16]. Parallel developments in the computational power allowed researchers to develop more powerful and accurate mathematical models to describe physical phenomena (mechanistic models). High-Throughput Process Development (HTPD) merged HTS with a greater mechanistic understanding of the process and computational abilities, allowing to fast-forward process development efforts [17]. There are many evidence of the successful application of HTPD for USP and DSP alike [18-21].

Continuous manufacturing has been implemented in many different industries, such as food, chemical, and pharmaceutical. While the biopharmaceutical industry has historically been operated in batch mode, the shift to Integrated Continuous Biomanufacturing (ICB) is welcomed by industry and regulatory agencies [22, 23]. It is

often associated with a reduction in the footprint and costs of the process and with a more streamlined product output [24, 25]. Process economics can improve drastically with the implementation of continuous manufacturing platforms, with cost reductions being as high as 55% [26]. Although the driving force for change is in place, there are some engineering considerations before implementing this mode of operation [27]. Several continuous chromatography systems have been proposed throughout the years: Annular chromatography [28], Simulated Moving Bed (SMB) [29], Multicolumn Countercurrent Solvent Gradient Purification (MCSGP) [30], Periodic Counter-current Chromatography (PCC) [29], just to name a few. Unfortunately, when chromatography is operated in a bind and elute mode in a packed bed, the operation intrinsically becomes a batch mode of operation. Strategies to overcome this limitation have been proposed and will be elaborated further in this dissertation.

1.3. Motivation and aim of the thesis

The motivation for this thesis is to improve the production process of monoclonal antibodies with respect to productivity, yield and costs, and proposing a strategy for faster, less time and resource expensive process development. The final goal of achieving a continuous process helps to reduce operational costs while improving the sustainability of the mAb production processes. Therefore, the aim of this thesis is to evaluate different HTS techniques for fast and efficient HTPD of continuous chromatography for the purification of high titers monoclonal antibodies, preparing for the future needs of biomanufacturing. The development of a novel microfluidic chip and the use of advanced HTS equipment allows to build the necessary database to feed a mechanistic model used in process development for continuous chromatography. Using this model, an *in-silico* optimization tool is developed for the optimization of different Key Performance Indicators (KPIs) in the continuous chromatography operation.

1.4. CODOBIO project

The thesis is part of the project *Continuous Downstream Processing of Biologics (CODOBIO)*, which was established in the framework of European Union's Horizon 2020 research and innovation program (codobio.eu). Different research institutions and companies collaborated to find answers to the challenges that the future transition to continuous biomanufacturing pose. By pooling together a consortium with expertise in different fields such as process control, statistical modelling, high end protein analytics, and process engineering, the most urgent questions in continuous downstream bioprocessing were addressed:

- Process control and modelling of continuous downstream processes.
- Miniaturization, scale-up and scale-down of continuous downstream processes.

- Process design and development of integrated continuous downstream processes.

1.5. Thesis outline

An overview of the contents of the thesis is provided in **Figure 1.2**.

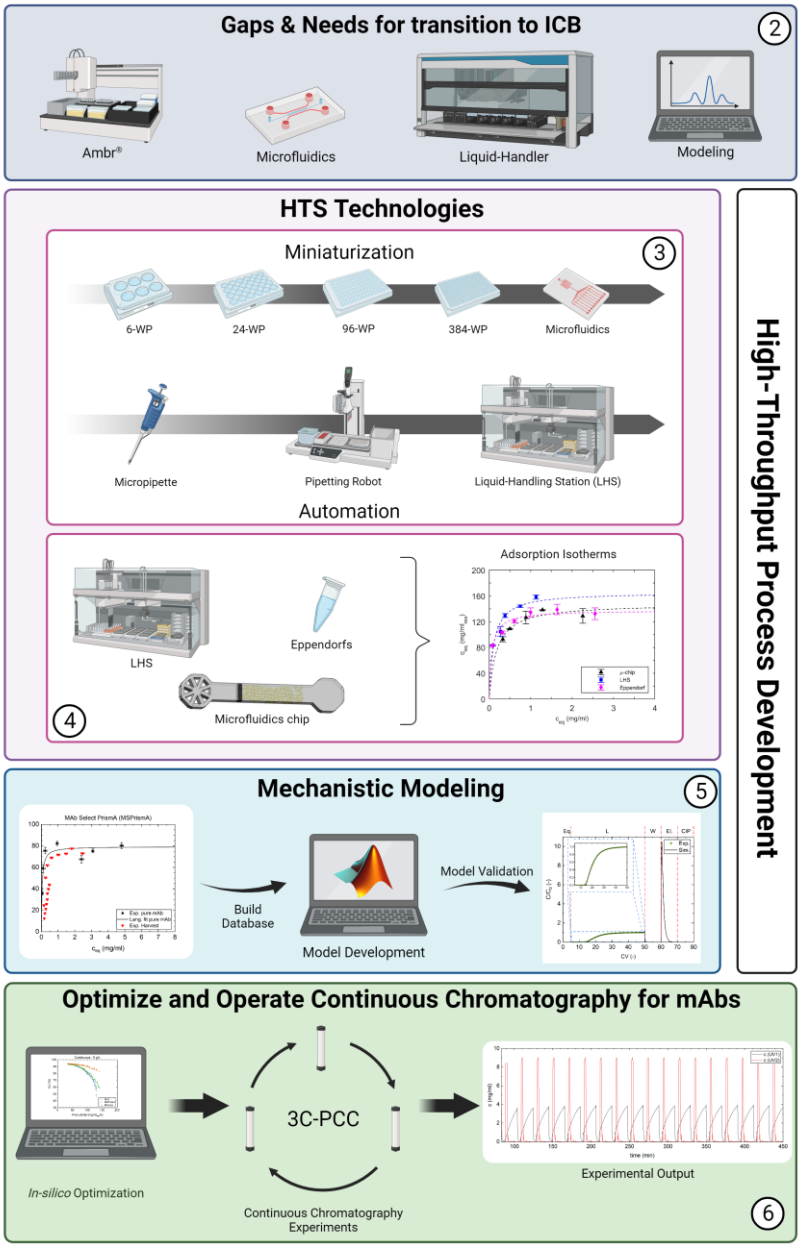

Figure 1.2 - Overview of the contents of the thesis. ICB – Integrated Continuous Biomanufacturing; HTS – High-Throughput Screening.

The introduction chapter of this thesis (**Chapter 1**) presents the background on the production and purification processes of biopharmaceuticals, focusing on the case of monoclonal antibodies, and defines the scope of this thesis.

Integrated continuous biomanufacturing can only be achieved with a joint effort between academia, industry, and regulatory agencies. **Chapter 2** provides information on what the leading experts in the biomanufacturing field perceive as needs and gaps for a smooth shift to continuous biomanufacturing, with information obtained from workshops during the Integrated Continuous Biomanufacturing IV (ICB IV) conference. It also presents the state-of-the-art in continuous biomanufacturing and discusses which technologies can fulfill the gaps identified.

One of the highlighted gaps of the previous chapter is in high-throughput technologies for different unit operations. **Chapter 3** provides an overview of different technologies used in the HTPD in continuous biomanufacturing. The important roles of automation and miniaturization are discussed, and a thorough overview of technologies is presented. In this chapter, there is also a summary of typical workflows for process development with different HTS techniques and a SWOT analysis of the two most widely used HTS techniques (liquid-handling stations and microfluidics).

The work developed in this thesis focuses on process development for chromatography steps for the purification of a monoclonal antibody. In **Chapter 4** a microfluidic platform for the determination of protein adsorption isotherms is presented. The microfluidic chip is developed in-house and is compared to the state-of-the-art HTS method (liquid-handling stations) and another screening method (Eppendorf tubes). A study on the cost considerations of using either one of the three techniques is conducted, with the goal of providing researchers in the academic and industrial field a more rational choice for the type of technique to employ, depending on the desired goal.

The work developed in **Chapter 4** allows to establish a methodology for the determination of protein adsorption isotherms, which provides relevant information on adsorption behavior of monoclonal antibodies to different resins. This serves as a database for the development of a mechanistic model, used to study the chromatographic behavior of this protein, by screening 13 protein A and 16 CEX resins (**Chapter 5**). In this chapter, the influence that components present in the supernatant have on the adsorption behavior of monoclonal antibodies is also discussed. Furthermore, this chapter also presents a rationale for the use of lumped kinetic models to describe chromatographic behavior and how feed concentration influences the overall mass transfer coefficient.

The mechanistic model developed in **Chapter 5** is used as a basis for the continuous chromatography model used in the work in **Chapter 6**. In this chapter, a continuous

chromatography model is developed and used for the optimization of a capture and polishing step for monoclonal antibodies. The optimization focuses on high titers to help researchers prepare for what is expected to be achieved in the (near) future. The model results are validated experimentally for three different protein A resins and the best performing resin is used for the continuous capture of mAb from a harvest solution. A subsequent continuous polishing step with CEX resin is performed using as feed the eluates from the capture step from the harvest.

Finally, **Chapter 7** summarizes the key findings of this thesis and provides an outlook for future research.

1.6. References

[1] G. Walsh, Biopharmaceutical benchmarks 2014, Nature Biotechnology 32(10) (2014) 992-1000. https://doi.org/10.1038/nbt.3040.

[2] G. Jagschies, E. Lindskog, K. Lacki, P.M. Galliher, Biopharmaceutical Processing: Development, Design, and Implementation of Manufacturing Processes, Elsevier2018. https://doi.org/10.1016/C2014-0-01092-1.

[3] A.C. Martins, M.Y. Oshiro, F. Albericio, B.G. de la Torre, G.J.V. Pereira, R.V.J.B. Gonzaga, Trends and Perspectives of Biological Drug Approvals by the FDA: A Review from 2015 to 2021, 10(9) (2022) 2325. https://doi.org/10.3390/biomedicines10092325.

[4] A.L. Grilo, A. Mantalaris, The Increasingly Human and Profitable Monoclonal Antibody Market, Trends in Biotechnology 37(1) (2019) 9-16. https://doi.org/10.1016/j.tibtech.2018.05.014.

[5] G. Walsh, E. Walsh, Biopharmaceutical benchmarks 2022, Nature Biotechnology 40(12) (2022) 1722-1760. https://doi.org/10.1038/s41587-022-01582-x.

[6] S.O.o.t.E.U.-. Eurostat, Government expenditure on health, 2023. https://ec.europa.eu/eurostat/statistics-explained/index.php?title=Government_expenditure_on_health.

[7] C.B.v.d.S.-. CBS, Zorguitgaven; kerncijfers, 2023. https://www.cbs.nl/nl-nl/cijfers/detail/84047NED.

[8] G. Walsh, Biopharmaceutical benchmarks 2018, Nature biotechnology 36(12) (2018) 1136-1145. https://doi.org/10.1038/nbt.4305.

[9] F. Li, N. Vijayasankaran, A. Shen, R. Kiss, A. Amanullah, Cell culture processes for monoclonal antibody production, MAbs, Taylor & Francis, 2010, pp. 466-479.

[10] A.A. Shukla, J. Thömmes, Recent advances in large-scale production of monoclonal antibodies and related proteins, Trends in Biotechnology 28(5) (2010) 253-261. https://doi.org/10.1016/j.tibtech.2010.02.001.

[11] D. Pfister, L. Nicoud, M. Morbidelli, Continuous biopharmaceutical processes: chromatography, bioconjugation, and protein stability, Cambridge University Press2018.

[12] A.M. Azevedo, P.A. Rosa, I.F. Ferreira, M.R. Aires-Barros, Chromatography-free recovery of biopharmaceuticals through aqueous two-phase processing, Trends in biotechnology 27(4) (2009) 240-247. https://doi.org/10.1016/j.tibtech.2009.01.004.

[13] A.C.A. Roque, A.S. Pina, A.M. Azevedo, R. Aires-Barros, A. Jungbauer, G. Di Profio, J.Y. Heng, J. Haigh, M. Ottens, Anything but conventional chromatography approaches in bioseparation, Biotechnology Journal 15(8) (2020) 1900274. https://doi.org/10.1002/biot.201900274.

[14] B. Kiss, U. Gottschalk, M. Pohlscheidt, New bioprocessing strategies: development and manufacturing of recombinant antibodies and proteins, Springer2018.

[15] J. Pollock, G. Bolton, J. Coffman, S.V. Ho, D.G. Bracewell, S.S. Farid, Optimising the design and operation of semi-continuous affinity chromatography for clinical and commercial manufacture, Journal of Chromatography A 1284 (2013) 17-27. https://doi.org/10.1016/j.chroma.2013.01.082.

[16] L.M. Mayr, D. Bojanic, Novel trends in high-throughput screening, Curr Opin Pharmacol 9(5) (2009) 580-8. https://doi.org/10.1016/j.coph.2009.08.004.

[17] A.T. Hanke, M. Ottens, Purifying biopharmaceuticals: knowledge-based chromatographic process development, Trends in Biotechnology 32(4) (2014) 210-20. https://doi.org/10.1016/j.tibtech.2014.02.001.

[18] B.K. Nfor, M. Noverraz, S. Chilamkurthi, P.D. Verhaert, L.A. van der Wielen, M. Ottens, High-throughput isotherm determination and thermodynamic modeling of protein adsorption on mixed mode adsorbents, Journal of Chromatography A 1217(44) (2010) 6829-50. https://doi.org/10.1016/j.chroma.2010.07.069.

[19] M. Bensch, P. Schulze Wierling, E. von Lieres, J. Hubbuch, High Throughput Screening of Chromatographic Phases for Rapid Process Development, Chemical Engineering & Technology 28(11) (2005) 1274-1284. https://doi.org/10.1002/ceat.200500153.

[20] S.W. Benner, J.P. Welsh, M.A. Rauscher, J.M.J.J.o.C.A. Pollard, Prediction of lab and manufacturing scale chromatography performance using mini-columns and mechanistic modeling, 1593 (2019) 54-62. https://doi.org/10.1016/j.chroma.2019.01.063.

[21] K.A. Shah, J.J. Clark, B.A. Goods, T.J. Politano, N.J. Mozdzierz, R.M. Zimnisky, R.L. Leeson, J.C. Love, K.R. Love, Automated pipeline for rapid production and screening of HIV-specific monoclonal antibodies using pichia pastoris, Biotechnology and bioengineering 112(12) (2015) 2624-2629. https://doi.org/10.1002/bit.25663.

[22] A.C. Fisher, M.-H. Kamga, C. Agarabi, K. Brorson, S.L. Lee, S. Yoon, The current scientific and regulatory landscape in advancing integrated continuous biopharmaceutical manufacturing, Trends in biotechnology 37(3) (2019) 253-267. https://doi.org/10.1016/j.tibtech.2018.08.008.

[23] K.B. Konstantinov, C.L. Cooney, White paper on continuous bioprocessing. May 20–21, 2014 continuous manufacturing symposium, Journal of pharmaceutical sciences 104(3) (2015) 813-820.

[24] B. Somasundaram, K. Pleitt, E. Shave, K. Baker, L.H. Lua, Progression of continuous downstream processing of monoclonal antibodies: Current trends and challenges, Biotechnology and bioengineering 115(12) (2018) 2893-2907. https://doi.org/10.1002/bit.26812.

[25] A.A. Shukla, L.S. Wolfe, S.S. Mostafa, C.J.B. Norman, T. Medicine, Evolving trends in mAb production processes, 2(1) (2017) 58-69. https://doi.org/10.1002/btm2.10061.

[26] J. Walther, R. Godawat, C. Hwang, Y. Abe, A. Sinclair, K. Konstantinov, The business impact of an integrated continuous biomanufacturing platform for recombinant protein production, Journal of biotechnology 213 (2015) 3-12. https://doi.org/10.1016/j.jbiotec.2015.05.010.

[27] M. Drobnjakovic, R. Hart, B.S. Kulvatunyou, N. Ivezic, V. Srinivasan, Current challenges and recent advances on the path towards continuous biomanufacturing, Biotechnology Progress (2023). https://doi.org/10.1002/btpr.3378.

[28] A. Jungbauer, Continuous downstream processing of biopharmaceuticals, Trends in biotechnology 31(8) (2013) 479-492. https://doi.org/10.1016/j.tibtech.2013.05.011.

[29] G. Carta, A. Jungbauer, Protein chromatography: process development and scale-up, John Wiley & Sons2020. https://doi.org/10.1002/9783527630158.

[30] T. Müller-Späth, L. Aumann, G. Ströhlein, H. Kornmann, P. Valax, L. Delegrange, E. Charbaut, G. Baer, A. Lamproye, M. Jöhnck, Two step capture and purification of IgG2 using multicolumn countercurrent solvent gradient purification (MCSGP), Biotechnology and bioengineering 107(6) (2010) 974-984. https://doi.org/10.1002/bit.22887

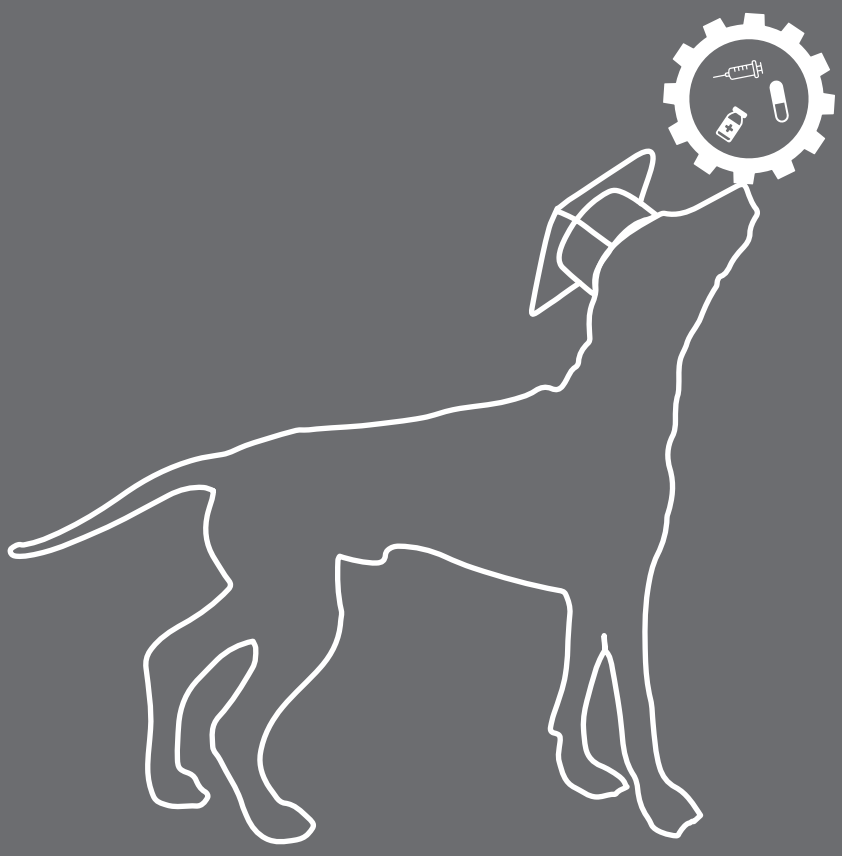

Chapter 2

White Paper on High Throughput Process Development for Integrated Continuous Biomanufacturing

Abstract

Continuous manufacturing is an indicator of a maturing industry, as can be seen by the example of the petrochemical industry. Patent expiry promotes a price competition between manufacturing companies, and more efficient and cheaper processes are needed to achieve lower production costs. Over the last decade, continuous biomanufacturing has had significant breakthroughs, with regulatory agencies encouraging the industry to implement this processing mode. Process development is resource and time consuming and, although it is increasingly be-coming less expensive and faster through high-throughput process development (HTPD) implementation, reliable HTPD technology for integrated and continuous biomanufacturing is still lacking and is considered to be an emerging field. There-fore, this paper aims to illustrate the major gaps in HTPD and to discuss the major needs and possible solutions to achieve an end-to-end Integrated Continuous Biomanufacturing, as discussed in the context of the 2019 Integrated Continuous Biomanufacturing conference. The current HTPD state-of-the-art for several unit operations is discussed, as well as the emerging technologies which will expedite a shift to continuous biomanufacturing.

Keywords: High-Throughput Process Development, Integrated Continuous Biomanufacturing, Microfluidics, Modeling, Process Analytical Technology

---

***Published as*:** São Pedro, M.N., Silva, T.C., Patil, R. and Ottens, M., 2021. White paper on high-throughput process development for integrated continuous biomanufacturing. Biotechnology and Bioengineering, 118(9), pp.3275-3286. DOI: https://doi.org/10.1002/bit.27757

2.1. Introduction

A possible solution to establish more efficient and flexible processes in the biopharmaceutical industry is to transition to continuous integrated manufacturing: an improvement in productivity, product quality and consistency can be achieved while drastically reducing the facility footprint and manufacturing costs [1-3]. Continuous bioprocessing utilizes a continuous flow of material through the various unit operations such that, at steady state, product of consistent quality is being produced as long as the operation runs [2].

Many manufacturing sectors, such as chemical, food and pharmaceutical have long adopted continuous manufacturing, but its implementation in biotechnology manufacturing, particularly of biotherapeutics, is still behind [2, 4]. However, Walther, Godawat, Hwang, Abe, Sinclair and Konstantinov [5] conducted an economic analysis into an integrated continuous biomanufacturing platform, and concluded that it would allow to reduce costs by 55% relative to conventional batch processing, demonstrating the promise of implementing a continuous bioprocess for the manufacturing of recombinant proteins. Therefore, there is a growing interest, from both academia and industrial researches, to develop continuous processing systems [6]. An example is the ongoing project Continuous Downstream Processing of Biologics - CODOBIO [7], a research program with the main goal of facing the future transition challenges to a continuous downstream process, implementing innovative integrated continuous manufacturing in the bio-industry.

The Integrated Continuous Biomanufacturing (ICB) conference aims to bring together academia and industry peers in order to shed some light on the recent advances and discoveries on bioprocesses, which could help to achieve the "holy grail" of a continuous end-to-end process and real time release. Within the fourth edition of the conference (ICB IV), held in Cape Cod (Massachusetts, USA) in 2019, a workshop entitled "High-Throughput Methodologies for ICB" brought together participants with different backgrounds (**Figure 2.1**). The workshop aimed to trigger the discussion on which are the perceived gaps in high-throughput (HT) technologies for process development, what are the current needs for ICB, the major problems and the correspondent expected solutions and what is currently being done in research to achieve this continuous biomanufacturing. With a total of 73 participants (from which the vast majority belonging to industry), the workshop aimed to collect relevant and up-to-date data on what is the view regarding the shift to continuous manufacturing in the biopharmaceutical realm, and what still needs to be done in order to put this industry closer to this objective. The attendees were asked to split and mix with their peers from different background and affiliation. This aimed to achieve a more diverse discussion between the groups and promote a greater need for consensus when posting an answer.

Overall, six out of the eight groups were mixed in terms of affiliation and a good mix of backgrounds was also possible to achieve (**Figure 2.1C**).

Although current trends in the production of biopharmaceuticals are to gradually move from batch processes to integrated continuous processing strategies, in order to perform the process in a continuous mode, an integration of the different unit operations in one single production and purification train is the ultimate goal, adding to each unit operation the capacity of recycling streams and the ability to purge impurities as required by the process [2]. Furthermore, analytical techniques must provide real-time information of each biomanufacturing step in order to gain knowledge and control over the overall process. Therefore, this white paper will discuss the major gaps in HTPD for the different unit operations, the integration problems present in a continuous manufacturing of biopharmaceuticals and the already available tools to overcome these challenges. By covering what is the state of the art for several established technologies, the paper aims to shed some light on the emerging tools for process development to enable and accelerate the shift to a continuous process.

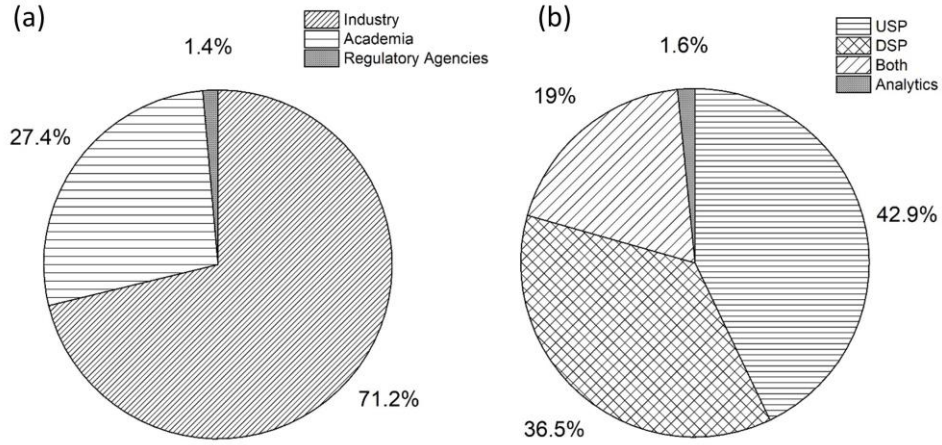

(c)

Groups	Industry	Academia	Regulatory Agencies	USP	DSP	Process Development	Analytics
1	6	4	-	5	2	2	1
2	6	3	1	2	4	3	-
3	4	5	-	*information not collected			
4	9	-	-	4	3	2	-
5	6	3	-	5	4	-	-
6	6	2	-	2	3	3	-
7	10	-	-	5	3	2	-
8	5	3	-	4	4	-	-

Figure 2.1 – Workshop participants background: (a) Area where the participants work in: Industry, academia, or regulatory agencies;(b) Function/Department where the participants work in: USP, upstream processing; DSP, downstream processing; process development, which implicates both USP and DSP function; and analytics. (c) Descriptive constitution of each of the eight groups formed during the workshop, according to the area/function of each participant.

2.2. Outcome of the workshop

After identifying the state of the art in HTPD, it was possible to pinpoint the gaps in HTPD for continuous biomanufacturing. In **Figure 2.2**, the unit operations/system components perceived by the participants as having a major gap for high-throughput process development are presented: cell culture was unanimously identified by every group, followed by the filtration unit operation and the current analytical tools for a continuous process. Some groups also pointed out potential gaps regarding cell media development, viral inactivation, chromatography and other unit operations, such as centrifugation and aqueous two-phase extraction.

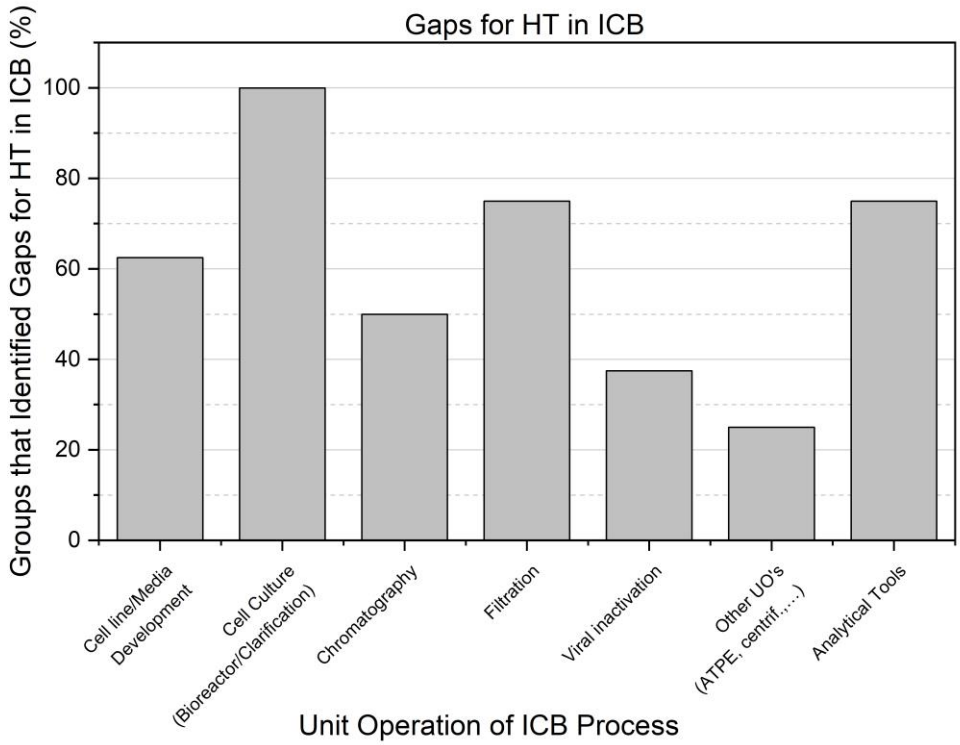

Figure 2.2 – Major gaps indicated for high-throughput (HT)development in integrated continuous biomanufacturing (ICB) by the participants in the workshop.

Cell culture has had the industry's attention for several years, with higher titer producing strains being developed. There is already equipment available for the HTPD of cell culture, still such systems come at a high price, as will be discussed further, which make it to be perceived by all groups as being an area where a significant gap is present.

On the other hand, filtration has been an overlooked unit operation when it comes to HTPD. When many researchers focused efforts in the optimization of chromatography, most likely due to being one of the most expensive unit operations, filtration steps have

stayed behind when it comes to HT alternatives. Although a batch filtration step can easily be implemented in a continuous process, the optimization of such step can become costly, as scale-down models are lacking, with a large investment to find optimal operating conditions needed. Therefore, there usually exists a compromise between oversizing the equipment or spending a considerable amount for the optimization of this unit operation. However, recent studies developed by Fernandez-Cerezo, Rayat, Chatel, Pollard, Lye and Hoare [8] used a downscale method for a filtration unit resorting to using a combination of critical flow regime analysis, modelling and experimentation to predict the performance of a pilot-scale system, therefore showing a possible HT tool for future conditions studies in this unit operation.

On the other hand, filtration has been an overlooked unit operation when it comes to HTPD. When many researchers focused efforts in the optimization of chromatography, most likely due to being one of the most expensive unit operations, filtration steps have stayed behind when it comes to HT alternatives. Although a batch filtration step can easily be implemented in a continuous process, the optimization of such step can become costly, as scale-down models are lacking, with a large investment to find optimal operating conditions needed. Therefore, there usually exists a compromise between oversizing the equipment or spending a considerable amount for the optimization of this unit operation. However, recent studies developed by Fernandez-Cerezo, Rayat, Chatel, Pollard, Lye and Hoare [8] used a downscale method for a filtration unit resorting to using a combination of critical flow regime analysis, modelling and experimentation to predict the performance of a pilot-scale system, therefore showing a possible HT tool for future conditions studies in this unit operation.

Regarding the analytical tools needed for implementation in a continuous process, the major gaps indicated are related to the quantity of samples and different techniques necessary to obtain information on the overall process. Furthermore, there are still great limitations in the available HT analytical tools used in ICB, highlighted by the limited number of techniques which were able to be integrated in HT platforms. A possible explanation for this limitation is related to the lengthy analysis times of each technique, which can make it difficult to employ for process monitoring and control. The current trend to tackle these analytical shortcomings is the creation of at-line sensors, which can provide a real-time measurement and data on a continuous process, titled Process Analytical Techniques (PAT), and will be further discussed in this paper.

2.3. State-of-the-Art in Continuous Biomanufacturing

The workshop participants were tasked to come up with HT technologies that are currently in use in process development for continuous biomanufacturing. Although some unit operations got more attention than others, the main goal of this activity was

to understand what are the mainly used equipment and tools involved in the development of processes for the desired successful shift to a continuous operation. The main tools already in place are the automated systems for liquid-handling, where there is the possibility to use tailored equipment for a specific unit operation or an equipment with a broader capability that can have minor adaptions for different uses. In **Table 2.1**, the state of the art of HTPD tools for the development of different unit operations are summarized.

Table 2.1 - State of the art in the integrated continuous biomanufacturing field; (*) Mainly a description of what is being done in the scope of ICB and not completely related to HT; (**) Few groups answered this question: either they had some struggles to find an answer or didn't consider this technology to be a bottleneck.

Technology	Answers	References from literature
Cell Line / Media Development	Ambr® 15/250/P	[11, 12]
	Liquid Handling Systems (Tecan)	[13]
	Beacon®	[14]
	Spin Tubes	[15]
Cell culture (Bioreactor)	Ambr® 15/250/P	[11, 12]
	Small Scale Bioreactors	[16]
Cell culture (Clarification) (*)	Pendotech	[17, 18]
	Filtration Skids	[19]
	Acoustic Wave	[20, 21]
	ATF/TFF	[18, 19]
	Centrifugation	[22, 23]
Chromatography	Tecan	[24, 25]
	Predictor Plates	[26]
	RoboColumns	[10, 27]
	Mechanistic Understanding using HT	[28-30]
	ÄKTA™	[27]
	Multi Column Chromatography (MCC)	[31]
Filtration (*) (**)	SPTFF	[8, 32]
	UF Membranes	[33]
	96-Well Plate	[34]
Viral inactivation (*) (**)	Low pH/Mixing	[35-38]
	Solvents/Detergents	[39, 40]
	Filters	[34, 41]
	Temperature	[35]
	Purification Steps	[42]
	Tubular Reactor	[35, 36, 38]
	Two Chambers (not continuous)	[42]

Table 2.1 (cont.) - State of the art in the integrated continuous biomanufacturing field; (*) Mainly a description of what is being done in the scope of ICB and not completely related to HT; (**) Few groups answered this question: either they had some struggles to find an answer or didn't consider this technology to be a bottleneck.

Technology	Answers	References from literature
Analytical Tools (*) (**)	UV	[43, 44]
	pH	[35, 45]
	Conductivity	[45]
	Raman Spectroscopy	[46-48]
	NIR/MIR Spectroscopy	[49-52]
	MALS	[53, 54]
	Online LC	[55-57]
	Mass Spectrometry	[58-60]

The use of liquid-handling stations for the determination of best operating conditions for cell media development and antibody purification has gained popularity over the past years [60]. The work developed by Schmidt, Abdo, Butcher, Yap, Scotney, Ramunno, Martin-Roussety, Owczarek, Hardy and Chen [25] shows an improvement of previous studies where a platform for the purification of an antibody in an automated two-step chromatography purification was developed. The HT system showed limitations in the flow rate that could be used in the RoboColumns, which affected the value for the Dynamic Binding Capacity (DBC) that could be obtained, but the results were comparable to the previously used ÄKTA™ systems. This platform process allows for the purification of hundreds of monoclonal antibodies per week, even at low feed concentrations..

In terms of available HTPD tools for viral inactivation and viral clearance, even though the participants indicated to be a considerable gap in development, recent studies have been published demonstrating the potential of developing a virus filter micro-scale HTPD model. Tang, Ramos, Newell and Stewart [33] used, in combination with an automated liquid handling system, a 96-well filter plate to assess its suitability to be a novel micro-scale HTPD scale-down model. With these types of tools, HT virus filtration optimization is now an option, enabling rapid process development for the continuous biomanufacturing. Additionally, in order to make this important step continuous, several lab-scale models of viral inactivation system have been simulated, designed and built: for example, Gillespie, Holstein, Mullin, Cotoni, Tuccelli, Caulmare and Greenhalgh [34] tested multiple incubation chamber designs to allow narrow residence time distributions; whereas Parker, Amarikwa, Vehar, Orozco, Godfrey, Coffman, Shamlou and Bardliving [35] used a comprehensive Computational Fluid Dynamics (CFD) model to create a laminar flow tubular reactor.

2.4. Current Needs in the Integrated Continuous Bioprocessing

From the information gathered during the workshop, the major challenges pointed out by the participants in HTPD for the implementation of continuous bioprocessing are presented in **Table 2.2**. Furthermore, it was requested to the participants to propose possible solutions for each of the challenges discussed. Modelling and micro/nanofluidics were the main suggestions for the fields to further invest/prioritize to make an easier and smoother transition to continuous biomanufacturing. These proposed solutions and other current needs in ICB will be further discussed, with a particular focus given to PAT tools and unit operation connection.

Table 2.2 - (a) Major problems indicated by the participants of the workshop, with the proposed solutions/fields to invest/prioritize for ICB process development; (b) Summary of the suggested tools by the participants (only six groups answered this question) as solutions for current gaps/problems with HTPD in ICB

(a)

Major Problem	Suggested Solution
Scale Down of Filtration Processes	Microfluidics
USP-DSP Integration	Microfluidics Modelling
Low-throughput Cell Line and Media Development	Integrate robotics into existing systems
Cell culture development (bioreactor/cell retention device) is not mechanistic	Big Data / Smart HTPD (Artificial Intelligence / Mechanistic Modelling)
Process development for Cell Culture	Microfluidics
Scalability of mini-columns (done in batch mode)	Modelling
Integration of chromatographic steps	Modelling

(b)

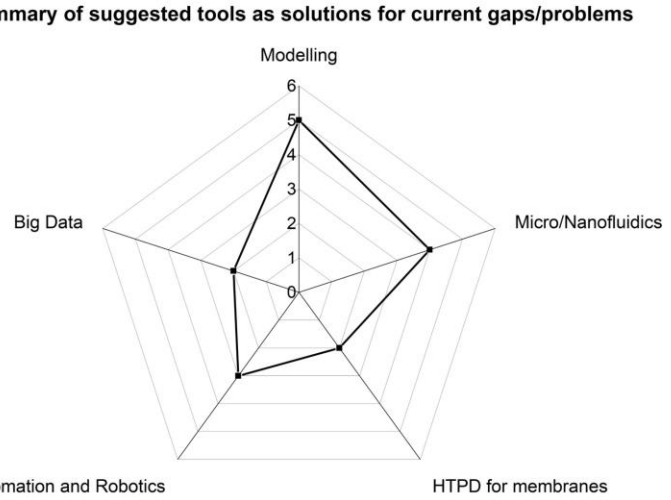

2.4.1. Process Analytical Technique (PAT)

PAT was defined as "a system for designing, analysing, and controlling manufacturing through timely measurements (*i.e.*, during processing) of critical quality and performance

attributes of raw and in-process materials and processes, with the goal of ensuring final product quality" [61]. The ultimate goal of implementing PAT in the biopharmaceutical industry is to design and develop well-understood processes that will reliably ensure a predefined quality in the final product by either monitoring the raw material or in-process product attributes in real-time to control the process, the critical quality attributes (CQAs) [62, 63]. The clear process control and understanding provided by the PAT framework supports as well the Quality by Design (QbD) approach adopted by the biopharmaceutical industry. QbD was defined as "a systematic approach to development that begins with predefined objectives and emphasizes product and process understanding and process control, based on sound science and quality risk management" [64]. Hence, PAT implementation will aid this systematic process development method, QbD, by providing a better understanding of the products and design processes that will ensure consistent product quality.

The crucial element for PAT applications in a continuous process is to be able to gather CQA information for the process and elicit a timely response to facilitate control. It is necessary for the analytical measurements to be available in the time-frame necessary to facilitate real-time decision making [62]. Additionally, to easily implement a PAT tool, the cost required for the instrumentation should not be high, at least until it does not drastically increase the biopharmaceutical production cost. Furthermore, the chosen analytical technique has to be precise, accurate and robust [65]. Although a continuous process has a lot of gain from PAT implementation, these types of tools have been fairly unexplored [56, 62] and for the advancement of continuous processes, important improvements in sensor technology, configuration, and robustness are still required [66].

Regarding the upstream processing, classical process sensors provide information on process variables such as temperature, pH, dissolved gases, and foam levels [66]. However, more robust techniques, involving spectrometric sensors, have been successfully implemented for process monitoring. For example, near infrared (NIR) spectroscopy has been most extensively studied to determine the concentration of individual components in cell culture broth, as demonstrated by Arnold, Gaensakoo, Harvey and McNeil [67]. Furthermore, Raman spectroscopy can be used not only to analyse broth component profiles as well as to monitor structural/chemical changes in proteins, of particular interest to on-line monitor aggregate formation [68] or quality attributes such as glycosylation [47]. Recently, liquid chromatography-mass spectrometry (LC-MS) based multiattribute methods (MAM) has emerged as an important PAT, allowing for a simultaneous monitoring of the product quality attributes such as glycan profile, charge variants, and purity of biotherapeutics [64]. By developing a platform with the collection of cell-free samples from bioreactors, followed by automated HT purification using an automated liquid handling system, Dong, Migliore, Mehrman,

Cunningham, Lewis and Hu [59] demonstrated that it was possible to produce a "near-real-time" measurement, laying out a solid foundation towards using this technique to monitor multiple CQAs during the entire biomanufacturing process.

For the downstream processing, PAT implementation is still fairly limited due to, in part, a lack of sensor options: pH, conductivity, absorbance and pressure sensors do not actually measure quality attributes of the biomolecule, such as protein aggregation. However, Kamga, Woo Lee, Liu and Yoon [43] employed multiwave UV spectra to effectively determine the concentration of individual components in a protein mixture, accurately predicting aggregate concentration relative to the protein of interest. Additionally, for the chromatography steps, implementing PAT can be challenging because of the typical short process times of these unit operations [62]. Sharma, Chilin and Rathore [56] demonstrated that, with on-line analytical liquid chromatography, continuous monitoring of the chromatography step for aggregate peaks can be achieved. An on-line HPLC system was used to investigate the real-time pooling of a process chromatography column and it was programmed to stop collecting when the aggregate peak starts, showing the feasibility of using PAT in order to facilitate real-time decisions for column pooling based on product quality attributes.

Therefore, in a continuous process, a PAT tool must provide decisive information for subsequent process steps on-line, making continuity of processing possible [65]. In the future, the development and implementation of these PAT will allow for the design of a manufacturing process that will deliver a consistent, well-defined quality product and improve process efficiency. Foreseeable challenges include implementing non-invasive process monitoring techniques and incorporating advanced sensors into automated process control strategies [66].

2.4.2. Data Collection/Modeling

The biological processes in the biotechnology industry present many challenges and are usually, if not always, less straightforward than in other industries. The complexity of the operations, especially fermentation, drove the industry to a trial-and-error mode of optimization for years. However, in recent years with the application of QbD and PAT initiatives [69, 70], there has been a greater push for better understanding of the process. This has empowered scientists and engineers to have greater knowledge and details of each operation and not treat processes purely as black boxes.

The ability to translate a process, whether it is a relatively complex process, such as a fermentation, or a simpler process, such as a mixing tank, into a mathematical model has not only allowed a greater process understanding but also a reduction in time and experiments needed for optimization [71, 72]. Mechanistic models (MM) aim to accurately describe the physico-chemical phenomena of the system to be described, and

several examples of such models have been published for bioprocesses [27, 28, 73, 74]. Besides models that are purely mechanistic, hybrid approaches using MM and machine learning, like Artificial Neural Networks (ANNs), can help to ease up the computational load on the computer, *e.g.* by using data sets for the determination of certain parameters and then use these as input to the models. This accelerates the process development and provides faster results, as has been shown in literature, for estimation of process parameters [75] and optimization of full downstream processes [76]. Once such models are tuned and trained, the output of these computations will provide valuable insight on the processes. It is clear that models are of great importance for the leap into integrated continuous biomanufacturing, both in the process development stage and also once such processes are implemented in the production facilities. Modelling cannot, however, be completely detached from the experimental work and data. It needs data to estimate parameters, to train models and ultimately to validate them. Moreover, mathematical models are important for the implementation and realization of much needed control strategies, which are crucial for ensuring the proper functioning of such a complex production train.

The use of models is now widely accepted by industry and is certainly a critical feature of the future continuous processes. The ability to make decisions on the fly depending on unexpected changes to the process based on an accurately described model is something the industry requires. This also raises the need for a reliable and accurate data collection. Coupled to increasingly improved sensors, there is a great need to have very fast and accurate analytics in order to not only collect data on the process's behaviour in order for fast action to take place, but also to be able to monitor and control the CQAs and maintain the final product quality. Considering all the unit operations and processes taking place in a production facility, the amount of data generated at once can be overwhelming. While this generation of large amounts of data is of paramount importance for the process understanding and monitoring, automation of the analyses of the data is crucial [77]. The integrated continuous biomanufacturing initiatives are longing for ways to accommodate and make good use of all the generated data, whether it is destined to process control, process overview or process development.

2.4.3. Upstream/Downstream Processing Connection (& Unit Operations)

For a truly integrated continuous biomanufacturing, the uninterrupted connection of continuous unit operations (upstream and downstream) is necessary, with no or minimal isolated intermediate or hold steps occurring between them.

Several examples of integrating a continuous upstream process with immediate capture have been established [78, 79], with the use of perfusion culture to continuously remove media and extracellular material from the bioreactor. A major challenge with integrating

both processes is synchronizing the upstream perfusion flow rate with the downstream purification flow rate [66]. Synchronized control systems between upstream and downstream systems are also lacking. Therefore, a deviation in the upstream process will not be detected by downstream systems (feedforward control) or vice versa (feedback control). This type of system needs to be developed and implemented since several upstream parameters can impact subsequent downstream operations. Karst, Steinebach, Soos and Morbidelli [79] demonstrated the possibility of implementing feedback control with the installation of an at-line HPLC to provide titer data on bioreactor harvest to modulate the operating conditions of the capture step and regulate the continuous volumetric flow rate by using control loops.

While continuous upstream bioprocessing is reasonably well established, the integration of a full continuous downstream processing is still a developing field. For a continuous capture and polishing chromatography, two main systems can be applied: periodic counter-current chromatography (PCC) and simulated moving bed (SMB) chromatography. In a truly integrated continuous chromatography platform, process synchronization can be achieved by enforcing the residence time in a column to exceed the successive column steps. To ensure that poor quality eluent material from one column is not pooled with material to next functioning column, real-time monitoring and feedback control is necessary. The pooling between columns might also introduce the risk of cross-contamination, which this feedback control strategy might be able to detect and divert the effluent away from the second column [66]. At a small scale, the connection between different chromatography columns and an ultrafiltration unit for the purification of a recombinant protein was developed by Gomis-Fons, Lofgren, Andersson, Nilsson, Berghard and Wood [80]. An external controller, Orbit, was used to make the system automated and open and closed-loop control strategies were applied: UV was monitored in-line and used for automatic product pooling based on cut-off absorbance levels, for example. Furthermore, in an integrated continuous downstream process, a significant reduction in consumable needs, such as chromatography media and buffer consumption, will lead to a drastic reduction in operating and costs. Gjoka, Gantier and Schofield [41] converted four purification unit operations into a continuous process, reducing the resin volume and buffer required by more than 95% and 44% compared to the corresponding batch process, respectively, and significantly decreasing consumables consumption.

Therefore, a fully integrated continuous process has potential to improve quality, cost, speed, and flexibility, with the most urgent challenge to be tackled being the creation of a global monitoring and control strategy for the entire biomanufacturing process. This would entail not only the monitoring and control of continuous measurements at all inlet and outlet streams (PAT framework), but also a realistic feedback and feedforward

control strategy to ensure the final product quality. Thus far, to the author's knowledge, a complete end-to-end integration in manufacturing processes has still to be reported. However, Godawat, Konstantinov, Rohani and Warikoo [81] was able to combined a perfusion bioreactor with two periodic PCC units for initial capture and successive ion-exchange steps, showing it is feasible to fully create and integrate an end-to-end continuous bioprocessing platform. More recently, Coolbaugh et al. (2021) have demonstrated such end-to-end continuous processes are scalable by showing a successful proof-of-concept at pilot-scale.

2.4.4. Other Needs

The aforementioned needs represent three big realms where further development is needed. However, there are also some needs that are missing and others that despite not being totally missing still lack the practicality and/or affordability in order to be reliable solutions. The increased democratization of High-Throughput Screening (HTS) has led facilities around the world to more automated labs and miniaturized assays.

The use of automated liquid-handling systems has long been established as the standard for HTPD in downstream (mainly chromatography), as methods for the determination of adsorption isotherms and even full chromatographic runs have been described [82-85]. The use of such equipment allows for the automation of the assays while keeping the used volumes low, yielding a faster and more cost-effective analysis. For upstream, there have been solutions for HTPD, however these usually come with a very high price tag such as the Ambr® systems [10], which can discourage scientists and companies from investing. Industry is therefore calling for affordable alternatives and sees in microfluidics a good opportunity to fill this need. When it comes to cell line development, the current state-of-the-art for companies without the Ambr® system is to take the better performing strains in batch mode and then test it in perfusion mode. There is therefore a need for deeper understanding on cell biology which will ultimately lead to the development of better cell lines at affordable prices, and microfluidics steps up to offer that [86].

Microfluidics has already shown to be a powerful scale-down model of equipment capable of mimicking several unit operations with the advantage of using less sample volume and achieving faster assays. These devices are still paving their way into the repertoire of process development but have already shown promising results for different unit operations such as crystallization [87], chromatography [88], cell culture [89], aqueous two-phase systems [90], biocatalysis [91] and as a promising scale-down model for HTS equipment, where parallel assays at a manifold volume and time reduction has been previously demonstrated [92]. However, filtration have lacked a scale-down model that would allow for HTPD of the specific unit operations.

Membrane filtration is also not widely used in microfluidics, with both inertial and membrane filtration being reported as alternatives [93, 94]. The adaption of liquid-handling stations to the HTPD of such unit operation is still in very early stages. Filtration process development usually needs a large amount of materials and time-consuming work. The use of a HTS equipment for such system emphasizes on reducing reagent consumption in process development while avoiding the oversizing of equipment, consequence of a poorer process knowledge [33].

2.5. Conclusions

The change to continuous processing is a natural path for a maturing industry, and biopharmaceutical industries are following it, with technological advancements empowering this shift more and more. The advantages of this technology are great and well demonstrated, and it has been evidenced that it allows for process cost reductions at different scales, even when compared to the most established batch processing modes and different production scales [95].

Continuous processing allows, in general, for more efficient processes while reducing the footprint. Increasing the volumetric flow translates into a smaller increase in equipment and consumables cost for continuous processing than for what is observed for batch processes, due to a more efficient use of equipment. The counterpart of continuous bioprocessing is the increased need for fast analytics and control, that can provide real-time responses for fluctuations in operational conditions in order to guarantee product quality.

Although the technological breakthroughs have been immense over the past 20 years, we can understand that academia and industry are eager for better processing technologies. From the workshop outcome it is possible to conclude that although there are plenty options for process development and optimization, the room for improvement is still quite large, either to have new technologies or to find a way to cut down the prices of existing technologies in order to democratize process development. Among the tools perceived as the most promising to fulfil current gaps in ICB are modelling and micro/nanofluidics. This goes in accordance with current demands of regulatory agencies translated in PAT and QbD initiatives, where a higher process understanding is in order and a control of the final product quality is achieved, reducing the product variance in meeting CQA's.

Recent advances in both upstream and downstream processing research allowed to achieve competitive unit operations running in continuous mode, allowing these new processes to outperform the previously established ones. As the upstream and downstream processing have been developed separately throughout the years, the

challenge now relies on integrating all these continuous unit operations into a continuous end-to-end manufacturing process [96]. The integration of software and hardware is important to achieve a fully continuous process, as well as process control, both feedforward and feedback, so that faster decisions are made according to what is happening in other unit operations. The further development of PAT and a synchronization of control systems will be the key enablers of the shift to an end-to-end continuous process in the biopharmaceutical industry [66].

Reducing the time to market usually hinders the implementation of a continuous process, as it is easier to "play safe" and assure that the "race is won". Biosimilars can, however, take advantage of the patent expiry and bet on such processing mode, aiming to achieve a more efficient and less expensive process allowing the biosimilars producing companies to compete with major players.

2.6. Acknowledgements

The authors wish to thank the European Union's Horizon 2020 research and innovation programme under the Marie Skłodowska-Curie grant agreement No 812909 CODOBIO, within the Marie Skłodowska-Curie European Training Networks framework. The authors also wish to thank the 2019 ICB conference chairs for providing the opportunity to conduct this workshop and get valuable feedback from participants.

2.7. References

[1] B. Somasundaram, K. Pleitt, E. Shave, K. Baker, L.H.L. Lua, Progression of continuous downstream processing of monoclonal antibodies: Current trends and challenges, Biotechnol Bioeng 115(12) (2018) 2893-2907. https://doi.org/10.1002/bit.26812.

[2] A.S. Rathore, H. Agarwal, A.K. Sharma, M. Pathak, S. Muthukumar, Continuous processing for production of biopharmaceuticals, Prep Biochem Biotechnol 45(8) (2015) 836-49. https://doi.org/10.1080/10826068.2014.985834.

[3] A.A. Shukla, L.S. Wolfe, S.S. Mostafa, C. Norman, Evolving trends in mAb production processes, Bioeng Transl Med 2(1) (2017) 58-69. https://doi.org/10.1002/btm2.10061.

[4] A.L. Zydney, Continuous downstream processing for high value biological products: A Review, Biotechnol Bioeng 113(3) (2016) 465-75. https://doi.org/10.1002/bit.25695.

[5] J. Walther, R. Godawat, C. Hwang, Y. Abe, A. Sinclair, K. Konstantinov, The business impact of an integrated continuous biomanufacturing platform for recombinant protein production, J Biotechnol 213 (2015) 3-12. https://doi.org/10.1016/j.jbiotec.2015.05.010.

[6] K.B. Konstantinov, C.L. Cooney, White paper on continuous bioprocessing. May 20-21, 2014 Continuous Manufacturing Symposium, J Pharm Sci 104(3) (2015) 813-20. https://doi.org/10.1002/jps.24268.

[7] CODOBIO, Continuous Downstream Processing of Biologics, https://www.codobio.eu/ (2018 - 2022).

[8] L. Fernandez-Cerezo, A. Rayat, A. Chatel, J.M. Pollard, G.J. Lye, M. Hoare, An ultra scale-down method to investigate monoclonal antibody processing during tangential flow filtration using ultrafiltration membranes, Biotechnol Bioeng 116(3) (2019) 581-590. https://doi.org/10.1002/bit.26859.

[9] V. Sandner, L.P. Pybus, G. McCreath, J. Glassey, Scale-Down Model Development in ambr systems: An Industrial Perspective, Biotechnology Journal 14(4) (2019) 1700766. https://doi.org/10.1002/biot.201700766.

[10] P. Xu, C. Clark, T. Ryder, C. Sparks, J. Zhou, M. Wang, R. Russell, C. Scott, Characterization of TAP Ambr 250 disposable bioreactors, as a reliable scale-down model for biologics process development, Biotechnology Progress 33(2) (2017) 478-489. https://doi.org/10.1002/btpr.2417.

[11] S. Shi, R.G. Condon, L. Deng, J. Saunders, F. Hung, Y.-S. Tsao, Z. Liu, A high-throughput automated platform for the development of manufacturing cell lines for protein therapeutics, JoVE (Journal of Visualized Experiments) (55) (2011) e3010. https://doi.org/10.3791/3010.

[12] K. Le, C. Tan, H. Le, J. Tat, E. Zasadzinska, J. Diep, R. Zastrow, C. Chen, J. Stevens, Assuring Clonality on the Beacon Digital Cell Line Development Platform, Biotechnology Journal 15(1) (2020) 1900247. https://doi.org/10.1002/biot.201900247.

[13] J. Strnad, M. Brinc, V. Spudić, N. Jelnikar, L. Mirnik, B. Čarman, Z. Kravanja, Optimization of cultivation conditions in spin tubes for Chinese hamster ovary cells producing erythropoietin and the comparison of glycosylation patterns in different cultivation vessels, Biotechnology Progress 26(3) (2010) 653-663. https://doi.org/10.1002/btpr.390.

[14] H. Schwarz, Y. Zhang, C. Zhan, M. Malm, R. Field, R. Turner, C. Sellick, P. Varley, J. Rockberg, V. Chotteau, Small-scale bioreactor supports high density HEK293 cell perfusion culture for the production of recombinant Erythropoietin, Journal of Biotechnology 309 (2020) 44-52. https://doi.org/10.1016/j.jbiotec.2019.12.017.

[15] D. Fedorenko, A.K. Dutta, J. Tan, J. Walko, M. Brower, N.D.S. Pinto, A.L. Zydney, O. Shinkazh, Improved protein A resin for antibody capture in a continuous countercurrent tangential chromatography system, Biotechnol Bioeng 117(3) (2020) 646-653. https://doi.org/10.1002/bit.27232.

[16] N.D.S. Pinto, W.N. Napoli, M. Brower, Impact of micro and macroporous TFF membranes on product sieving and chromatography loading for perfusion cell culture, Biotechnol Bioeng 117(1) (2020) 117-124. https://doi.org/10.1002/bit.27192.

[17] A. Arunkumar, N. Singh, M. Peck, M.C. Borys, Z.J. Li, Investigation of single-pass tangential flow filtration (SPTFF) as an inline concentration step for cell culture harvest, Journal of Membrane Science 524 (2017) 20-32. https://doi.org/10.1016/j.memsci.2016.11.007.

[18] R.P. Baptista, D.A. Fluri, P.W. Zandstra, High density continuous production of murine pluripotent cells in an acoustic perfused bioreactor at different oxygen concentrations, Biotechnol Bioeng 110(2) (2013) 648-55. https://doi.org/10.1002/bit.24717.

[19] G. Granicher, J. Coronel, F. Trampler, I. Jordan, Y. Genzel, U. Reichl, Performance of an acoustic settler versus a hollow fiber-based ATF technology for influenza virus production in perfusion, Appl Microbiol Biotechnol 104(11) (2020) 4877-4888. https://doi.org/10.1007/s00253-020-10596-x.

[20] A.S. Tait, J.P. Aucamp, A. Bugeon, M. Hoare, Ultra scale-down prediction using microwell technology of the industrial scale clarification characteristics by centrifugation of mammalian cell broths, Biotechnol Bioeng 104(2) (2009) 321-31. https://doi.org/10.1002/bit.22393.

[21] C.E. Hogwood, A.S. Tait, N. Koloteva-Levine, D.G. Bracewell, C.M. Smales, The dynamics of the CHO host cell protein profile during clarification and protein A capture in a platform antibody purification process, Biotechnol Bioeng 110(1) (2013) 240-51. https://doi.org/10.1002/bit.24607.

[22] P. McDonald, B. Tran, C.R. Williams, M. Wong, T. Zhao, B.D. Kelley, P. Lester, The rapid identification of elution conditions for therapeutic antibodies from cation-exchange chromatography resins using high-throughput screening, Journal of Chromatography A 1433 (2016) 66-74. https://doi.org/10.1016/j.chroma.2015.12.071.

[23] V.N. Sisodiya, J. Lequieu, M. Rodriguez, P. McDonald, K.P. Lazzareschi, Studying host cell protein interactions with monoclonal antibodies using high throughput protein A chromatography, Biotechnology Journal 7(10) (2012) 1233-1241. https://doi.org/10.1002/biot.201100479.

[24] T. Bergander, K. Nilsson-Välimaa, K. Öberg, K.M. Lacki, High-throughput process development: determination of dynamic binding capacity using microtiter filter plates filled with chromatography resin, Biotechnology Progress 24(3) (2008) 632-639. https://doi.org/10.1021/bp0704687.

[25] P.M. Schmidt, M. Abdo, R.E. Butcher, M.-Y. Yap, P.D. Scotney, M.L. Ramunno, G. Martin-Roussety, C. Owczarek, M.P. Hardy, C.-G. Chen, A robust robotic high-throughput antibody purification platform, Journal of Chromatography A 1455 (2016) 9-19. https://doi.org/j.chroma.2016.05.076.

[26] W.R. Keller, S.T. Evans, G. Ferreira, D. Robbins, S.M. Cramer, Use of MiniColumns for linear isotherm parameter estimation and prediction of benchtop column performance, Journal of chromatography A 1418 (2015) 94-102. https://doi.org/10.1016/j.chroma.2015.09.038.

[27] B.K. Nfor, J. Ripić, A. van der Padt, M. Jacobs, M. Ottens, Model-based high-throughput process development for chromatographic whey proteins separation, Biotechnology Journal 7(10) (2012) 1221-1232. https://doi.org/10.1002/biot.201200191.

[28] V. Kumar, S. Leweke, E. von Lieres, A.S. Rathore, Mechanistic modeling of ion-exchange process chromatography of charge variants of monoclonal antibody products, Journal of Chromatography A 1426 (2015) 140-153. https://doi.org/10.1016/j.chroma.2015.11.062.

[29] S.M. Pirrung, D. Parruca da Cruz, A.T. Hanke, C. Berends, R.F. Van Beckhoven, M.H. Eppink, M. Ottens, Chromatographic parameter determination for complex biological feedstocks, Biotechnology Progress 34(4) (2018) 1006-1018. https://doi.org/10.1002/btpr.2642.

[30] X. Gjoka, K. Rogler, R.A. Martino, R. Gantier, M. Schofield, A straightforward methodology for designing continuous monoclonal antibody capture multi-column chromatography processes, Journal of Chromatography A 1416 (2015) 38-46. https://doi.org/10.1016/j.chroma.2015.09.005.

[31] A. Clutterbuck, P. Beckett, R. Lorenzi, F. Sengler, T. Bisschop, J. Haas, Single-Pass Tangential Flow Filtration (SPTFF) in Continuous Biomanufacturing, Continuous Biomanufacturing: Innovative Technologies and Methods (2017) 423-456.

[32] Y. Baek, N. Singh, A. Arunkumar, M. Borys, Z.J. Li, A.L. Zydney, Ultrafiltration behavior of monoclonal antibodies and Fc-fusion proteins: Effects of physical properties, Biotechnology and Bioengineering 114(9) (2017) 2057-2065. https://doi.org/10.1002/bit.26326.

[33] A. Tang, I. Ramos, K. Newell, K.D. Stewart, A novel high-throughput process development screening tool for virus filtration, Journal of Membrane Science 611 (2020). https://doi.org/10.1016/j.memsci.2020.118330.

[34] C. Gillespie, M. Holstein, L. Mullin, K. Cotoni, R. Tuccelli, J. Caulmare, P. Greenhalgh, Continuous In-Line Virus Inactivation for Next Generation Bioprocessing, Biotechnol J 14(2) (2019) e1700718. https://doi.org/10.1002/biot.201700718.

[35] S.A. Parker, L. Amarikwa, K. Vehar, R. Orozco, S. Godfrey, J. Coffman, P. Shamlou, C.L. Bardliving, Design of a novel continuous flow reactor for low pH viral inactivation, Biotechnol Bioeng 115(3) (2018) 606-616. https://doi.org/10.1002/bit.26497.

[36] L. David, B. Maiser, M. Lobedann, P. Schwan, M. Lasse, H. Ruppach, G. Schembecker, Virus study for continuous low pH viral inactivation inside a coiled flow inverter, Biotechnol Bioeng 116(4) (2019) 857-869. https://doi.org/10.1002/bit.26872.

[37] R. Orozco, S. Godfrey, J. Coffman, L. Amarikwa, S. Parker, L. Hernandez, C. Wachuku, B. Mai, B. Song, S. Hoskatti, J. Asong, P. Shamlou, C. Bardliving, M. Fiadeiro, Design, construction, and optimization of a novel, modular, and scalable incubation chamber for continuous viral inactivation, Biotechnol Prog 33(4) (2017) 954-965. https://doi.org/10.1002/btpr.2442.

[38] A.L. Lofgren, J.G. Fons, N. Andersson, B. Nilsson, L. Berghard, C.L.H. Hagglund, An integrated continuous downstream process with real-time control: A case study with periodic countercurrent chromatography and continuous virus inactivation, (2020). https://doi.org/10.22541/au.160029924.40393430.

[39] D.L. Martins, J. Sencar, N. Hammerschmidt, B. Tille, J. Kinderman, T.R. Kreil, A. Jungbauer, Continuous Solvent/Detergent Virus Inactivation Using a Packed-Bed Reactor, Biotechnol J 14(8) (2019) e1800646. https://doi.org/10.1002/biot.201800646.

[40] S. Lute, J. Kozaili, S. Johnson, K. Kobayashi, D. Strauss, Development of small-scale models to understand the impact of continuous downstream bioprocessing on integrated virus filtration, Biotechnol Prog 36(3) (2020) e2962. https://doi.org/10.1002/btpr.2962.

[41] X. Gjoka, R. Gantier, M. Schofield, Transfer of a three step mAb chromatography process from batch to continuous: Optimizing productivity to minimize consumable requirements, J Biotechnol 242 (2017) 11-18. https://doi.org/10.1016/j.jbiotec.2016.12.005.

[42] S.W. Li, H.P. Song, Y. Leng, Rapid determination of lovastatin in the fermentation broth of Aspergillus terreus using dual-wavelength UV spectrophotometry, Pharm Biol 52(1) (2014) 129-35. https://doi.org/10.3109/13880209.2013.833947.

[43] M.H. Kamga, H. Woo Lee, J. Liu, S. Yoon, Quantification of protein mixture in chromatographic separation using multi-wavelength UV spectra, Biotechnol Prog 29(3) (2013) 664-71. https://doi.org/10.1002/btpr.1712.

[44] M. Zelger, S. Pan, A. Jungbauer, R. Hahn, Real-time monitoring of protein precipitation in a tubular reactor for continuous bioprocessing, Process Biochemistry 51(10) (2016) 1610-1621. https://doi.org/10.1016/j.procbio.2016.06.018.

[45] M. Kornecki, J. Strube, Process Analytical Technology for Advanced Process Control in Biologics Manufacturing with the Aid of Macroscopic Kinetic Modeling, Bioengineering (Basel) 5(1) (2018). https://doi.org/10.3390/bioengineering5010025.

[46] B. Nagy, A. Farkas, M. Gyurkes, S. Komaromy-Hiller, B. Demuth, B. Szabo, D. Nusser, E. Borbas, G. Marosi, Z.K. Nagy, In-line Raman spectroscopic monitoring and feedback control of a continuous twin-screw pharmaceutical powder blending and tableting process, Int J Pharm 530(1-2) (2017) 21-29. https://doi.org/10.1016/j.ijpharm.2017.07.041.

[47] M.Y. Li, B. Ebel, C. Paris, F. Chauchard, E. Guedon, A. Marc, Real-time monitoring of antibody glycosylation site occupancy by in situ Raman spectroscopy during bioreactor CHO cell cultures, Biotechnol Prog 34(2) (2018) 486-493. https://doi.org/10.1002/btpr.2604.

[48] G. Thakur, V. Hebbi, A.S. Rathore, An NIR-based PAT approach for real-time control of loading in Protein A chromatography in continuous manufacturing of monoclonal antibodies, Biotechnol Bioeng 117(3) (2020) 673-686. https://doi.org/10.1002/bit.27236.

[49] G. Thakur, S. Thori, A.S. Rathore, Implementing PAT for single-pass tangential flow ultrafiltration for continuous manufacturing of monoclonal antibodies, Journal of Membrane Science 613 (2020). https://doi.org/10.1016/j.memsci.2020.118492.

[50] F. Capito, R. Skudas, H. Kolmar, B. Stanislawski, Host cell protein quantification by Fourier transform mid infrared spectroscopy (FT-MIR), Biotechnol Bioeng 110(1) (2013) 252-9. https://doi.org/10.1002/bit.24611.

[51] F. Capito, A. Zimmer, R. Skudas, Mid-infrared spectroscopy-based analysis of mammalian cell culture parameters, Biotechnol Prog 31(2) (2015) 578-84. https://doi.org/10.1002/btpr.2026.

[52] B.A. Patel, A. Gospodarek, M. Larkin, S.A. Kenrick, M.A. Haverick, N. Tugcu, M.A. Brower, D.D. Richardson, Multi-angle light scattering as a process analytical technology measuring real-time molecular weight for downstream process control, MAbs 10(7) (2018) 945-950. https://doi.org/10.1080/19420862.2018.1505178.

[53] D.G. Sauer, M. Melcher, M. Mosor, N. Walch, M. Berkemeyer, T. Scharl-Hirsch, F. Leisch, A. Jungbauer, A. Durauer, Real-time monitoring and model-based prediction of purity and quantity during a chromatographic capture of fibroblast growth factor 2, Biotechnol Bioeng 116(8) (2019) 1999-2009. https://doi.org/10.1002/bit.26984.

[54] A.S. Rathore, R. Wood, A. Sharma, S. Dermawan, Case study and application of process analytical technology (PAT) towards bioprocessing: II. Use of ultra-performance liquid chromatography (UPLC) for making real-time pooling decisions for process chromatography, Biotechnol Bioeng 101(6) (2008) 1366-74. https://doi.org/10.1002/bit.21982.

[55] A.S. Rathore, M. Yu, S. Yeboah, A. Sharma, Case study and application of process analytical technology (PAT) towards bioprocessing: use of on-line high-performance liquid chromatography (HPLC) for making real-time pooling decisions for process chromatography, Biotechnol Bioeng 100(2) (2008) 306-16. https://doi.org/10.1002/bit.21759.

[56] A. Sharma, D. Chilin, A.S. Rathore, Applying Process Analytical Technology to Biotech Unit Operations, BioPharm International 19(8) (2006).

[57] R.F. Steinhoff, D.J. Karst, F. Steinebach, M.R. Kopp, G.W. Schmidt, A. Stettler, J. Krismer, M. Soos, M. Pabst, A. Hierlemann, M. Morbidelli, R. Zenobi, Microarray-based MALDI-TOF mass spectrometry enables monitoring of monoclonal antibody production in batch and perfusion cell cultures, Methods 104 (2016) 33-40. https://doi.org/10.1016/j.ymeth.2015.12.011.

[58] Y. Liu, J. Fernandez, Z. Pu, H. Zhang, L. Cao, I. Aguilar, D. Ritz, R. Luo, A. Read, A. Laures, K. Lan, A. Ubiera, A. Smith, P. Patel, A. Liu, Simultaneous Monitoring and Comparison of Multiple Product Quality Attributes for Cell Culture Processes at Different Scales Using a LC/MS/MS Based Multi-Attribute Method, J Pharm Sci 109(11) (2020) 3319-3329. https://doi.org/10.1016/j.xphs.2020.07.029.

[59] J. Dong, N. Migliore, S.J. Mehrman, J. Cunningham, M.J. Lewis, P. Hu, High-Throughput, Automated Protein A Purification Platform with Multiattribute LC-MS Analysis for Advanced Cell Culture Process Monitoring, Anal Chem 88(17) (2016) 8673-9. https://doi.org/10.1021/acs.analchem.6b01956.

[60] K. Treier, S. Hansen, C. Richter, P. Diederich, J. Hubbuch, P. Lester, High-throughput methods for miniaturization and automation of monoclonal antibody purification processes, Biotechnol Prog 28(3) (2012) 723-32. https://doi.org/10.1002/btpr.1533.

[61] F.a.D.A.F. U.S. Department of Health and Human Services, Center for Drug Evaluation and Research (CDER), Center for Veterinary Medicine (CVM), Office of Regulatory Affairs (ORA), PAT- A Framework for Innovative Pharmaceutical Development Manufacturing and Quality Assurance, 2004.

[62] E.K. Read, J.T. Park, R.B. Shah, B.S. Riley, K.A. Brorson, A.S. Rathore, Process analytical technology (PAT) for biopharmaceutical products: Part I. concepts and applications, Biotechnol Bioeng 105(2) (2010) 276-84. https://doi.org/10.1002/bit.22528.

[63] J. Glassey, K.V. Gernaey, C. Clemens, T.W. Schulz, R. Oliveira, G. Striedner, C.F. Mandenius, Process analytical technology (PAT) for biopharmaceuticals, Biotechnol J 6(4) (2011) 369-77. https://doi.org/10.1002/biot.201000356.

[64] D.P. Wasalathanthri, M.S. Rehmann, Y. Song, Y. Gu, L. Mi, C. Shao, L. Chemmalil, J. Lee, S. Ghose, M.C. Borys, J. Ding, Z.J. Li, Technology outlook for real-time quality attribute and process parameter monitoring in biopharmaceutical development-A review, Biotechnol Bioeng 117(10) (2020) 3182-3198. https://doi.org/10.1002/bit.27461.

[65] C.-F. Mandenius, R. Gustavsson, Mini-review: soft sensors as means for PAT in the manufacture of bio-therapeutics, Journal of Chemical Technology & Biotechnology 90(2) (2015) 215-227. https://doi.org/10.1002/jctb.4477.

[66] A.C. Fisher, M.H. Kamga, C. Agarabi, K. Brorson, S.L. Lee, S. Yoon, The Current Scientific and Regulatory Landscape in Advancing Integrated Continuous Biopharmaceutical Manufacturing, Trends Biotechnol 37(3) (2019) 253-267. https://doi.org/10.1016/j.tibtech.2018.08.008.

[67] S.A. Arnold, R. Gaensakoo, L.M. Harvey, B. McNeil, Use of at-line and in-situ near-infrared spectroscopy to monitor biomass in an industrial fed-batch Escherichia coli process, Biotechnol Bioeng 80(4) (2002) 405-13. https://doi.org/10.1002/bit.10383.

[68] C.M. Gryniewicz, J.F. Kauffman, Multivariate calibration of covalent aggregate fraction to the raman spectrum of regular human insulin, J Pharm Sci 97(9) (2008) 3727-34. https://doi.org/10.1002/jps.21326.

[69] A.S. Rathore, Roadmap for implementation of quality by design (QbD) for biotechnology products, Trends in Biotechnology 27(9) (2009) 546-553. https://doi.org/10.1016/j.tibtech.2009.06.006.

[70] F.a.D.A.F. U.S. Department of Health and Human Services, Center for Drug Evaluation and Research (CDER), Center for Veterinary Medicine (CVM), Office of Regulatory Affairs (ORA), Guidance for Industry: Process Validation: General Principles and Practices, 2011.

[71] B.K. Nfor, T. Ahamed, G.W. van Dedem, P.D. Verhaert, L.A. van der Wielen, M.H. Eppink, E.J. van de Sandt, M. Ottens, Model-based rational methodology for protein purification process synthesis, Chemical Engineering Science 89 (2013) 185-195. https://doi.org/10.1016/j.ces.2012.11.034.

[72] S. Chhatre, S.S. Farid, J. Coffman, P. Bird, A.R. Newcombe, N.J. Titchener-Hooker, How implementation of quality by design and advances in biochemical engineering are enabling efficient bioprocess development and manufacture, Journal of Chemical Technology & Biotechnology 86(9) (2011) 1125-1129. https://doi.org/10.1002/jctb.2628.

[73] V. Hebbi, S. Roy, A.S. Rathore, A. Shukla, Modeling and prediction of excipient and pH drifts during ultrafiltration/diafiltration of monoclonal antibody biotherapeutic for high concentration formulations, Separation and Purification Technology 238 (2020) 116392. https://doi.org/10.1016/j.seppur.2019.116392.

[74] B.B. Yahia, L. Malphettes, E. Heinzle, Macroscopic modeling of mammalian cell growth and metabolism, Applied microbiology and biotechnology 99(17) (2015) 7009-7024. https://doi.org/10.1007/s00253-015-6743-6.

[75] G. Wang, T. Briskot, T. Hahn, P. Baumann, J. Hubbuch, Estimation of adsorption isotherm and mass transfer parameters in protein chromatography using artificial neural networks, Journal of Chromatography A 1487 (2017) 211-217. https://doi.org/10.1016/j.chroma.2017.01.068.

[76] S.M. Pirrung, L.A. van der Wielen, R.F. van Beckhoven, E.J. van de Sandt, M.H. Eppink, M. Ottens, Optimization of biopharmaceutical downstream processes supported by mechanistic models and artificial neural networks, Biotechnology Progress 33(3) (2017) 696-707. https://doi.org/10.1002/btpr.2435.

[77] A.L. Oliveira, Biotechnology, big data and artificial intelligence, Biotechnology Journal 14(8) (2019) 1800613. https://doi.org/10.1002/biot.201800613.

[78] M.H. Kamga, M. Cattaneo, S. Yoon, Integrated continuous biomanufacturing platform with ATF perfusion and one column chromatography operation for optimum resin utilization and productivity, Prep Biochem Biotechnol 48(5) (2018) 383-390. https://doi.org/10.1080/10826068.2018.1446151.

[79] D.J. Karst, F. Steinebach, M. Soos, M. Morbidelli, Process performance and product quality in an integrated continuous antibody production process, Biotechnol Bioeng 114(2) (2017) 298-307. https://doi.org/10.1002/bit.26069.

[80] J. Gomis-Fons, A. Lofgren, N. Andersson, B. Nilsson, L. Berghard, S. Wood, Integration of a complete downstream process for the automated lab-scale production of a recombinant protein, J Biotechnol 301 (2019) 45-51. https://doi.org/10.1016/j.jbiotec.2019.05.013.

[81] R. Godawat, K. Konstantinov, M. Rohani, V. Warikoo, End-to-end integrated fully continuous production of recombinant monoclonal antibodies, J Biotechnol 213 (2015) 13-9. https://doi.org/10.1016/j.jbiotec.2015.06.393.

[82] M. Wiendahl, P. Schulze Wierling, J. Nielsen, D. Fomsgaard Christensen, J. Krarup, A. Staby, J. Hubbuch, High Throughput Screening for the Design and Optimization of Chromatographic Processes – Miniaturization, Automation and Parallelization of Breakthrough and Elution Studies, Chemical Engineering & Technology 31(6) (2008) 893-903. https://doi.org/10.1002/ceat.200800167.

[83] B.K. Nfor, M. Noverraz, S. Chilamkurthi, P.D. Verhaert, L.A. van der Wielen, M. Ottens, High-throughput isotherm determination and thermodynamic modeling of protein adsorption on mixed mode adsorbents, J Chromatogr A 1217(44) (2010) 6829-50. https://doi.org/10.1016/j.chroma.2010.07.069.

[84] A. Kiesewetter, P. Menstell, L.H. Peeck, A. Stein, Development of pseudo-linear gradient elution for high-throughput resin selectivity screening in RoboColumn® Format, Biotechnology Progress 32(6) (2016) 1503-1519. https://doi.org/10.1002/btpr.2363.

[85] S.T. Evans, K.D. Stewart, C. Afdahl, R. Patel, K.J. Newell, Optimization of a micro-scale, high throughput process development tool and the demonstration of comparable process performance and product quality with biopharmaceutical manufacturing processes, Journal of Chromatography A 1506 (2017) 73-81. https://doi.org/10.1016/j.chroma.2017.05.041.

[86] T. Kwon, H. Prentice, J. De Oliveira, N. Madziva, M.E. Warkiani, J.-F.P. Hamel, J. Han, Microfluidic cell retention device for perfusion of mammalian suspension culture, Scientific Reports 7(1) (2017) 1-11. https://doi.org/10.1038/s41598-017-06949-8.

[87] L. Li, R.F. Ismagilov, Protein crystallization using microfluidic technologies based on valves, droplets, and SlipChip, Annual Review of Biophysics 39 (2010) 139-158. https://doi.org/10.1146/annurev.biophys.050708.133630

[88] I.F. Pinto, D. Santos, R. Soares, M. Aires-Barros, V. Chu, A. Azevedo, J. Conde, A regenerable microfluidic device with integrated valves and thin-film photodiodes for rapid optimization of chromatography conditions, Sensors and Actuators B: Chemical 255 (2018) 3636-3646. https://doi.org/10.1016/j.snb.2017.09.167.

[89] M. Mehling, S. Tay, Microfluidic cell culture, Current Opinion in Biotechnology 25 (2014) 95-102. https://doi.org/10.1016/j.copbio.2013.10.005.

[90] D. Silva, A. Azevedo, P. Fernandes, V. Chu, J. Conde, M. Aires-Barros, Determination of aqueous two phase system binodal curves using a microfluidic device, Journal of Chromatography A 1370 (2014) 115-120. https://doi.org/10.1016/j.chroma.2014.10.035.

[91] Y. Zhu, Q. Chen, L. Shao, Y. Jia, X. Zhang, Microfluidic immobilized enzyme reactors for continuous biocatalysis, Reaction Chemistry & Engineering 5(1) (2020) 9-32. https://doi.org/10.1039/C9RE00217K.

[92] H.S. Rho, A.T. Hanke, M. Ottens, H. Gardeniers, A microfluidic device for the batch adsorption of a protein on adsorbent particles, Analyst 142(19) (2017) 3656-3665. https://doi.org/10.1039/c7an00917h.

[93] A.A.S. Bhagat, S.S. Kuntaegowdanahalli, I. Papautsky, Inertial microfluidics for continuous particle filtration and extraction, Microfluidics and Nanofluidics 7(2) (2008) 217-226. https://doi.org/10.1007/s10404-008-0377-2.

[94] X. Chen, J. Shen, Review of membranes in microfluidics, Journal of Chemical Technology & Biotechnology 92(2) (2017) 271-282. https://doi.org/10.1002/jctb.5105.

[95] J. Hummel, M. Pagkaliwangan, X. Gjoka, T. Davidovits, R. Stock, T. Ransohoff, R. Gantier, M. Schofield, Modeling the downstream processing of monoclonal antibodies reveals cost advantages for continuous methods for a broad range of manufacturing scales, Biotechnology Journal 14(2) (2019) 1700665. https://doi.org/10.1002/biot.201700665.

[96] P. Gronemeyer, H. Thiess, S. Zobel-Roos, R. Ditz, J. Strube, Integration of Upstream and Downstream in Continuous Biomanufacturing, Continuous Biomanufacturing-Innovative Technologies and Methods: Innovative Technologies and Methods (2017) 481-510. https://doi.org/10.1002/9783527699902.ch17.

Chapter 3

Automation and miniaturization: enabling tools for fast, high-throughput process development in integrated continuous biomanufacturing

Abstract

Process development in the biotech industry leads to investments around hundred of millions of dollars. It is important to mitigate costs without neglecting the quality of process development. Biopharmaceutical process development is important for companies to develop new processes and be first to market, improve a pre-established process, or start manufacturing a product available by patent expiry (biosimilars). Laboratory automation enables methodical and standardized process development. Miniaturization and parallelization empower laboratories to screen several experimental conditions and define operating windows for purification processes, improving process robustness. Together, they allow for fast and accurate process development in a fraction of the time and cost of nonminiaturized/nonparallel process development approaches. The most widely used High-Throughput Screening technique is a liquid-handling station and microfluidics is taking its first steps in process development. Both are attractive scale-down tools for the characterization of bioprocesses and allow thousands of experiments to be performed per day. High-Throughput Process Development (HTPD) has helped to achieve major breakthroughs in process optimization, both for upstream and downstream processing. Continuous processing is the next step in process development which leads to cost reduction, higher productivity and better quality control; the integration of upstream and downstream processes is seen as a major challenge. In this review, we will focus on the state-of-the-art of miniaturized techniques for process development in the biotechnology industry, and how automation and miniaturization drive process development. A comparison between liquid-handling stations and microfluidics is made and an indication is given of which tools are still lacking for HTPD in the context of Integrated Continuous Biomanufacturing.

Keywords: Automation; Miniaturization; Integrated Continuous Biomanufacturing; High-Throughput Process Development; Microfluidics; Liquid-Handling Stations.

***Published as*:** Silva, T.C., Eppink, M. and Ottens, M., 2022. Automation and miniaturization: enabling tools for fast, high-throughput process development in integrated continuous biomanufacturing. Journal of Chemical Technology & Biotechnology, 97(9), pp.2365-2375. DOI: https://doi.org/10.1002/jctb.6792

3.1. Introduction

In recent years, an evolution in medicine and available treatments has taken place. The available drugs for different therapies keep increasing and competition grows fiercely with patent expiry. Companies that want to remain competitive need fast and inexpensive process development for new products.

With patent expiry, competition rises and consumers profit, as prices go down. One example of heavy market competition is the monoclonal antibody (mAb) market, where the expiry of patents held by major players in USA and Europe allowed the emergence of the so-called biosimilars – molecules similar to the therapeutic mAbs available at a fraction of the price - with the first mAb biosimilar (infliximab) registering a decrease of up to 72% of the original molecule price [1]. Companies have tried to counteract the emergence of similar drugs through the discovery of new applications for already available drugs [2].

R&D represents a considerable slice of the budget of (bio)pharma companies, but it is also what allows them to differentiate. The challenge in obtaining novel products with profitable processes has led to a decrease of drugs available in the market. In the last 70 years we have seen a reduction of about 80 times of drugs approved per billion-dollar R&D investment [3].

High-throughput screening (HTS) methods make use of developments in several scientific fields and combine automation and miniaturization to test and screen products, processes, and conditions inherent to these processes. The use of HTS caught the eye of (Bio)Pharma companies, that soon shifted to this technology to test and generate data in the order of tens and hundreds of thousands of data points per day [4]. Fast experimentation, low sample consumption and reliable data makes HTS attractive for both companies and academia peers.

The true impact of HTS started more than 20 years ago, with a shift being made in early-stage screening. The evolution of this field equipped researchers with powerful tools that allowed for fast screening and generation of genetic libraries of mutants[5] and products [6]. The optimization of microorganisms and the increasing product titers achieved drifted the attention of HTS from upstream to downstream processing (USP/DSP), that needs to be able to deliver the final product as quickly and robustly as possible (**Table 3.1**) [7].

Process development techniques evolved greatly as they need to adapt to an ever-changing market and capitalize on the availability of cutting-edge technologies. The evolution of the available tools and the introduction of initiatives like Quality by Design and Process Analytical Tools pushed for the need to have better understanding of the

process and clear definition of the design space [8]. The increasing computational power enabled researchers to use more complex modelling tools, freeing them from the heuristic modelling chains, that although useful rarely allow for extrapolation and don't promote process understanding. As the industry matured, high-throughput process development (HTPD) combined HTS, a greater mechanistic understanding of processes, and a higher computational capability for smarter process development, which helped to guide experiments in order to achieve better performing processes faster at a lower cost [9].

Initial evidence of HTS in the biotechnology field started with the appearance of 96-well microtiter plates. These were used to screen chemical compounds and widespread use by the pharmaceutical industry was adopted. Later, with increasing pipetting precision, it was introduced the 384 and 1536-well microtiter plates [4]. There is also another option for HTS. Microfluidics started more than 20 years ago, getting traction over the years. These systems are known for the handling of very small amounts of liquids and allow for sample saving, taking this one step further. Their small size often allows for the analysis to occur faster than conventional tests, saving time and allowing for multiple data points to be generated with low lab space utilization [10].

Turning processes that are composed of discrete unit operations (UO) into one end-to-end continuous process is a sign of a maturing industry. Operating in steady-state, better equipment utilization, better control and quality, better productivities are some of the advantages of having a continuous process [11]. Biopharmaceutical industries are pushing for this shift which is welcomed by regulatory agencies [12]. All these advantages culminate in lower cost of goods making this shift ever more necessary and attractive [13].

The shift of processes from discrete operation to continuous is also achieved through HTPD. This is a key tool for today's process development and by making use of HTPD, researchers aim to achieve continuous processes faster, resulting in Integrated Continuous Biomanufacturing (ICB). To do this, classical HTS methods are used. Although HTS is the cheapest and fastest alternative for process development, the needed equipment is expensive. A paradigm shift is needed to achieve lower costs of HTPD tools, together with more adequate analytical tools [14]. Furthermore, some unit operations still lack proper scale-down models and, for the ones already in place, the translation of the results obtained to manufacturing scale needs to be investigated [15].

This article aims to shed a light on the evolution of high-throughput experimentation (HTE) and the evolution in the role this approach has gained over the years, providing an overview on the automation and miniaturization and how it has influenced the biopharmaceutical and food industries for the development of continuous processes.

Table 3.1 - Examples of HTS applicability in different stages of process development. The three process stages included are Pre-Process Screening, Upstream Processing and Downstream Processing [9, 16]. HTS can also be used to study formulation which was discussed in other publications [17, 18].

Preliminary Screening	Upstream Processing	Downstream Processing
Screening for molecular properties that can help determine processing steps	Build mutant library - titer and host organisms are important	Development of complete downstream process [9]
Determination of Critical Quality Attributes (CQAs)	Screen for best producing strains (usually highest titer)	Definition of UO based on separation efficiency and yield
	Optimize bioreactor design	Optimize purification train for minimal number of UO at highest possible yield - expensive steps are usually the ones getting tackled first (*e.g.* chromatography)
	Define best operating conditions for fermentation and to test in scale-up setup [19]	Test new UO for already established processes (*e.g.,* ATPS for mAb purification) [20]
	Toxicity testing for producing strains	Define window of operation for different UO [21]
	Test processing mode (Batch vs Continuous)	
	Establish KPI for the processes	

3.2. Microplates and microfluidics: automation and miniaturization

Bioindustries soon captured the advantages of miniaturization of assays for process development, which allows for faster processing using less samples. With a smaller footprint needed for the performance of assays, the parallelization of such assays arose innately. This translates to a reduction in cost and time. The technological advances in mechanical engineering in the second half of the 20th century allowed for an ever-increasing level of automation that benefits process development, analytics, quality control and quality assurance. Automation enabled the use of automatic equipment for the processing of samples, and the first evidence of automation in the drug discovery industry can be traced back to Japan [22, 23], where the first automated tasks were the transport of samples throughout the laboratory. Shortly after, the technology started making its way to the mainstream and equipment that combines automation and miniaturization arose, allowing for the first HTS, through microtiter plates [4].

Microfluidics is the area that studies systems that allow for fluid handling in small dimension channels, in the micrometer range, allowing for handling liquids even in the nanoliter range [10]. With the development of technology, microfluidics also has its own

sub-disciplines like, among others, droplet microfluidics [24]. Liquid-handling stations (LHS) also allow for the miniaturization of experiments and empowered researchers to have automated systems that could perform trials in the microliter range with great precision. The importance of automation and miniaturization, for both LHS and microfluidics, will be covered, along with a discussion regarding the different uses these two methodologies have. The rise of 3D-printing will also be covered, as a promising tool for HTPD.

3.2.1. The power and role of automation and miniaturization

Liquid handling is paramount for research in life sciences and is a crucial part of experimentation in this field. While assays moved to a smaller scale, accurate liquid handling became ever more important for the assays to remain reliable. This brought together automation and miniaturization in the form of LHS. While miniaturization has the power of reducing sample volume consumption to very low volumes, automation has the power of removing humans from the experimental realm, helping to reduce human-prone errors, and allowing for more time to be dedicated to designing the experiments rather than performing them.

Liquid-handling robots have proven to be very useful tools for process development and screening, fulfilling the automation and high-throughput needs in such a competitive market as the life sciences. There are several different assays that can be done with robotic workstations, and these can be tailored to a lab's needs. Accuracy and precision naturally are key performance parameters for LHS, independent of the working volumes. For a more thorough analysis of the advances in the liquid dispensing field, the reader is directed to another review [25]. Here, the authors cover the different components of robotic workstations (*e.g.,* dispensing parts, robots, and sensors) and compare different commercially available systems and their performance regarding the minimum dispensing volume and speed.

The level of miniaturization employed in microfluidics is many folds higher than for LHS [10]. The advantages of this degree of miniaturization are not exclusive to reagent saving as at such small scales the physico-chemical conditions will be different. Besides allowing for the handling of samples in the nanoliter range, microfluidics also allows for a deep understanding of the physical properties of a system. The characteristic dimensions of such systems allow for a precise fluid flow characterization as a result of the well-ordered laminar flow through dimensionless numbers, such as the Reynolds number (Re) and Péclet number (Pe).

Reynolds number predicts if the system will be dominated by inertial or viscous forces, whereas Péclet number expresses the relation between convective and diffusive transport. In microfluidics, laminar flows are dominant with Re values remaining usually

below 1, meaning that the flow is clearly dominated by viscous forces. This makes it easier for the modelling of the fluid flow and the behavior of chemical species inside such systems, where mixing, diffusion and reactions can be modelled with great precision [26, 27]. The Péclet number can help predict the length of a channel and the time needed until a desired degree of mixing is achieved. These characteristics can even improve performance of miniaturized unit operations, a concept described as "positive downscaling" [28].

3.2.1.1. Automation in microfluidic devices

Automation in microfluidics is achieved by integrating different components in the microfluidic device, through implementation of different features in the design, using external equipment or by exploiting the microscale characteristics. Fluid flow in microfluidic devices can take many shapes and forms and several have been applied in different applications [28]. Although pressure-driven flows may seem the most intuitive for microfluidic devices, both this and electroosmotic flow are applied when performing chromatographic separations [29, 30], the latter allowing for flow control without the need of external pumps or valves.

Microvalves and micropumps greatly aid in the operation and automation of microfluidic devices, which come at residual incremental material cost but at a high complexity cost both in design and fabrication [31]. Microfluidic integrated valves and pumps enabled scientists to achieve the concept of Lab-on-a-chip, using a methodology that allows for the discretization of fluid flow in the microchannels, as well as flow control and mixing, which can be important for the micro-integration of several operations in the same microchip [32]. However, it is important to highlight that most of these types of valves and pumps cannot be transversely employed in all microdevices, since for some there is a need to have a flexible material, *e.g.,* an elastomer like polydimethylsiloxane (PDMS), and not all devices use this material. The type of materials in which microfluidic devices are built can vary greatly depending on the desired purpose and this has been deeply covered in other publications [33, 34].

Several methodologies with a high degree of automation have been employed in microfluidics experimentation that showed an increase in throughput. Droplet microfluidics makes use of immiscible fluids with different properties and through the manipulation of fluid flow rate, droplets of very precise diameter can be generated [35], although several advances have been made and different methodologies can be employed for the control of droplet formation [36], being geometry one of the most important [37]. This discipline of microfluidics has shown good advancements in this field and several studies showcase its prowess in the screening and selection of

microorganisms, from selecting for antibody secretion to the selection through cell viability or to select specific oxygen uptake rates [38].

The relevance of automation and miniaturization is evident for the implementation of laboratory HTS. It has empowered researchers to deliver results very fast and reliably with the use of automated systems, while keeping the costs low by miniaturizing assays. Either by using microfluidics or robotic systems, the present and future of HTPD involves automation and miniaturization as there is a push for more automated systems dealing with the least amount of volume possible.

3.2.2. Brute Force (liquid-handling robot) *VS* design freedom (Microfluidics)

Robotic workstations have established their role in the biotechnology field through the ability of performing several experiments with minimal human intervention. Besides this, the evolution of such devices has been mainly related to achieving a greater number of tests per unit of time and integrating more systems (both for liquid handling and analytics) in one single equipment. The liquid handling by such devices can be done in several manners, either by pipetting or with acoustic energy [39] and both of these technologies are suitable for the dispensing of very small volumes (as low as the nL range). The dispensing can also be done by having contact or non-contact liquid dispensing and the latter is most suitable to avoid cross-contamination. The LHS are often connected to plate readers, which report results in a very fast manner. Furthermore, LHS's software can be tailored to report the readings directly as results, with built-in data analysis. This allows for time saving whilst avoiding human-prone errors in the calculations. LHS have allowed researchers to adopt a "brute force" method when performing experiments by allowing them to carry out a large number of experiments in a short amount of time. More advanced process development tools are increasingly available and smart process development is taking over the field [40]. The main advantages of LHS compared to its miniaturized counterpart are the level of automation that can be achieved in such systems and the generalized acceptance from researchers of the field.

Microfluidics is often perceived and portrayed as a cheap screening technique. While this is true for consumables, the fabrication of mastermolds for subsequent soft lithography is not cheap. Silicon wafers bought in bulk can cost up to 30 $ per 4-inch wafer, which translates to 3700 $/m^2. Besides the cost of wafers, clean room equipment for the fabrication of the microchips and maintenance of a clean environment inside the fabrication facilities are also expensive. Therefore, research groups usually share facilities and companies outsource the production of devices. The greatest advantage is the level of detail achieved, with structures showing very good accordance to the desired design in very small scale (μm and nm).

Microfluidics has evolved in a different way than the LHS. It also aims to reduce assay time and sample consumption, and although automation is a desired trait it is not mandatory, and most of the times this methodology takes advantage of its very small characteristic dimensions. With technological advancements, more complete systems were developed, and the design freedom achieved with microfluidics is unprecedented. Unit operations and processes have been scaled down for the separation of products or biocatalysis [41-43]. Complex micro bioreactors have also been developed where perfusion bioreactors were developed making use of microbubbles for both aeration and convection of the system [44].

Where microfluidics lacks in ease of automation it makes up for with its "Design Freedom". Effective scale-down models can be achieved with high precision at a sample consumption several orders of magnitude smaller. Furthermore, the entrance cost is also several orders of magnitude lower when compared to LHS. The rise of 3D-printing has enabled researchers to reduce the time from design-to-chip and fabrication costs. Instead of cleanroom facilities, it is now possible to produce microchips using 3D-printers [45], a natural low-cost solution for microfluidics.

3.2.3. 3D-printing: An enabling technology

3D-printing dates back to the 80's, but major breakthroughs of this technology that allowed it to reach mainstream status happened in recent years. Commercially available 3D-printers have seen a major evolution throughout the past ten years and printers' prices plummeted.

3D-printing techniques breakdown the 3D design into different layers, which are then built additively on top of one another (additive manufacturing), despite the type of technique used. 3D-printers have the advantage of easing the fabrication of the devices when three-dimensional structures are desired for microfluidics, as no extra steps nor skill-dependent assemblies are needed. Within the realm of 3D-printing, there are different techniques that are employed: Stereolithography (SL), Laser Sintering (LS), Multi Jet Modelling (MJM) and Fused Deposition Modelling (FDM) more commonly known as thermoplastic extrusion [46]. SL has been evolving as a natural technique for fast prototyping at a low cost and high resolution. Traditional SL resolution (minimum feature size) is strongly dependent on the laser spot size and the spectrum of absorption of the used resins [47]. Initially, SL was the only technique that was able to consistently fabricate closed channel devices with no extra assembly steps required [46], despite the fact that SL needs a post processing step for removal of non-polymerized resin. The fast development of 3D-printers and the materials used have allowed for a broader range of techniques and materials to be employed in microfluidics, and FDM has also shown to be a valid option for microfluidics [48]. Moreover, one of the main advantages of

cleanroom fabricated microfluidic devices compared to 3D-printed devices was the ability to include valves, to automate the apparatus. The automation of 3D-printed microfluidic devices has been demonstrated by Lee *et al.* [49]. The authors printed a device with a "Quake-style" valve, a technique often employed in clean room fabricated microchips, with a biocompatible resin using SL in a 3D-printer. The proof-of-concept of such valves raised the standard for automation of 3D-printed microfluidic devices for the future to come, as coupling such control mechanisms to three-dimensional designs can yield promising devices.

The fast evolution of 3D-printers enabled the technology to fill in the gaps for it to be recognized as a viable alternative to clean room microfluidics. The evolution of mechanics and materials coupled with a considerably lower price and easiness of handling makes 3D-printing a fierce alternative to clean room fabricated devices, as can be seen in **Figure 3.1**.

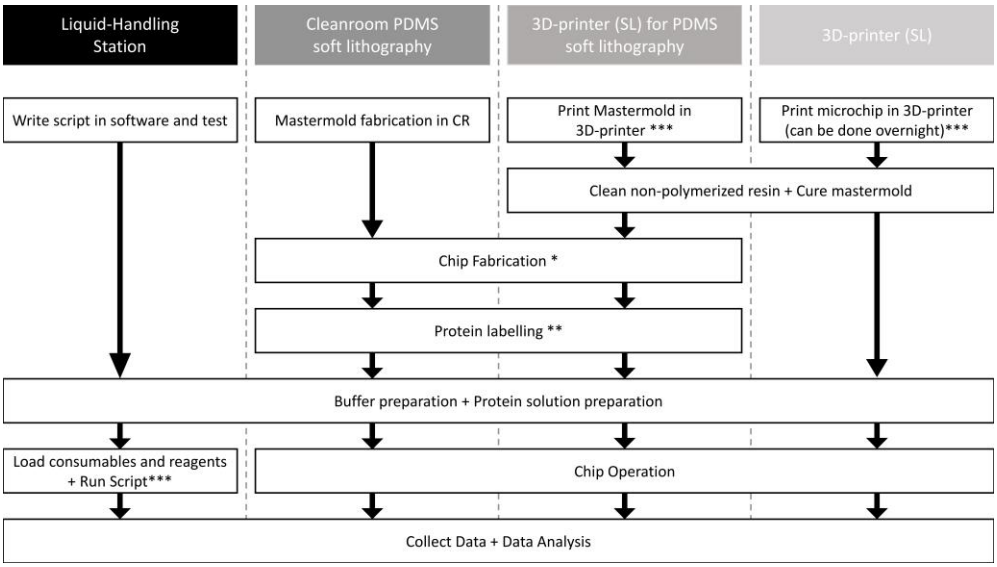

Figure 3.1 - Typical workflows when operating different high-throughput techniques. The operation using the 3D-printer for the production of a mastermold for further PDMS soft lithography has the biggest number of steps in the workflow, however this does not necessarily mean that it is the lengthiest process, as a mastermold fabrication in the clean room is very time consuming. * - Indicates that there are several steps to consider when doing microchip fabrication by PDMS soft lithography: i) Prepare PDMS; ii) Cure PDMS in mastermold and glass slides; iii) Aligning (optional: if one or more layers are used in the microchip) and bonding of the layers; iv) Chip sealing and bonding of the structure to the glass slide (which usually happens overnight) [51]. ** - Protein labelling may be necessary as fluorescence is still the mainstream detection method for PDMS microfluidics. *** – Fully automated steps (no human labor is needed – script and printing also run on their own).

HTS revolutionized the biotechnology sector. It allows for time and sample saving while maintaining or achieving greater quality data than was possible before. LHS seemed to have moved towards increasing assay performance and microfluidics towards eccentric

designs that are able to achieve good results and often mimic lab scale performance. This led to greater acceptance of liquid-handling stations from industry and academia, as microfluidics seems unable to captivate industrial attention. Even though microfluidics has the size advantage, and its portability also is a differentiation factor, Lab-on-a-chip is still of great interest for point-of-care diagnosis [50].

3.3. ICB and HTPD

The way that ICB and HTPD are interconnected depends on how the different technologies/tools can come together. Some of these will be further discussed: the need for compatible of analytical tools, the lack of scale-down models for different UO, the importance of data management and modelling and the affordability of HTPD tools.

3.3.1. Compatible Analytical Tools

With the increased miniaturization of assays, the analytical tools used needed to adapt. Further development of analytical tools was needed and lower volume requirements for analysis helped to propel the shift. The incorporation of multi-well plate readers into LHS and adaptation of the microfluidic device analytics, both on-chip and off-chip, for accurate assays that have results in real time highlight the importance of having analytical tools that are adequate to the screening scale [52]. Furthermore, using the already established tools for more complex or precise analysis, such as precise determination of resin volume using optical methods in a 384 well-plate [53], or coupling the analytical tools with models to aid in the analysis of complex systems, where recent work highlights the use of such methodology for the study of complex systems as multicomponent isotherms in HTS platforms [54-56].

3.3.2. Scale-down models for different Unit Operations

Another important aspect to consider is the feasibility of scale-down models in translating the results obtained at smaller scales into manufacturing scale processing [15]. Although some UO have favored from a lot of attention from research peers, such as chromatography, some still lack feasible or practical scale-down models. Only recently proper scale-down models for fermentation processes have arisen, both in LHS systems (with the Ambr® systems) and microfluidics [44, 57]. Moreover, membrane processes are present in every (bio)pharmaceutical process and are crucial to ICB mode of operation. However only recently studies on the adaptation of this unit operations have been published [58, 59], denoting a big room for improvement and can help to justify why these processes often operate in sub-optimal conditions in manufacturing. These scale-down models need to be accurate representations of their production scale counterparts in order to add value to the process development stage. This is why models

that can accurately translate miniaturized scale data into process scale are so valuable [60].

3.3.3. Data management and modelling

HTPD makes use of HTS methods and models for the development of optimal processes. It will in turn lead to the generation of large amounts of data both from experiments and simulation. Now that most experimentation is automated, data analysis needs to be automated too [61]. This is of paramount importance for the successful implementation of HTPD.

3.3.4. Affordable HTPD

HTPD for continuous manufacturing follows similar trends to HTPD for batch processes: fast and cheap process developments are achieved due to lower consumption of materials. However, the platforms used for HTS usually come at a high price tag, hence why some companies keep away from such methodology. The advancements in both automation and miniaturization are reducing this gap and helping to democratize such equipment, by lowering the price and reducing the equipment complexity.

3.4. Analytical methods in HT methodologies

Analytical methods are pivotal in every experimental field. For HT methodologies to be efficient the detection must allow for "high-throughputness". Optical methods are the most widely used in HTS as they're easily adapted to such equipment: for LHS is absorbance analysis and for microfluidics there is a wide range of methods available, although microscopic-based assays, such as fluorescence, remain amongst the most popular (**Table 3.2**).

Several assays in the biopharmaceutical industry rely on optical analytical methods (absorbance measurement of samples). The detection of impurities in a bioprocess is of the utmost importance and usually leads to tedious and time expensive laboratory work and LHS allow for more automated analytics. On the other hand, microfluidic devices allow for the use of different analytical methods due to their very small size, as they can be fitted to numerous spectroscopy equipment (contrary to microplates). This has shown a wide variety of applications and analytics implemented in microfluidic assays [67, 74].

LHS can be tailored to a lab's needs. This is the great power of automation and the advantage of increased miniaturization of assays. As equipment size decreases the integration of analytical equipment in one single workstation becomes easier. Workstations working in 360 degrees offer the possibility to integrate a greater number

Table 3.2 – Comparison of some of the different analytical methods available in liquid-handling stations and microfluidic devices.

Analytical Method	LHS		Microfluidics	
	Ref	Comments	Ref	Comments
Absorbance	There are plenty of commercially available microplate readers that are easily integrated in the liquid-handling stations (Tecan, for example)	Any type of absorbance assays can be performed (ELISA, UV-Vis measurement, etc.)	[27, 62]	
Fluorescence		-	[63]	-
Luminescence		-	[64]	-
Mass Spectrometry (MS)	[65]	This paper has a workflow where the MALDI-TOF MS is integrated in the HTS workflow, with several liquid handlers and the MALDI-TOF MS analyzer in the end	[66, 67]	-
Raman	[68]	Sample volumes of 160 – 200 µL are analysed in the Raman module coupled to the Ambr® system	[69, 70]	-
Near Infra-red (NIR)	-	-	[71]	The authors correlated the absorbance difference spectra with the solutes concentration and were able to obtain clear images of the acid-base reaction and the salt formation from the neutralization reaction

Table 3.2 (cont.) – Comparison of some of the different analytical methods available in liquid-handling stations and microfluidic devices.

Analytical Method	LHS		Microfluidics	
	Ref	Comments	Ref	Comments
Dynamic Light Scattering (DLS)	[72]	There are commercially available DLS plate readers: DynaPro II Plate Reader DLS instrument from Wyatt and Zetasizer APS from Malvern	[73]	-
Surface Plasmon Resonance (SPR)	-	-	BIAcore X100 (BIAcore, Cytiva)	Commercially available device

of equipment in the same space [75]. However, lab space is often limited, and linear workflows are often preferred (like the solutions offered by Tecan®, Switzerland). These systems are frequently commercialized as a package but are limited to a smaller number of plates that can be handled and to limited analytics to be performed (optical analytical methods with plate readers, such as absorbance, fluorescence and luminescence).

Raman spectroscopy has been used for upstream process development for some years, and more recently this analytical tool is being considered for use in DSP. It offers a broad range of applications from screening raw materials and culture media, to the monitorization of the process and assess chemical or structural changes in proteins [76]. It has not been until recently that the adoption of Raman spectroscopy to HTS platforms took place [68] and further implementation to downstream process development could bring important developments to the ICB landscape.

In **Table 3.2** we can see an overview of commonly used detection methods in HTS with LHS and microfluidics. The discussed analytical methods do not cover all the available methodologies for both LHS and microfluidics. However, it is possible to conclude that more analytical methods are more easily adapted to microfluidics. It is important to understand the limitations of each device hence why such methodologies are still not widespread, and some challenges need to be targeted to allow for a generalized use of the technology [66].

3.5. Upstream and Downstream process development with high throughput experimentation

3.5.1. High-Throughput Process Development – the case of chromatography

HTPD allows for a fast-forward in process development, allowing for a clear reduction in the time needed for optimization operations to be carried and optimum process design. As bioprocesses evolve to the final form of optimized continuous USP and DSP, there comes the task of integrating the bioprocess in one single continuous process.

The transition from up- to downstream in a bioprocess is always challenging. Several factors influence downstream processing, especially if the process relies on chromatographic steps in the early stages of the process, as small changes in the environment or the handling of the process can greatly affect the product's ability to undergo purification (for instance, the ability of a product to adsorb to a resin), as optimal operating conditions are not always met in a manufacturing environment. HTS is useful to find optimal operating conditions but also a great tool to determine operating windows. This is of great use, in an attempt to minimize the impact that batch-to-batch variations and human error have in downstream processing [77].

Chromatography is still the workhorse of several biopharmaceutical products, which is reflected both in its high product purification factors as well as percentage of overall process costs, which can be greater than 50% of the total batch costs [78]. In chromatographic separations there are several interactions to consider, and consequently several aspects to optimize: finding the optimal resin (defining the protein-ligand interactions, such as binding capacities) and buffers to use (loading, washing and elution buffers can have different pH and salt concentration), estimating adequate linear velocity for the desired separation. Consequently, there is the need to comprehend what is happening in the process. Modelling is the state of the art of chromatography process development [79], especially hybrid approaches that make use of mechanistic modelling and HTS [80]. Albeit modelling is getting more acceptance and implementation in process development, it still goes hand in hand with experimentation, whether for parameter estimation, "model training" or validation of modelling results. Hanke and Ottens have reduced the chromatographic process development to three main realms: trial and error, process development based on molecular properties and process development based on molecular interactions [81].

3.5.2. Examples of LHS and microfluidics for HT Experimentation in biotechnology

3.5.2.1. Liquid-handling stations

Cell culture in microtiter plates offers the advantage of automated pipetting, useful for screening several media components, but can be challenging to achieve proper oxygen transfer to the growth media. Several parameters can influence cell cultivation, and this also holds true for microtiter cell cultivation. Work from Neha *et al.* showed that well format, shaking frequency, among others were important parameters in achieving cultures of *Pichia pastoris* with a higher cell density in 96 well-plates [82]. The advantage of having cell cultures in LHS is that it can be introduced in a workflow for the full automation of expression, extraction, purification and evaluation of the protein of interest, like Shah *et al.* demonstrated for a HIV-specific mAb produced by *P. pastoris* [83]. Although the aforementioned parameters are important and impactful, LHS remain the state-of-the-art for upstream HTPD in the biopharmaceutical industry [84, 85].

Bensch *et al.* extensively cover in a review the developments and challenges faced when using HTS of chromatographic phases for process development [86]. The authors show the "thought process" behind the development of this purification step, covering subjects such as resin and column screening. This is very useful in early-stage process development. The next step is to verify if behavior remains the same in column experimentation and optimization and validation of the proposed experimental protocol is needed. Konstantinidis *et al.* developed a new methodology for the operation of

miniature columns in a liquid handling station [87]. These have the advantage of providing more insight on the separation process by mimicking large-scale operation. Miniaturized columns don't allow for linear gradients for elution, as liquids are loaded to the columns discretely. This work shows an automated way of experimenting in 8 miniature columns in parallel and the output file already has automated calculation of the blanks and normalized spectroscopy measurements. The power of automation is clear in this study, as it was shown that with the same setup it was possible to study the purification of ovalbumin from a mixture with conalbumin and BSA and capture of mAbs. Recently, implementation of a HTS setup coupled to mechanistic modelling showed how data retrieved from MiniColumns can be translated to lab scale chromatography [60, 88, 89]0 By analyzing the Péclet number at different scales the authors concluded that an increased axial dispersion is observed at smaller scales, compared to larger scales, leading to larger elution pool volumes [60]. The results were then used to correct the model, allowing for accurate prediction of elution pool volumes at larger scales using MiniColumns for experimentation.

Aqueous Two-Phase Systems (ATPS) recently arose as an important process and can represent an alternative to chromatographic processes for the purification of mAbs [90]. ATPS process development involves the preparation of systems with different phase compositions of polymer-polymer or polymer-salt solutions for the discovery of binodal curves and tie line length, which play an important role in the purification process. Azevedo *et al.* unveiled the potential ATPS and achieved recovery yields for IgG of 99% and purity of 76%. These studies were performed in 15 mL graduated tubes, which represent a great expense in consumables and reagents when considering the number of optimizable parameters, such as phase and salt compositions, and involves tedious and possibly erroneous work [91]. Implementing the same methodology in a LHS would allow to reduce the time needed for process development [92]. Oelmeier *et al.* also evaluated ATPS for the separation of mAbs from Host Cell Proteins [20]. This was performed in a LHS for a total system volume of 650 µL. The methodology described by the authors highlights the powerful features of LHS, such as liquid-level detection and liquid class definition, for aspiration of liquids with varying viscosities. The authors were able to screen a total of 552 systems and estimated that on microtiter plate could screen 33 systems in 2.5-3h. Studies with ATPS of 300 µL have also been reported [93].

Recently, Antibody Drug Conjugates (ADCs) have captured the attention of industry for its potential in cancer treatment. Andris *et al.* developed a HT process for the development of new ADC molecules and showcased how LHS can aid, through parallelization and automation, achieve faster process development [94]. A HT-compatible monitoring tool was also developed for the monitoring of these conjugation reactions [95].

3.5.2.2. Microfluidic devices

Downscaling operations like fermentations offer great advantages and can provide valuable insight. PDMS is the go-to material for microfluidic devices and its gas permeability and elasticity features can be used to the researchers' advantage for the production of micro bioreactors. Micro reactors' ability to be assembled in a microscope setup allows for real time *in situ* visualization of the experiments. The very small scale means that the analytical methods need to be accurate and have a low limit of detection (LOD) hence why the use of very sensitive techniques such as fluorescence are popular. A picolitre volume bioreactor has been described for single cell cultivation of *Escherichia coli* and *Corynebacterium glutamicum* [96]. This study demonstrated that the behavior of the culture under specific environmental conditions could be tested in a smaller amount of time. It was used to screen the influence of different media in cell growth, and an increase of 1.5-fold growth rate was registered for *C. glutamicum*. Different studies have also showed the use of microfluidics for the cultivation of *Saccharomyces cerevisiae* with integrated sensors in micro bioreactors [97] and the cultivation and transfection of CHO cells [57].

Microfluidic particle liquid chromatography has been recently reviewed [98]. With the design freedom available and advanced manufacturing techniques, there are many possibilities to study chromatography. Several applications, modes of operation and analytical techniques are discussed in the publication. Pinto *et al.* demonstrated an efficient screening of different operating conditions using multimodal chromatographic resin for the purification of a mAb [99]. The authors achieved recovery yields of 95% at the microscale, compared to 98% of lab scale, with 100 nL of resin per reactor. Furthermore, an automated device that makes use of Quake valves has demonstrated the usefulness of microfluidics, allowing for the determination of one full chromatographic isotherm (with 9 different protein concentrations tested in parallel) [100]. Although this device only allows for small-sized beads, it portraits the powerful combination of miniaturization and automation. ATPS have also been explored in microfluidic devices for the determination of binodal curves [101] and purification of mAbs [102]. By using the same systems studied at macroscale, the authors take advantage of the miniaturization feature of an increased surface area to phase volume ratio, which allows for comparable extraction at a fraction of the time.

Microfluidics still lacks generalized acceptance and widespread implementation of the many versatile devices that have been produced. Small steps have been taken in this direction and there are already commercialized microfluidic devices for different applications. Examples of these devices are the 2100 BioAnalyzer from Agilent Technologies that provides an automated electrophoresis with very high resolution, Biacore™ X100 from Cytiva that provides a microchip for the analysis of samples using

SPR or the LabChip GXII from Perkin Elmer® used for automated SDS-PAGE analysis.

The described examples for LHS and microfluidic devices are a few representations of what is being done in process development with both technologies. Microfluidic applications are not exclusive to bioprocesses, as there are many examples of diagnosis applications, however this review aims to shed light on process development in the biotechnology industry. Microfluidics is still aiming for general acceptance and validation of the technology for a broader audience, and 3D-printed microfluidics can help to achieve this.

3.6. Concluding Remarks

LHS and microfluidic devices have drastically reduced process development costs while allowing for major time savings. Automation and miniaturization have increased the throughput of data and reduced time to market. Although LHS have a higher price tag, the widespread use of the technology and regulatory acceptance make it a demanded technology. Microfluidics offers a bigger versatility in analytical methods that can be used, and its major banner is the technology's portability. 3D-printing technologies will enable labs to have a very cheap prototyping and manufacturing equipment for microfluidic devices [104].

The greater need for deep understanding of processes and a more wide-spread use of modelling doesn't leave room for "blind" testing in the hope of a technological breakthrough. When such screening technology is so easily available, it is tempting to perform a multitude of experiments leading to needless over-screening of the systems, while providing still little understanding on the underlying process mechanisms. As regulatory agencies are pushing for a greater process understanding, rational and more standardized approaches are needed.

This is mainly achieved by hybrid process-development which is the combination of mechanistic modelling with HTE [40]. These two methods can be coupled and will form a symbiotic relationship in process development, where the strengths of one can easily make up for the flaws of the other [81]. Opting for a mechanistic model for process-development allows for great process understanding at a low experimental effort. This process understanding is pivotal in current manufacturing strategies and it has been shown that the predictive nature of these mathematical models (white box models) allows to significantly decease experimental effort compared to having no available models, while improving process robustness [56, 80, 105]. Although mechanistic models still need calibration/parameterization partially via a selected set of experiments, this can be achieved quickly and at minimum experimental effort in the current landscape of

HTS [106]. The available methods for HTE have showed that with minimum effort a wide variety of experiments can be carried out in the same equipment or set of equipment which will alleviate the financial and learning endeavor of researchers. The need for rapid screening and fast process development is more evident when occurrences like the current pandemic caused by the virus SARS-CoV-2 arise. The development of the vaccines often made use of already established processes that needed tailoring to the specificity of the current virus.

The last 10 years in manufacturing saw an evolution in bioreactors where smaller reactors are preferred, outputting lower volumes and higher titers [107]. However, the industry has not stagnated and is moving towards continuous manufacturing, where higher productivities and facility flexibility are needed, and ICB caters to this [15]. The productivity driver is still in place and the key to deal with this is to find the necessary process innovations, as the ones offered by continuous processing.

It is only a matter of time before it is possible to achieve a full integration of biopharmaceutical processes into one single end-to-end process. HTS allowed to push for very optimized upstream and downstream processes, which now need to be integrated into one single process. This is desired not only by the manufacturing companies, as it allows for cost savings, but also by regulatory agencies. Automation and miniaturization enable faster process development and are pivotal for the continuous integration and improvement of these processes.

Moreover, while LHS seem to have reached a plateau in terms of new applications, microfluidics is constantly mutating and evolving and is more and more perceived as a valuable asset for HTPD and the emergence of 3D-printing microfluidics is a perfect example and is starting to get traction. The authors expect that LHS will continue to see the integration of more systems and will see a diversification in the investigated processes within a single piece of equipment. Microfluidics has reached mainstream use in a few instances. It is expected that the near future will show the emergence of novel applications of single use disposable systems through 3D-printing technologies making this technology more readily available at low cost to the biopharmaceutical process development and analytical community. A further increase in automation together with simpler production and operation will probably push microfluidics one step further into the research labs worldwide (**Figure 3.2**). The opportunity now lies in being capable to provide HTS solutions at affordable prices for the different processes and develop analytics that can keep up with the increased reduction of volume for assays, while implementing models that are capable of correlating miniaturized scale experimentation with the manufacturing scale. These developments, which are expected in the near future, will broaden applications of LHS and will pave the way in integrating microfluidics as an additional tool in biopharmaceutical process-development.

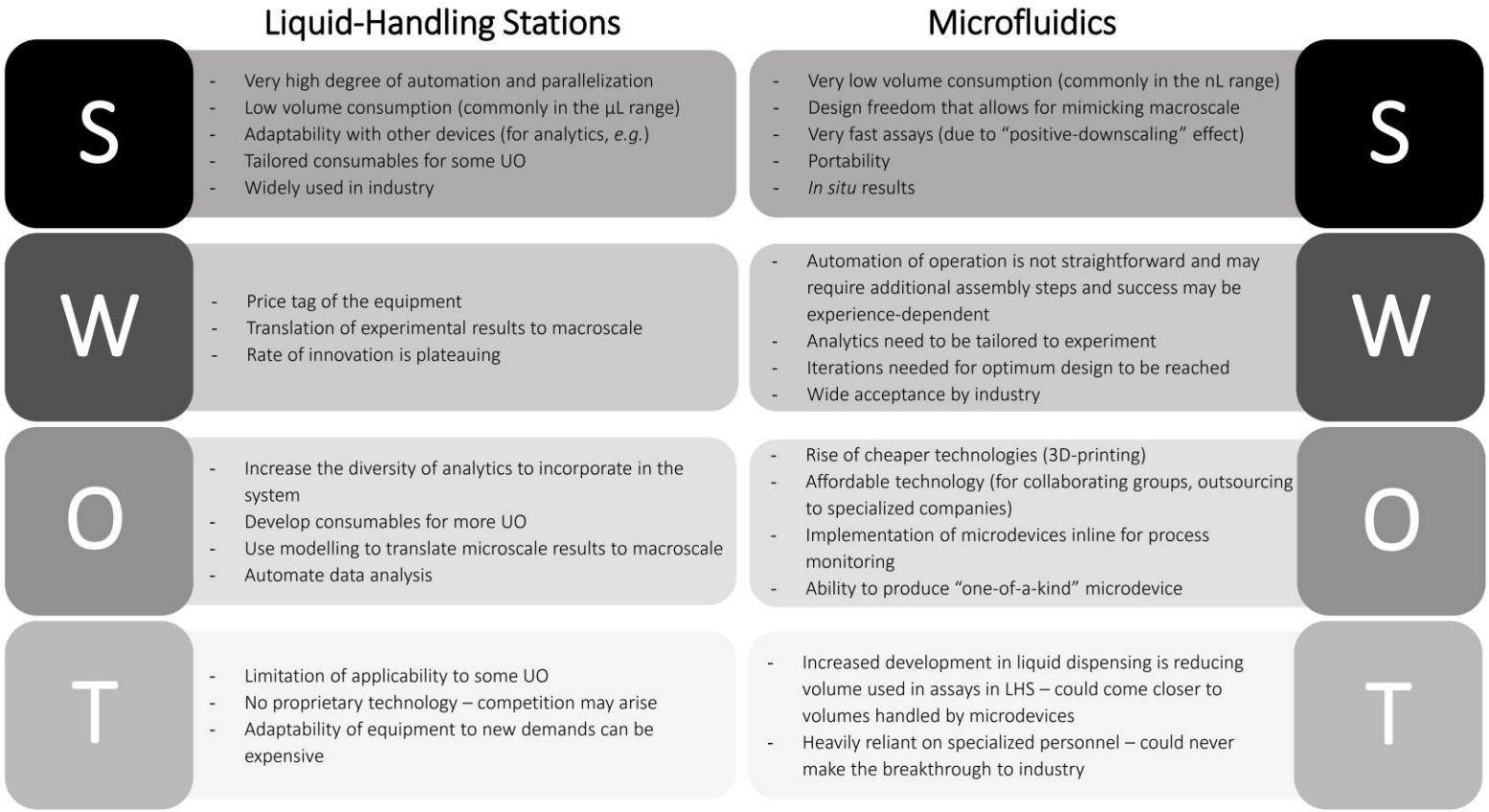

Figure 3.2 – SWOT (Strengths, Weaknesses, Opportunities, Threats) analysis of Liquid-Handling Stations and Microfluidics [25, 50, 103].

3.7. Acknowledgements

This work has received funding from the European Union's Horizon 2020 research and innovation program under the Marie Skłodowska-Curie grant agreement No 812909 CODOBIO, within the Marie Skłodowska-Curie International Training Networks framework.

3.8. References

[1] G. Jagschies, E. Lindskog, K. Lacki, P.M. Galliher, Biopharmaceutical Processing: Development, Design, and Implementation of Manufacturing Processes, Elsevier2018. https://doi.org/10.1016/C2014-0-01092-1.

[2] A.L. Grilo, A. Mantalaris, The Increasingly Human and Profitable Monoclonal Antibody Market, Trends in Biotechnology 37(1) (2019) 9-16. https://doi.org/10.1016/j.tibtech.2018.05.014.

[3] J.W. Scannell, A. Blanckley, H. Boldon, B. Warrington, Diagnosing the decline in pharmaceutical R&D efficiency, Nature Reviews Drug Discovery 11(3) (2012) 191. https://doi.org/10.1038/nrd3681.

[4] L.M. Mayr, D. Bojanic, Novel trends in high-throughput screening, Curr Opin Pharmacol 9(5) (2009) 580-8. https://doi.org/10.1016/j.coph.2009.08.004.

[5] D. Wahler, J.-L. Reymond, High-throughput screening for biocatalysts, Current Opinion in Biotechnology 12(6) (2001) 535-544. https://doi.org/10.1016/S0958-1669(01)00260-9.

[6] R.M. de Wildt, C.R. Mundy, B.D. Gorick, I.M. Tomlinson, Antibody arrays for high-throughput screening of antibody–antigen interactions, Nature Biotechnology 18(9) (2000) 989. https://doi.org/10.1038/79494.

[7] G. Guiochon, L.A. Beaver, Separation science is the key to successful biopharmaceuticals, Journal of Chromatography A 1218(49) (2011) 8836-8858. https://doi.org/10.1016/j.chroma.2011.09.008.

[8] R. Bhambure, K. Kumar, A.S. Rathore, High-throughput process development for biopharmaceutical drug substances, Trends Biotechnol 29(3) (2011) 127-35. https://doi.org/10.1016/j.tibtech.2010.12.001.

[9] K.M. Łącki, High throughput process development in biomanufacturing, Current Opinion in Chemical Engineering 6 (2014) 25-32. https://doi.org/10.1016/j.coche.2014.08.004.

[10] G.M. Whitesides, The origins and the future of microfluidics, Nature 442(7101) (2006) 368-73. https://doi.org/10.1038/nature05058.

[11] V. Warikoo, R. Godawat, K. Brower, S. Jain, D. Cummings, E. Simons, T. Johnson, J. Walther, M. Yu, B. Wright, Integrated continuous production of recombinant therapeutic proteins, Biotechnology and Bioengineering 109(12) (2012) 3018-3029. https://doi.org/10.1002/bit.24584.

[12] A.C. Fisher, M.-H. Kamga, C. Agarabi, K. Brorson, S.L. Lee, S. Yoon, The current scientific and regulatory landscape in advancing integrated continuous biopharmaceutical manufacturing, Trends in biotechnology 37(3) (2019) 253-267. https://doi.org/10.1016/j.tibtech.2018.08.008.

[13] J. Walther, R. Godawat, C. Hwang, Y. Abe, A. Sinclair, K. Konstantinov, The business impact of an integrated continuous biomanufacturing platform for recombinant protein production, Journal of Biotechnology 213 (2015) 3-12. https://doi.org/10.1016/j.jbiotec.2015.05.010.

[14] P. Gronemeyer, H. Thiess, S. Zobel-Roos, R. Ditz, J. Strube, Integration of Upstream and Downstream in Continuous Biomanufacturing, Continuous Biomanufacturing-Innovative Technologies and Methods: Innovative Technologies and Methods (2017) 481-510. https://doi.org/10.1002/9783527699902.ch17.

[15] A. Jungbauer, Continuous downstream processing of biopharmaceuticals, Trends in biotechnology 31(8) (2013) 479-492. https://doi.org/10.1016/j.tibtech.2013.05.011.

[16] Q. Long, X. Liu, Y. Yang, L. Li, L. Harvey, B. McNeil, Z. Bai, The development and application of high throughput cultivation technology in bioprocess development, Journal of Biotechnology 192 (2014) 323-338. https://doi.org/10.1016/j.jbiotec.2014.03.028.

[17] D.S. Goldberg, R.A. Lewus, R. Esfandiary, D.C. Farkas, N. Mody, K.J. Day, P. Mallik, M.B. Tracka, S.K. Sealey, H.S. Samra, Utility of high throughput screening techniques to predict stability of monoclonal antibody formulations during early stage development, Journal of Pharmaceutical Sciences 106(8) (2017) 1971-1977. https://doi.org/10.1016/j.xphs.2017.04.039.

[18] V.I. Razinkov, M.J. Treuheit, G.W. Becker, Accelerated formulation development of monoclonal antibodies (mAbs) and mAb-based modalities: review of methods and tools, Journal of Biomolecular Screening 20(4) (2015) 468-483. https://doi.org/10.1177/1087057114565593.

[19] S.R. Velugula-Yellela, A. Williams, N. Trunfio, C.J. Hsu, B. Chavez, S. Yoon, C. Agarabi, Impact of media and antifoam selection on monoclonal antibody production and quality using a high throughput micro-bioreactor system, Biotechnology Progress 34(1) (2018) 262-270. https://doi.org/10.1002/btpr.2575.

[20] S.A. Oelmeier, F. Dismer, J. Hubbuch, Application of an aqueous two-phase systems high-throughput screening method to evaluate mAb HCP separation, Biotechnology and Bioengineering 108(1) (2011) 69-81. https://doi.org/10.1002/bit.22900.

[21] R. Bhambure, A. Rathore, Chromatography process development in the quality by design paradigm I: Establishing a high-throughput process development platform as a tool for estimating "characterization space" for an ion exchange chromatography step, Biotechnology Progress 29(2) (2013) 403-414. https://doi.org/10.1002/btpr.1705.

[22] M. Sasaki, T. Kageoka, K. Ogura, H. Kataoka, T. Ueta, S. Sugihara, Total laboratory automation in Japan: Past, present and the future, Clinica Chimica Acta 278(2) (1998) 217-227. https://doi.org/10.1016/S0009-8981(98)00148-X.

[23] C.D. Hawker, Nonanalytic laboratory automation: a quarter century of progress, Clinical Chemistry 63(6) (2017) 1074-1082. https://doi.org/10.1373/clinchem.2017.272047.

[24] N. Convery, N. Gadegaard, 30 years of microfluidics, Micro and Nano Engineering 2 (2019) 76-91. https://doi.org/10.1016/j.mne.2019.01.003.

[25] F. Kong, L. Yuan, Y.F. Zheng, W. Chen, Automatic liquid handling for life science: a critical review of the current state of the art, Journal of Laboratory Automation 17(3) (2012) 169-185. https://doi.org/10.1177/2211068211435302.

[26] K. Malecha, L.J. Golonka, J. Bałdyga, M. Jasińska, P. Sobieszuk, Serpentine microfluidic mixer made in LTCC, Sensors and Actuators B: Chemical 143(1) (2009) 400-413. https://doi.org/10.1016/j.snb.2009.08.010.

[27] M. Yu, T.C. Silva, A. van Opstal, S. Romeijn, H.A. Every, W. Jiskoot, G.-J. Witkamp, M. Ottens, The Investigation of Protein Diffusion via H-Cell Microfluidics, Biophysical journal 116(4) (2019) 595-609. https://doi.org/10.1016/j.bpj.2019.01.014.

[28] T.M. Squires, S.R. Quake, Microfluidics: Fluid physics at the nanoliter scale, Reviews of Modern Physics 77(3) (2005) 977. https://doi.org/10.1103/RevModPhys.77.977.

[29] H.V. Fuentes, A.T. Woolley, Electrically actuated, pressure-driven liquid chromatography separations in microfabricated devices, Lab on a Chip 7(11) (2007) 1524-1531. https://doi.org/10.1039/B708865E.

[30] A.S. Chan, M.K. Danquah, D. Agyei, P.G. Hartley, Y. Zhu, A simple microfluidic chip design for fundamental bioseparation, Journal of Analytical Methods in Chemistry 2014 (2014). https://doi.org/10.1155/2014/175457.

[31] T. Thorsen, S.J. Maerkl, S.R. Quake, Microfluidic large-scale integration, Science 298(5593) (2002) 580-584. https://doi.org/10.1126/science.1076996.

[32] J.W. Hong, V. Studer, G. Hang, W.F. Anderson, S.R. Quake, A nanoliter-scale nucleic acid processor with parallel architecture, Nature Biotechnology 22(4) (2004) 435-439. https://doi.org/10.1038/nbt951.

[33] K. Ren, J. Zhou, H.J.A.o.c.r. Wu, Materials for microfluidic chip fabrication, 46(11) (2013) 2396-2406. https://doi.org/10.1021/ar300314s.

[34] X. Hou, Y.S. Zhang, G.T.-d. Santiago, M.M. Alvarez, J. Ribas, S.J. Jonas, P.S. Weiss, A.M. Andrews, J. Aizenberg, A. Khademhosseini, Interplay between materials and microfluidics, Nature Reviews Materials 2(5) (2017). https://doi.org/10.1038/natrevmats.2017.16.

[35] Y.-C. Tan, V. Cristini, A.P. Lee, Monodispersed microfluidic droplet generation by shear focusing microfluidic device, Sensors and Actuators B: Chemical 114(1) (2006) 350-356. https://doi.org/10.1016/j.snb.2005.06.008.

[36] P. Zhu, L. Wang, Passive and active droplet generation with microfluidics: a review, Lab on a Chip 17(1) (2017) 34-75. https://doi.org/10.1039/C6LC01018K.

[37] R. Dangla, S.C. Kayi, C.N. Baroud, Droplet microfluidics driven by gradients of confinement, Proceedings of the National Academy of Sciences 110(3) (2013) 853-858. https://doi.org/10.1073/pnas.1209186110.

[38] S.M. Bjork, H.N. Joensson, Microfluidics for cell factory and bioprocess development, Current Opinion in Biotechnology 55 (2019) 95-102. https://doi.org/10.1016/j.copbio.2018.08.011.

[39] B. Hadimioglu, R. Stearns, R. Ellson, Moving liquids with sound: the physics of acoustic droplet ejection for robust laboratory automation in life sciences, Journal of laboratory automation 21(1) (2016) 4-18. https://doi.org/10.1177/2211068215615096.

[40] B.K. Nfor, P.D. Verhaert, L.A. van der Wielen, J. Hubbuch, M. Ottens, Rational and systematic protein purification process development: the next generation, Trends in biotechnology 27(12) (2009) 673-679. https://doi.org/10.1016/j.tibtech.2009.09.002.

[41] M.P. Marques, N. Szita, Bioprocess microfluidics: applying microfluidic devices for bioprocessing, Current Opinion in Chemical Engineering 18 (2017) 61-68. https://doi.org/10.1016/j.coche.2017.09.004.

[42] S. Hardt, T. Hahn, Microfluidics with aqueous two-phase systems, Lab on a Chip 12(3) (2012) 434-442. https://doi.org/10.1039/C1LC20569B.

[43] J.P. Kutter, Liquid phase chromatography on microchips, Journal of Chromatography A 1221 (2012) 72-82. https://doi.org/10.1016/j.chroma.2011.10.044.

[44] R. Krull, G. Peterat, Analysis of reaction kinetics during chemostat cultivation of Saccharomyces cerevisiae using a multiphase microreactor, Biochemical Engineering Journal 105 (2016) 220-229. https://doi.org/10.1016/j.bej.2015.08.013.

[45] K. Kadimisetty, J. Song, A.M. Doto, Y. Hwang, J. Peng, M.G. Mauk, F.D. Bushman, R. Gross, J.N. Jarvis, C. Liu, Fully 3D printed integrated reactor array for point-of-care molecular diagnostics, Biosensors and Bioelectronics 109 (2018) 156-163. https://doi.org/10.1016/j.bios.2018.03.009.

[46] A.K. Au, W. Huynh, L.F. Horowitz, A. Folch, 3D-Printed Microfluidics, Angew Chem Int Ed Engl 55(12) (2016) 3862-81. https://doi.org/10.1002/anie.201504382.

[47] N. Fang, C. Sun, X. Zhang, Diffusion-limited photopolymerization in scanning micro-stereolithography, Applied Physics A 79(8) (2004) 1839-1842. https://doi.org/10.1007/s00339-004-2938-x.

[48] V. Romanov, R. Samuel, M. Chaharlang, A.R. Jafek, A. Frost, B.K. Gale, FDM 3D printing of high-pressure, heat-resistant, transparent microfluidic devices, Analytical Chemistry 90(17) (2018) 10450-10456. https://doi.org/10.1021/acs.analchem.8b02356.

[49] Y.S. Lee, N. Bhattacharjee, A. Folch, 3D-printed Quake-style microvalves and micropumps, Lab Chip 18(8) (2018) 1207-1214. https://doi.org/10.1039/C8LC00001H.

[50] A. Folch, Introduction to bioMEMS, CRC Press2016.

[51] J.C. McDonald, D.C. Duffy, J.R. Anderson, D.T. Chiu, H. Wu, O.J. Schueller, G.M. Whitesides, Fabrication of microfluidic systems in poly (dimethylsiloxane), ELECTROPHORESIS 21(1) (2000) 27-40. https://doi.org/10.1002/(SICI)1522-2683(20000101)21:1<27::AID-ELPS27>3.0.CO;2-C.

[52] H. Yang, M.A. Gijs, Micro-optics for microfluidic analytical applications, Chemical Society Reviews 47(4) (2018) 1391-1458. https://doi.org/10.1039/C5CS00649J.

[53] J. Kittelmann, M. Ottens, J. Hubbuch, Robust high-throughput batch screening method in 384-well format with optical in-line resin quantification, Journal of Chromatography B 988 (2015) 98-105. https://doi.org/10.1016/j.jchromb.2015.02.028.

[54] N. Field, S. Konstantinidis, A. Velayudhan, High-throughput investigation of single and binary protein adsorption isotherms in anion exchange chromatography employing multivariate analysis, Journal of Chromatography A 1510 (2017) 13-24. https://doi.org/10.1016/j.chroma.2017.06.012.

[55] P. Baumann, T. Huuk, T. Hahn, A. Osberghaus, J. Hubbuch, Deconvolution of high-throughput multicomponent isotherms using multivariate data analysis of protein spectra, Engineering in Life Sciences 16(2) (2016) 194-201. https://doi.org/10.1002/elsc.201400243.

[56] B.K. Nfor, M. Noverraz, S. Chilamkurthi, P.D. Verhaert, L.A. van der Wielen, M. Ottens, High-throughput isotherm determination and thermodynamic modeling of protein adsorption on mixed mode

adsorbents, Journal of Chromatography A 1217(44) (2010) 6829-50. https://doi.org/10.1016/j.chroma.2010.07.069.

[57] K. Woodruff, S.J. Maerkl, A high-throughput microfluidic platform for mammalian cell transfection and culturing, Scientific Reports 6(1) (2016) 1-12. https://doi.org/10.1038/srep23937.

[58] A. Tang, I. Ramos, K. Newell, K.D. Stewart, A novel high-throughput process development screening tool for virus filtration, Journal of Membrane Science (2020) 118330. https://doi.org/10.1016/j.memsci.2020.118330.

[59] L. Fernandez-Cerezo, A.C. Rayat, A. Chatel, J.M. Pollard, G.J. Lye, M. Hoare, An ultra scale-down method to investigate monoclonal antibody processing during tangential flow filtration using ultrafiltration membranes, Biotechnology and Bioengineering 116(3) (2019) 581-590. https://doi.org/10.1002/bit.26859.

[60] S.W. Benner, J.P. Welsh, M.A. Rauscher, J.M.J.J.o.C.A. Pollard, Prediction of lab and manufacturing scale chromatography performance using mini-columns and mechanistic modeling, 1593 (2019) 54-62. https://doi.org/10.1016/j.chroma.2019.01.063.

[61] A.L. Oliveira, Biotechnology, big data and artificial intelligence, Biotechnology Journal 14(8) (2019) 1800613. https://doi.org/10.1002/biot.201800613.

[62] K.W. Ro, K. Lim, B.C. Shim, J.H. Hahn, Integrated light collimating system for extended optical-path-length absorbance detection in microchip-based capillary electrophoresis, Analytical Chemistry 77(16) (2005) 5160-5166. https://doi.org/10.1021/ac050420c.

[63] N. Cohen, P. Sabhachandani, A. Golberg, T. Konry, Approaching near real-time biosensing: microfluidic microsphere based biosensor for real-time analyte detection, Biosensors and Bioelectronics 66 (2015) 454-460. https://doi.org/10.1016/j.bios.2014.11.018.

[64] X. Lin, K.-H. Leung, L. Lin, L. Lin, S. Lin, C.-H. Leung, D.-L. Ma, J.-M. Lin, Determination of cell metabolite VEGF165 and dynamic analysis of protein–DNA interactions by combination of microfluidic technique and luminescent switch-on probe, Biosensors and Bioelectronics 79 (2016) 41-47. https://doi.org/10.1016/j.bios.2015.11.089.

[65] K. Beeman, J. Baumgärtner, M. Laubenheimer, K. Hergesell, M. Hoffmann, U. Pehl, F. Fischer, J.-C. Pieck, Integration of an in situ MALDI-based high-throughput screening process: a case study with receptor tyrosine kinase c-MET, SLAS DISCOVERY: Advancing Life Sciences R&D 22(10) (2017) 1203-1210. https://doi.org/10.1177/2472555217727770.

[66] R.D. Pedde, H. Li, C.H. Borchers, M. Akbari, Microfluidic-mass spectrometry interfaces for translational proteomics, Trends in Biotechnology 35(10) (2017) 954-970. https://doi.org/10.1016/j.tibtech.2017.06.006.

[67] X. Wang, L. Yi, N. Mukhitov, A.M. Schrell, R. Dhumpa, M.G. Roper, Microfluidics-to-mass spectrometry: a review of coupling methods and applications, Journal of Chromatography A 1382 (2015) 98-116. https://doi.org/10.1016/j.chroma.2014.10.039.

[68] M. Sibley, A. Woodhams, M. Hoehse, B. Zoro, Novel Integrated Raman Spectroscopy Technology for Minibioreactors, BioProcess International 18 (2020) 9.

[69] A.F. Chrimes, K. Khoshmanesh, P.R. Stoddart, A. Mitchell, K. Kalantar-zadeh, Microfluidics and Raman microscopy: current applications and future challenges, Chemical Society Reviews 42(13) (2013) 5880-5906. https://doi.org/10.1039/C3CS35515B.

[70] Q. Zhou, T. Kim, Review of microfluidic approaches for surface-enhanced Raman scattering, Sensors and Actuators B: Chemical 227 (2016) 504-514. https://doi.org/10.1016/j.snb.2015.12.069.

[71] T. Uema, T. Ohata, Y. Washizuka, R. Nakanishi, D. Kawashima, N. Kakuta, Near-infrared imaging in a microfluidic channel of aqueous acid− base reactions, Chemical Engineering Journal (2020) 126338. https://doi.org/10.1016/j.cej.2020.126338.

[72] A.A. Bhirde, M.-J. Chiang, R. Venna, S. Beaucage, K. Brorson, High-throughput in-use and stress size stability screening of protein therapeutics using algorithm-driven dynamic light scattering, Journal of Pharmaceutical Sciences 107(8) (2018) 2055-2062. https://doi.org/10.1016/j.xphs.2018.04.017.

[73] F. Destremaut, J.-B. Salmon, L. Qi, J.-P. Chapel, Microfluidics with on-line dynamic light scattering for size measurements, Lab on a Chip 9(22) (2009) 3289-3296. https://doi.org/10.1039/B906514H.

[74] Y. Zhu, Q. Fang, Analytical detection techniques for droplet microfluidics—A review, Analytica Chimica Acta 787 (2013) 24-35. https://doi.org/10.1016/j.aca.2013.04.064.

[75] M. Winter, R. Ries, C. Kleiner, D. Bischoff, A.H. Luippold, T. Bretschneider, F.H. Büttner, Automated MALDI target preparation concept: providing ultra-high-throughput mass spectrometry–based screening for drug discovery, SLAS TECHNOLOGY: Translating Life Sciences Innovation 24(2) (2019) 209-221. https://doi.org/10.1177/2472630318791 98.

[76] K. Buckley, A.G. Ryder, Applications of Raman spectroscopy in biopharmaceutical manufacturing: a short review, Applied Spectroscopy 71(6) (2017) 1085-1116. https://doi.org/10.1177/0003702817703270.

[77] B.K. Nfor, J. Ripić, A. van der Padt, M. Jacobs, M. Ottens, Model-based high-throughput process development for chromatographic whey proteins separation, Biotechnology Journal 7(10) (2012) 1221-1232. https://doi.org/10.1002/biot.201200191.

[78] J. Pollock, G. Bolton, J. Coffman, S.V. Ho, D.G. Bracewell, S.S. Farid, Optimising the design and operation of semi-continuous affinity chromatography for clinical and commercial manufacture, Journal of Chromatography A 1284 (2013) 17-27. https://doi.org/10.1016/j.chroma.2013.01.082.

[79] V. Kumar, A.M. Lenhoff, Mechanistic Modeling of Preparative Column Chromatography for Biotherapeutics, Annual Review of Chemical and Biomolecular Engineering 11 (2020) 235-255. https://doi.org/10.1146/annurev-chembioeng-102419-125430.

[80] S.M. Pirrung, L.A. van der Wielen, R.F. van Beckhoven, E.J. van de Sandt, M.H. Eppink, M. Ottens, Optimization of biopharmaceutical downstream processes supported by mechanistic models and artificial neural networks, Biotechnology Progress 33(3) (2017) 696-707. https://doi.org/10.1002/btpr.2435.

[81] A.T. Hanke, M. Ottens, Purifying biopharmaceuticals: knowledge-based chromatographic process development, Trends in Biotechnology 32(4) (2014) 210-20. https://doi.org/10.1016/j.tibtech.2014.02.001.

[82] K. Neha, L. Urpo, K. Navin, B. Gaurav, Enhanced cell density cultivation and rapid expression-screening of recombinant Pichia pastoris clones in microscale, Scientific Reports 10(1) (2020). https://doi.org/10.1038/s41598-020-63995-5.

[83] K.A. Shah, J.J. Clark, B.A. Goods, T.J. Politano, N.J. Mozdzierz, R.M. Zimnisky, R.L. Leeson, J.C. Love, K.R. Love, Automated pipeline for rapid production and screening of HIV-specific monoclonal antibodies using pichia pastoris, Biotechnology and Bioengineering 112(12) (2015) 2624-2629. https://doi.org/10.1002/bit.25663.

[84] J. Ehret, M. Zimmermann, T. Eichhorn, A. Zimmer, Impact of cell culture media additives on IgG glycosylation produced in Chinese hamster ovary cells, Biotechnology and Bioengineering 116(4) (2019) 816-830. https://doi.org/10.1002/bit.26904.

[85] F.V. Ritacco, Y. Wu, A. Khetan, Cell culture media for recombinant protein expression in Chinese hamster ovary (CHO) cells: History, key components, and optimization strategies, Biotechnology Progress 34(6) (2018) 1407-1426. https://doi.org/10.1002/btpr.2706.

[86] M. Bensch, P. Schulze Wierling, E. von Lieres, J. Hubbuch, High Throughput Screening of Chromatographic Phases for Rapid Process Development, Chemical Engineering & Technology 28(11) (2005) 1274-1284. https://doi.org/10.1002/ceat.200500153.

[87] S. Konstantinidis, H.Y. Goh, J.M. Martin Bufájer, P. de Galbert, M. Parau, A. Velayudhan, Flexible and accessible automated operation of miniature chromatography columns on a liquid handling station, Biotechnology Journal 13(3) (2018) 1700390. https://doi.org/10.1002/biot.201700390.

[88] A.T. Hanke, E. Tsintavi, M.d.P. Ramirez Vazquez, L.A. van der Wielen, P.D. Verhaert, M.H. Eppink, E.J. van de Sandt, M. Ottens, 3D-liquid chromatography as a complex mixture characterization tool for knowledge-based downstream process development, Biotechnology Progress 32(5) (2016) 1283-1291. https://doi.org/10.1002/btpr.2320.

[89] S.M. Pirrung, D. Parruca da Cruz, A.T. Hanke, C. Berends, R.F. Van Beckhoven, M.H. Eppink, M. Ottens, Chromatographic parameter determination for complex biological feedstocks, Biotechnology Progress 34(4) (2018) 1006-1018. https://doi.org/10.1002/btpr.2642.

[90] A.M. Azevedo, P.A. Rosa, I.F. Ferreira, M.R. Aires-Barros, Chromatography-free recovery of biopharmaceuticals through aqueous two-phase processing, Trends in biotechnology 27(4) (2009) 240-247. https://doi.org/10.1016/j.tibtech.2009.01.004.

[91] A.M. Azevedo, A.G. Gomes, P.A.J. Rosa, I.F. Ferreira, A.M.M.O. Pisco, M.R. Aires-Barros, Partitioning of human antibodies in polyethylene glycol–sodium citrate aqueous two-phase systems, Separation and Purification Technology 65(1) (2009) 14-21. https://doi.org/10.1016/j.seppur.2007.12.010.

[92] B.C. Bussamra, J.C. Gomes, S. Freitas, S.I. Mussatto, A.C. da Costa, L. van der Wielen, M. Ottens, A robotic platform to screen aqueous two-phase systems for overcoming inhibition in enzymatic reactions, Bioresource Technology 280 (2019) 37-50. https://doi.org/j.biortech.2019.01.136.

[93] M. Marchel, H.R. Soares, P. Vormittag, J. Hubbuch, A.S. Coroadinha, I.M. Marrucho, High-throughput screening of aqueous biphasic systems with ionic liquids as additives for extraction and purification of enveloped virus-like particles, Engineering Reports 1(1) (2019) e12030. https://doi.org/10.1002/eng2.12030.

[94] S. Andris, M. Wendeler, X. Wang, J. Hubbuch, Multi-step high-throughput conjugation platform for the development of antibody-drug conjugates, Journal of Biotechnology 278 (2018) 48-55. https://doi.org/10.1016/j.jbiotec.2018.05.004.

[95] S. Andris, M. Rüdt, J. Rogalla, M. Wendeler, J. Hubbuch, Monitoring of antibody-drug conjugation reactions with UV/Vis spectroscopy, Journal of biotechnology 288 (2018) 15-22. https://doi.org/10.1016/j.jbiotec.2018.10.003.

[96] A. Grünberger, N. Paczia, C. Probst, G. Schendzielorz, L. Eggeling, S. Noack, W. Wiechert, D. Kohlheyer, A disposable picolitre bioreactor for cultivation and investigation of industrially relevant bacteria on the single cell level, Lab on a Chip 12(11) (2012) 2060-2068. https://doi.org/10.1039/C2LC40156H.

[97] S. Lladó Maldonado, P. Panjan, S. Sun, D. Rasch, A.M. Sesay, T. Mayr, R. Krull, A fully online sensor-equipped, disposable multiphase microbioreactor as a screening platform for biotechnological applications, Biotechnology and Bioengineering 116(1) (2019) 65-75. https://doi.org/10.1002/bit.26831.

[98] A. Kecskemeti, A. Gaspar, Particle-based liquid chromatographic separations in microfluidic devices - A review, Analytica Chimica Acta 1021 (2018) 1-19. https://doi.org/10.1016/j.aca.2018.01.064.

[99] I.s.F. Pinto, R.R. Soares, S.A. Rosa, M.R. Aires-Barros, V. Chu, J.o.P. Conde, A.M. Azevedo, High-throughput nanoliter-scale analysis and optimization of multimodal chromatography for the capture of monoclonal antibodies, Analytical Chemistry 88(16) (2016) 7959-7967. https://doi.org/10.1021/acs.analchem.6b00781.

[100] H.S. Rho, A.T. Hanke, M. Ottens, H. Gardeniers, A microfluidic device for the batch adsorption of a protein on adsorbent particles, Analyst 142(19) (2017) 3656-3665. https://doi.org/10.1039/c7an00917h.

[101] D. Silva, A. Azevedo, P. Fernandes, V. Chu, J. Conde, M. Aires-Barros, Determination of aqueous two phase system binodal curves using a microfluidic device, Journal of Chromatography A 1370 (2014) 115-120. https://doi.org/10.1016/j.chroma.2014.10.035.

[102] D. Silva, A. Azevedo, P. Fernandes, V. Chu, J. Conde, M. Aires-Barros, Design of a microfluidic platform for monoclonal antibody extraction using an aqueous two-phase system, Journal of Chromatography A 1249 (2012) 1-7. https://doi.org/10.1016/j.chroma.2012.05.089.

[103] S. Trietsch, T. Hankemeier, H. Van der Linden, Lab-on-a-chip technologies for massive parallel data generation in the life sciences: A review, Chemometrics and Intelligent Laboratory Systems 108(1) (2011) 64-75. https://doi.org/10.1016/j.chemolab.2011.03.005.

[104] N. Bhattacharjee, A. Urrios, S. Kang, A. Folch, The upcoming 3D-printing revolution in microfluidics, Lab on a Chip 16(10) (2016) 1720-1742. https://doi.org/10.1039/C6LC00163G.

[105] E.J. Close, J.R. Salm, D.G. Bracewell, E. Sorensen, A model based approach for identifying robust operating conditions for industrial chromatography with process variability, Chemical Engineering Science 116 (2014) 284-295. https://doi.org/10.1016/j.ces.2014.03.010.

[106] F. Rischawy, D. Saleh, T. Hahn, S. Oelmeier, J. Spitz, S. Kluters, Good modeling practice for industrial chromatography: Mechanistic modeling of ion exchange chromatography of a bispecific antibody, Computers & Chemical Engineering 130 (2019) 106532. https://doi.org/10.1016/j.compchemeng.2019.106532.

[107] A.A. Shukla, J. Thömmes, Recent advances in large-scale production of monoclonal antibodies and related proteins, Trends in Biotechnology 28(5) (2010) 253-261. https://doi.org/10.1016/j.tibtech.2010.02.001.

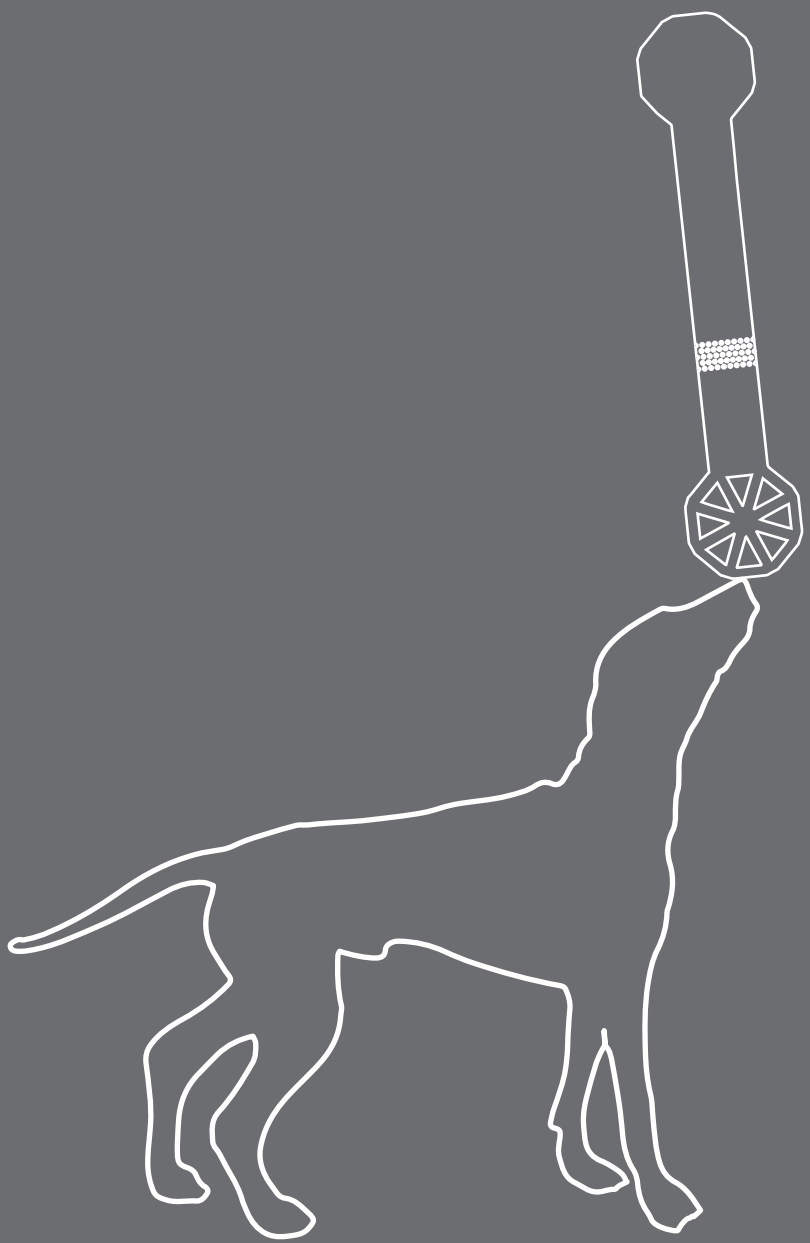

Chapter 4

Small, smaller, smallest: Miniaturization of chromatographic process development

Abstract

Biopharmaceuticals are becoming increasingly important in modern healthcare. Monoclonal antibodies (mAb) are one of the most widely used therapeutic proteins and are important for the treatment of cancer and autoimmune diseases, among others. After cell culture there are still large amounts of other impurities (*e.g.,* host cell proteins) in solution. Chromatography is usually the first purification step, allowing to increase purity and reduce volume. This comes associated with high costs and chromatography accounts for a significant portion of total production costs for therapeutic proteins. Chromatographic process development may be time consuming and use large amounts of resins. Therefore, there is increased interest in finding cheaper techniques for chromatographic process development without compromising accuracy. This paper presents a highly sophisticated microfluidic chip approach for efficient adsorption isotherm determinations compared to current chromatographic process development. Implementation of an image analysis software ensures that chromatographic resin volume is accurately determined. The adsorption isotherm performance of microfluidics was compared to the robotic Liquid-handling Station (LHS) and labor-intensive Eppendorf tubes. The microfluidic chip allows a 15-fold volume reduction and resin consumptions as low as 100/200 nl (200/100-fold reduction). The microfluidic chip performed comparably to the other miniaturized techniques, using less liquid and resin volume. For process development of expensive products (*e.g.,* monoclonal antibodies), miniaturization (provided by the microfluidic chip) proved to be the most cost effective alternative whereas for less valuable products (*e.g.,* lysozyme) automation (provided by the LHS) was the most cost-effective alternative.

Keywords: High-Throughput Screening; Batch adsorption protein isotherms; Microfluidic chromatography; Liquid-Handling Stations; Miniaturization

---

***Published as*:** Silva, T.C., Eppink, M. and Ottens, M., 2022. Small, smaller, smallest: Miniaturization of chromatographic process development. Journal of Chromatography A, 1681, 463451. DOI: https://doi.org/10.1016/j.chroma.2022.463451

4.1. Introduction

The past few years have seen increasing general public interest in the biopharmaceutical industry, mainly in the field of vaccine production due to the Covid pandemic. For the industry, a fast, reliable, and preferably cost-effective process development is important to respond to the market's needs. Patient accessibility to therapeutic proteins depends on several aspects, such as the cost of treatment or product availability. Although patent expiration considerably decreases the retail price of monoclonal antibodies (mAb), the price may still be prohibitive for patients [1, 2]. High-Throughput Screening (HTS) is used to decrease time to market and reduce development costs, especially in the early stages of process development. Moreover, increased use of mechanistic modelling of the processes combined with the ability to determine different parameters faster originated High-Throughput Process Development (HTPD). In the past decades HTPD has proven to be a valuable tool for faster and cheaper process development [3].

Chromatography plays a key role in the purification of biopharmaceuticals, as it usually is the first purification step in the downstream process and the one responsible for high purification factors [4]. However, this comes associated with high costs, since preparative chromatography can be very expensive. Therefore, chromatography accounts for a significant portion of the cost of producing therapeutic proteins [5]. Process development for chromatography involves the screening of different consumables (chromatographic resins, buffers) and conditions to find a suitable purification process. Equilibrium adsorption isotherms are amongst the important parameters to be determined for model based chromatographic process development [6]. Batch uptake experiments in 96 well-plates have also been used to calculate the partition coefficient and separation factor [7, 8]. These give an indication of the purification capabilities of the tested systems. Isotherms provide insight on the thermodynamics of the studied systems, which are composed of the different buffers and the resin-protein pairs [9]. Previously, protein adsorption isotherms in batch uptake mode were determined using agitated vessels, with sample volume reaching up to hundreds of milliliters [10]. This method required large amounts of sample and resin. Current technology enabled researchers to reduce the amount of samples and materials, by using microtiter plates both with 96-well and 384-well format [11, 12].

Researchers started to push for a manifold volume reduction, due to the high costs of chromatographic resin and sample waste and limited amount of samples available in early stages of process development (*e.g.,* clinical trials). Different formats to determine adsorption isotherms emerged, like the use of plastic (Eppendorf) tubes, with volume requirements in the milliliter range [13]. Subsequently, Liquid-Handling Stations (LHS) were employed, reducing volume requirements to the sub-milliliter range. These offer great automation to screen a plethora of consumables available for chromatographic

process development [14]. Although LHS have become the *status quo* for both industry and academia [12, 15], these platforms and consumables are expensive and still require a fair amount of product, which can be scarce in early stages of process development. It would be beneficial to reduce volume consumption in early-stage process development while maintaining accurate results. Microfluidics presents itself as a viable alternative for analytics and process development in many areas of the life sciences, often operating in the nanoliter range [16]. Although it has the obvious advantage of reducing volume (and, therefore, cost), microfluidics can also be more flexible and versatile than LHS, when the devices can be designed and produced from zero (for devices already commercialized this does not apply). Microfluidic devices have also been used for studying and screening conditions to determine protein adsorption isotherms [17], and protein purification [18]. Although these studies show the great miniaturization achieved by microfluidics, the use of a fluorescent label has been proven to interfere with the protein, altering its properties [19, 20]. A clear comparison of different miniaturization techniques is currently not available in open literature.

This paper compares different miniaturization techniques for the determination of protein adsorption isotherms. It discusses the accuracy, usability, and technology readiness level (TRL) of each technique. Additionally, the cost of each screening solution is evaluated. Finally, this work shows how to use the small volume (Eppendorfs), smaller volume (LHS), and smallest volume (microfluidics) tools for chromatographic process development.

4.2. Materials and Methods

4.2.1. Materials

Two different proteins were used in this study: lysozyme from chicken egg white (M_w of 14 300 Da, pI ≈ 11; Sigma-Aldrich Chemie GbmH, Steinheim, Germany) and purified monoclonal antibody (M_w of 148 220 Da, pI ≈ 8.6; Byondis B.V., Nijmegen, The Netherlands).

Sodium phosphate monobasic dihydrate, acetic acid (≥99.8%) and Tween® 20 were purchased from Sigma-Aldrich Chemie GbmH, Steinheim, Germany. Phosphoric acid (85%) and sodium hydroxide were purchased from Mallinckrodt Baker, Deventer, The Netherlands. Sodium Chloride was purchased from VWR-Chemicals, Leuven, Belgium. Di-sodium hydrogen phosphate was purchased from Merck KGaA, Darmstadt, Germany. SU-8 2100 photoresist was purchased from MicroChem, Newton, MA, USA and Developer mr-Dev 600 was purchased from micro resist technology GmbH, Berlin, Germany. Polydimethylsiloxane (PDMS) was purchased as a Sylgard 184 elastomer kit (Dow Corning; Midland, MI, USA).

The resin used in the study was SP Sepharose™ Fast Flow (SP-Sepharose-FF) from Cytiva, Uppsala, Sweden. This is a strong cation-exchange agarose-based resin and has a mean particle size of 90 μm.

4.2.2. Buffers and solutions preparation

The lysozyme experiments were performed with sodium phosphate buffer containing 10 mM Na_2HPO_4 and varying NaCl concentrations adjusted to pH 6.5 with phosphoric acid. The mAb experiments were performed with buffer containing 25 mM NaOAc and 5 mM NaCl adjusted to pH 4.5 with 2 M NaOH. NaCl was added to the buffer solutions to adjust the total Na^+ concentration of the solutions. All experiments were performed at room temperature. 0.01% w/v Tween® 20 was added to acetate buffer for the mAb experiments. The different buffers and solutions were prepared by dissolving the appropriate amount of chemical in Milli-Q water.

Lysozyme solutions were prepared by dissolving the appropriate amount of protein in the corresponding buffer. MAb solutions were used in the conditioning buffer that the protein was provided (mentioned above). All buffers and solutions were filter-sterilized using 0.20 μm filters.

4.2.3. Microfluidic chip fabrication

The microfluidic chips were fabricated in two main steps: fabrication of the mastermolds and of the PDMS structures.

4.2.3.1. Production of mastermolds

The SU-8 mold (mastermold) was fabricated using direct write optical lithography (DWL). A SU-8 2100 layer of 100 μm was spin coated on top of a clean Si substrate. The substrate was soft baked in a hotplate for 5 min at 65 °C and subsequently for 30 min at 95 °C. The mold was placed in the laserwriter (μMLA Tabletop Maskless Aligner; Heidelberg Instruments Mikrotechnik, Heidelberg, Germany), where it was exposed with a 365 nm laser. The exposure energy used for this fabrication was 225 mJ/cm2. After exposure, the substrate was placed in a hotplate for post exposure bake for 5 min at 65 °C and 10 min at 95 °C. Afterwards, the mastermold was developed by immersing it in mr-Dev 600 and hand stirring for a minimum of 10 min. After this, it was rinsed with isopropyl alcohol (IPA) and spin-dried. Finally, the mastermold was hard baked for 15 min at 150 °C.

4.2.3.2. Fabrication of PDMS structures

The PDMS microchips were fabricated using standard PDMS soft lithography [21]. PDMS elastomer was prepared by mixing the elastomer base and curing agent in a (7:1) ratio. The mixture was degassed and placed on top off the mold. Simultaneously, a (20:1)

mixture of elastomer base and curing agent was also prepared and degassed. This mixture was poured on top of glass slides and spin coated at 2500 rpm for 1 min. The covered mold and glass slides were baked at 80 °C for 45 min. After baking, the structure was peeled from the mold, and access holes (inlets and outlets) of 1.25 mm were punched using a hole-puncher. The structure was then placed on the PDMS-covered glass slides and sealed. The final structures were baked overnight at 80 °C.

4.2.4. Batch uptake adsorption isotherms

Adsorption isotherms provide information on the equilibrium concentration of a solute adsorbed to a solid phase (chromatographic resin) at different liquid concentrations. A known amount of protein is contacted with a known amount of resin and the equilibrium liquid concentrations are measured. The time to reach equilibrium varies according to the different systems. The amount of protein adsorbed to the solid phase was calculated by a mass balance, described by the following equation:

$$q_{eq} = \frac{V_l \times \left(c_{l,initial} - c_{l,eq}\right)}{V_r} \quad (1)$$

where q_{eq} is the protein adsorbed to the resin in equilibrium, V_l is the volume of liquid, V_r is the volume of resin, and $c_{l,initial}$ and $c_{l,eq}$ are the protein concentrations in the liquid phase in the beginning and after equilibrium is reached, respectively. Equilibrium adsorption isotherms were obtained with triplicate experiments.

4.2.4.1. LHS

Batch adsorption isotherm data were generated using a LHS (Tecan EVO Freedom 200 robotic station; Tecan, Switzerland). The LHS was equipped with an orbital mixer (Te-Shake), an automated vacuum system (Te-VacS), a multi-well plate reader (InfiniTe Pro 200), a robotic manipulator (RoMa) arm, two different liquid-handling arms (LiHa and MCA96) and a centrifuge system (Rotanta).

A known amount of resin (20.8 µL) was added to a 96-well filter plate (Pall Corporation, NY, USA) using a MediaScout® ResiQuot resin loader device from Atoll (Weingarten, Germany). To wash the resin, an equilibration buffer was pipetted into the filter plate, and it was shaken for 5 min at 1200 rpm, after which the solution was removed using the vacuum system. This cycle was performed 3 times in total. Protein solutions were subsequently pipetted (800 µL) inside the well plates, and the plates were agitated at 1200 rpm until equilibrium was reached (2h for lysozyme and 18h for mAb). Once equilibrium was reached, the filter plate was placed on top of a 2 mL deep-well plate (Eppendorf AG, Hamburg, Germany) and these were centrifuged together using the centrifugation system. The supernatant was collected from the deep well plates to a UV star plate and

the equilibrium concentrations were measured using the plate reader. Equilibrium concentrations were estimated using appropriate calibration curves, obtained using the LHS.

4.2.4.2. Eppendorfs

The batch adsorption isotherms in Eppendorf tubes were estimated using a similar method to the one described above. The studies were performed in 1.5 mL tubes. 800 µL of protein solutions were prepared by hand into each of the tubes. The solutions were then contacted with 20.8 µL of resin (generated using the same method as described for LHS). The tubes were rotated end-over-end at 10 rpm, until equilibrium was reached (the same was described above). After equilibrium was reached, the tubes were centrifuged (Sigma 112 from De Spatel B.V., The Netherlands), and the supernatant was hand-pipetted to a UV star plate, and the equilibrium concentrations were measured using the plate reader mentioned above. Equilibrium concentrations were estimated using appropriate calibration curves.

4.2.4.3. Microfluidic chip

4.2.4.3.1. Setup and mode of operation

The batch adsorption isotherms in the microfluidics devices were determined by recirculating protein solution through the microchip, that contained beads trapped inside. This is achieved with a closed system, where the same liquid is continuously pumped through the same resin volume, until equilibrium is reached. In the system, an inline UV-Vis detector (SPD-20AV; Shimadzu, Kyoto, Japan) with a microflow cell (0.2 µL), allows to monitor the evolution of the adsorption over time.

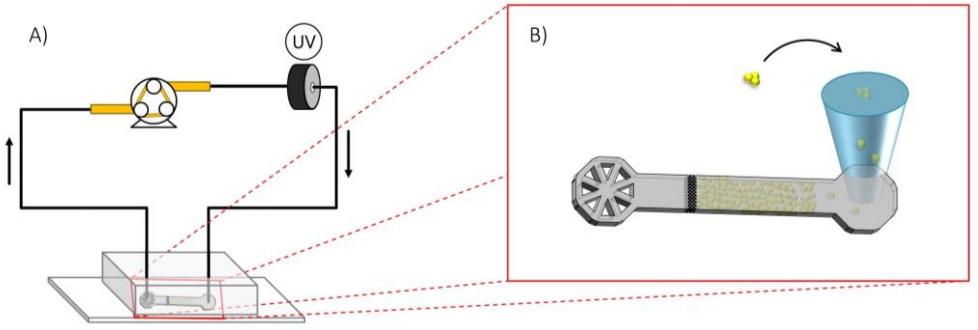

Figure 4.1 - Microfluidic experimental setup for the determination of protein adsorption isotherms. A) Schematics of the setup. Yellow lines represent the PharMed® BPT tube that is connected to the peristaltic pump; black lines represent the PEEK tubing. Arrows show the direction of fluid flow through the system. B) Zoomed in image of the microfluidic chip with schematics for resin loading into the microchip. The resin is loaded using a micropipette tip and the chromatographic beads are trapped by the frits further down the channel.

Figure 4.1 shows a schematic setup of the microfluidic chip. A peristaltic pump (ISM596D from Cole-Parmer, Wertheim, Germany) was used to recirculate the solution through the microchip. The pump used a PharMed® BPT tube (0.51 mm ID; Cole-Parmer, Wertheim, Germany), which was connected to PolyEtherEtherKetone (PEEK) tubes (0.18 mm ID; BGB, Harderwijk, The Netherlands). The PEEK tubes were directly connected to the microfluidic chip. The calculation of the equilibrium concentration was done using a calibration curve performed before each trial.

To perform the adsorption trials, the tube system was continuously primed with protein solutions of known concentrations, until a plateau was reached in the UV detector. After the plateau was reached, a protein solution of another concentration was successively primed until all the solutions for the calibration curve were primed. After this, the last solution to prime was the solution with the desired initial protein concentration. When the plateau of the signal was observed the pumping was stopped, and the PEEK tubes were directly connected to the microchip containing the chromatographic resin (see **Figure 4.1**). After connecting, the pumping was resumed and the solution was recirculated until equilibrium was reached. Equilibrium was assumed to be reached when the signal stopped changing over time. The equilibrium concentration was used to calculate the mass balance to determine the amount of adsorbed protein in each trial.

4.2.4.3.2. Bead loading and volume determination for microfluidic chip

A suspension of 0.5% v/v chromatographic resin in storage buffer was prepared, by pipetting appropriate amounts of settled resin and storage buffer. The solution was vortexed and approximately 150 µL of this solution was promptly pipetted directly into the microchip inlet using a micropipette. By suspending the resin and rapidly pipetting it into the microchip, it is avoided that the resin settles in the bottom of the pipette tip. This would block the microchip and hinder the entrance of the resin in the channel. Downstream of the channel there are frits. These structures, spaced 50 µm from each other vertically and horizontally, will trap the beads inside the microchannel. After a sufficient amount of resin is loaded into the channel, the tip is removed and the microchip is analyzed in the microscope to estimate the total bead volume.

An accurate bead volume determination is paramount for the determination of the adsorption isotherms. Pictures of the loaded channel allow to estimate the number of beads and their radius. These images are then loaded into a MatLab script for image analysis. Using the built-in function *imfindcircles* and appropriate parameters, it is possible to estimate the number of beads detected and the radius, in pixels, of each bead. Using an appropriate calibration (for example the channel's width, of 1000 µm), it is possible to correlate the bead radius in pixels with the distance per pixel (µm/px). With the information of the bead radius in micrometers, the bead volume is calculated using the

formula for the volume of a sphere. An example of this bead volume determination can be found in **Figure 4.2**. The beads are then washed with 200 µL of equilibration buffer. The interstitial porosity of the channel was not calculated since the experiments focus on studying the adsorption equilibrium of different proteins to a chromatographic resin. The microfluidic chip is used to mimic the batch adsorption mode of operation. Therefore, this parameter was considered to not be important since it provides information for the performance of packed columns but no relevant information for the equilibrium data between ligand and solute of interest.

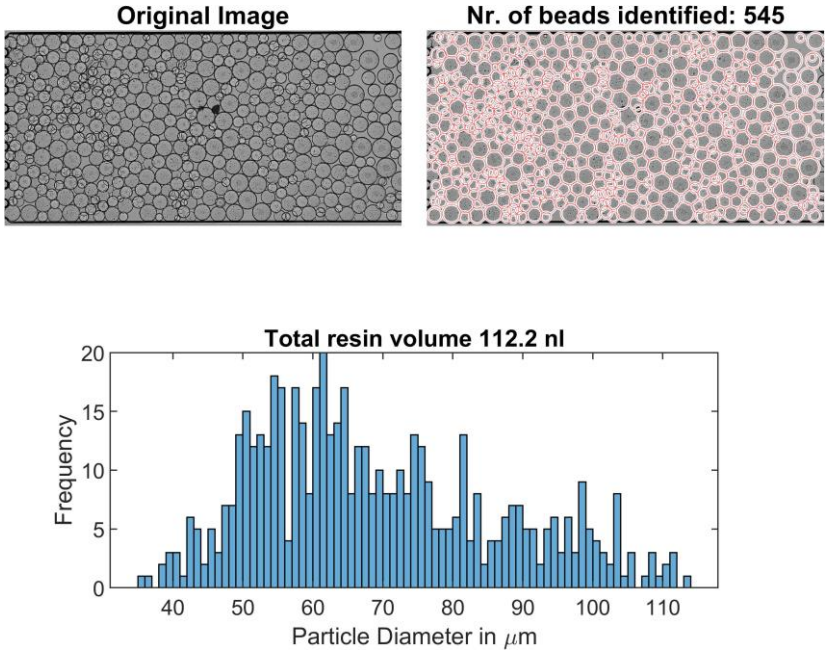

Figure 4.2 - Image Analysis software. Top Left: Original image used as input for the program. Top right: visualization of the bead radius determination by the MatLab function imfindcircles. Bottom: Histogram distribution of the bead radius.

4.2.4.3.3. Mass Balance in microfluidic chip

The mass balance for the microfluidic chip is similar to the one presented in equation (1). However, for the microchip system, the initial protein concentration is determined for the tubing system, which doesn't account for the buffer volume present in the microchip. Therefore, an adjustment to the previous mass balance equation is needed:

$$q_{eq} = \frac{c_{l,initial} \times V_{tubing} - c_{l,eq} \times V_{system}}{V_r} \quad (2)$$

$$V_{system} = V_{tubing} + V_{\mu-chip} + V_{liquid\ plugs} \quad (3)$$

Where V_{tubing} is the volume of the tubes and the detector of the spectrophotometer, and $V_{\mu-chip}$ is the volume of the microchip. With these equations, all the buffer volume present in the final system (after the tubes are connected to the microchip) is considered. The volume of the "liquid plugs" ($V_{liquid\ plugs}$) in the mass balance was determined experimentally by measuring the height of the plug and considering a diameter of each inlet of 1.25 mm. This was also confirmed experimentally by running a test without resin inside the microchip and calculating the final liquid volume with the concentration after recirculation (data not shown). The total liquid volume for each microfluidics experiment was 56 µl and the resin volume per trial was around 200 nl (slight variations from experiment to experiment). The microchip system has a significantly larger volume than the microchip itself, mostly due to the tubing needed to operate the system. To reduce this volume further, the tube length reduction of the peristaltic pump can be considered. The total adsorbent and liquid volume used in each methodology is summarized in **Table 4.1**.

Table 4.1 - Overview of liquid and adsorbent volumes used in each experiment with each of the different methods.

Method	Adsorbent Volume (µl)	Liquid Volume (µl)
LHS	20.8	800
Eppendorf	20.8	800
µ-chip	0.2	1.12
µ-chip system (chip+tubing)	0.2	56

4.3. Results and Discussion

4.3.1. Microchip design and operation

A microfluidic chip was designed to determine protein adsorption isotherms in batch uptake mode. The liquid phase (buffer solution containing protein) is permanently contacted with the solid phase (chromatographic resin). Usually this is achieved by means of stirrers (*e.g.,* magnetic stirrer in a glass flask), or by shaking the solution in shake flasks or orbital shakers (*e.g.*, for the case of LHS). In the presented microfluidic chip, the batch uptake is achieved by continuously pumping (by means of a peristaltic pump, **Figure 4.1**) the protein solution through a microchannel where the chromatographic resin is trapped. The channel has a height of 100 µm, which can accommodate a plethora of resins used in the biopharmaceutical field (*e.g.,* SP Sepharose FF (SP Seph FF) has an average diameter of 90 µm). To trap the beads, frits (pillar-like structures) were included in the design of the microchip. There are different methods one can apply to achieve this [22, 23]. The chosen method was to have 5 frit columns next to each other. Compared to the studied alternatives (shafts, which are achieved by differences in height

channels, narrowing the channel height to trap the resin), the frit design showed less flow constraints when performing simple flow simulations (data not shown). Each frit has a diameter of 50 µm, and the vertical and horizontal distance between frits was also set at 50 µm (**Figure 4.3**). The liquid inlet (**Figure 4.3 A**, right) was designed to have a circular shape that would allow for the bead loading, whereas the liquid outlet (**Figure 4.3 A**, left) was designed with triangles to easily guide the liquid to the outlet and serve as an extra barrier in case of defected frits that would fail to trap the beads, thus avoiding major fouling in the tubes.

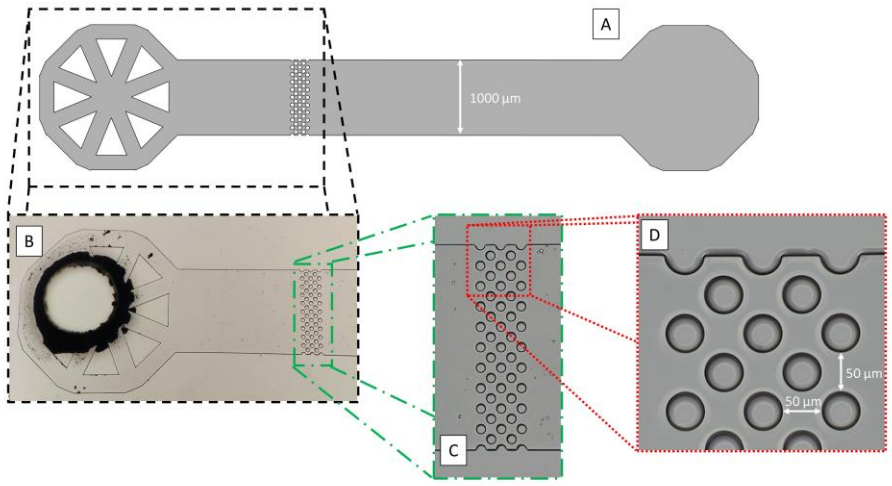

Figure 4.3 - Microfluidic chip design. A – Schematics of the whole microchip. B – Microscope image of the frits and outlet. The black circle is the hole punched with the punching tool and where the tube will be fit. C – Zoomed in image of the whole frit structure used. D – Zoomed in image of the top frits and indication of distance between frits. B, C and D are microscope pictures of the same structure, under different magnifications.

The liquid flow was ensured by a peristaltic pump. The liquid flowed from the inlet (**Figure 4.3 A**, right circular shape) to the outlet (**Figure 4.3 A**, left circular shape with triangle shapes). The beads were successfully trapped by the frit system, which is important to avoid fouling of the PEEK tubes used in the system. Besides SP Seph FF, beads of average particle diameter of 75 µm were also successfully trapped in the frit system. PDMS-based microfluidic chips can fail at relatively low pressures, so it is important that the pressure inside the flowing channel is as low as possible [24]. Therefore, a flow rate of 50 µl/min was employed, which enabled a good balance between a relatively low pressure in the channel, low bead compression against the frits, and fast enough recirculation through the system.

4.3.2. Image Analysis

To determine protein adsorption isotherms and ensure results are reliable, it is important to have a good characterization of the concentration of protein in the liquid phase as well as the total resin volume that the protein solution contacts. For the first, inline monitoring of the absorbance values is used whereas for the second an image analysis program was developed. The crude images were uploaded to the program and the only processing required was the conversion from red green blue (RGB) to black and white and snipping the area to evaluate.

By using the function described in section 4.2.4.3.2, it was possible to determine the radius of the chromatographic beads, given in pixels. The calibration used the channel's width (as shown in **Figure 4.3 A**) to convert the radius to μm. **Figure 4.2** shows the output of the program. The implementation of an appropriate calibration is important for the microfluidic chip results. Furthermore, ImageJ software was also used as an alternative to the described program to determine the resin volume. It had a worse performance for the intended purpose, as it was labor intensive and less accurate (data not shown). Therefore, it was decided that the most suitable method for chromatographic resin volume determination in the microchip was with the aforementioned program.

4.3.3. Determination of time to equilibrium

The monitoring of the adsorption of protein to the chromatographic resin was achieved by inline monitoring of the absorbance values at a wavelength of 280 nm (A_{280}). This allows to monitor in real time the adsorption of protein. In **Figure 4.4** it is possible to see the absorbance signal of two different systems throughout the time the experiments were performed. From this figure it is obvious that each system has its own characteristic time to equilibrium, which is the time it takes for the adsorption and desorption of protein molecules to the chromatographic resin to reach an equilibrium, meaning that the concentrations in the liquid and solid phase no longer change with time. The time to equilibrium varies dependent on the protein, buffer, and resin used in each experiment

After recirculation is started (time = 0 min), there is a lag time before a signal drop is observed. This is because the system was primed with a protein solution, which is still present in the tubes between the microchip and the detector. The first valley that can be seen in **Figure 4.4**, and is highlighted in **Figure 4.4 A**, is representative of two phenomena: i) the adsorption of the first "protein front" upon passing through the chromatographic resin for the first time, and ii) a local dilution of the solution due to the presence of protein-free buffer inside the microchip. The signal gradually smoothens as a result of a better mixing and adsorption throughout the duration of the experiment. Eventually, the signal flattens and reaches a plateau, which indicates the time to

equilibrium. It is noteworthy that for the tested resin and systems, the mAb showed the longest time to equilibrium (around the 1000-minute mark), whereas for lysozyme the systems reached equilibrium before the 120-minute mark. This difference can be explained by the smaller effective diffusivities that mAbs have compared to Lysozyme on SP Seph FF [25]. The larger mAb molecules take longer to migrate through the pores into the center of the particles, contributing to a longer time needed to access all available binding sites.

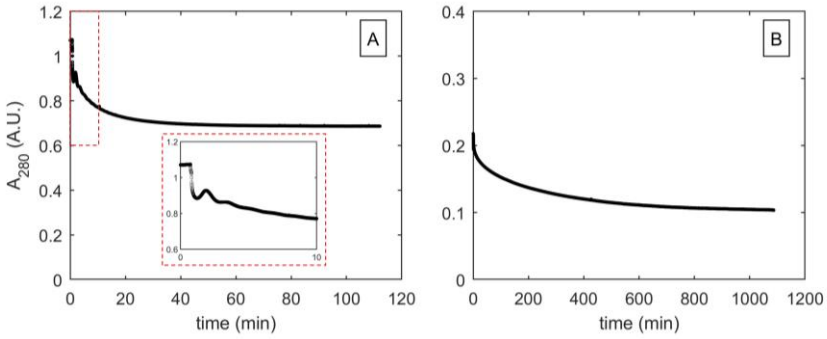

Figure 4.4 - Time to equilibrium of Lysozyme (A) and mAb (B) on Sp Seph FF. A – Lysozyme in 10 mM Phosphate buffer, pH 6.5, [Na+] = 50 mM; B – mAb in 25 mM Acetate Buffer, pH 4.5, [NaCl] = 5 mM. Dashed line in A shows a closer look at the first 10 min of recirculation, where the signal oscillation can be explained by the presence of two phenomena: i) already some adsorption from the first pass of protein through the chromatographic beads and ii) local dilution of the solution due to the presence of protein-free solution present inside the microchip that is reaching the detector. Lysozyme systems reached a plateau around the 100-minute mark whereas mAb system reached a plateau around the 1000-minute mark.

4.3.4. Protein Adsorption Isotherms

4.3.4.1. Lysozyme on SP Seph FF

The adsorption of Lysozyme to SP Seph FF was studied. Lysozyme has a very high pI, meaning that at the tested conditions its net charge will always be positive. Since SP Seph FF is a Cation-Exchange (CEX) resin, it was expected that a favorable adsorption behavior would be observed [26].

The isotherm data presented in **Figure 4.5** shows the adsorption isotherms of Lysozyme determined with the 3 different methodologies, as well as the fitted results to a Langmuir isotherm model (eq. (4)). The adsorption of Lysozyme to SP Seph FF is highly favorable, visible by the rectangular shape of the three isotherm curves.

$$q = \frac{q_{max} K C}{1 + K C} \tag{4}$$

The regressed parameter values for the q_{max} and K estimated from the fitting of the experimental data to eq. (4) are summarized in **Table 4.2**. From the aforementioned figure and table, it is noticeable that the microfluidic chip estimated higher adsorption

values of Lysozyme to the SP Seph FF for the studied system. Although the estimated values for the microchip are higher than for the other two methodologies, these are still within the same order of magnitude. The fitted isotherms also show a similar shape, meaning that the microchip also predicts the highly favorable adsorption behavior of Lysozyme to SP Seph FF.

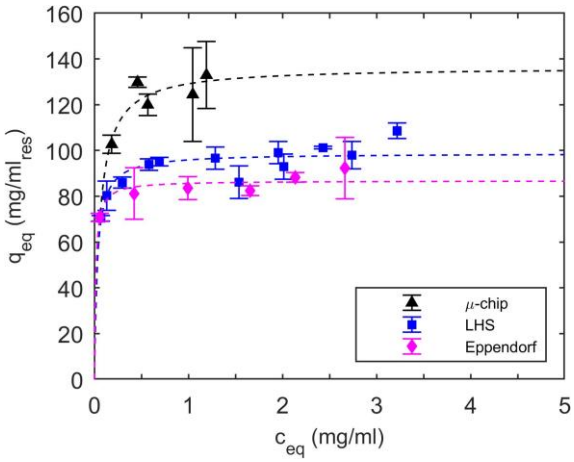

Figure 4.5 - Adsorption isotherms of Lysozyme on SP Seph FF, in 10 mM Phosphate buffer pH 6.5, [Na+] = 50 mM, using 3 different methodologies: (▲) microfluidic chip, (■) LHS and (♦) Eppendorf tubes. Dashed lines represent the fitting of the different data sets to the Langmuir model. The parameters of the fitting can be found in **Table 4.2**.

Proteins can interact with PDMS and non-specific adsorption of proteins to the PDMS surface has been previously reported [27]. To understand if this phenomenon was occurring in our system, some experiments with no resin inside the microchannel were performed. The results showed a flat signal over the duration of the trial (data not shown). Furthermore, there is a very low area of PDMS that contacts the solution at any given point in time and the liquid is being continuously pumped through the channel. Not only it is unlikely that there is non-specific adsorption, but this is greater when the solution is contacted statically with the PDMS surface [27]. The fluid flow through the microfluidic chip would contribute to prevent the non-specific adsorption of Lysozyme to the PDMS surface.

4.3.4.2. mAb on SP Seph FF

The adsorption of mAbs to SP Seph FF was also studied using the same setup. Initial experiments showed some instability in the UV signal of the solution containing mAb throughout the recirculation time. A recent study showed that different kinds of peristaltic pump tubes can affect the solutions [28]. The authors saw that the amount of nano and microparticles in solution increased over the pumping trials with water and buffer solutions, meaning that some particle shedding from the tubes to the solution is

occurring. The study showed that there is particle shedding from the tube's material to the solution, and from the tested tubes, the one that shed the most particles was PharMed® BPT. Although the amount of particles present in protein-free solutions increased with the peristaltic pumping, this was much more pronounced when protein solutions were pumped. This could help explain that the pumping and particle shedding can influence the stability of the studied protein solution, potentially leading to more aggregation. Another study by Deiringer and Friess hypothesizes that protein particle formation is caused by the formation of a protein film in the surface of the tube and consequent tearing of the film caused by the pump rollers, thus releasing parts of this film in solution [29]. However, both studies show that the addition of surfactants to the protein's solutions would significantly reduce this phenomenon.

Keeping these studies' observations and our own in mind, the adsorption studies with the mAb were carried out with a solution containing 0.01% Tween® 20 to increase the solution's colloidal stability. LHS studies showed comparable adsorption between the solutions with and without the added surfactant (data not shown). Similarly, to what was observed for Lysozyme, it was expected that mAb would have a favorable adsorption to SP Seph FF at the tested pH, as it is positively charged in these conditions. The results of the inline monitoring of the signal with the microfluidic chip, shown in **Figure 4.4**, were used to define the time to equilibrium needed for this system.

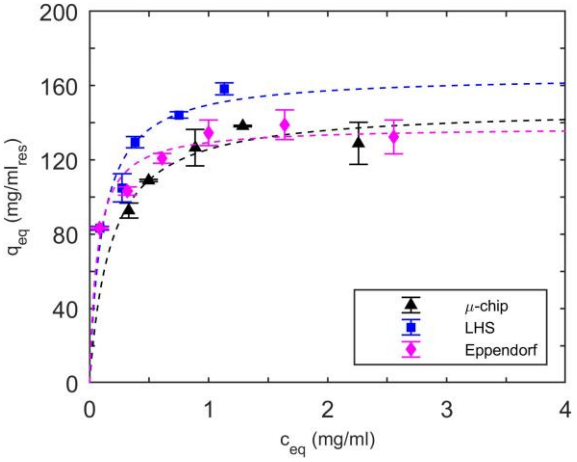

Figure 4.6 - Adsorption isotherms of mAb on SP Seph FF, in 25 mM Acetate buffer pH 4.5 and 5 mM NaCl, using 3 different methodologies: (▲) microfluidic chip, (■) LHS and (♦) Eppendorf tubes. Dashed lines represent the fitting of the different data sets to the Langmuir model. The parameters of the fitting can be found in **Table 4.2**.

Figure 4.6 shows the adsorption isotherms of mAb with the three different methodologies, as well as the fitted results to a Langmuir model. From these results, it is possible to see that the adsorption behavior of mAb to SP Seph FF is favorable,

characterized by the slope of the linear part of the isotherm. For this protein-resin pair it is noticeable the microchip results are more in line with what was determined by the other two methodologies. The regressed parameter values for the q_{max} and K estimated from the fitting of the experimental data to eq. (4) are summarized in **Table 4.2**.

Table 4.2 - Langmuir parameters of Lysozyme and mAb adsorption isotherms on SP Seph FF.

Lysozyme		
Method	q_{max} (mg/ml)	K (ml/mg)
µ-chip	136.4	17.8
LHS	98.8	33.1
Eppendorf	86.8	71.7
mAb		
Method	q_{max} (mg/ml)	K (ml/mg)
µ-chip	148.0	5.6
LHS	165.6	9.3
Eppendorf	137.7	15.4

This system showed the most agreement between the three methodologies, with the Langmuir fitting for the microfluidic chip placed between the fitted Langmuir isotherms for the LHS and Eppendorfs. The microfluidic chip can, therefore, capture the adsorption behavior of the Lysozyme and mAb.

4.3.5. Cost Considerations

The adsorption isotherms results show that the microfluidic chip, the LHS, and the Eppendorf tubes are different methodologies that achieve very similar results for the intended purpose. It would be good to have a comparison between the three methodologies in terms of costs and compare the key features of each. For the cost considerations, four different methodologies were considered: LHS (both renting and purchasing one), microfluidic chip, and Eppendorf tubes. Three cost categories were considered: equipment costs, material costs and labor costs. These cost considerations take into account the current technology state of each methodology used for the studies adsorption studies.

The equipment costs comprise all the necessary equipment for the operation of each of the methodologies. The renting price of the LHS includes all the necessary equipment integrated in the LHS that is used for the determination of adsorption isotherms. For the microfluidics systems a shorter depreciation period was considered for the tubings

and wafers due to the greater wear that these are subjected to and, therefore, shorter lifetimes. The equipment necessary for the fabrication of the mastermold, which is often very expensive, was not considered. The costs of the device used for the preparation of the resin plugs for the LHS and Eppendorf studies were not considered. The materials cost estimation is based on the materials and consumables needed to perform the experiments. The labor cost estimation is based on the hours needed of active labor, which is the time that an operator needs to actively work for the determination of the adsorption isotherms. For all the systems the reagent preparation (buffer and protein solutions) was considered. For the LHS studies, the operation was considered as the necessary time to prepare the LHS, resin plug preparation and supervision of initial stages of the operation, to ensure everything runs without errors. For the microfluidics studies, the chip production was considered, as well as microchip operation. The latter includes the time that the operator is required to operate the system and does not include the incubation time. For the Eppendorf studies, besides the reagent preparation, the pipetting of the solutions used for the study was also considered. The operation included the preparation of the resin plugs, the loading of the plugs to different Eppendorf tubes, and operating the rotor. The removal of the supernatant and subsequent dilution (when needed) of the solution in the 96 well-plate was also considered. A rate of 25€/h of labor costs was considered for the present study. The considered equipment, materials and labor hours per isotherm for each methodology are summarized in **Table 4.3**.

The cost determination of the protein isotherms was based on the three components described above. This was done for two different scenarios: one where a "cheap" protein was considered (*e.g.,* Lysozyme, which costs 0.03 €/mg) and another where an "expensive" protein was considered (*e.g.,* mAb, which was estimated to cost 2.29 €/mg, based on the average price of the infliximab biosimilar in 2016 [30]). This was considering the determination of 100 protein adsorption isotherms per year. Besides this, an estimation of the variation of the cost per isotherm with the number of isotherms determined per year was also performed.

It is possible to see that, out of all the 4 options, the LHS have the highest material cost, for both scenarios (**Figure 4.7**). This is because of the significantly larger liquid and resin volumes used by the technique (800 µl and 20.8 µl versus 56µl and 0.2 µl, respectively) per data point. The Eppendorfs also use the same amount of liquid and resin volumes, but require less disposables than the LHS, hence why the materials costs are lower. This difference becomes less evident for the "expensive" protein scenario since the costs related to the sample represent the higher portion of materials costs for these two methods (LHS and Eppendorfs). However, the lesser consumables use comes at the expense of added labor and, consequently, higher labor costs.

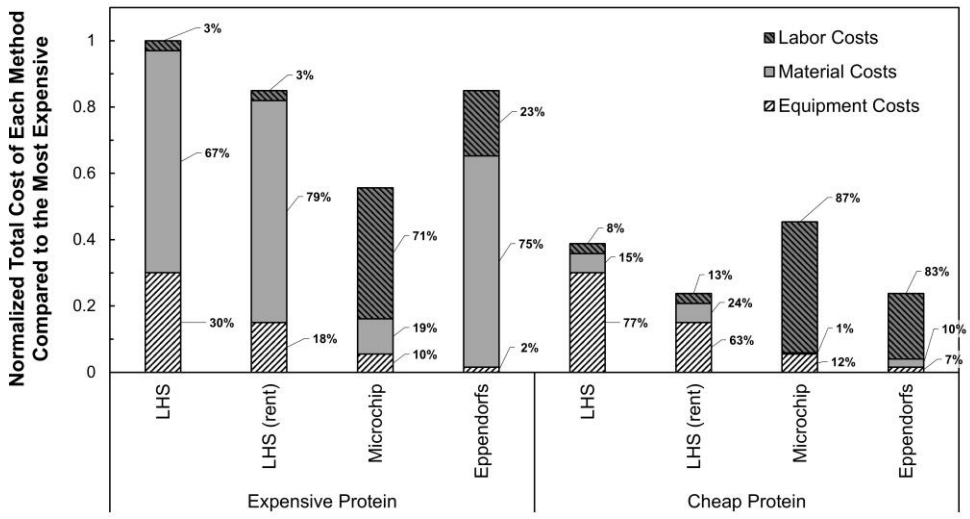

Figure 4.7 - Breakdown of the costs for the determination of protein adsorption isotherms, for a LHS (purchasing and renting), microfluidic chip and Eppendorf tubes, for a base case of 100 isotherms determined per year. The costs are normalized relative to the methodology of the scenario that has the highest overall cost (LHS for the Expensive Protein scenario). Left – Scenario for the "expensive" protein; the most expensive method for this scenario was the LHS (purchasing), with an isotherm estimated to cost 665€. Right – Scenario for the "cheap" protein; the most expensive method for this scenario was the microfluidic chip. The percentages show what is the percent contribution of the Labor, Materials and Equipment cost for each methodology in each scenario (e.g., for LHS in the "cheap" protein scenario, 8% of the isotherm costs were Labor costs, 15% Material costs and 77% Equipment costs).

The advantage of automation is reflected in the lower labor costs of the LHS in both scenarios and proves to be an advantage when low-value proteins are studied. On the other hand, the miniaturization of the adsorption studies proves to be very advantageous when high-value proteins are studied. Increasing protein costs will change the cost driver of LHS and Eppendorf to the materials whereas the cost driver of the microfluidic chip will always be the labor costs. The labor needed for the isotherms studies considered the microfluidic chip methodology as it was previously described. However, this could be reduced by increasing the automation of the system, bringing the Labor costs down. Therefore, the cost performance of the LHS is dependent on the materials' prices. Consequently, a high degree of miniaturization is preferred for very expensive proteins and a high degree of automation is preferred for cheap materials.

An increased number of isotherms to be determined per year also contributes to a "dilution" of the costs per isotherm for the LHS (see **Figure 4.8**). This is mainly due to a decreasing contribution of the equipment costs for an increasing number of isotherms determined per year. As expected, the microfluidics costs per isotherm plateau at a relatively low number of isotherms to be determined per year; this is because the labor

Table 4.3 - Overview of the needed equipment, materials and labor hours needed for the determination of protein adsorption isotherms for the different methodologies studied.

Equipment Costs

Method	Equipment	Cost (€)	Depreciation	Part used for isotherm	yearly equipment cost
LHS	LHS	400000	10	0.5	20000
LHS (rent)	LHS	10000	-	1	10000
Microfluidic chip	Peristaltic Pump	3508	10	1	350.8
	UV-Detector	15000	10	1	1500
	Other (tubes,	1000	1	1	1000
	Wafer	410	0.5	1	820
Eppendorf	Multi-well Plate Reader	10000	10	1	1000
	Rotor	586	10	1	58.6

Labor Hours

Method	Task	Hours spent per Task per isotherm
All	Reagent prep	1
LHS (Purch. & Rent.)	Operation	1
Microfluidic chip	Microchip production	0.5
	Operation	9
Eppendorfs	Pipetting to Eppendorf tubes	1
	Removing supernatant	1.5
	dilution to UV-Plate	0.75
	Operation	1

Table 4.3 (cont.) - Overview of the needed equipment, materials and labor hours needed for the determination of protein adsorption isotherms for the different methodologies studied.

Materials		
Method	Materials needed	Amount needed per isotherm
All	Resin	Dependent on methodology
	Buffer	Dependent on methodology
	Protein	Dependent on methodology
LHS (Purch. & Rent.)	Filter plate	0.5 (pieces)
	UV plate	0.5 (pieces)
	Deep-Well Plate	0.5 (pieces)
	Disposable Tips LHS	0.5 (pieces)
Microfluidic chip	PDMS + Curing Agent	7.5 g
Eppendorfs	Eppendorf tubes	48 (pieces)
	UV plate	0.5 (pieces)

costs are the main cost driver and the labor per isotherm is independent of the number of isotherms to be determined per year. A similar trend can be observed for the Eppendorfs, as the main cost driver for the cheap protein is labor, but for the expensive protein is the materials. For the renting of the LHS, it was considered that only 120 isotherms could be determined in a 3-month rental period (2 isotherm per day for a 60 working day period). Renting the equipment two times a year would already bring the yearly costs of the equipment to the same level as purchasing the LHS, which would then be considered to be more cost-effective. It is important to mention that maintenance costs are not being considered for this study, which could impact more the yearly equipment costs of owning the equipment and for renting this would not represent added costs.

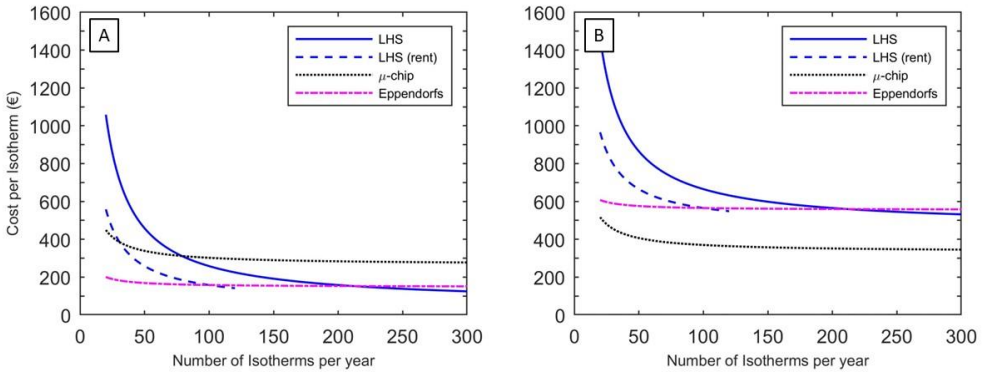

Figure 4.8 - Variation of the price per isotherm with increasing number of isotherms determined per year, for the 4 different methodologies considered. A minimum number of 20 isotherms to be determined per year was considered and for the LHS rent, a maximum number of 120 isotherms per year was considered. A – Scenario for the "cheap" protein; B – Scenario for the "expensive" protein.

4.3.6. Key Features of the Different Methodologies

LHS remain the *status-quo* for chromatographic process development for industry and academia. The LHS rely on their high degree of automation and precision and have a higher Technology Readiness Level than the other two methodologies presented in this study. Furthermore, and since it has been widely used by industry and academia for more than a decade, there is a wide variety of consumables dedicated to chromatographic process development. However, the equipment has a high price tag, which is not affordable for every lab.

Microfluidics has been taking steps in the field of bioengineering and there are some microfluidics devices that are commercialized (mainly for analytics [14]). At a lower TRL, the microfluidic chips present, generally, a low level of automation, and on-chip automation can hinder the versatility of the devices. If the operation of the microchips can have a higher level of automation, the labor costs can be reduced further.

Nevertheless, microfluidics still offers the highest degree of miniaturization possible, which in the case of this study, that used an external source for fluid pumping, still reduced the liquid volume to 56 µl. The tested devices were used only once, but further testing for the removal of the beads from inside the channel, by reverse flow, could prove that the devices are reusable. Since PDMS has a high compatibility with acid and base, the microfluidic chip can be cleaned with most solutions used for the removal of proteins and regeneration of chromatographic resins. The use of solvents may pose a problem for PDMS, as these can react with PDMS (e.g., acetone). However, using lower concentrations of these solves (e.g., 70% v/v EtOH) for short periods of time should be sufficient for the intended purpose and still safe to the PDMS chip. Using different materials for the microfluidic chip (e.g., glass or quartz) would also improve the microchip's mechanical and chemical resistance.

If the devices can be reused, it would help to reduce the labor costs. Furthermore, a common approach for microfluidics is parallelization, which for this case could also be an interesting option, provided that a system could be designed to allow this. Microfluidics is still trying to pave the way into HTS for chromatographic processes and the high skill required to design and produce the designs makes it a less attractive alternative. This could be overcome with outsourcing and mass production of the devices or by finding alternative production techniques (like 3D printers).

Of all the methodologies in this work, Eppendorfs proved to be the one with the lowest level of automation. The need to prepare all the solutions by hand, removal of supernatant and subsequent dilution in the UV-plate (when needed) required tremendous amounts of pipetting, leading to lengthy runs in the lab and tedious and cumbersome work. However, it made up by being the methodology with the most easily accessible materials (which are common in every lab) and the lowest equipment costs of the three methodologies.

4.4. Conclusions

Lysozyme and mAb adsorption isotherms were successfully determined using three different methodologies: microfluidic chip, Liquid-Handling Station, and Eppendorf tubes. An in-house designed and produced microfluidic chip showed comparable results to the other two methodologies. Inline monitoring of the absorbance of the protein solution allowed the microfluidics setup to estimate the time to equilibrium required for the different systems. This can be especially relevant when systems that are not reported in the literature are studied (e.g., the mAb used in this study), thus allowing for saving time and material for such study in a LHS. Industry perceives microfluidics as a viable option to contribute to HTPD [31], and our study showed that microfluidics can compete with the *status-quo* of HTPD for chromatography.

For the correct estimation of adsorbed protein, accurate protein concentration in the liquid phase is needed (usually achieved by using spectrophotometry) as well as accurate resin volume determination. For the latter, devices for the generation of resin plugs are used for the LHS (and the same device was used for the Eppendorf experiments in this study), but microfluidics resin volume determination was often imprecise [18] or cumbersome [17]. By implementing the Image Analysis in our studies, we were able to accurately estimate the resin volume in each microfluidics experiment.

The microfluidic chip allowed to perform protein adsorption studies to chromatographic resin using only 200 nl of resin and with a total system volume of 56 µl. This represents a 100-fold reduction in resin and a 15-fold reduction in solution. Such large reductions in material and sample proved to be advantageous when considering the cost of isotherm studies for expensive proteins. However, the large labor costs meant that it was not cost-competitive when cheap proteins were studied. Of the three methods used, microfluidics presents the lowest TRL. Further studies could help increase automation of the proposed system, thus reducing labor costs of microfluidics. The large level of automation offered by LHS is still very attractive, and depending on the desired total use, investing in one can be the best option. However, if no intensive studies are needed year-round, renting a LHS can be a viable option and the most cost-competitive (**Figure 4.8**). Although the Eppendorf studies showed a good cost performance, the experimental work involved in the isotherm studies does not allow for a good throughput and more workers would be needed.

Of the three methodologies, Eppendorfs are the least attractive but could still be used for lower throughputs if companies or academia are not willing to invest in a LHS or the microfluidic chip. For intensive studies on protein adsorption isotherms, the LHS is still the best option, since an increase in throughput (if needed) does not directly translate in an increase in labor. On the other hand, if the studied protein is very expensive and/or the amount of material is very low (e.g., due to low expression levels or in early stages of process development), the proposed microfluidic chip, in its current TRL stage, is an attractive alternative to the LHS. Further studies and improvements in the microfluidic chip production and possible parallelization could increase the competitiveness of the microfluidic chip, even for studies involving cheaper samples. This study showed that the microfluidic chip was able to generate protein adsorption isotherms using a fraction of the materials required by other methodologies.

4.5. Acknowledgements

This work has received funding from the European Union's Horizon 2020 research and innovation program under the Marie Skłodowska-Curie grant agreement No 812909

CODOBIO, within the Marie Skłodowska-Curie International Training Networks framework.

4.6. References

[1] A.L. Grilo, A. Mantalaris, The Increasingly Human and Profitable Monoclonal Antibody Market, Trends in Biotechnology 37(1) (2019) 9-16. https://doi.org/10.1016/j.tibtech.2018.05.014.

[2] G. Jagschies, E. Lindskog, K. Lacki, P.M. Galliher, Biopharmaceutical Processing: Development, Design, and Implementation of Manufacturing Processes, Elsevier2018. https://doi.org/10.1016/C2014-0-01092-1.

[3] K.M. Łącki, High throughput process development in biomanufacturing, Current Opinion in Chemical Engineering 6 (2014) 25-32. https://doi.org/10.1016/j.coche.2014.08.004.

[4] A.T. Hanke, M. Ottens, Purifying biopharmaceuticals: knowledge-based chromatographic process development, Trends in Biotechnology 32(4) (2014) 210-20. https://doi.org/10.1016/j.tibtech.2014.02.001.

[5] A.A. Shukla, J. Thömmes, Recent advances in large-scale production of monoclonal antibodies and related proteins, Trends in Biotechnology 28(5) (2010) 253-261. https://doi.org/10.1016/j.tibtech.2010.02.001.

[6] B.K. Nfor, J. Ripić, A. van der Padt, M. Jacobs, M. Ottens, Model-based high-throughput process development for chromatographic whey proteins separation, Biotechnology Journal 7(10) (2012) 1221-1232. https://doi.org/10.1002/biot.201200191.

[7] J.F. Kramarczyk, B.D. Kelley, J.L. Coffman, High-throughput screening of chromatographic separations: II. Hydrophobic interaction, Biotechnology and Bioengineering 100(4) (2008) 707-720. https://doi.org/10.1002/bit.21907.

[8] D.L. Wensel, B.D. Kelley, J.L. Coffman, High-throughput screening of chromatographic separations: III. Monoclonal antibodies on ceramic hydroxyapatite, Biotechnology and Bioengineering 100(5) (2008) 839-854. https://doi.org/10.1002/bit.21906.

[9] G. Carta, A. Jungbauer, Protein chromatography: process development and scale-up, John Wiley & Sons2020. https://doi.org/10.1002/9783527630158.

[10] C. Chang, A.M. Lenhoff, Comparison of protein adsorption isotherms and uptake rates in preparative cation-exchange materials, Journal of Chromatography A 827(2) (1998) 281-293. https://doi.org/10.1016/S0021-9673(98)00796-1.

[11] J. Kittelmann, M. Ottens, J. Hubbuch, Robust high-throughput batch screening method in 384-well format with optical in-line resin quantification, Journal of Chromatography B 988 (2015) 98-105. https://doi.org/10.1016/j.jchromb.2015.02.028.

[12] B.K. Nfor, M. Noverraz, S. Chilamkurthi, P.D. Verhaert, L.A. van der Wielen, M. Ottens, High-throughput isotherm determination and thermodynamic modeling of protein adsorption on mixed mode adsorbents, Journal of Chromatography A 1217(44) (2010) 6829-50. https://doi.org/10.1016/j.chroma.2010.07.069.

[13] A. Creasy, G. Barker, Y. Yao, G. Carta, Systematic interpolation method predicts protein chromatographic elution from batch isotherm data without a detailed mechanistic isotherm model, Biotechnology Journal 10(9) (2015) 1400-1411. https://doi.org/10.1002/biot.201500089.

[14] T.C. Silva, M. Eppink, M. Ottens, Automation and miniaturization: enabling tools for fast, high-throughput process development in integrated continuous biomanufacturing, Journal of Chemical Technology & Biotechnology (2021). https://doi.org/10.1002/jctb.6792.

[15] N. Field, S. Konstantinidis, A. Velayudhan, High-throughput investigation of single and binary protein adsorption isotherms in anion exchange chromatography employing multivariate analysis, Journal of Chromatography A 1510 (2017) 13-24. https://doi.org/10.1016/j.chroma.2017.06.012.

[16] L.J. Millet, J.D. Lucheon, R.F. Standaert, S.T. Retterer, M.J. Doktycz, Modular microfluidics for point-of-care protein purifications, Lab on a Chip 15(8) (2015) 1799-1811. https://doi.org/10.1039/C5LC00094G.

[17] H.S. Rho, A.T. Hanke, M. Ottens, H. Gardeniers, A microfluidic device for the batch adsorption of a protein on adsorbent particles, Analyst 142(19) (2017) 3656-3665. https://doi.org/10.1039/c7an00917h.

[18] I.s.F. Pinto, R.R. Soares, S.A. Rosa, M.R. Aires-Barros, V. Chu, J.o.P. Conde, A.M. Azevedo, High-throughput nanoliter-scale analysis and optimization of multimodal chromatography for the capture of monoclonal antibodies, Analytical Chemistry 88(16) (2016) 7959-7967. https://doi.org/10.1021/acs.analchem.6b00781.

[19] M.N. São Pedro, A.M. Azevedo, M.R. Aires-Barros, R.R. Soares, Minimizing the Influence of Fluorescent Tags on IgG Partition in PEG–Salt Aqueous Two-Phase Systems for Rapid Screening Applications, Biotechnology Journal 14(8) (2019) 1800640. https://doi.org/10.1002/biot.201800640.

[20] J. Romanowska, D.B. Kokh, R.C. Wade, When the label matters: Adsorption of labeled and unlabeled proteins on charged surfaces, Nano Letters 15(11) (2015) 7508-7513. https://doi.org/10.1021/acs.nanolett.5b03168.

[21] Y. Xia, G.M. Whitesides, Soft lithography, Annual Review of Materials Science 28(1) (1998) 153-184. https://doi.org/10.1146/annurev.matsci.28.1.153.

[22] A. Kecskemeti, A. Gaspar, Particle-based liquid chromatographic separations in microfluidic devices - A review, Analytica Chimica Acta 1021 (2018) 1-19. https://doi.org/10.1016/j.aca.2018.01.064.

[23] J.P. Kutter, Liquid phase chromatography on microchips, Journal of Chromatography A 1221 (2012) 72-82. https://doi.org/10.1016/j.chroma.2011.10.044.

[24] E. Sollier, C. Murray, P. Maoddi, D. Di Carlo, Rapid prototyping polymers for microfluidic devices and high pressure injections, Lab on a Chip 11(22) (2011) 3752-3765. https://doi.org/10.1039/C1LC20514E.

[25] T.E. Bankston, M.C. Stone, G. Carta, Theory and applications of refractive index-based optical microscopy to measure protein mass transfer in spherical adsorbent particles, Journal of Chromatography A 1188(2) (2008) 242-254. https://doi.org/10.1016/j.chroma.2008.02.076.

[26] F. Dismer, M. Petzold, J. Hubbuch, Effects of ionic strength and mobile phase pH on the binding orientation of lysozyme on different ion-exchange adsorbents, Journal of Chromatography A 1194(1) (2008) 11-21. https://doi.org/10.1016/j.chroma.2007.12.085.

[27] A. Gökaltun, Y.B.A. Kang, M.L. Yarmush, O.B. Usta, A. Asatekin, Simple surface modification of poly (dimethylsiloxane) via surface segregating smart polymers for biomicrofluidics, Scientific Reports 9(1) (2019) 1-14. https://doi.org/10.1038/s41598-019-43625-5.

[28] C. Her, L.M. Tanenbaum, S. Bandi, T.W. Randolph, R. Thirumangalathu, K.M. Mallela, J.F. Carpenter, Y. Elias, Effects of tubing type, operating parameters, and surfactants on particle formation during peristaltic filling pump processing of a mAb formulation, Journal of Pharmaceutical Sciences 109(4) (2020) 1439-1448. https://doi.org/10.1016/j.xphs.2020.01.009.

[29] N. Deiringer, W. Friess, Proteins on the rack: mechanistic studies on protein particle formation during peristaltic pumping, Journal of Pharmaceutical Sciences (2022). https://doi.org/10.1016/j.xphs.2022.01.035.

[30] M.I. Aladul, R.W. Fitzpatrick, S.R. Chapman, Impact of infliximab and etanercept biosimilars on biological disease-modifying antirheumatic drugs utilisation and NHS budget in the UK, BioDrugs 31(6) (2017) 533-544. https://doi.org/10.1007/s40259-017-0252-3.

[31] M.N. São Pedro, T.C. Silva, R. Patil, M. Ottens, White paper on high-throughput process development for integrated continuous biomanufacturing, Biotechnology and Bioengineering 118(9) (2021) 3275-3286. https://doi.org/10.1002/bit.27757.

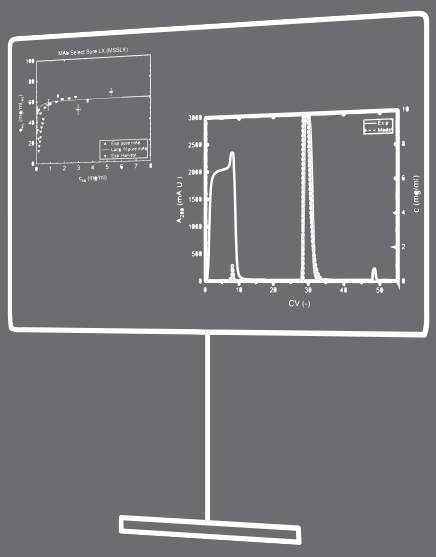
MAb Select SuRe LX (MSSLX)
CV (-)

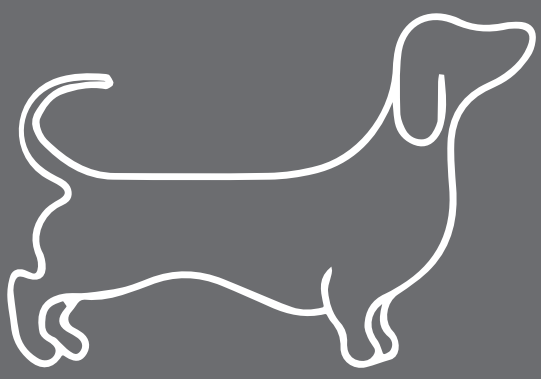

Chapter 5

Digital Twin in High Throughput Chromatographic Process Development for Monoclonal Antibodies

Abstract

The monoclonal antibody (mAb) industry is becoming increasingly digitalized. Digital twins are becoming increasingly important to test or validate processes before manufacturing. High-Throughput Process Development (HTPD) has been progressively used as a tool for process development and innovation. The combination of High-Throughput Screening with fast computational methods allows to study processes in-silico in a fast and efficient manner. This paper presents a hybrid approach for HTPD where equal importance is given to experimental, computational and decision-making stages. Equilibrium adsorption isotherms of 13 protein A and 16 Cation-Exchange resins were determined with pure mAb. The influence of other components in the clarified cell culture supernatant (harvest) has been under-investigated. This work contributes with a methodology for the study of equilibrium adsorption of mAb in harvest to different protein A resins and compares the adsorption behavior with the pure sample experiments. Column chromatography was modelled using a Lumped Kinetic Model, with an overall mass transfer coefficient parameter (k_{ov}). The screening results showed that the harvest solution had virtually no influence on the adsorption behavior of mAb to the different protein A resins tested. k_{ov} was found to have a linear correlation with the sample feed concentration, which is in line with mass transfer theory. The hybrid approach for HTPD presented highlights the roles of the computational, experimental, and decision-making stages in process development, and how it can be implemented to develop a chromatographic process. The proposed white-box digital twin helps to accelerate chromatographic process development.

Keywords: Harvest High-throughput Screening; High-Throughput Process Development; Lumped Kinetic Model; Overall Mass Transfer coefficient

---

This chapter has been submitted for publication: Silva, T.C., Eppink, M. and Ottens, M..

5.1. Introduction

The biopharmaceutical market has seen tremendous growth in the past 20 years, with more and more products getting approval from regulatory agencies [1, 2]. Monoclonal antibodies (mAbs) are important biopharmaceuticals that are used to treat a plethora of diseases, such as different types of cancer and autoimmune diseases [2]. MAbs are produced by cell culture, where a host (typically CHO cells) produces them and releases them into the cell culture. Together with the mAbs, many different components are present in the cell culture which cannot be present in the final product. For patient administration, mAbs have to be produced in a highly pure form.

The first step for the purification of mAbs is of great importance as it aims to separate it from all components present in a cell culture (media components, cell metabolites, Host Cell Proteins (HCP), etc.). It is desired to have a purification step that can both concentrate and purify the product to a good extent, further reducing the volumes to be handled downstream. Affinity chromatography is usually the preferred option, and Protein A (ProA) ligands' specificity to mAbs and robustness makes it a very attractive process choice [3, 4]. Even accounting for some disadvantages of ProA chromatography (expensive ligand, leaching of ProA) [5], efforts to dethrone this ligand as the first purification step of mAbs have been unsuccessful. Studies on the use of Cation-Exchange (CEX) and Multimodal (MM) ligands for the capture of mAbs from a complex mixture have demonstrated good results but still subpar compared to ProA results [6-8]. MM ligands are especially sensitive to changes in the loading conditions [8, 9]. Further chromatographic steps are used to polish the mixture, aiming at removing remaining HCPs, leached ProA, genetic material of the host, and aggregates. These are usually done with a combination of Ion-Exchange (IEX) and/or Hydrophobic Interaction (HIC) chromatography steps [2, 10, 11].

Process development strategies for biopharmaceuticals often relied on purely experimental work. Over the past 30 years, and with the emergence of robotic workstations, other tools have become available for chromatographic process development that aim at the miniaturization and automation of experiments [12]. Many studies have showed the applicability of High-Throughput Screening (HTS) for process development using Liquid-Handling Stations [13-17], as well as other tools, such as Eppendorf tubes [18, 19] and microfluidics [20, 21]. However, a purely empirical approach is both sample and time consuming. For that reason, High-Throughput Process Development (HTPD) uses a combination of HTS and mechanistic modelling to accelerate development and minimize costs [22, 23]. Ideally, one should aim at choosing the simplest model possible that still provides accurate results, as the computational data should be representative of the experimental data. More complex models will often require more experiments to calibrate but should also be more

accurate [24]. This is not always the case, as Altern *et al.* showed recently that a Steric Mass Action model (generally used for Ion Exchange ligands) provided the best description of the system, for the case of one of the multimodal chromatography resins tested with mAbs, compared to models that included terms for the hydrophobic interaction [25].

HTPD is usually done using pure protein solutions to determine parameters and investigate protein adsorption behavior. Important parameters that are then used in the adsorption model are hard to define mechanistically and are usually derived from HTS experiments. For process development to be both fast and effective, it is important to understand if the screening with pure mAb reflects what happens in the presence of other components. It still hasn't been shown in literature (to the authors' knowledge) that the equilibrium adsorption behavior of mAbs remains the same regardless of being in pure form or in the presence of Harvested Cell Culture (harvest). Furthermore, many different models have been reported for the description of chromatography [26-29]. The most complex model (General Rate Model – GRM) provides a full description of the transport of the molecule through the column and its adsorption to the resin, whereas the "ideal" model only provides information on convection and adsorption equilibrium [26, 28]. Lumped Kinetic Models (LKM) are less descriptive than GRM, usually lacking a detailed kinetic description of the system and several have been described [27, 28] and used extensively for the description of chromatography of different solutes and are broadly applicable [30-33]. Mass transfer parameters can be determined experimentally or using different correlations [26]. Adsorption models also take many shapes and depend on the type of molecule-ligand interaction, with more complex ligands (such as MM) needing more complex models for the description of the chromatographic behavior [13, 34, 35].

"Digital Twins" is an overarching term that can be broadly used within the biopharmaceuticals industry [36]. They are defined as an in-silico equivalent of a process and can be used for different purposes, such as virtual experiments and control [37]. Digital twins are often used in manufacturing for data management and life-cycle analysis, but its use in R&D is still limited[38]. With increasing computational power, digital twins have become more and more accessible from a computational point of view. Often, software that offers the "keys-in-hand" digital twins are limited and expensive, allowing for little customization which limits the "twinning" capabilities. The use of grey/white-box models allows for unprecedented levels of customization and increases process understanding at a cost of understanding any programming language. Industry seems to be reaching the inflexion point in the adoption of these models, with more and more companies willing to invest in in-house developed digital twins for process monitoring and development.

Taking into account all the design choices that can take place in process development of chromatography, this study presents a structured hybrid approach to HTPD for the capture and first polishing step of mAbs. It showcases the screening of dozens of different ProA and CEX resins and compares adsorption behavior of pure mAb and mAb in a harvest mixture for a number of selected ProA resins. It discusses the correlation of overall mass transfer parameter with equilibrium concentration. Finally, it shows the validation of the model and how the hybrid approach for HTPD helped to speed-up process development and how it can be used to screen more conditions without needing to perform experiments.

5.2. Theory

5.2.1. Hybrid Approach for High-Throughput Process Development

A hybrid approach was taken for the development of the chromatography step in this study. This kind of approach has been previously described [23], and can be applied to whole processes or to different processes or unit operations inside a larger process. The approach taken in this study is summarized in **Figure 5.1**. In this approach, three different separate parts are considered: experimental, computational, and (the often not mentioned) decision making. The decision making is always based on information provided by the experimental or computational parts of the hybrid approach. Important decisions such as "knock-out" criteria for the resins after HTS or which model to choose can influence the duration of the process development stage. For this case, the process development stage could be translated into: HTS, mathematical modelling of chromatography, *in-silico* column experiments, column experiments for model validation, final process design.

The first stage of our approach involved the selection of different ProA and CEX resins for HTS. Since HTS was available, the selection criteria for this weren't too tight, and the criteria to leave out some resins was mainly based on operating constraints of the resins (pressure limitations, cleaning conditions, etc.) rather than adsorption parameters provided by the manufacturer. If enough sample is available and there is the possibility to HTS the resins, it is always advisable to screen the resins. There can be some unexpected positive/negative results, and to build a wide database on adsorption is always desirable. After HTS and data processing, the first "real" decision making stage arises, based on the adsorption data. Out of all the resins screened, the best candidates were the ones that showed a high enough q_{max} and and with the most rectangular isotherm shape.

After, there is the need to select an appropriate model for the chromatographic system. There is an abundance of models to choose from, and the choice will depend on the

case study and available resources (more complicated models require higher computational power) [26]. After the model is built, some column experiments are required to calibrate the model. The choice of the model is important since, generally speaking, the more complex a model is, the more experiments are needed for its calibration. This comes from a higher characterization of all phenomena involved in chromatography, which in turn means that more parameters need to be estimated [26]. From these column experiments, the necessary parameters are fit, finalizing the model building stage.

Finally, some *in silico* runs can be performed. This is the time to evaluate if the output of the model matches the steps defined by the user and if the model appears to be working. Provided that everything is in order, experimental runs with the same conditions as the ones from the *in-silico* runs are performed, and the results can be compared. If the results are comparable to the user's satisfaction, then different conditions can be tested and a decision on the best process for the case study can be made.

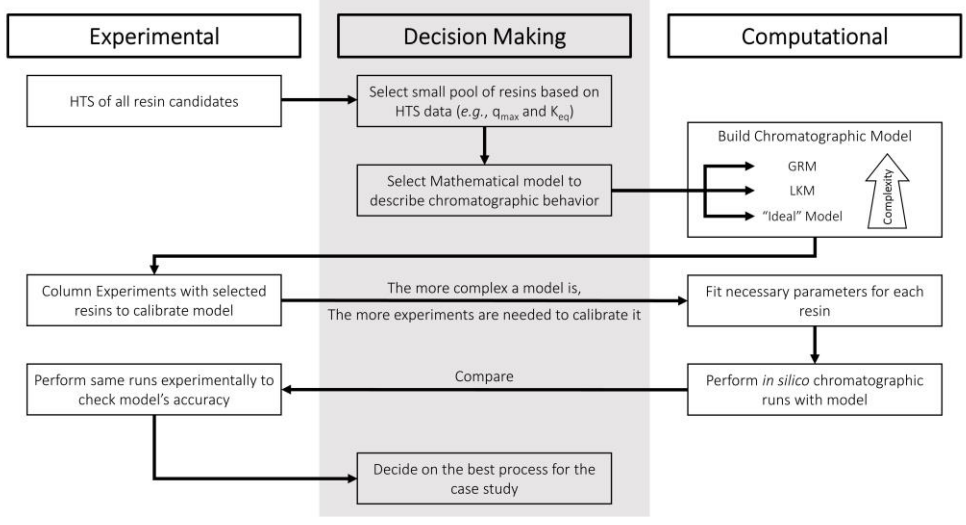

Figure 5.1 - Hybrid Approach for Process Development of Chromatography. HTS – High-Throughput Screening; GRM – General Rate Model; LKM – Lumped Kinetic Model.

5.2.2. Adsorption Column Model

The chosen model had to be as accurate and simple as possible. Naturally, the most complex models are very accurate, such as the General Rate Model (GRM). However, these models are often the most complex and simplifications have been proposed [38], such as the Lumped Pore Model and the Lumped Kinetic Model (LKM). For this work, the Transport-Dispersive Model (TDM) was chosen. TDM is a LKM, which in this case the simplification assumes that there are no intraparticle pores ($\varepsilon_p = 0$), meaning that there is no longer a separate mass balance for the pores. This model is simpler than the

GRM but will still provide enough accuracy to describe the system, and is shown in equation (1):

$$\frac{\partial c}{\partial t} = -u_{int} \cdot \frac{\partial c}{\partial x} + D_L \cdot \frac{\partial^2 c_i}{\partial x^2} - \frac{1-\varepsilon}{\varepsilon} \cdot \frac{\partial \bar{q}}{\partial t} \quad (1)$$

where, c is the concentration of protein in the liquid (mg/ml), ε is the bed porosity, u_{int} the interstitial velocity of the mobile phase (m/s), and D_L is the axial dispersion coefficient (m^2/s). The mass transfer in this system is described by the Solid-Film Linear Driving Force (SLDF) model [28]. The average solid phase concentration $\bar{q}$ is described in the following equation:

$$\frac{\partial \bar{q}}{\partial t} = k_{ov} \cdot (q - \bar{q}) \quad (2)$$

Where q is the interface concentration in the stationary phase, k_{ov} is a lumped mass transfer coefficient (designated overall mass transfer coefficient) (s^{-1}).

The adsorption equilibrium can be described using many different models. The Langmuir isotherm model is a relatively simple adsorption model that is based on a number of assumptions [26], that usually can describe the adsorption of pure mixtures accurately. It is often used for affinity chromatography due to the ligands specificity. Furthermore, it is safe to assume that no competitive adsorption will happen with the ProA or the CEX ligands (for this case study), discarding the need to use more complex models. Therefore, the concentration of protein at the interface of the resin (q) is in equilibrium with the concentration of protein in the bulk of the liquid (c) and can be estimated using the Langmuir isotherm equation:

$$q_{eq} = \frac{q_{max} K_{eq} c_{eq}}{1 + K_{eq} c_{eq}} \quad (3)$$

where q_{max} is the maximum adsorption capacity (in mg/ml_{resin}), and K_{eq} is the adsorption equilibrium constant of the resin (in ml_{liquid}/mg). D_L was assumed to be 4 times the product of u_{int} and d_p, where d_p is the adsorbent's particle diameter (in m) [27, 40]. The column is assumed to be free of protein at the initial time point $\left(c|_{t=0,\ 0\le x\le L} = 0 \text{ and } q|_{t=0,\ 0\le x\le L} = 0\right)$ and the boundary conditions of the column are described by the Danckwerts boundary conditions for dispersive systems [41]:

for $x = 0$

$$c = c_{inlet} + \frac{D_L}{u_{int}} \cdot \frac{\partial c}{\partial x} \quad (4)$$

for $x = L$

$$\frac{\partial c}{\partial x} = 0 \quad (5)$$

where x the axial position, and L the length of the column. The column was modelled as a loading-elution operation, with c_{inlet} given by:

for $t_{Eq} \leq t \leq t_{Eq} + t_{pulse}$

$$c_{inlet}(t) = c_{feed} \quad (6)$$

for $t_{Eq} > t$ or $t > t_{Eq} + t_{pulse}$

$$c_{inlet}(t) = 0 \quad (7)$$

where c_{inlet} is the feed concentration of protein, and t_{Eq} and t_{pulse} are the equilibration time and pulse time, respectively. The pulse duration is given by $t_{pulse} = \frac{V_{inj}}{F_{v_{inj}}}$, where V_{inj} is the injection volume and $F_{v_{inj}}$ the volumetric flow rate of the injection step.

The partial differential equation (equation (1)) is dependent on time and axial position. Spatial discretization using the method of lines was used to transform the partial differential equations (PDEs) into ordinary differential equations (ODEs). The first and second order spatial derivatives were discretized using a fourth-order central difference scheme, with 100 grid points (N), and a step size of $\Delta x = \frac{L_c}{N}$, where L_c is the length of the column. This ODE together with SLDF equation ODE comprise the set of ODEs to be solved. The set of ordinary differential equations was solved in MATLAB® R2021a using *ode15s* as the ODE solver.

5.3. Materials and Methods

5.3.1. Materials

The monoclonal antibody (M_w of 148 220 Da, pI ≈ 8.6) used in this study was provided by Byondis B.V., Nijmegen, The Netherlands, both in purified form and with the Clarified Cell Culture (harvest). A summary of the resins used for the HTS studies can be found in **Table 5.1**.

For breakthrough curve (BTC) experiments, 1 ml MAbSelect SuRe pcc (MSSpcc) and MSPrismA HiTrap® columns from Cytiva, Uppsala, Sweden, were used. The bed height is 25 mm, the inner diameter 7 mm, and the bed volume 1 ml. The MSS column was packed using the resin mentioned above in an Omnifit™ column housing from Thermo

Fisher Scientific, Waltham, MA, with an inner diameter of 6.6 mm, a bed height of approximately 2.8 cm and a bed volume of approximately 0.96 ml. The asymmetry of all columns was measured with a pulse experiment using 25 µl of a 1% acetone solution and a 1 M NaCl solution, and was within specifications for all columns.

5.3.2. Buffers and solutions preparation

The different buffers and solutions were prepared by dissolving the appropriate amount of chemicals in Milli-Q water. For the protein A resin studies, a 1x Phosphate Buffer Saline (PBS) buffer was prepared and the pH corrected to 7.14 for all the experiments, to mimic the pH values of the harvest solution. For the CEX resin studies, a 25 mM NaOAc solution with 20 mM NaCl at pH 4.5 was prepared, to mimic the solution properties of the eluate of protein A after viral inactivation and subsequent pH correction. The elution buffers used for the protein A and CEX resins were 25 mM NaOAc, pH 3.5 and 25 mM NaOAc with 1M NaCl, pH 4.5, respectively.

Table 5.1 - Summary of the resins used in the HTS studies. (*) - resins that are multimodal CEX resins.

Mode	Resin Name	Manufacturer
ProA	MAbSelect SuRe (MSS) MAbSelect PrismA™ (MSPrismA) MAbSelect SuRe LX (MSSLX) Capto™ L	Cytiva, Uppsala, Sweden
	Eshmuno® A (EMA)	Merck KGaA, Darmstadt, Germany
	CaptivA® PriMAB (CPMAB)	Repligen, Waltham, Massachusetts
	Praesto® AP (PAP) Praesto® Jetted (PJet)	Purolite, King of Prussia, PA
	KanCapA (KCA)	KANEKA, Tokyo, Japan
	Amsphere™ A3 (Amsphere ProA – ASPA)	JSR Life Sciences (Sunnyvale, CA)
	Toyopearl AF-rProtein A-650F (AF650F)	Tosoh Biosciences, Tokyo, Japan
	POROS™ MabCapture™ A (POROSA)	Thermo Fisher Scientific, Waltham, MA
CEX	SP Sepharose FF (SPSephFF) SP Sepharose Big Beads (SPSephBB) CM Seph FF (CMSephFF) Capto™ S ImpAct (CapSImp) CM Sephadex C-25 (CMSeph25)	Cytiva, Uppsala, Sweden
	Fractogel® EMD COO- (M) (FractoEMD) Eshmuno® S (EshS) Eshmuno® HCX (EshHCX) (*) Eshmuno® CPX (EshCPX) Eshmuno® CP-FT (EshCPFT)	Merck KGaA, Darmstadt, Germany
	Toyopearl Mx-trp-650M (ToyoMxTrp) (*) Toyopearl CM 650-S (ToyoCM) Toyopearl GigaCap-650M (ToyoGiga)	Tosoh Biosciences, Tokyo, Japan
	CHT Ceramic Hydroxyapatite Type II Media Nuvia™ S (NuS)	Bio-Rad Laboratories, Hercules, CA
	POROS™ 50 HS (POROS50HS)	Thermo Fisher Scientific, Waltham, MA

The provided mAb in purified form was buffer-exchanged to the buffer solutions mentioned above (depending on the resins studied) and diluted until the desired concentration was achieved. This was done using Vivaspin® 15 Turbo Centrifugal Concentrator from Sartorius (Gottingen, Germany) or Amicon® ultra-15 centrifugal filters from Merck KGaA (Darmstadt, Germany). A highly concentrated solution of mAb in PBS buffer was used to increase the concentration of mAb in the harvest for the HTS experiments using the harvest.

5.3.3. Analytical Methods

Protein concentration of pure samples was determined using a CTechTM SoloVPE® system (Repligen, Waltham, Massachusetts). The concentration, aggregation, and purity of the harvest HTS samples was determined by analytical size-exclusion (SEC) chromatography in a Acquity H-class bio system (Waters Corp., Milford, MA). 2 µl of sample was injected in a Tosoh TSKgel UP-SW3000 2 µm column (Tosoh Biosciences, Tokyo, Japan), using as running buffer a mixture of 400 mM NaCl, 15% Isopropanol, 150 mM PO4 buffer pH 6.2, a flowrate of 0.2 ml/min and absorbance of 280 nm. Protein concentration in the studies with pure mAb was determined using appropriate calibration curves obtained using the LHS (for the HTS studies) and the ÄKTA system (for the column studies).

5.3.4. Breakthrough Curve Experiments

The breakthrough curve experiments were performed in different ÄKTA systems: Avant 150, Avant 25, and Pure 25 (Cytiva). Protein concentrations from the ÄKTA were determined using appropriate calibration curves measured in each of the systems' UV detectors at 280 nm. BTCs at different feed concentrations (fixed flow rate) and different flow rates (fixed concentration) were performed, until a plateau in the outlet concentration was achieved (meaning the resin was saturated).

5.3.5. Adsorption Equilibrium Isotherms

Adsorption isotherms provide information on the equilibrium concentration of a solute adsorbed to a solid phase (chromatographic resin) at different liquid concentrations. To understand this, known amounts of protein and resin are contacted until an equilibrium is reached. Time to reach equilibrium can vary from system to system.

5.3.5.1. Batch Uptake Adsorption Equilibrium Isotherms

Batch uptake experiments contact a liquid with a given initial concentration with a known amount of resin. After sufficient time is given to the system to reach equilibrium, the concentration of the liquid phase can be measured and by using a mass balance it is

possible to estimate what is the amount of protein adsorbed to the solid phase, in the conditions tested (eq. (8)):

$$q_{eq} = \frac{V_l \times \left(c_{l,initial} - c_{eq}\right)}{V_r} \quad (8)$$

where, q_{eq} is the protein adsorbed to the resin in equilibrium (in mg/ml$_{resin}$), V_l is the volume of liquid (in ml$_{liquid}$), V_r is the volume of resin (in ml$_{resin}$), and $c_{l,initial}$ and $c_{l,eq}$ are the protein concentrations in the liquid phase in the beginning and after equilibrium is reached, respectively (in mg/ml$_{liquid}$).

Batch adsorption isotherm data was generated using a Tecan EVO Freedom 200 liquid-handling station (LHS) (Tecan, Switzerland). The LHS was equipped with an orbital mixer (Te-Shake), a multi-well plate reader (InfiniTe Pro 200), a robotic manipulator (RoMa) arm, two different liquid-handling arms (LiHa and MCA96) and a centrifuge system (Rotanta).

A known amount of resin (20.8 µL) was added to a 96-well filter plate (Pall Corporation, NY, USA) using a MediaScout® ResiQuot resin loader device from Atoll (Weingarten, Germany). To wash the resin, equilibration buffer was pipetted into the filter plate, and it was shaken for 10 min at 1200 rpm, after which the solution was removed using the vacuum system. This cycle was performed 3 times in total. Protein solutions were subsequently pipetted (600 µL) inside the well plates, and the plates were agitated at 1200 rpm until equilibrium was reached (minimum 24h). Once equilibrium was reached, the filter plate was placed on top of a 2 mL deep-well plate (Eppendorf AG, Hamburg, Germany) and these were centrifuged together using the centrifugation system. The supernatant was transferred from the deep well plates to a UV star plate and the equilibrium concentrations were measured using the plate reader. Equilibrium concentrations were estimated using appropriate calibration curves, obtained using the LHS. The results shown for the isotherms of all resins except MSSpcc were generated using this method.

5.3.5.2. Equilibrium Isotherms from Column Experiments

To determine the adsorption isotherms of MSSpcc, the resulting BTCs at different feed concentrations were used. The equilibrium concentration of the liquid phase is the feed concentration of the different trials. This is done by calculating the equilibrium binding capacity (EBC), which is the binding capacity at which 100% of the dynamic binding capacity (DBC$_{100\%}$) is achieved [27]. This can be estimated by calculating the area above the BTC (which corresponds to the adsorbed protein) (eq. (9)).

$$q_{eq} = \frac{m_{adsorbed}}{V_{resin}} = \frac{q_{EBC}}{V_{resin}} = \frac{\left(c_{feed} \cdot t_{DBC_{100\%}} - \int_0^{t_{DBC_{100\%}}} c_{out}\, dt\right) \cdot F_v}{V_{resin}} \quad (9)$$

where, c_{feed} and c_{out} are the feed and outlet concentration (in mg/ml), respectively, $t_{DBC_{100\%}}$ is the time it takes to reach 100% of DBC (in min), V_{resin} the volume of resin (in ml) and F_v the flow rate used (in ml/min).

5.3.5.3. Equilibrium Isotherms using Harvest

Equilibrium adsorption isotherms using the Harvest were obtained by contacting a mAb containing harvest solution with different ProA resins. Two different stock solutions were used: the original harvest solution, and a "spiked" harvest solution (with a c_{mAb} = 5 mg/ml). This solution was only 10% of the volume of the final "spiked" harvest solution. The isotherms experiments were performed using the same methodology described in (3.5.1 - Batch Uptake Adsorption Equilibrium Isotherms), with a few changes. Due to the inability to inject high protein content solutions in the UPLC system, a slight modification to the experimental procedure had to be done, compared to the pure mAb isotherms. After the 24h incubation period, the filter plates were centrifuged and the supernatant collected in the deep-well plates. Then, 600 µl of elution buffer was pipetted onto the filter plates and the resin was incubated for at least 1 h. The supernatant was then collected and analyzed using the UPLC system. Contrary to the pure mAb experiments, the adsorbed mass is used to calculate the c_{eq} of the harvest HTS trials:

$$q_{eq} = \frac{m_{adsorbed}}{V_{resin}} = \frac{V_{HTS_{eluate}} \times c_{HTS_{eluate}}}{V_{resin}} \quad (10)$$

$$c_{eq} = \frac{m_{init} - m_{adsorbed}}{V_{resin}} \quad (11)$$

where $m_{adsorbed}$ is the adsorbed mass to the resin (in mg), $V_{HTS_{eluate}}$ the volume of eluate used in the harvest trials (in ml), $c_{HTS_{eluate}}$ the concentration of mAb in the eluate in the harvest trials (in mg/ml) and m_{init} the initial mass of mAb present in each well for the harvest trials (in mg).

5.3.6. Parameter Estimation

The Langmuir isotherm parameters were regressed using the pair of c_{eq} and q_{eq} for each of the resins. This was performed using the *lsqcurvefit* function in MATLAB. The fitting function was the Langmuir isotherm, as shown in eq. (3). The error of the fitted parameters was calculated with an appropriate error propagation, described in 3.7 - Statistical Analysis. The overall mass transfer coefficient was estimated using the

experimental data from the BTC experiments at different feed concentrations. The *fmincon* function in MATLAB was used and the default tolerances (1e-6) were used for the fit.

5.3.7. Statistical Analysis

The reported uncertainties were calculated taking into account the systematic error and the statistical error resulting from random variation of measured values. The sample standard deviation and error propagation was calculated according to Young [42]. For the systematic error, only the uncertainty associated with the parameter regression of the calibration was considered, as other equipment errors were considerably smaller and thus negligible. The error of the regressed isotherm parameters was obtained using the variance-covariance matrix *M*, which is calculated by multiplying the variance of the residuals of the best fit with the Jacobian matrix (*J*) of the fitting function, as shown in eq. (12):

$$M = \frac{(J^T J)^{-1} \sum_{i=1}^{n} res_i^2}{n - p} \qquad (12)$$

where, n is the number of data points, and p the number of regressed parameters. The diagonal of the covariance matrix contains the variance of each parameter [43].

5.4. Results and Discussion

5.4.1. Adsorption Isotherms pure mAb

The approach mentioned in section 5.2.1 was followed. The first step was the screening of the different stationary phases of both ProA and CEX ligands. This was done using pure mAb solutions, which will provide some insight into the adsorption capacity and affinity of the different resins. The buffer choices were done already considering what would be found in a manufacturing scenario: the buffer chosen for the ProA experiments mimics the pH and conductivity of the harvest solution, and the buffer chosen for the CEX experiments mimics the salt content, pH and conductivity of the solution after viral inactivation and subsequent pH correction.

5.4.1.1. Protein A resins

The HTS results for the equilibrium adsorption isotherms ProA ligand resins are shown in **Figure 5.2** (Capto® L data shown in **Figure SI 5.1**). The isotherm data were fitted using the Langmuir isotherm (eq. (3)), and the fitted values can be found in **Table 5.2**. The results show that most of the resins possess highly favorable adsorption isotherms, which is in agreement with affinity chromatography (Praesto AP and CaptivA PriMAB are the exceptions, which are still favorable but with a less rectangular profile). This is

also confirmed by the high K_{eq} values for the resins, with some even in the order of magnitude of thousands. This is a mathematical artifact from the fitting of the experimental data to the Langmuir equation and is a consequence of the rectangular shape of the isotherm for these resins, which lack experimental points in the linear part of the isotherm, skewing the fitting.

Considering the performance of the resins, it is possible to see that MAb Select PrismA, MAb Select SuRe pcc, Praesto Jetted, and Praesto AP present the highest maximum capacity values for the studied mAb (between 65-95 mg/ml$_{resin}$), with MSPrismA and MSSpcc clearly outperforming the other resins and Praesto AP presenting a smaller affinity constant. CaptivA PriMAB, MAb Select SuRe, MAb Select SuRe LX, KanCapA, and Amsphere ProA all showed maximum capacity values in the middle range (between 52-62 mg/ml$_{resin}$), with the first presenting a smaller affinity constant than the rest. The remainder of the resins (Eshmuno A, AF-rProtein A-650F, POROS Mab Capture A, Capto® L) showed maximum capacity values in the lower range of all the tested resins (between 25-44 mg/ml$_{resin}$). This first screening stage served as a first step to understand which resins would be used for the isotherm studies using harvest solution.

Since the HTS for the harvest required more experimental effort, it was decided that 4 resins would be selected for the harvest study, out of the 13 resin pool: MSS, MSPrismA, MSSLX, and PJet. MSSpcc was not chosen because it was not available in bulk form (only in pre-packed column). The resins were chosen based on their maximum adsorption capacity and affinity constant. Although Praesto AP had a higher maximum binding capacity than MSSLX, the smaller affinity constant lead to it being discarded for this trial. MSS was selected because of its relevance and widespread use in industry-relevant processes.

5.4.1.2. CEX resins

The results with the different CEX ligands are presented in **Figure 5.3** (CM Sephadex C-25 and Toyopearl CM 650-S data shown in **Figure SI 5.2**). The isotherm data were fit using the Langmuir isotherm (eq. (3)), and the fitted values can be found in **Table 5.2**. Under the operating conditions (pH 4.5), the mAb is positively charged since the pH is below the pI. This means that it is expected that the adsorption isotherms will be favorable, and that is what can be seen from the experimental data. Only for the case of CM Sephadex C-25 (**Figure SI 5.2**) there was virtually no adsorption of mAb to the resin. This happened because CMSeph25 is a weak CEX resin, and the recommended operating pH is between 6 and 10, which means that the ligand will not be charged at pH 4.5, thus not adsorbing any protein. Four main clusters were chosen for the CEX resins, according to their ligand/backbone characteristics: **Figure 5.3 A** shows multimodal CEX resins, **Figure 5.3 B** shows sepharose resins, **Figure 5.3 C** shows

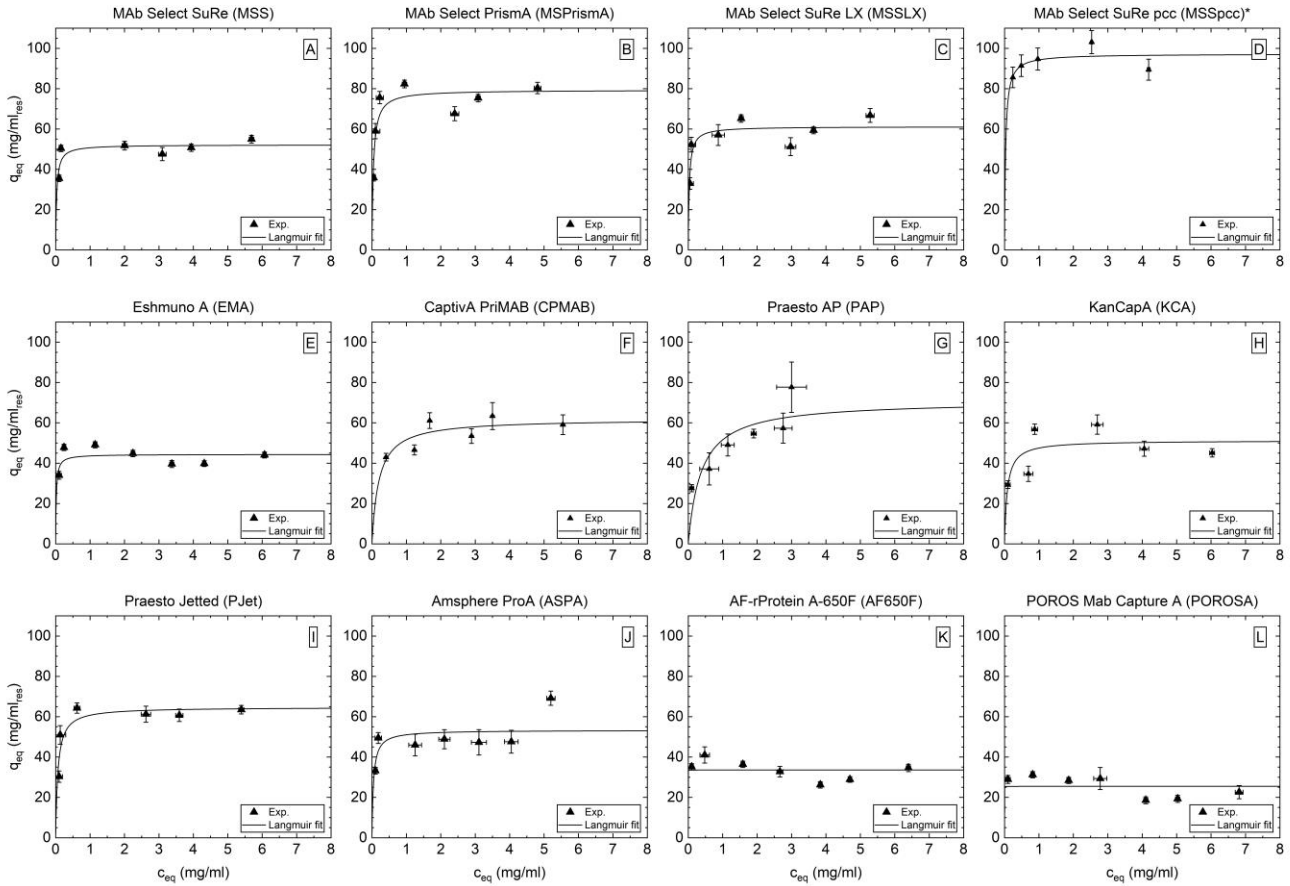

Figure 5.2 - Adsorption isotherms of mAb on different Protein A resins, in 1x PBS buffer, pH 7.14. Solid lines represent the fit of the experimental data to the Langmuir isotherm. A – MSS; B – MSPrismA; C – MSSLX; D – MSSpcc; E – EMA; F – CPMAB; G – PAP; H – KCA; I – PJet; J – ASPA; K – AF650F; L – POROSA.

resins with SO_3^- functional group, and **Figure 5.3 D** shows resins with sulfoisobutyl and sulfopropyl functional groups.

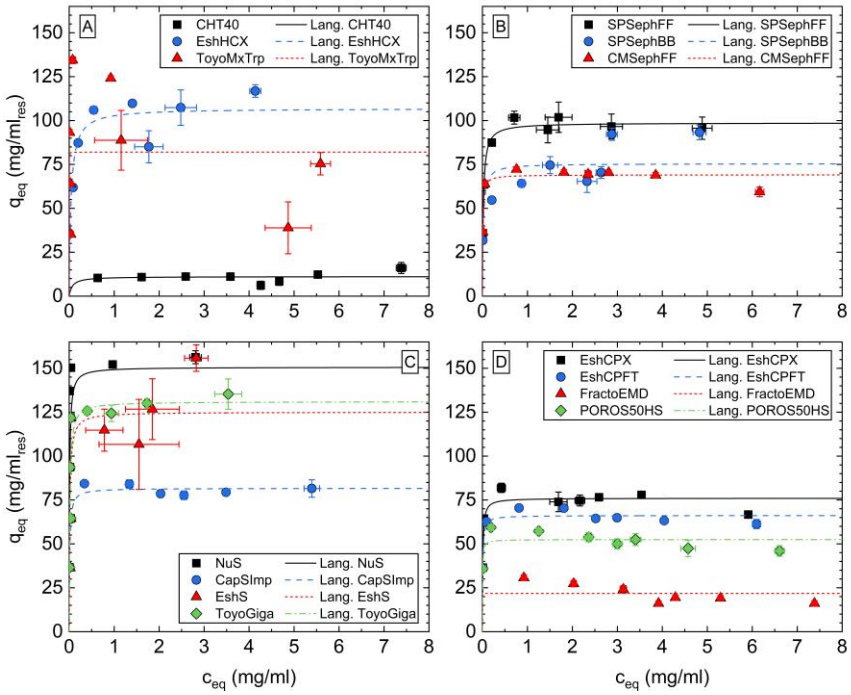

Figure 5.3 - Adsorption isotherms of mAb on different CEX resins in 25 mM NaOAc buffer, pH 4.5. A – Multimodal CEX resins; B – Sepharose resins; C – -SO3- functional group resins; D – Sulfoisobutyl (Eshmuno CPX and CPFT and Fractogel EMD COO-) and sulfopropyl (POROS 50 HS) functional group resins).

The Langmuir fits show rectangular shapes for all the tested resins, with 3 resins showing very sharp rectangular shapes: Toyopearl MX-trp-650M and Fractogel EMD COO^- in **Figure 5.3 A** and **D**, respectively, and Toyopearl CM 650-S in **Figure SI 5.2** right. For the last two resins, this is mainly a mathematical artifact from the Langmuir fit due to a lack of experimental data points in the low c_{eq} range. However, for Toyopearl MX-trp-650M there is a large amount of data over the low c_{eq} range with corresponding high values of q_{eq}, which then decrease at high c_{eq} values. Since the Langmuir fit is made for isotherms that have an asymptote shape (with cap on the fitted q_{max} value), the fit will then converge to the values of q_{max} and K_{eq} that minimize the error, resulting in such a Langmuir isotherm shape. From the manufacturer's data it is clear that the pH can influence drastically the adsorption capacity of ToyoMxTrp, with a pH change from 4.8 to 5 decreasing the binding capacity as much as 60% (from approx. 95 to 35 mg/ml) in a solution at roughly the same ionic strength [44]. Antibodies possess tenths and even up to one hundred buffering amino acid side chains per molecule [45], which means that despite the buffer's pH being 4.5, the solution's pH at higher mAb concentrations may

be different than the target 4.5. For experiments at higher c_{eq} a higher initial concentration of mAb is present in each well, possibly leading to a stronger effect of the buffering capacity of the mAb in the solution's pH value, explaining the lower q_{eq} values for this resin at higher mAb concentrations.

The resins with the SO_3^- functional group showed the highest maximum capacity of the different clusters, whereas the resins with sulfoisobutyl and sulfopropyl functional groups showed the most variability between the resins in terms of maximum capacity. It was expected that the adsorption capacity of SP Seph FF and SP Seph BB would be similar since the resins have the same ligand. However, we see that the adsorption of SP Seph BB is inferior to what is observed to SP Seph FF. Although the resin beads of SP Seph BB have a particle diameter of 100-300 μm, which is bigger than the 45-165 μm of SP Seph FF, the resins have different pore sizes, with pore size of SP Seph BB being reported at around 7 nm [46] and SP Seph FF pore size being reported at around 60 nm [47]. It is hypothesized that the smaller pore size hinders protein transport inside the SP Seph BB resin beads, thus preventing more protein to adsorb to the binding sites closer to the core of the resin leading to lower adsorption being observed.

Overall, the screening of CEX resins with pure solutions of mAb suits a logical choice for process development since it is expected that the solution will already be very pure after the ProA step. The same rationale applies to the buffer choices, since the goal is to have less buffer-exchanges in the whole purification train, as these are time consuming and expensive steps. There could be a more suitable buffer for each of the resins, but by choosing this buffer it is guaranteed that operationally it will require very little manipulation after the viral inactivation step. Furthermore, it was decided that no additional screening with CEX resins was needed since the goal was to generate a database that could handle a CEX step after a ProA step, and the ProA step generates a highly pure sample of mAb (confirmed by the results of the harvest adsorption equilibrium experiments).

5.4.2. Adsorption Isotherms Harvest – Protein A resins

Although the pure mAb experiments already give a good indication on the maximum binding capacity and affinity constants of each resin, it is important to understand if the adsorption behavior of mAb in harvest or pure solutions changes. To achieve this, it was decided to perform HTS with mAb in a harvest solution, using similar methodology to the one described for the pure mAb approach. Since the flowthrough of the filter plates for these experiments is a harvest solution with a multitude of components, a calibration curve using the UV plate reader was not possible.

Therefore, for the analysis of the equilibrium concentrations, the UPLC was used. However, the method used was SEC-UPLC and not Analytical Protein A

Table 5.2 - Summary of the Langmuir parameters fitted to the experimental data of mAb adsorption isotherms to the different Protein A and CEX resins. (*) – Isotherm of CaptoL shown in SI. (**) – Isotherms of CM Sephadex 25 and Toyopearl CM 650-S shown in SI (these resins have a functional group of carboxymethyl).

ProA		
Resin	q_{max} (mg/ml$_{res}$)	K_{eq} (ml/mg)
MSS	52.17 ± 1.15	34.39 ± 7.82
MSPrismA	79.35 ± 1.66	23.82 ± 3.27
MSSLX	61.19 ± 1.31	33.18 ± 5.62
MSSpcc	97.25 ± 2.02	31.79 ± 11.65
EMA	44.39 ± 0.96	55.23 ± 20.82
CPMAB	61.92 ± 1.82	5.00 ± 1.13
PAP	70.92 ± 5.32	2.66 ± 0.91
KCA	51.23 ± 2.32	12.75 ± 4.61
PJet	64.69 ± 1.75	15.30 ± 2.60
ASPA	53.32 ± 1.83	22.40 ± 6.98
AF650F	33.57 ± 0.96	9.87E+03 ± 7.21E+05
POROSA	25.47 ± 1.00	7.95E+03 ± 6.52E+05
CaptoL(*)	38.20 ± 2.12	66.20 ± 68.93
CEX		
Resin	q_{max} (mg/ml$_{res}$)	K_{eq} (ml/mg)
CHT40	11.13 ± 0.62	14.39 ± 20.72
EshHCX	106.89 ± 2.31	24.47 ± 4.12
ToyoMxTrp	82.04 ± 6.37	5.96E+03 ± 7.23E+04
SPSephFF	98.68 ± 0.66	49.74 ± 2.55
SPSephBB	75.48 ± 2.04	53.83 ± 15.80
CMSephFF	69.10 ± 0.72	126.44 ± 12.81
NuS	150.64 ± 9.80	106.75 ± 29.86
CapSImp	81.70 ± 0.52	86.66 ± 4.69
EshS	125.09 ± 6.26	74.45 ± 20.30
ToyoGiga	131.05 ± 4.09	73.86 ± 11.90
EshCPX	76.01 ± 0.84	109.07 ± 10.61
EshCPFT	66.17 ± 0.55	126.67 ± 10.92
FractoEMD	21.82 ± 1.56	9.70E+03 ± 1.36E+07
POROS50HS	52.47 ± 0.76	234.49 ± 44.18
CMSeph25(**)	0.00 ± 2.76E+07	0.00 ± 5.21E+04
ToyoCM(**)	19.84 ± 1.18	9.68E+03 ± 4.22E+06

Chromatography (APAC). In turn, this means that the equilibrium solutions could not be injected directly in the column due to their high protein content. Consequently, after incubation was achieved, the equilibrium solution was collected in a deep-well plate and the resin present in the 96WP was incubated with elution buffer, to desorb all mAb that adsorbed during the first incubation. After sufficient time was given for the desorption of mAb, the solution was collected in a different deep-well plate and the concentrations were measured using the SEC-UPLC. This means that, contrary to what happened for the pure mAb, this measurement provides information on what was adsorbed to the resins, rather than what remained in solution. The 4 resins chosen for the harvest study

were MSS, MSPrismA, MSSLX, and PJet. The reasoning behind the selection of these resins is discussed in section 5.4.1.1.

The results of the adsorption equilibrium isotherms with the harvest solution are shown in **Figure 5.4**. The results show very good agreement between the pure mAb experiments and the harvest solution experiments. Even though the harvest solution experiments required extra experimental steps, this seems to not have affected the results. These results also confirm what had been seen for the pure mAb experiments, with MSPrismA showing higher maximum adsorption capacity than the other three resins. The harvest data shows that the screening with the pure mAb gives enough confidence in the estimation of relevant adsorption parameters for ProA resins. This implies that for future ProA-based process development it is most likely not necessary to screen resins using the harvest solution.

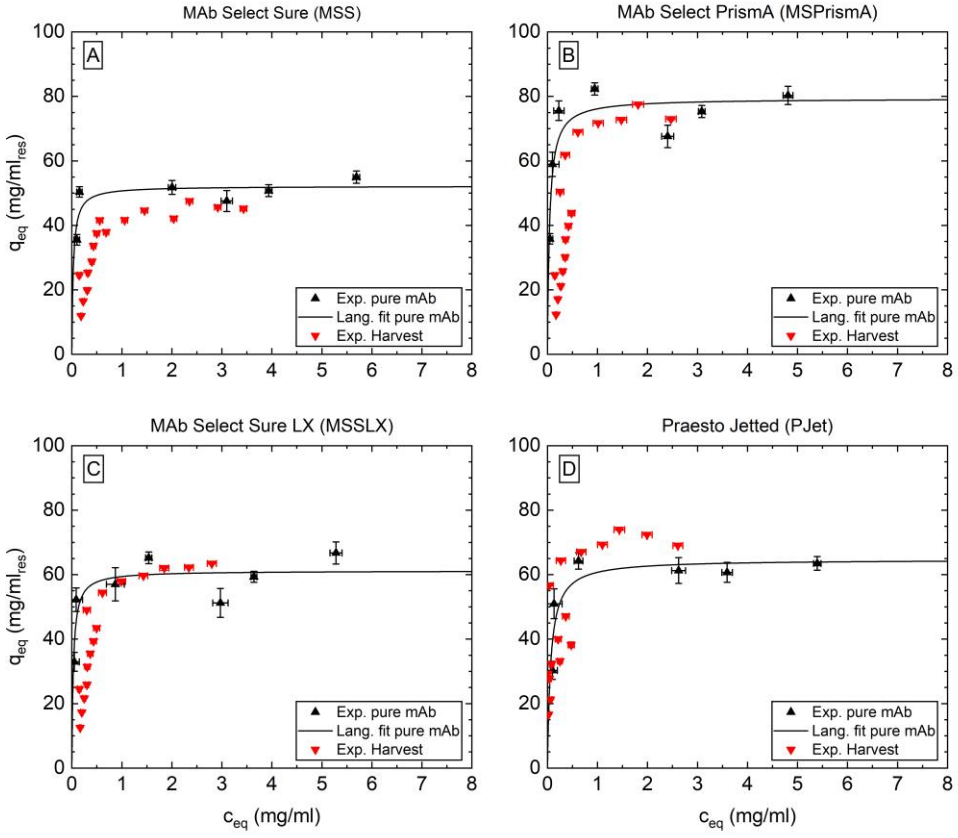

Figure 5.4 - Comparison of the adsorption of mAb to four different Protein A resins from pure sample and harvest. A – Mab Select SuRe (MSS); B – Mab Select PrismA (MSPrismA); C – Mab Select SuRe LX (MSSLX); D – Praesto Jetted.

5.4.3. Column Experiments

Following the hybrid approach described in section 5.2.1, after the first screenings and model choice are done, it is time to perform some column experiments (BTC) with the selected resins to calibrate the model. These usually involve, but are not limited to, experiments with varying loading concentration and constant flowrate and with constant loading concentration and varying flowrate. These experiments first serve as a check of the model suitability and, if that is confirmed, to estimate or fit some parameters that cannot be determined using mathematical correlations. In the case of the present work, these experiments were used to estimate the overall mass transfer coefficient of our system, since the axial dispersion coefficient was estimated using the correlation mentioned in section 5.2.2.

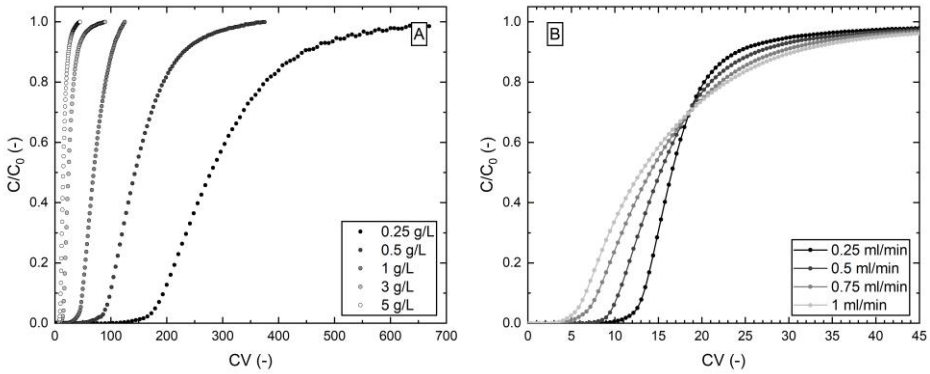

Figure 5.5 - Column experiments used for the calibration of the mechanistic model for MSPrismA with pure mAb solutions. A - Different initial concentration and constant flow rate (Fv = 0.5 ml/min); B - Different flow rate and constant concentration (cmAb = 5 g/L). Dots represent 100 data points from every experiment. In B, the line connecting the experimental data points is used to guide the reader's eye. C/C_0 – normalized concentration (concentration observed divided by inlet concentration). CV – column volumes.

The BTCs for MSPrismA are shown in **Figure 5.5** and for MSS and MSSpcc are shown in **Figure SI 5.3**. MSPrismA and MSSpcc were chosen because they showed the highest maximum adsorption capacity and MSS as the industry standard. The results of the experimental BTCs are in line with the expected results. As it can be seen in **Figure 5.5 A**, for less concentrated solutions, more column volumes (CV) will have to be flowed through the column to saturate all the resin's binding sites. **Figure 5.5 B** shows the BTCs at different flowrates (and, therefore, different residence times). It is noticeable that at higher flowrates (lower residence times), there is earlier breakthrough of protein from the column, and the shape of the BTC is less sharp (flatter). This can be attributed to the shorter times allowed for adsorption to take place, since the residence time is shorter. Other authors have also reported that some resins present a decrease in DBC with decrease of residence times [48-50]. A flatter BTC will lead to an under-utilization

of the resin in the column since less CV will be required to reach the defined %DBC defined for the process. The flowrate (or residence time) is an important parameter for the design of chromatography, mainly due to its influence in the shape of BTCs. This becomes increasingly important in the design of continuous chromatography systems that do not operate in flowthrough mode.

5.4.4. Parameter Estimation

The selected model for mass transfer in the present work was a lumped-parameter model. These models assume that changes in the concentration occur very near to the boundary of the solid-liquid interface but that far from this interface the system is "well-mixed", so that the concentration in the solid and liquid interface does not change the further we are from the interface [51]. It was assumed that the kinetics of adsorption and desorption was much faster than the mass transfer kinetics, therefore the model used was the Transport-Dispersive Model [28]. In the SLDF model, all contributing mechanisms for band broadening are lumped in a coefficient, which in the case of this work is defined by k_{ov}. The lumped phenomena include pore, solid, and free diffusivities, film mass transfer coefficient, among others [26, 28].

Correlations have been proposed to describe the overall mass transfer coefficient of LKMs, for example, based on the external film mass transfer coefficient [52], and have been extensively used [29, 31]. These correlations are proposed for the liquid-film linear driving force model. For the current work this was not applicable, since the SLDF was used.

Ruthven has described that the diffusivities are not independent of the solute's concentration, at either low or high solute concentration [52]. A recent study by Yu *et al.* also found that the diffusion coefficient of proteins is a function of the protein's concentration in solution, with a higher diffusion coefficient in more concentrated solutions [53]. For the SLDF model, concentration dependence between the rate coefficient and solute concentration has been previously described [28, 54, 55]. Furthermore, recent work has described this dependence in the rate coefficient expressions, for example with the rate depending on the partition ratio, which in turn depends on the solute concentration [56]. Other authors have also described this correlation in terms of mathematical equations for constant pattern behavior [57]. Furthermore, it has been reported that apparent diffusion coefficients are dependent on the isotherm chord, which in turn is dependent on the solute's concentration [28].

Therefore, it was concluded that the rate coefficient, in this case the overall mass transfer coefficient, had a concentration dependence. To evaluate this, the k_{ov} was fit to BTCs with varying protein concentration. The obtained values for k_{ov} VS c are shown in **Figure 5.6**. Comparing the results of the three different resins tested, it is noticeable

that the obtained values are different from resin to resin. This was expected because there are different phenomena playing a role in the mass transfer in chromatographic separations, from pore diameter, particle radius, among others, and these depend on the resin's characteristics. The results obtained from this work's estimation are similar to the ones obtained by Chen *et al.* [57], even though the authors present a modification to the model described by LeVan and Carta [56].

The fitting of k_{ov} to the experimental BTC was easily achieved and provided results with good confidence intervals. This method of determining the mass transfer coefficient eliminates the need to have laborious mathematical descriptions for this parameter, whilst providing accurate results without requiring extra experiments. The linearity of the correlation could be easily implemented in the model and provided good forecasting abilities even for concentrations that were not tested experimentally, thus adding to the predictive capabilities of the model.

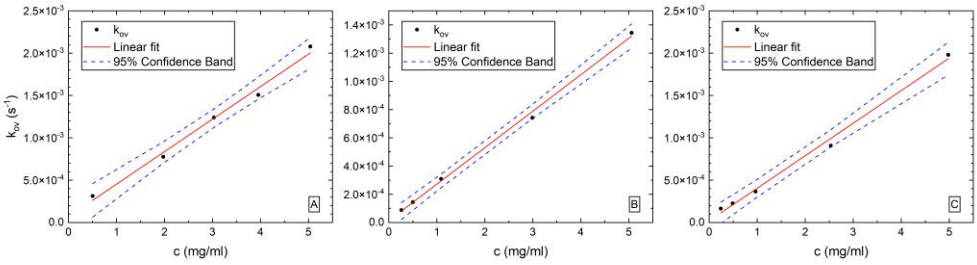

Figure 5.6 - Variation of k_{ov} with concentration for 3 different Protein A resins. A – MSS; B – MSPrismA; C – MSSpcc. The red line (—) represents the linear fitting and the blue dashed lines (- - -) represents the 95% confidence band of each fitting.

The k_{ov} estimated in the context of this work is a function of the feed concentration and it represents the k_{ov} averaged over the length of the column over the time it takes to fully saturate the column in the context of BTC experiments. This is, of course, a simplification of the physical phenomena responsible for mass transfer and adsorption inside the column. In reality, with the aforementioned references, the mass transfer parameters are a function of protein concentration. Since protein concentration changes along the length of the column and with time, due to the progression of the protein front through the column and the protein that gets retained through adsorption, one could say that the overall mass transfer coefficient (or any mass transfer coefficient, for that matter, such as film mass transfer coefficient or pore mass transfer coefficient) depends simultaneously on feed concentrations, axial position and time. The inclusion of this dependence in the k_{ov} parameter would increase the complexity of the fitting while not improving the accuracy of the model. The model presented in this work aims at providing the most accurate results possible with the simplest possible model, while still maintaining physical description of the system. The proposed correlation between k_{ov}

and feed concentration achieved this goal, hence why it was decided to use the presented model for the current study.

5.4.5. Model Validation

In **Figure 5.1** it is highlighted that the first "Computational" task is the choice of the model. In this step, prior knowledge of the system and of chromatography in general can play an important role into making a first choice of model as close to an appropriate one as possible. The LKMs offer detailed descriptions of chromatographic behavior at a low computational expense, compared for example with the GRM. The LKMs can be described by Linear Driving Force (LDF) models, based either on the liquid or solid phase concentration of protein. In the case of linear isotherms, the results are not expected to change much between the two LKM [27, 52]. However, the same does not hold for non-linear isotherms, which is almost always the case for the biopharmaceutical industry. For systems with favorable adsorption isotherms it has been described that the SLDF model is preferred when intra-particle resistance is the dominant mass transfer resistance [27]. In the case of this work, the film (external) mass transfer resistance was considered negligible compared to the internal mass transfer resistance [58]. The fit (or misfit) of the experimental results with the model's results can prove/disprove the validity of the assumptions taken and, in case the assumptions were not correct, a re-evaluation of the chosen model may be needed.

Following the steps described in **Figure 5.1**, after fitting the necessary parameters to the model, the first *in-silico* runs can be performed. These runs serve as a first screening step to understand if there are any major flaws in the model. This is done based on the output chromatogram and how this looks. After the experimental conditions are set *in-silico*, the same experiment can be run in the chromatographic equipment in order to understand if the model's and experiment's results are in agreement. **Figure 5.7 A** shows the validation of the model, by comparing a loading step to 100% breakthrough of a 5 g/L mAb solution. It is possible to see from the experimental results that the model was able to capture the adsorption behavior accurately, with a good prediction of the initial breakthrough and the shape of the BTC. Similar results were achieved for the other two resins (data not shown).

The model was able to capture the essence of the chromatogram for all the different steps. The loading behavior (the most important step) was accurately described as discussed above. The washing profile was also consistent to what is expected, with a decrease in the concentration of protein at the outlet of the column, consistent to what is expected experimentally, since the non-adsorbed mAb present in the interstitial fluid flows out of the column during the wash step. The model also shows a sharp elution profile with a little tailing. This is consistent with ProA elution profiles, which generally

use low pH solutions as modifiers that will make the mAb almost instantly elute, generating a very concentrated protein front, which then tails off due to axial dispersion. Simulations with different loading volumes showed results consistent to what is expected. When loading the column to DBC10% and DBC50% (Figure 5.7 B and C, respectively) the elution peaks were smaller than for DBC100%, with DBC10% and DBC50% having the smallest and second smallest elution peaks, respectively, which was expected due to the lower amount of mAb loaded onto the columns.

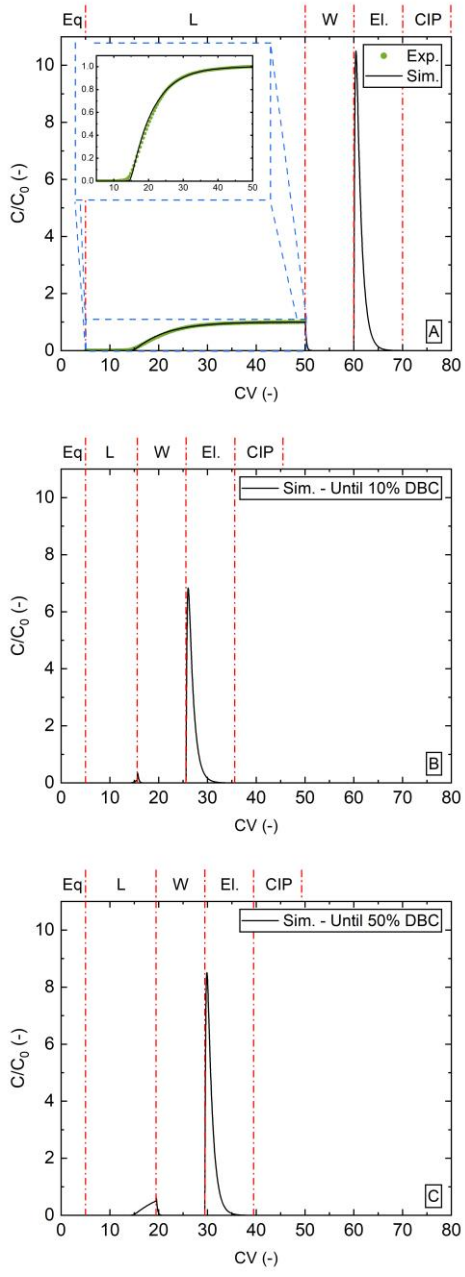

Figure 5.7 - Validation of the used mechanistic model for the simulation of protein chromatographic behavior with MSPrismA at a loading concentration of 5 g/L and a loading flow rate of 0.5 ml/min. A – Model validation by loading the column to 100% Breakthrough: experimental data points (•) ; B & C – Example of model applicability, by testing the loading of the column until 10% and 50% Breakthrough, respectively. Vertical red dash-dot lines (–•–) represent the different phases. Different column volumes were used for different phases: Equilibration (Eq.) – 5 CV, Load (L) – variable, Wash (W) – 10 CV, Elution (El.) – 10 CV, CIP – 10 CV. These are represented above each plot.

5.4.6. Model Application: Preparing for higher USP titers

The applicability of chromatography models in the biopharmaceutical industry has been thoroughly discussed [59]. Increasingly higher titers in the Upstream Processing have shifted the costs to Downstream Processing, of which ProA represents a big portion of the costs [2, 5]. The approach followed in this work showed how chromatographic process development could be tackled, from beginning to end.

The model showed good results for a variety of feed concentrations (data not shown), of which a comparison between model and experimental results are shown for a 5 g/L feed concentration. This concentration was chosen because it is becoming an industry standard to achieve such titers of mAb during cell culture. Since ProA is the first step in the purification of mAbs, it is important to have a good mechanistic understanding of the process, which the results above show. Furthermore, and considering how much titer has increased throughout the last two decades [2], a model that can accurately predict this increase in feed concentration is important for process design and is provided in this work.

To provide further clarity on this, a mAb at a titer of 5 mg/ml was purified from a harvest solution using a ProA resin (**Figure 5.8**). The experimental results show a great initial increase in the UV signal due to the presence of impurities in the harvest solution. This signal starts plateauing at around 2000 mA.U. and after some CV, there is again an increase in the UV signal, marking the beginning of breakthrough of mAb, which is clearly captured by the model. Model results were generated for pure mAb solutions since it was considered that for a purification scheme that includes a ProA step it would be unnecessary to attempt to model the interactions between the ProA resins and the components in the harvest solution. Elution results also show good agreement between model data and experimental data. CIP shows that some mAb was stripped from the column in the experiment and not in the model. This is because when modelling this step, it was considered that all mAb would be removed in the elution phase. Nonetheless, the amount of mAb in the CIP is negligible compared to the elution phase.

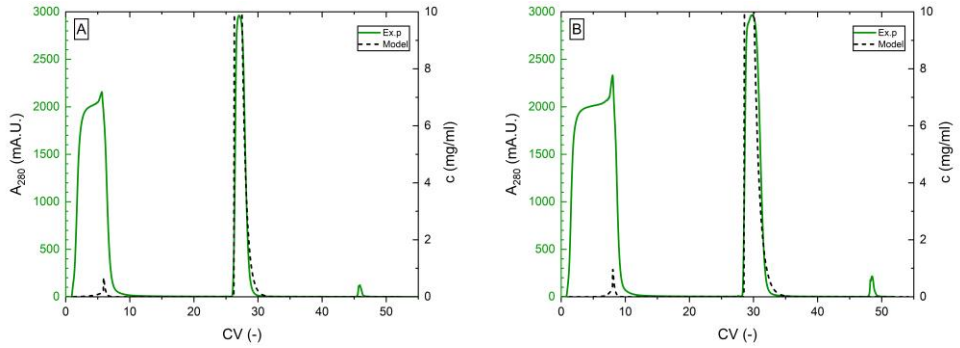

Figure 5.8 - Purification of the mAb from harvest solution using MSS (A) and MSPrismA (B) with a titer of 5 mg/ml and a flowrate of 0.49 and 0.68 ml/min, respectively. Experimental data is given in Absorbance Units (mA.U.) and model data is given in concentration (secondary y-axis). Model data was obtained for a pure mAb scenario, since the impurities were not modelled. Initial breakthrough of mAb can be observed by the slight shift in the plateauing curve during loading (approximately at around 2000 mA.U.) and was accurately predicted by the model. Elution was also accurately predicted by the model. There are some discrepancies between experiments and model in the CIP, since in the model it is assumed that no mAb is lost in this phase. The used volumes for each phase were: Loading – 4.7 CV (MSS – A) and 8 CV (MSPrismA – B); Wash – 20 CV; Elution – 15 CV; CIP – 10 CV. UV signal saturated at 3000 mA.U., which would correspond to a 10 mg/ml solution in case the used calibration would be extrapolated to the maximum mA.U. value, hence why the maximum of each axis was set to these values.

The proposed model showed that with a small number of experiments it is possible to reach an accurate model. With the linear mass transfer coefficient correlations, it would even be possible to extrapolate the results to calculate a k_{ov} for higher concentrations, with an experimental check being recommended. The obtained results are pivotal for the design of the capture step. Anything ranging from appropriate loading flowrate, to Yield and productivity predictions and capacity needed, can be predicted using the developed model. In addition to what was described, models are great tools that can be used for the control of chromatographic processes, provided that they are accurate and fast enough [60]. The capabilities of this model in accurately predicting chromatographic behavior highlight its use as a Digital Twin for the chromatography step. The step can be further studied and optimized in-silico by varying a multitude of parameters, from flowrates to feed concentrations or column dimensions, without the need to test every design idea experimentally. This reduces the experimental burden in early development stages, helping to achieve the desired process faster and cheaper. Furthermore, such chromatographic models help to enhance process knowledge and helps to achieve a Quality by Design approach in biopharmaceutical process development.

5.5. Conclusions

This work focused on the development of a hybrid approach for the development of a chromatographic step for the purification of monoclonal antibodies (**Figure 5.1**). This

approach focused on minimizing experiments and applying mechanistic models that are as simple as possible whilst providing a good prediction for the chromatographic behavior. The approach made use of HTS of several resins (both ProA and CEX) and the development of a mechanistic model for chromatography.

The initial HTS step (29 resins studied – 13 ProA and 16 CEX) aimed at reducing the number of resins to study in subsequent steps. After ProA chromatography it is expected that most impurities are removed from the solution, yielding the pure mAb screening of CEX resins a good enough model for polishing steps. The adsorption behavior of the mAb in a harvest solution was further studied using 4 ProA resins (MSS, MSPrismA, MSSLX, and PJet) to assess the influence of the impurities in mAb adsorption. The results show comparable adsorption isotherms. Therefore, it can be concluded that the parameters estimated from the HTS using pure mAb can be used when modelling a ProA-based mAb purification process from harvest solution.

The choice of model used to study mAb chromatography was based on achieving the best description of the chromatographic behavior with the least complexity possible. A LKM with SLDF model, using Langmuir adsorption model, was used and the overall mass transfer coefficient was determined through breakthrough curve (BTC) experiments. The linear correlation between feed concentration and the mass transfer coefficient simplified the model compared to other methodologies proposed for the estimation of this parameter [56, 57]. This linear correlation can be used to extrapolate the overall mass transfer coefficient for solutions with a higher mAb concentration, provided that there is experimental validation. The model results were then compared to an experiment and showed great agreement between the model's predictions and the experimental results at a feed concentration of 5 g/L, showing the model's validity and applicability.

5.6. Acknowledgements

This work has received funding from the European Union's Horizon 2020 research and innovation program under the Marie Skłodowska-Curie grant agreement No 812909 CODOBIO, within the Marie Skłodowska-Curie International Training Networks framework.

5.7. References

[1] A.L. Grilo, A. Mantalaris, The Increasingly Human and Profitable Monoclonal Antibody Market, Trends in Biotechnology 37(1) (2019) 9-16. https://doi.org/10.1016/j.tibtech.2018.05.014.

[2] G. Jagschies, E. Lindskog, K. Lacki, P.M. Galliher, Biopharmaceutical Processing: Development, Design, and Implementation of Manufacturing Processes, Elsevier2018. https://doi.org/10.1016/C2014-0-01092-1.

[3] A.A. Shukla, J. Thömmes, Recent advances in large-scale production of monoclonal antibodies and related proteins, Trends in Biotechnology 28(5) (2010) 253-261. https://doi.org/10.1016/j.tibtech.2010.02.001.

[4] A.A. Shukla, B. Hubbard, T. Tressel, S. Guhan, D. Low, Downstream processing of monoclonal antibodies—application of platform approaches, Journal of Chromatography B 848(1) (2007) 28-39. https://doi.org/10.1016/j.jchromb.2006.09.026.

[5] S. Vunnum, G. Vedantham, B. Hubbard, Protein A-based affinity chromatography, in: U. Gottschalk (Ed.), Process Scale Purification Of Antibodies, John Wiley & Sons, Inc., USA and Canada, 2009, pp. 79-102. https://doi.org/10.1002/9780470444894.ch4.

[6] T. Ahamed, S. Chilamkurthi, B.K. Nfor, P.D. Verhaert, G.W. van Dedem, L.A. van der Wielen, M.H. Eppink, E.J. van de Sandt, M. Ottens, Selection of pH-related parameters in ion-exchange chromatography using pH-gradient operations, Journal of Chromatography A 1194(1) (2008) 22-29. https://doi.org/10.1016/j.chroma.2007.11.111.

[7] G. Miesegaes, S. Lute, D. Strauss, E. Read, A. Venkiteshwaran, A. Kreuzman, R. Shah, P. Shamlou, D. Chen, K.J.B. Brorson, bioengineering, Monoclonal antibody capture and viral clearance by cation exchange chromatography, Biotechnology and Bioengineering 109(8) (2012) 2048-2058. https://doi.org/10.1002/bit.24480.

[8] K.A. Kaleas, M. Tripodi, S. Revelli, V. Sharma, S.A. Pizarro, Evaluation of a multimodal resin for selective capture of CHO-derived monoclonal antibodies directly from harvested cell culture fluid, Journal of Chromatography B 969 (2014) 256-263. https://doi.org/10.1016/j.jchromb.2014.08.026.

[9] T. Hahn, N. Geng, K. Petrushevska-Seebach, M.E. Dolan, M. Scheindel, P. Graf, K. Takenaka, K. Izumida, L. Li, Z. Ma, Mechanistic modeling, simulation, and optimization of mixed-mode chromatography for an antibody polishing step, Biotechnology Progress (2022) e3316. https://doi.org/10.1002/btpr.3316.

[10] D.E. Steinmeyer, E.L. McCormick, The art of antibody process development, Drug discovery today 13(13-14) (2008) 613-618. https://doi.org/10.1016/j.drudis.2008.04.005.

[11] D. Pfister, L. Nicoud, M. Morbidelli, Continuous biopharmaceutical processes: chromatography, bioconjugation, and protein stability, Cambridge University Press2018.

[12] T.C. Silva, M. Eppink, M. Ottens, Automation and miniaturization: enabling tools for fast, high-throughput process development in integrated continuous biomanufacturing, Journal of Chemical Technology & Biotechnology (2021). https://doi.org/10.1002/jctb.6792.

[13] B.K. Nfor, M. Noverraz, S. Chilamkurthi, P.D. Verhaert, L.A. van der Wielen, M. Ottens, High-throughput isotherm determination and thermodynamic modeling of protein adsorption on mixed mode adsorbents, Journal of Chromatography A 1217(44) (2010) 6829-50. https://doi.org/10.1016/j.chroma.2010.07.069.

[14] M. Bensch, P. Schulze Wierling, E. von Lieres, J. Hubbuch, High Throughput Screening of Chromatographic Phases for Rapid Process Development, Chemical Engineering & Technology 28(11) (2005) 1274-1284. https://doi.org/10.1002/ceat.200500153.

[15] M. Wiendahl, P. Schulze Wierling, J. Nielsen, D. Fomsgaard Christensen, J. Krarup, A. Staby, J. Hubbuch, High Throughput Screening for the Design and Optimization of Chromatographic Processes –

Miniaturization, Automation and Parallelization of Breakthrough and Elution Studies, Chemical Engineering & Technology 31(6) (2008) 893-903. https://doi.org/10.1002/ceat.200800167.

[16] P.M. Schmidt, M. Abdo, R.E. Butcher, M.-Y. Yap, P.D. Scotney, M.L. Ramunno, G. Martin-Roussety, C. Owczarek, M.P. Hardy, C.-G. Chen, A robust robotic high-throughput antibody purification platform, Journal of Chromatography A 1455 (2016) 9-19. https://doi.org/j.chroma.2016.05.076.

[17] J. Feliciano, A. Berrill, M. Ahnfelt, E. Brekkan, B. Evans, Z. Fung, R. Godavarti, K. Nilsson-Välimaa, J. Salm, U. Saplakoglu, Evaluating high-throughput scale-down chromatography platforms for increased process understanding, Engineering in Life Sciences 16(2) (2016) 169-178. https://doi.org/10.1002/elsc.201400241.

[18] A. Creasy, G. Barker, Y. Yao, G. Carta, Systematic interpolation method predicts protein chromatographic elution from batch isotherm data without a detailed mechanistic isotherm model, Biotechnology Journal 10(9) (2015) 1400-1411. https://doi.org/10.1002/biot.201500089.

[19] T.M. Pabst, J. Thai, A.K. Hunter, Evaluation of recent Protein A stationary phase innovations for capture of biotherapeutics, Journal of Chromatography A 1554 (2018) 45-60. https://doi.org/10.1016/j.chroma.2018.03.060.

[20] T.C. Silva, M. Eppink, M. Ottens, Small, smaller, smallest: Miniaturization of chromatographic process development, Journal of Chromatography A 1681 (2022) 463451. https://doi.org/10.1016/j.chroma.2022.463451.

[21] I.s.F. Pinto, R.R. Soares, S.A. Rosa, M.R. Aires-Barros, V. Chu, J.o.P. Conde, A.M. Azevedo, High-throughput nanoliter-scale analysis and optimization of multimodal chromatography for the capture of monoclonal antibodies, Analytical Chemistry 88(16) (2016) 7959-7967. https://doi.org/10.1021/acs.analchem.6b00781.

[22] A.T. Hanke, M. Ottens, Purifying biopharmaceuticals: knowledge-based chromatographic process development, Trends in Biotechnology 32(4) (2014) 210-20. https://doi.org/10.1016/j.tibtech.2014.02.001.

[23] B.K. Nfor, P.D. Verhaert, L.A. van der Wielen, J. Hubbuch, M. Ottens, Rational and systematic protein purification process development: the next generation, Trends in biotechnology 27(12) (2009) 673-679. https://doi.org/10.1016/j.tibtech.2009.09.002.

[24] H. Schmidt-Traub, M. Schulte, A. Seidel-Morgenstern, H. Schmidt-Traub, Preparative Chromatography, Wiley Online Library2012. https://doi.org/10.1002/9783527816347.

[25] S.H. Altern, J.P. Welsh, J.Y. Lyall, A.J. Kocot, S. Burgess, V. Kumar, C. Williams, A.M. Lenhoff, S.M. Cramer, Isotherm model discrimination for multimodal chromatography using mechanistic models derived from high-throughput batch isotherm data, Journal of Chromatography A 1693 (2023) 463878. https://doi.org/10.1016/j.chroma.2023.463878.

[26] A. Seidel-Morgenstern, H. Schmidt-Traub, M. Michel, A. Epping, A. Jupke, Modeling and Model Parameters, Preparative Chromatography2012, pp. 321-424. https://doi.org/10.1002/9783527649280.ch6.

[27] G. Carta, A. Jungbauer, Protein chromatography: process development and scale-up, John Wiley & Sons2020. https://doi.org/10.1002/9783527630158.

[28] G. Guiochon, A. Felinger, D.G. Shirazi, Fundamentals of preparative and nonlinear chromatography, Elsevier2006.

[29] B.K. Nfor, D.S. Zuluaga, P.J. Verheijen, P.D. Verhaert, L.A. van der Wielen, Ottens, Marcel, Model-based rational strategy for chromatographic resin selection, Biotechnology Progress 27(6) (2011) 1629-1643. https://doi.org/10.1002/btpr.691.

[30] S.M. Pirrung, D. Parruca da Cruz, A.T. Hanke, C. Berends, R.F. Van Beckhoven, M.H. Eppink, M. Ottens, Chromatographic parameter determination for complex biological feedstocks, Biotechnology Progress 34(4) (2018) 1006-1018. https://doi.org/10.1002/btpr.2642.

[31] M. Moreno-González, D. Keulen, J. Gomis-Fons, G.L. Gomez, B. Nilsson, M. Ottens, Continuous adsorption in food industry: The recovery of sinapic acid from rapeseed meal extract, Separation and Purification Technology 254 (2021) 117403. https://doi.org/10.1016/j.seppur.2020.117403.

[32] F. Steinebach, M. Angarita, D.J. Karst, T. Müller-Späth, M. Morbidelli, Model based adaptive control of a continuous capture process for monoclonal antibodies production, Journal of Chromatography A 1444 (2016) 50-56. https://doi.org/10.1016/j.chroma.2016.03.014.

[33] M. Ostrihoňová, P. Cabadaj, M. Polakovič, Design of frontal chromatography separation of 1-phenylethanol and acetophenone using a hydrophobic resin, Separation and Purification Technology 314 (2023) 123578. https://doi.org/10.1016/j.seppur.2023.123578.

[34] C.A. Brooks, S.M. Cramer, Steric mass-action ion exchange: displacement profiles and induced salt gradients, AIChE Journal 38(12) (1992) 1969-1978. https://doi.org/10.1002/aic.690381212.

[35] Y.-C. Chen, S.-J. Yao, D.-Q. Lin, Parameter-by-parameter method for steric mass action model of ion exchange chromatography: Theoretical considerations and experimental verification, Journal of Chromatography A 1680 (2022) 463418. https://doi.org/10.1016/j.chroma.2022.463418.

[36] M. Sokolov, M. von Stosch, H. Narayanan, F. Feidl, A. Butté, Hybrid modeling—a key enabler towards realizing digital twins in biopharma?, Current Opinion in Chemical Engineering 34 (2021) 100715. https://doi.org/10.1016/j.coche.2021.100715.

[37] R.M. Portela, C. Varsakelis, A. Richelle, N. Giannelos, J. Pence, S. Dessoy, M. von Stosch, When is an in silico representation a digital twin? A biopharmaceutical industry approach to the digital twin concept, Digital Twins: Tools and Concepts for Smart Biomanufacturing (2021) 35-55. https://doi.org/10.1007/10_2020_138.

[38] Y. Chen, O. Yang, C. Sampat, P. Bhalode, R. Ramachandran, M. Ierapetritou, Digital twins in pharmaceutical and biopharmaceutical manufacturing: a literature review, Processes 8(9) (2020) 1088. https://doi.org/10.3390/pr8091088.

[39] A. Felinger, G. Guiochon, Comparison of the kinetic models of linear chromatography, Chromatographia 60(1) (2004) S175-S180. https://doi.org/10.1365/s10337-004-0288-7.

[40] J. Van Deemter, F. Zuiderweg, A.v. Klinkenberg, Longitudinal diffusion and resistance to mass transfer as causes of nonideality in chromatography, Chemical Engineering Science 5(6) (1956) 271-289. https://doi.org/10.1016/0009-2509(56)80003-1.

[41] P.V. Danckwerts, Continuous flow systems: distribution of residence times, Chemical Engineering Science 2(1) (1953) 1-13. https://doi.org/10.1016/0009-2509(53)80001-1.

[42] H.D. Young, Statistical Treatment of Experimental Data, McGraw-Hill Book Company, Inc., USA, 1962.

[43] D.A. Skoog, F.J. Holler, S.R. Crouch, Principles of Instrumental Analysis, Cengage Learning2017.

[44] TosohBiosciencesLLC, TOYOPEARL MX-Trp-650M - Performance Data, 2023. https://www.separations.us.tosohbioscience.com/Process_Media/id-7015/TOYOPEARL_MX-Trp-650M. (Accessed 03/07/2023 2023).

[45] A.R. Karow, S. Bahrenburg, P. Garidel, Buffer capacity of biologics—from buffer salts to buffering by antibodies, Biotechnology Progress 29(2) (2013) 480-492. https://doi.org/10.1002/btpr.1682.

[46] B.C. de Neuville, A. Tarafder, M. Morbidelli, Distributed pore model for bio-molecule chromatography, Journal of Chromatography A 1298 (2013) 26-34. https://doi.org/10.1016/j.chroma.2013.04.074.

[47] F. Hagemann, P. Adametz, M. Wessling, V. Thom, Modeling hindered diffusion of antibodies in agarose beads considering pore size reduction due to adsorption, Journal of Chromatography A 1626 (2020) 461319. https://doi.org/10.1016/j.chroma.2020.461319.

[48] E. Müller, J. Vajda, Routes to improve binding capacities of affinity resins demonstrated for Protein A chromatography, Journal of Chromatography B 1021 (2016) 159-168. https://doi.org/10.1016/j.jchromb.2016.01.036.

[49] V. Natarajan, A.L. Zydney, Protein a chromatography at high titers, Biotechnology and Bioengineering 110(9) (2013) 2445-2451. https://doi.org/10.1002/bit.24902.

[50] K. Swinnen, A. Krul, I. Van Goidsenhoven, N. Van Tichelt, A. Roosen, K. Van Houdt, Performance comparison of protein A affinity resins for the purification of monoclonal antibodies, Journal of Chromatography B 848(1) (2007) 97-107. https://doi.org/10.1016/j.jchromb.2006.04.050.

[51] E.L. Cussler, Diffusion: mass transfer in fluid systems, 3rd ed., Cambridge University Press, USA, 2009.

[52] D.M. Ruthven, Principles of adsorption and adsorption processes, John Wiley & Sons, USA and Canada, 1984.

[53] M. Yu, T.C. Silva, A. van Opstal, S. Romeijn, H.A. Every, W. Jiskoot, G.-J. Witkamp, M. Ottens, The Investigation of Protein Diffusion via H-Cell Microfluidics, Biophysical journal 116(4) (2019) 595-609. https://doi.org/10.1016/j.bpj.2019.01.014.

[54] S. Golshan-Shirazi, G. Guiochon, Comparison of the various kinetic models of non-linear chromatography, Journal of Chromatography A 603(1-2) (1992) 1-11. https://doi.org/10.1016/0021-9673(92)85340.

[55] N.K. Hiester, T. Vermeulen, Saturation performance of ion exchange and adsorption columns, Chemical Engineering Progress 48(10) (1952) 505-516.

[56] M.D. LeVan, G. Carta, Adsorption and ion exchange, in: D.W. Green (Ed.), Perry's Chemical Engineers' Handbook, McGraw-Hill, New York, 2008, pp. 16-1 - 16-54.

[57] C.-S. Chen, F. Konoike, N. Yoshimoto, S. Yamamoto, A regressive approach to the design of continuous capture process with multi-column chromatography for monoclonal antibodies, Journal of Chromatography A 1658 (2021) 462604. https://doi.org/10.1016/j.chroma.2021.462604.

[58] R. Hahn, P. Bauerhansl, K. Shimahara, C. Wizniewski, A. Tscheliessnig, A. Jungbauer, Comparison of protein A affinity sorbents: II. Mass transfer properties, Journal of Chromatography A 1093(1-2) (2005) 98-110. https://doi.org/10.1016/j.chroma.2005.07.050.

[59] A.S. Rathore, S. Nikita, G. Thakur, S. Mishra, Artificial intelligence and machine learning applications in biopharmaceutical manufacturing, Trends in Biotechnology (2022). https://doi.org/10.1016/j.tibtech.2022.08.007.

[60] A.S. Rathore, S. Nikita, G. Thakur, N. Deore, Challenges in process control for continuous processing for production of monoclonal antibody products, Current Opinion in Chemical Engineering 31 (2021) 100671. https://doi.org/j.coche.2021.100671.

Supplementary Information

Tables

Table SI 5.1 – Percentage of monomer (Mon.) and monomer plus High Molecular Weight species (Mon. + HMW) in the samples after batch uptake adsorption with harvest solution, measured by the UHPLC. Results shown are triplicate results, with the error representing the standard deviation of the triplicates. Results for different initial concentrations are shown (0.6 to 2 mg/ml are the low concentration trials, and 1 to 5 are the high concentration trials). The results show the data from the adsorption trials with the same four resins mentioned in section 4.2.

$c_{initial}$ (mg/ml)	MSS		MSPrismA		MSSLX		PJet	
	Mon. (%)	Mon. + HMW (%)	Mon. (%)	Mon. + HMW (%)	Mon. (%)	Mon. + HMW (%)	Mon. (%)	Mon. + HMW (%)
0.6	97.8 ± 0.4	99.7 ± 0.1	97.5 ± 0.2	99.5 ± 0.0	97.5 ± 0.3	99.5 ± 0.0	96.3 ± 0.2	99.5 ± 0.0
0.8	96.5 ± 0.7	99.5 ± 0.0	97.1 ± 0.1	99.5 ± 0.0	97.2 ± 0.1	99.5± 0.1	96.1 ± 0.9	99.5 ± 0.0
1	96.4 ± 0.1	99.5 ± 0.1	97.1 ± 0.0	99.5 ± 0.0	96.8 ± 0.1	99.5± 0.1	96.3 ± 0.5	99.6 ± 0.0
1.2	96.0 ± 0.1	99.3 ± 0.0	96.9 ± 0.0	99.4 ± 0.0	96.5 ± 0.1	99.4 ± 0.0	96.4 ± 0.1	99.5 ± 0.0
1.4	95.7 ± 0.3	99.4 ± 0.1	96.9 ± 0.0	99.5 ± 0.0	96.6 ± 0.1	99.5 ± 0.0	96.1 ± 0.3	99.5 ± 0.0
1.6	95.8 ± 0.0	99.5 ± 0.0	96.7 ± 0.0	99.5 ± 0.0	96.2 ± 0.3	99.4 ± 0.2	95.0 ± 1.7	99.5 ± 0.0
1.8	95.7 ± 0.1	99.4 ± 0.0	95.4 ± 1.7	99.5 ± 0.0	96.3 ± 0.1	99.4 ± 0.0	95.3 ± 0.6	99.5 ± 0.0
2	94.3 ± 0.9	99.1 ± 0.2	96.4 ± 0.2	99.5 ± 0.0	96.3 ± 0.1	99.5 ± 0.0	94.8 ± 0.5	99.5 ± 0.0
1	96.6 ± 0.4	99.7 ± 0.0	96.4 ± 0.1	99.6 ± 0.0	96.2 ± 0.0	99.7 ± 0.0	95.1 ± 0.3	99.8 ± 0.0
2	95.8 ± 0.1	99.7 ± 0.0	95.7 ± 0.1	99.6 ± 0.1	95.9 ± 0.5	99.7 ± 0.0	94.9 ± 0.4	99.7 ± 0.0
2.5	96.6 ± 0.1	99.7 ± 0.0	96.7 ± 0.0	99.6 ± 0.0	96.5 ± 0.2	99.5 ± 0.2	94.2 ± 0.1	99.7 ± 0.0
3	95.1 ± 0.8	99.4 ± 0.0	95.3 ± 1.3	99.4 ± 0.2	95.7 ± 0.7	99.5 ± 0.2	94.1 ± 0.2	99.5 ± 0.1
3.5	95.1 ± 0.8	99.4 ± 0.1	95.1 ± 0.7	99.4 ± 0.2	94.6 ± 1.1	99.3 ± 0.1	94.2 ± 0.9	99.3 ± 0.1
4	94.3 ± 0.2	99.3 ± 0.1	94.2 ± 0.1	98.7 ± 0.4	94.0 ± 0.8	99.3 ± 0.1	94.0 ± 0.1	99.2 ± 0.0
4.5	94.1 ± 0.0	99.2 ± 0.0	94.2 ± 0.0	99.0 ± 0.0	94.2 ± 0.0	99.2 ± 0.0	92.5 ± 0.7	99.4 ± 0.2
5	93.9 ± 0.2	99.2 ± 0.0	93.5 ± 0.8	99.3 ± 0.5	94.1 ± 0.0	98.8 ± 0.5	93.9 ± 0.2	99.1 ± 0.0

Table SI 5.2 – Parameters used in the chromatographic model for MSPrismA and MSS.

Parameter	Resin		Units
	MSPrismA	**MSS**	
Bed porosity (ε_b)	0.3	0.31	-
Pore porosity (ε_p)	0.89	0.92	-
Total porosity (ε_t)	0.92	0.94	-
Particle/bead diameter (d_p)	$60x10^{-6}$	$85x10^{-6}$	m
Radius of the pore (r_{pore}) [18]	$3.27x10^{-8}$	$4.18x10^{-8}$	m
q_{max}	79.35	57.17	mg/ml_{resin}
K_{eq}	23.82	34.39	ml_{liquid}/mg
Column Inner diameter (D_i)	$7 x10^{-3}$		m
Column Length (L_c)	$2.5 x10^{-2}$		m
Column Volume (V_c)	1		mL
Liquid viscosity (μ)	$1 x10^{-3}$		Pa·s
Liquid density (ϱ)	1000		kg/m^3

5

Figures

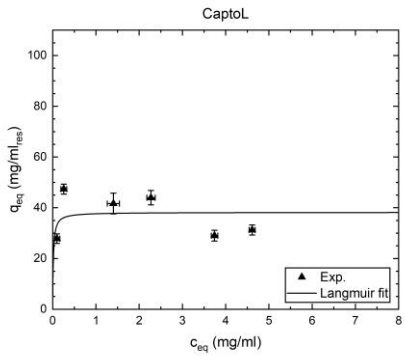

Figure SI 5.1 - Adsorption isotherms of mAb on CaptoL resin in 1x PBS buffer, pH 7.14.

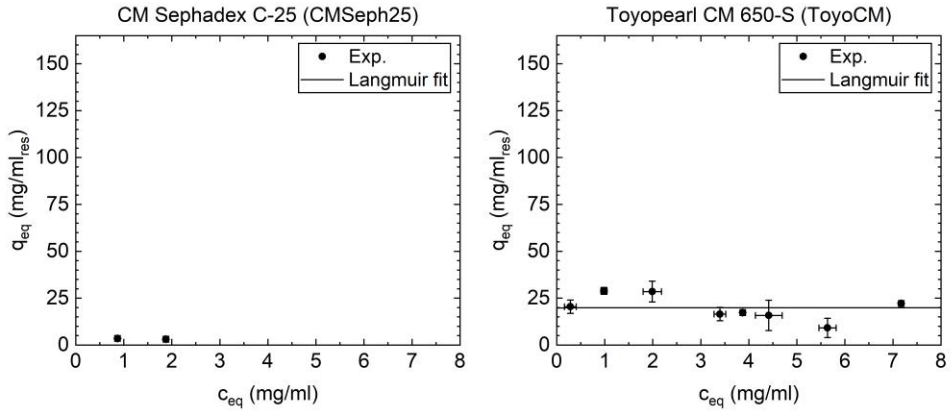

Figure SI 5.2 - Adsorption isotherms of mAb on CM Sephadex C-25 (left) and Toyopearl CM 650-S (right) in 25 mM NaOAc buffer, pH 4.5.

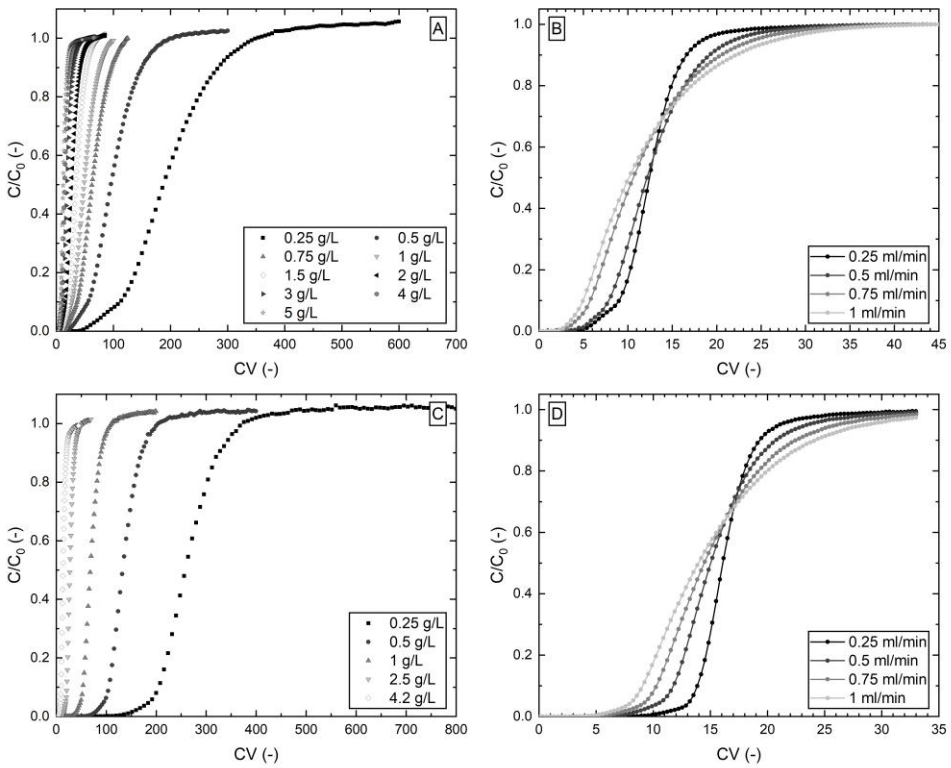

Figure SI 5.3 - Column experiments used for the calibration of the mechanistic model of MSS (A & B) and MSSpcc (C & D). A & C – Different initial concentrations and constant flow rate (F_v = 0.5 ml/min); B & D – Different flow rate and constant concentration (c_{mAb} = 5 g/L). Dots represent 100 data points from every experiment. In B and D, the line connecting the experimental data points is used to guide the reader's eye. C/C_0 – normalized concentration (concentration observed divided by inlet concentration). CV – column volumes.

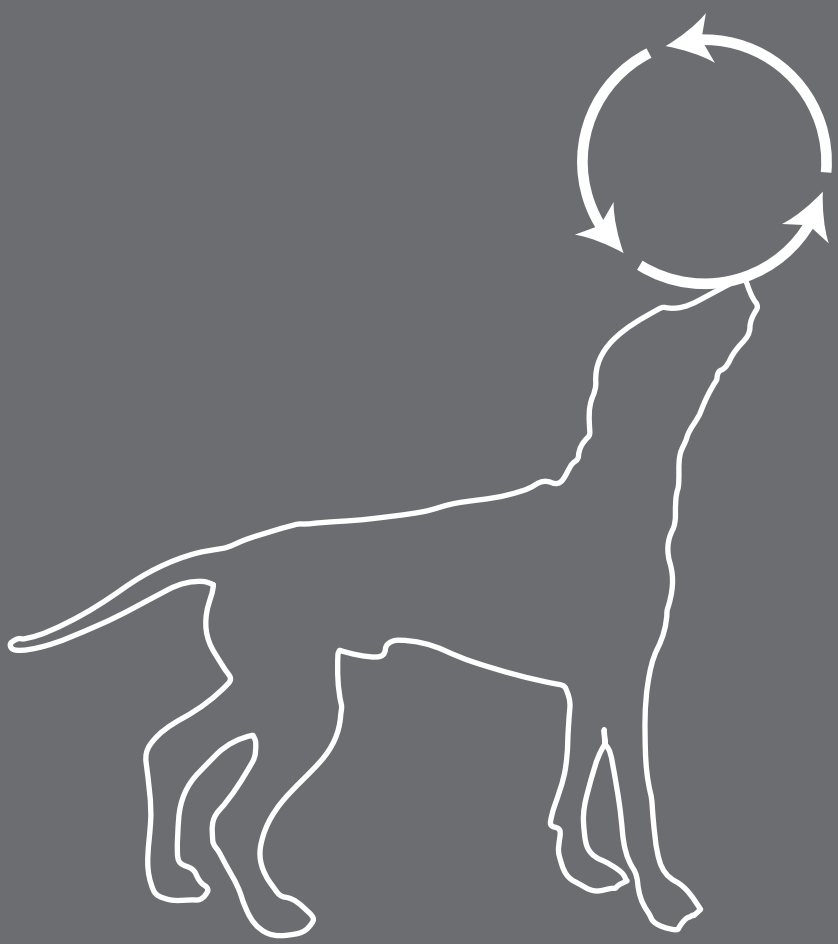

Chapter 6

Integrated Continuous Chromatography for Capture and Polishing at High Protein Load

Abstract

Integrated Continuous Biomanufacturing reduces manufacturing costs while maintaining product quality. A key contributor for high biopharmaceuticals costs, especially monoclonal antibodies (mAbs), is chromatography. Protein A ligands are usually preferred but still expensive in the manufacturing context, and batch chromatography under-utilizes the columns' capacity, compromising productivity to maintain high yields. Continuous chromatography increases columns' Capacity Utilization (CU) without sacrificing yield or productivity. This work presents the *in-silico* optimization of a 3 Column Periodic Counter-current Chromatography (3C-PCC) of a capture and polishing step for mAbs. The 3C-PCC was modeled and Pareto-fronts were used to optimize the 3C-PCC steps varying the flowrate and percentage of breakthrough achieved in the interconnected loading, maximizing Productivity and CU. Breakthrough curve shape significantly impacts the optimization of 3C-PCC. The model output was validated for three different protein A ligands using a pure mAb solution MAb Select SuRe pcc was selected to continuously capture mAb from a high-titer clarified cell culture supernatant (harvest). The eluates of this were pooled and used for continuous polishing using a Cation-Exchange resin. Experimental results validated model predictions (<7% deviation in the worst case) and a process with two 3C-PCC in sequence was proposed, with a productivity of approximately 100 mg/ml_{res}/h.

Keywords: Continuous Chromatography; High titers; Integrated Continuous Biomanufacturing; Modeling; Periodic Counter-current Chromatography

---

This chapter has been submitted for publication: Silva, T.C., Isaksson, M., Nilsson, B., Eppink, M. and Ottens, M..

6.1. Introduction

Demand for monoclonal antibodies (mAbs) is rising every year, making this one of the fastest growing biopharmaceuticals [1]. Simultaneously, mAbs are historically expensive to produce and new solutions to reduce the price have arisen, mostly in the form of biosimilars [2]. Operational strategies and process improvements have also been implemented to increase production capacity, notably recent developments in Upstream Processing (USP) where increasingly higher titers are being achieved [3]. Naturally, USP improvements to the cell line's productivity at a fractional increase of the costs have shifted the cost pressure of these biopharmaceuticals to the Downstream Processing (DSP), where costs can be as high as 80% of the total production costs [4]. Of all unit operation in a DSP train, chromatography is the most cost demanding. This is mainly due to resin prices (in general expensive, especially protein A ligands) and to the fact that there are usually three chromatographic steps [5, 6]. Despite this, chromatography is still the most viable option for the purification of mAbs, since other alternatives have still not been able to compete with it [7].

Integrated Continuous Biomanufacturing can help tackle the aforementioned problems by increasing the productivity and reducing costs of the whole process [8]. The biopharmaceutical community and regulatory agencies are joining efforts to make the transition to continuous manufacturing [9, 10]. Chromatography is, for most cases, an inherently batch process. If operated in bind and elute mode, product collection will unavoidably be discrete. Different strategies to convert batch chromatography to continuous have been proposed: (Capture) Simulated Moving Bed (CaptureSMB/SMB) in the case of operating in bind and elute mode or not, respectively [11]; Multicolumn Countercurrent Solvent Gradient Purification (MCSGP) [12]; Periodic Counter-current Chromatography (PCC); among others [11]; and various systems are already commercially available [13].

One very important design element for PCC are Breakthrough Curves (BTCs). These provide information on the protein's Dynamic Binding Capacity (DBC) at specific operating conditions (flow rate, buffer conditions, etc.). Figure 6.1 A shows how a BTC looks and an example of what is usually done in batch chromatography, where the loading step goes to about 1% of DBC (DBC1%). The area in light green above the BTC curve shows the protein adsorbed to the resin until DBC1%, whereas the grey area with right diagonal lines and red area with left diagonal lines represent the protein that would be lost and what could still be adsorbed to the column in case the column would be loaded to DBC100%, respectively. By interconnecting the columns in the loading step it is possible to go to higher percentages of DBC. In Figure 6.1 B one can see that by interconnecting the loading, it is possible to reach a higher DBC without losing product (it is captured by the subsequent column, represented by area in white). In the loaded

column, more protein will be adsorbed (sum of the areas of light and dark green). The reduction of the red area means that more of the resin is used to adsorb product, increasing the resin utilization.

Empirical optimization studies on PCC can be laborious and expensive, as both a significant amount of product and time would be required to find optimum processes. By using Mechanistic Models (MM) to describe chromatographic behavior it is possible to test several scenarios in-silico before having to make the shift to the lab [14]. There are several parameters that need to be addressed in such optimization [15], therefore the computer-based optimization will help to reduce process development times. The choices of the model and optimization framework are important, as there is often a compromise between accuracy and optimization times. Furthermore, the feasibility of different process alternatives can be evaluated in-silico, saving time and sample [16].

This work presents a model-based optimization for a batch and a 3 column PCC (3C-PCC) capture step and a 3C-PCC polishing Cation-Exchange (CEX) step. The selected resins were optimized *in-silico* for different feed concentrations. The continuous model was validated with pure sample for a feed concentration of 5 g/L. The best performing ProA resin was selected for a study with harvest solution and the eluates were then used as feed solution for the 3C-PCC of CEX, mimicking a continuous capture and polishing step. Finally, model data is compared to experimental data to assess the model's feasibility to describe the system and its accuracy.

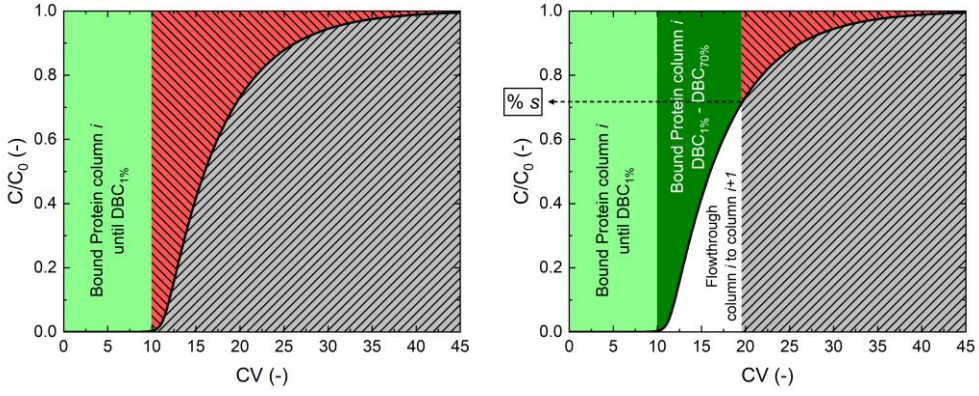

Figure 6.1 - Breakthrough curve of importance for the design of continuous chromatography. A – Scenario where only one column is connected; B – Scenario where columns are interconnected. Light green represents the protein adsorbed to the chromatographic resin until 1% of DBC; Dark green represents the protein adsorbed in column i until a specified percentage of breakthrough is achieved (represented by % s). Red with left diagonal dashes represents the protein that could still be adsorbed to the column if 100% DBC was achieved. Grey with tight diagonal dashes represents what is lost in the flow through.

6.2. Materials and Methods

6.2.1. Theory: Continuous Chromatography Model

6.2.1.1. 3C-PCC process and model

3C-PCC was modelled using the Transport Dispersive Model (TDM) and the mass transfer is described by the Solid-Film Linear Driving Force (SLDF) model, both described elsewhere [17]. BTC experiments used to calibrate the model have been previously described and performed [17] (for ProA resins). BTC experiments for the CEX resins are shown in SI.

In this system, feed continuity was assured by guaranteeing that the duration of the non-loading steps was shorter than that for the loading step [18]. As in the case for the experimental setup, the model connects the outlet of one column to another (for the interconnected loading and interconnected washing), which in the model is achieved by setting the inlet boundary condition of the receiving column as the outlet of the giving column. In this system, the Danckwerts boundary conditions for dispersive systems apply [19], where the inlet concentration is provided by the mathematical solution of the previous column. This is done in the ordinary differential equations (ODE) axial and time-dependent system, and the spatial discretization is achieved using the method of lines.

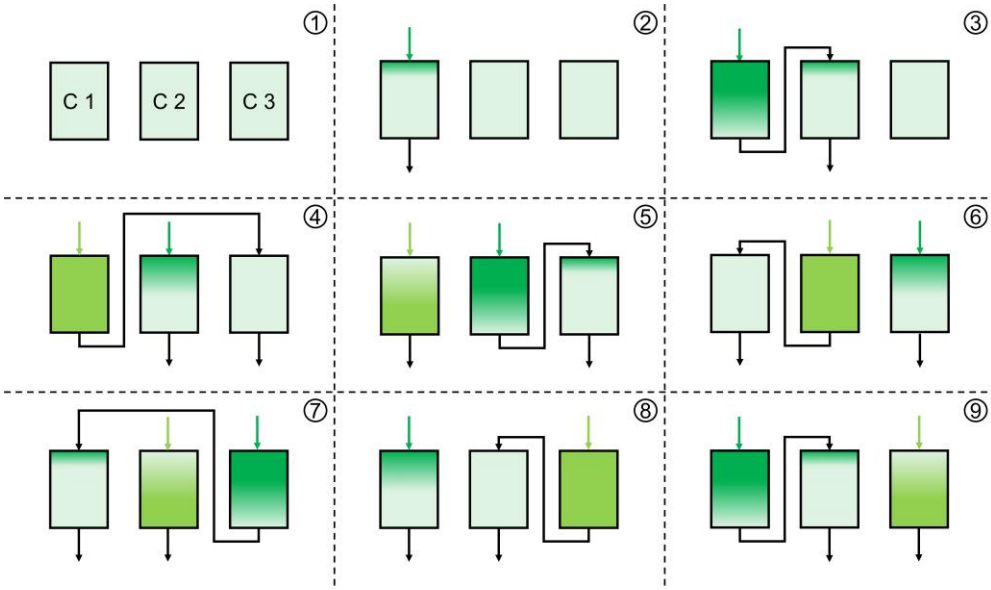

Figure 6.2 - Diagram with the different phases in the operation of a 3 Column Periodic Counter-current Chromatography (3C-PCC). Numbers 1 to 3 represent the start-up phase and numbers 4 to 9 represent the cyclic operation.

Figure 6.2 shows a schematic representation of the system. **Figure 6.2 - 1** to **3** represent the start-up phase, where column 1 (C1) is loaded disconnected (**Figure 6.2 – 2**) and then interconnected to C2 (**Figure 6.2 – 3**). In **Figure 6.2 – 4**, C2 is loaded disconnected and C1 is washed interconnected to C3, minimizing product loss. In **Figure 6.2 – 5**, C1 undergoes elution (el.), CIP and equilibration (eq.) while C2 is loaded interconnected to C3. In **Figure 6.2 – 6**, C2 is washed interconnected to C1 while C3 is loaded disconnected. In **Figure 6.2 – 7**, C2 undergoes el., CIP, and eq., while C3 is washed interconnected to C1. In **Figure 6.2 – 8**, C3 is washed interconnected to C2, while C1 is loaded disconnected. Finally, in **Figure 6.2 – 9**, C1 is loaded interconnected to C2, while C3 is undergoing el., CIP and eq. and will be ready to receive the wash from C1, thus completing one full cycle.

6.2.1.2. Batch and Continuous Optimization

In a PCC process, feed continuity is ensured by guaranteeing that the time it takes to completely load one column (t_{cycle}) is larger than the time required to perform all other steps. Two common performance indicators are the productivity (P), which is the protein adsorbed per resin volume and time, and the capacity utilization (CU), which is the effective adsorbed product divided by the maximum product that could be adsorbed at the tested feed concentration and depends on the chosen isotherm (in this case the Langmuir isotherm). The indicators are calculated according to the following equations:

$$P\ (mg_{mAb}/ml_{resin}/h) = \frac{t_{all\ cycles} \cdot c_{feed} \cdot F_{v_{inj}} - Mass\ Lost}{CV \cdot (1 - \varepsilon_b) \cdot N_{columns} \cdot t_{all\ cycles}} \quad (1)$$

$$CU\ (\%) = \frac{t_{all\ cycles} \cdot c_{feed} \cdot F_{v_{inj}} - Mass\ Lost}{CV \cdot (1 - \varepsilon_b) \cdot N_{columns} \cdot \left(N_{cycles} - 1\right) \cdot \left(\frac{q_{max} \cdot K_{eq} \cdot c_{feed}}{1 + K_{eq} \cdot c_{feed}}\right)} \quad (2)$$

where $t_{all\ cycles}$ is the cycle time for all cycles, c_{feed} is the feed concentration, $F_{v_{inj}}$ is the loading flow rate, $Mass\ Lost = \frac{\int_0^{t_{end}} c|_{z=L}\, dt}{c_{feed} \cdot t_{all\ cycles}}$ is the mass lost in the cycle, CV is the column volume, ε_b is the bed porosity, $N_{columns}$ is the number of columns, N_{cycles} is the number of cycles, and q_{max} and K_{eq} are the maximum adsorption capacity and adsorption equilibrium constant of each resin, in the Langmuir model, respectively.

For the defined process, a Yield (Y) constraint was set, to minimize product loss both in the interconnected loading step (by early breakthrough in the second column) and in the interconnected wash step. This can be defined as the recovered product divided by the total loaded product:

$$Y\ (\%) = \frac{t_{cycle} \cdot c_{feed} \cdot F_{v_{inj}} - Mass\ Lost}{t_{cycle} \cdot c_{feed} \cdot F_{v_{inj}}} \quad (3)$$

Additionally, there is another parameter that can be used to design the PCC step and check its performance, which is the percentage of breakthrough achieved in the first column when two columns are interconnected (*% s*). This can be defined as:

$$\%\ s\ (\%) = \frac{c|_{z=L}\ \ (at\ t = t_{end\ IC\ phase})}{c_{feed}} \quad (4)$$

The design variables for the optimization of the continuous step were the loading flow rate and the percentage of breakthrough achieved in the first column at the end of an interconnected load. The constraints set for the system were feed continuity (meaning that t_{cycle} must be larger than the time to recover the product and prepare the column to be interconnected for the wash (t_{RR})), and a yield constraint, to avoid product loss. The only design variable for the optimization of the batch chromatography was the loading flow rate, since *% s* is fixed to 1% because of the yield constraint. The optimization procedure for the continuous steps can be summarized in:

$$objective\ =\ max(Prod\ ,\ CU)$$
$$variables\colon\ x = [F_{v_{inj}}\ ,\ \%\ s] \text{ with } \begin{cases} 0.1/0.25\ \leq\ F_{v_{inj}}\ \leq\ 1\ ml/min \\ 20\ \leq\ \%\ s\ \leq 90 \end{cases} \quad (5)$$
$$Constraints\colon\ \begin{cases} Y\ >\ 99\% \\ t_{cycle} > t_{RR} \end{cases}$$

The lower limits of $F_{v_{inj}}$ were 0.1 and 0.25 ml/min for the PCC CEX and ProA optimization, respectively. In case where the optimal solution of an objective function hurts the results of the other, Pareto fronts find non-inferior solutions to the problem, which form the Pareto front. An optimization was run for every resin and different feed concentrations. The used optimization solver was *paretosearch*, an in-built function of the Global optimization toolbox in MATLAB, that allows to solve constrained multi-objective optimization problems. Another solver (*gamultiobj*) was also tested, but the yielded results were the same, but at larger computational times, so the first was used for the present work. The selected population size was 150, and maximum iterations of 50, and default tolerances were used. Each optimization was computed in parallel in a 10-core computer and ran for approximately 18h each.

6.2.2. Materials

1 ml HiTrap® columns of Protein A (ProA) resins Mab Select SuRe (MSS), Mab Select PrismA (MSPrismA), and Mab Select SuRe pcc (MSSpcc) and Cation-Exchange (CEX) resins Capto™ S ImpAct (CapSImp), and SP Sepharose Fast Flow (SPSephFF) were purchased from Cytiva, Uppsala, Sweden. The bed height is 25 mm, the inner diameter 7 mm, and the bed volume 1 ml. The mAb (M_w of 148 220 Da, pI ≈ 8.6) used in this study was provided by Byondis B.V., Nijmegen, The Netherlands, both in purified form and with the Clarified Cell Culture (harvest). The titer of mAb present in the harvest was 1.4 g/L.

6.2.3. Buffers and solutions preparation

The different buffers and solutions were prepared by dissolving the appropriate amount of chemicals in Milli-Q water. For the protein A resin studies, a 1x Phosphate Buffer Saline (PBS) buffer was prepared and the pH corrected to 7.14 for all the experiments, to mimic the pH values of the harvest solution. For the CEX resin studies, a 25 mM NaOAc solution at pH 4.5 was prepared. The elution buffers used for the protein A and CEX resins were 25 mM NaOAc pH 3.5, and 25 mM NaOAc with 1M NaCl pH 4.5, respectively. The provided mAb in purified form was buffer-exchanged to the buffer solutions mentioned above (depending on the resins studied) and diluted until the desired concentration was achieved. A highly concentrated solution of mAb in 1x PBS buffer was used to increase the concentration of mAb in the harvest for the HTS experiments using the harvest.

6.2.4. Analytical Methods

The concentration, aggregation, and purity of the eluates of harvest samples was determined by analytical size-exclusion (SEC) chromatography UltiMate 3000 UHPLC System (Thermo Fisher Scientific, Waltham, MA). 5 µl of each sample was injected in an ACQUITY UPLC Protein BEH SEC 200 Å column (Waters Corp., Milford, MA), using the running buffer 100 mM sodium phosphate buffer pH 6.8, a flowrate of 0.3 ml/min and absorbance of 280 nm. Protein concentration in the studies with pure mAb (until 5 mg/ml) was determined using appropriate calibration curves obtained using the ÄKTA system.

6.2.5. Criteria for resin selection

The selection of the pool of ProA and CEX resins used for this study was based on previous work [17]. Three ProA resins were chosen for the optimization studies, and from the output of these studies, the operating conditions of the pure mAb PCC experiments were chosen, both to validate the continuous model and compare the performance of the resins. A productivity of around 100 $mg/ml_{resin}/h$ was chosen for all

resins. After the experimental runs, and provided that the experimental results were in line with the *in-silico* results, the ProA resin that showed the best results of productivity and CU was chosen for the PCC with the Harvest. The CEX resin chosen for the subsequent polishing step was based only on the optimization results from the two optimized resins, since it was expected that experimental and *in-silico* results would not differ.

6.2.6. Continuous runs – Pure mAb and Harvest

For the capture experiments, a concentration of 5 mg/ml of mAb was selected and the process was run for a total of 8 cycles. The 3C-PCC experimental runs with pure mAb were used to validate the model results and compare the performance of the resins. The best performing resin in terms of the selection criteria was used for the capture step from the Harvest mixture, at a mAb concentration of 5 mg/ml.

The capture step eluates from the harvest trials were stored in elution buffer for a minimum of 1h, then mixed, and the pH was corrected to 4.5. This solution was then used as input for the 3C-PCC run of the CEX resin. Due to the concentrating ability of chromatography, the available solution for the CEX trials allowed to run 4 cycles, instead of the 8 cycles for the ProA resin.

6.2.7. Continuous experimental setup and process control

The experimental setup for the 3C-PCC runs (pure mAb and continuous) is shown in **Figure 6.3**. This setup is similar to the one used by Gomis-Fons *et al.*, applied in an ÄKTA Avant 25 unit [16]. The column valve (ColV) is used to dictate the flow path of the loading of sample (green line). The versatile valves (VVs) and outlet valve (OutV) are used to direct the flow after each column. In **Figure 6.3** is shown an example where C1 and C2 are in the interconnected loading phase, whereas C3 is undergoing the non-loading steps (blue line). The UV1 monitor is used to monitor the loading and wash phases of each column and the UV2 monitor is used to monitor the elution steps and what leaves column in the position *i+1* in the interconnected wash step. Lastly, the loop valve (LV) is used to fractionate the eluates, whenever the pooling is active. The chromatography system is controlled by the research software Orbit [20], which was previously used for the control and monitoring of continuous purification processes [21].

6.2.8. Statistical Analysis

The reported uncertainties were calculated considering the systematic error and the statistical error resulting from random variation of measured values. The sample standard deviation and error propagation was calculated according to Young [22]. For the systematic error, only the uncertainty associated with the parameter regression of the

calibration was accounted, as other equipment errors were considerably smaller and thus negligible.

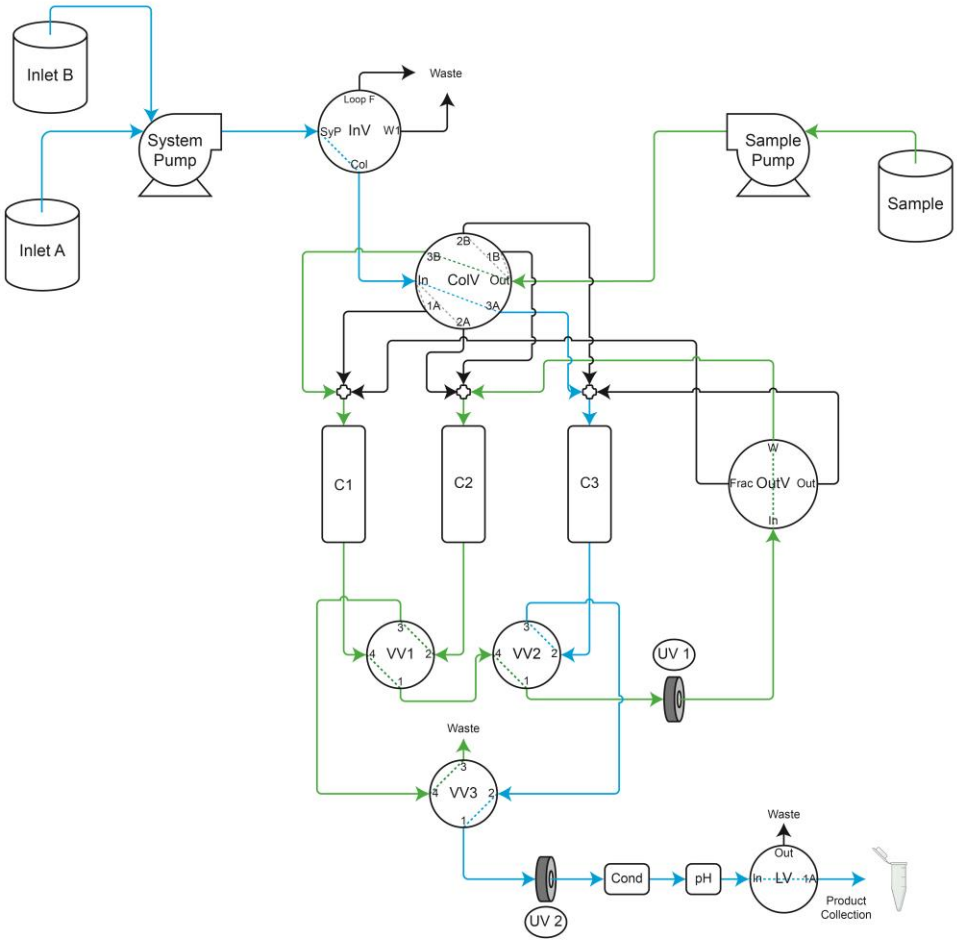

Figure 6.3 - Experimental set-up of the 3C-PCC process on the ÄKTA Avant 25. The example shows the interconnected loading from column 1 to column 2 (green line) while column 3 undergoes the non-loading steps (blue line) (in this case the elution step, where there is product collection).

6.3. Results and Discussion

6.3.1. Optimization PCC – Protein A

The optimization of the ProA 3C-PCC was accomplished by estimating the Pareto fronts for Productivity and CU. The Pareto fronts can be calculated for any combination of KPIs, which can be Purity, Yield, CU, concentration factor, Productivity, among others [16, 23]. In case of the present work, the Yield was used as a constraint and the

Productivity and CU were regarded as more important KPIs to optimize, since it was expected that the purity would be high after the ProA step. The optimization was carried out for three different resins, at four different feed concentrations for the 3C-PCC system and one feed concentration for the batch system.

6.3.1.1. Resin Selection

There is a wide variety of ProA ligand resins available in the market, which makes it difficult to narrow down to one single resin. The three resins chosen for optimization were based on previous HTS work [17], based on the maximum binding capacity and affinity constant values from the isotherm study, and operating stability: MSS (chosen due to its industrial relevance to date), MSPrismA, and MSSpcc. As mentioned in **Figure 6.1**, the BTC shape also plays a role in the suitability of the resins to be used in a 3C-PCC system. Previous work with these three resins showed that all BTCs showed promising profiles to be used in a 3C-PCC system [17].

6.3.1.2. Different Concentrations tested in optimization: preparing for the future

The optimization of the 3C-PCC was run for four different concentrations: 2, 5, 7.5, and 10 g/L. Titers as high as these are becoming the norm for USP [1], thus in a process intensification point-of-view it is imperative that DSP prepares for the future. 2 g/L is already the norm in mAb titers and 5 g/L titers are becoming more and more common [24], with titers as high as 10 g/L being rarer but having already been reported [25]. The model calibration was performed for mAb concentrations up to 5 g/L, and varying flowrate with constant feed concentration of 5 g/L [17], which implies that the higher concentrations are extrapolations of the model. Although the experimental verification of such results is advised, we are confident that the linear correlation that was reported between the mass transfer coefficient and feed concentration holds true for higher concentrations [17]. Thus, it is anticipated that the extrapolated results show no major deviations from what is expected and were deemed reasonable and trustable.

Figure 6.4 shows the Pareto fronts for the different ProA resins (A-MSS; B-MSPrismA; C-MSSpcc). The shape of the Pareto fronts for all resins is mainly influenced by the BTC profiles of the resins under different operating conditions. The productivity is mainly affected by the flow rate, since at a higher flow rate and constant feed concentration it is possible to process more product at the same processing time. However, higher flow rate will lead to flattening of BTCs, which means that the columns will have to be interconnected for the load phase earlier. Furthermore, to reach high values of *%s* the columns will have to be interconnected for longer periods, which could lead to a breakthrough in the second column while the first is still not loaded to the required *%s*, thus the capacity will be affected to have the yield within the requirements. This is noticeable for the lower concentrations tested (2 and 5 g/L) and especially for MSS.

Since MSS has the lowest capacity of the three columns, it will be the most negatively affected by an increase in the flowrate, and in **Figure 6.4 A** it is clear that small increases in productivity (achieved by increasing the flow rate) lead to increasingly larger decreases in CU, due to flattening of the BTCs. Similar phenomena has been previously reported [16].

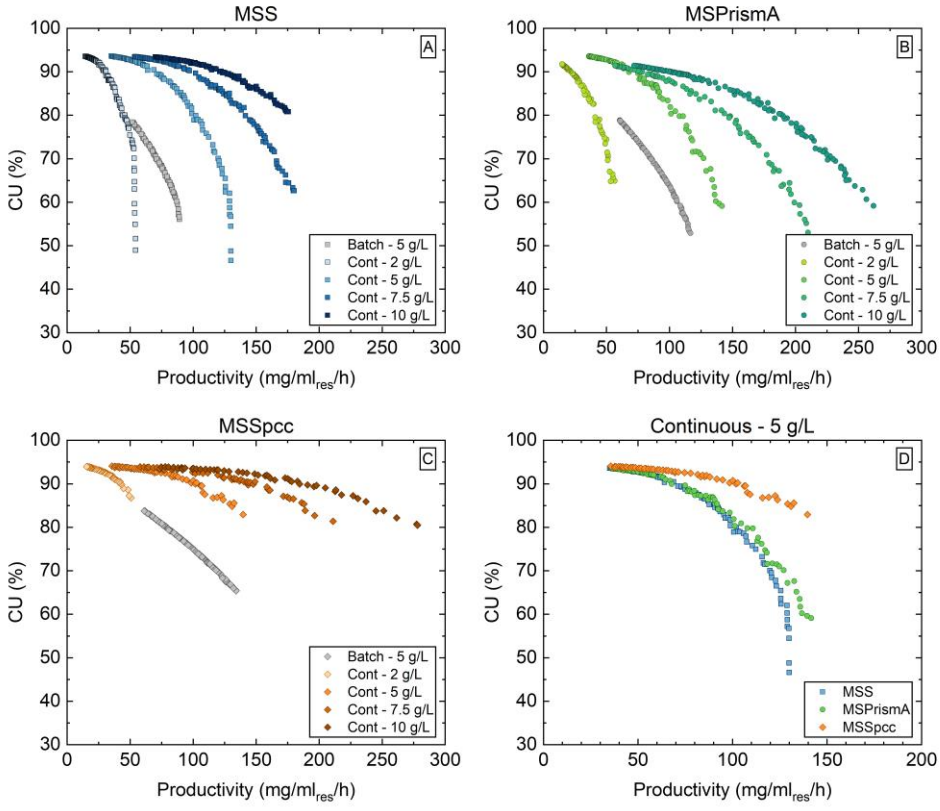

Figure 6.4 - Optimization plots of the three different Protein A resins studied for the capture step of mAb. A, B, and C are the Pareto fronts for MSS, MSPrismA, and MSSpcc, respectively. The optimization was done for batch mode (at cmAb of 5 g/L) and continuous mode (at cmAb of 2.5, 5, 7.5, and 10 g/L). D – Comparison of the optimizations for continuous chromatography of the three different resins at a 5 g/L concentration of mAb.

In **Figure 6.4 C**, it is interesting to observe that MSSpcc is the resin that shows the least variation in the slope of the Pareto fronts between the different concentrations. This resin, which was designed to have improved mass transfer capabilities, is the least affected by a change in the flow rate, hence why the "drop" that is observed for the other two resins is not observed. For MSSpcc the BTCs did not become significantly shallower at increased flow rates, and showed the later breakthrough time out of the three resins. In fact, from **Figure 6.4 A** to **C** one can see a decrease in the slope of the

Pareto fronts, which directly correlates with decreasing particle radius (MSS – 85 μm, MSPrismA – 60 μm; MSSpcc – 50 μm) and inversely correlates with the increasing maximum binding capacity (MSS – 52 mg/ml, MSPrismA – 79 mg/ml; MSSpcc – 97 mg/ml) [17].

The improved mass transfer from smaller resin particles [26] and higher binding capacities will allow for sharper BTCs at higher flow rates, allowing to increase productivity without greatly hampering the CU. **Figure 6.4 D** shows the Pareto fronts for each of the resins for the 3C-PCC at 5 g/L feed concentration. The Pareto fronts follow the trend discussed above, and this comparison highlights that for a similar Productivity a much higher CU can be achieved using MSSpcc compared to MSPrismA and MSS. For productivities above 70 $mg/ml_{res}/h$, MSSpcc has CU values of 5% or above compared with the other resins, which means that if the desired productivity is above such value, MSSpcc would be the best alternative at this feed concentration.

A Pareto-front for the different systems using a feed concentration of 20 g/L was also tested. However, the results showed no feasible process was possible to achieve at this feed concentration. This is because the highly concentrated feed will saturate the binding sites in the column with very little volume and the inter-connected load phase volume will be a fraction of the non-interconnected load phase volume, meaning that very little time is available for the non-loading steps of the column. Therefore, the condition of feed continuity in this system would not be met, meaning that a continuous system could not be achieved. The described system is based on 1 mL columns, which are very small. Performing the same optimization for columns of bigger dimensions would possibly lead to a feasible process for that feed concentration.

6.3.1.3. Batch VS Continuous

The comparison between the batch and continuous mode of operation is important to understand if the continuous operation is able to deliver a process that has higher productivities and capacity utilization [18]. Since in 3C-PCC the loading is interconnected, it is expected that the Pareto-front for the continuous process is above the Pareto-front for the batch process. In fact, this is what is observed for all resins (**Figure 6.4**). Higher productivities are achieved by having a higher flow rate and, therefore, a higher throughput of material. An increase in the flow rate will lead to earlier breakthrough times and shallower BTCs, meaning that interconnecting the columns is needed to increase CU without compromising productivity and yield. Interconnected loading allows to increase the *%s*, which leads to more protein being loaded onto the column and consequently more protein adsorbing to the available binding sites, leading to higher CU. Since the optimizations are constrained to 99% Yield, the batch processes

will consequently have lower CU, since the *%s* achieved by this process will be much lower than what can be achieved for the continuous processes.

A comparison of Pareto fronts for batch and continuous processes has been previously shown [16]. In this study, and since the focus is to optimize for the current titers and prepare for higher titers in the future, the comparison between batch and continuous modes of operation was done for 5 g/L. For all resins, the batch Pareto-front follows the continuous Pareto-front in a seemingly parallel fashion. This is because of what was mentioned above, with the interconnecting of the columns allowing to reach higher %DBC in the first column, increasing CU for the same productivity. For example, for a productivity of 70 mg/ml$_{res}$/h, the CU of continuous increased 27, 19, 13 % compared to batch, for MSS, MSPrismA, and MSSpcc, respectively. For a CU of 80%, productivity is 91, 67, 82 % higher compared to batch, for MSS, MSPrismA, and MSSpcc, respectively. This shows the potential of continuous chromatography, with large increases in productivity and CU being possible using this mode of operation. Nonetheless, it is noticeable that the batch processes for this feed concentration can still go to high productivities. This comes at the cost of lower CU, caused by the earlier breakthrough times for processes with higher flowrates. Ultimately, continuous mode of operation is able to offer better KPIs for the process compared to the batch mode of operation. However, this comes at a higher operational complexity and the choice between batch and continuous mode of operation depends on the manufacturing scenario and the manufacturer's goal.

6.3.2. Continuous runs pure mAb – Protein A

The results of the optimization provide some insight on the performance of the three different resins. However, it is important to understand if the model's results are in agreement with experimental results. To do this, a 3C-PCC experiment was performed with each of the different resins, for a feed concentration of 5 g/L, and the experimental KPIs compared with the model's KPIs. To compare the different resins, the productivity of 100 mg/ml$_{res}$/h was chosen for all the resins and the corresponding loading flow rate and *%s* was used for each of the resins' experiments. **Figure 6.5** shows the resulting chromatograms of this comparison for MSPrismA. A total of 8 cycles (fully loading the three columns) were done, where the first cycle is the startup phase and the last cycle is considered to be the shutdown phase. The first injection is done in C3, meaning that the injection in C1 of the first cycle is the second peak in the total chromatogram.

Figure 6.5 A shows the total chromatogram of the continuous run. The concentration was estimated from the UV-signal and appropriate calibration curve in the ÄKTA Avant system, which is linear until 5 g/L. The elution peaks' concentration maximum is well

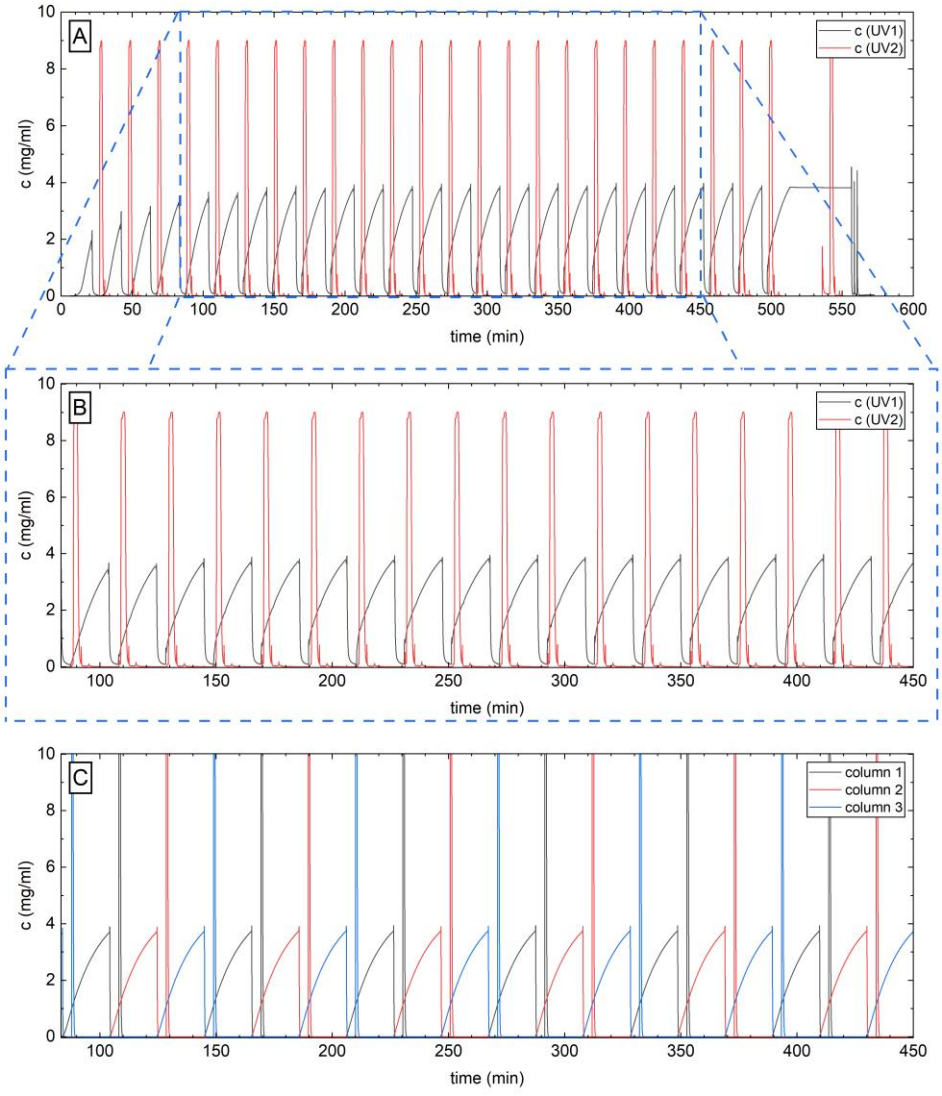

Figure 6.5 - Experimental validation of the continuous chromatography model for the capture step with a pure sample of mAb using MSPrismA. The initial concentration is 5 g/L and the loading flowrate is 0.71 ml/min. A – total chromatogram; B – Zoom in on the steady-state of the cyclic operation of the 3C-PCC; C – Model data for the same cyclic period as shown in B. In A and B, black and red represent the concentration observed in UV1 and UV2, respectively. In C, black, red, and blue represent the outlet concentrations observed for columns 1, 2, and 3, respectively.

above 9 g/L, and what can be seen in the figure is an artifact from the signal saturation in the ÄKTA system's UV-detector. **Figure 6.5 B** shows the steady-state part of this operation. It is possible to see that from the second cycle the operation is already at steady-state through the similarities in the shapes of the BTCs of different cycles.

Figure 6.5 C shows the steady-state operation of the same process performed *in-silico*, with the operating conditions chosen to be the same as the ones used in the experiments. The experimental profile of the 3C-PCC run is very similar to the model's profile for all the different chromatographic stages, like the loading profiles (shape of the breakthrough curve in the different cycles) and the washing and elution profiles. The model even captured the miniscule "peak" that can be seen in the beginning of the washing, which is an artifact due to the use of a higher flow rate for the wash stage compared to the loading stage (also observed in the experiments). The model's washing curves show a sharper decrease in concentration when compared to the experimental curve, which can mainly be attributed to the lack of ideality of the experiments compared to the model. The model also did not capture the small peak of the CIP. This is because when modelling the system it was assumed that no mAb would be irreversibly bound to the column, therefore the model predicted that all the mAb adsorbed in the loading phase would be collected in the eluate. Nonetheless, it was already expected that there would be some loss of product in the CIP stage, which was observed experimentally.

Table 6.1 shows a comparison between the KPIs predicted by the model in the optimization and what was obtained experimentally, for a target productivity of 100 $mg/ml_{res}/h$, for the three different resins. The target productivity was based on the optimization using the feed concentration of 5 g/L. In reality, the solutions prepared for the 3C-PCC experiments had a slightly different concentration than 5 g/L (MSS – 4.92 g/L; MSPrismA – 4.83 g/L; MSSpcc – 4.9 g/L), and the concentration of the solutions used experimentally was used to estimate the KPIs of the different resins and provide a fair comparison. The experimental results for the different resins show a very good agreement between the KPIs predicted by the model and the experimental KPIs. The yield values were lower than the model's estimations because the model was set to optimize based on a 99% yield constraint. As mentioned above, the model assumed that all the protein adsorbed in the would be recovered in the eluate, with the yield losses mainly being attributed to losses in breakthrough of the second column in the interconnected phase. However, in practice this is not what happens, and there can be some "irreversible" binding, and some of the protein can only be displaced with harsher chemical conditions, such as the ones of the CIP stage, explaining the small peaks observed in the CIP stage in **Figure 6.5**. Nonetheless, the deviation for all the resins is below 4 %.

The experimental productivity values are also in agreement with the experimental values for the 3 resins studied. Productivity values depend on the yield values, since it is a measurement of the output of the process. If the output is lower due to a lower yield, the productivity of the process will also be lower. This is confirmed by the larger

deviations in productivity coming from the resins that had the larger deviations in yield, which for the productivity are not larger than 3.9 % for all the resins.

CU is the measurement of the amount of mAb that is actually adsorbed to the resin in a cycle compared to the total theoretical amount of mAb that the resin could adsorb (if all binding sites would be occupied), and it also depends on, among other things, the yield values. Overall, the CU of the model's predictions and the experimental values are in good agreement, but vary between the different resins, contrary to yield and productivity. This is because yield was a constraint and productivity was the KPI chosen to keep the same for all resins. All resins present quite a high CU (all above 78%), with MSSpcc showing the highest CU, at 88%, which was already expected from the optimization results.

The *%s* values for MSPrismA and MSSpcc followed the predictions from the model. However, the experimental *%s* for MSS was higher than the model predicted. The main difference between model and experiments is that the model was built with no dead volumes between the columns, since tubing could have to be replaced during operation, and it was decided to model assuming no dead volume between the columns. This assumption is acceptable because the dead volume between columns was not expected to be large enough to affect operation, and therefore the complexity of the model was reduced. It is hypothesized that the dead volume between the tubes still had some protein solution when there was a switch between the loading and the washing phases. Since the BTC for MSS has a relatively sharp profile at the operated flow rate between *%s* of 65 to 85%, this dead volume that is not accounted for in the model could help explain the difference between model and experimental %s values. For MSPrismA and MSSpcc, the curves at the respective operational flow rates are slightly less sharp, explaining why the deviations are not considerable.

Table 6.1 - Comparison of the model and experimental Key Performance Indicators (KPIs) for the pure mAb experiments, with the 3 different Protein A resins tested. The feed concentrations used for the model's values were the same as for each experiment's feed concentration: MSS – 4.92 g/L; MSPrismA – 4.83 g/L; MSSpcc – 4.9 g/L. Loading flow rate for each resin: MSS – 0.70 ml/min; MSPrismA – 0.71 ml/min; MSSpcc – 0.72 ml/min.

	MSS		**MSPrismA**		**MSSpcc**	
	Model	Experimental	Model	Experimental	Model	Experimental
Yield (%)	99.57	95.88 ± 3.75	99.61	98.47 ± 3.85	99.15	95.88 ± 3.75
Prod.	97.98	94.35 ± 3.69	96.18	96.07 ± 3.76	98.74	96.51 ± 3.78
CU (%)	78.90	76.24 ± 2.98	81.62	79.68 ± 3.12	90.01	88.24 ± 3.45
% s (%)	67.80	78.03 ± 2.23	79.96	77.91 ± 2.38	89.68	87.68 ± 3.67

The results show that the mechanistic model for the chromatographic columns [17] and the continuous model employed in the context of this work are validated, both by the concentration profiles from the *in-silico* and lab experiments as well as by the KPIs obtained. The presented continuous model is capable of optimizing the operation of a 3C-PCC chromatography with great accuracy. Given the KPIs of the different resins, MSSpcc was the selected resin for the harvest trials since it showed the best performance of all evaluated resin candidates.

6.3.3. Continuous runs Harvest – MSSpcc

After performing the 3C-PCC experiments with pure mAb for the different resin candidates, the best performing resin (MSSpcc) was selected for the capture of mAb from a harvest solution. **Figure 6.6** shows the resulting chromatogram of the experiment with the harvest solution. In the case of the 3C-PCC for the harvest solution, the base UV signal was considerably higher than what was observed for the pure mAb study, due to the presence of different components in solution (HCPs, genetic material, among others). Consequently, a direct translation from the UV-signal to concentration of mAb was not possible for the harvest experiment.

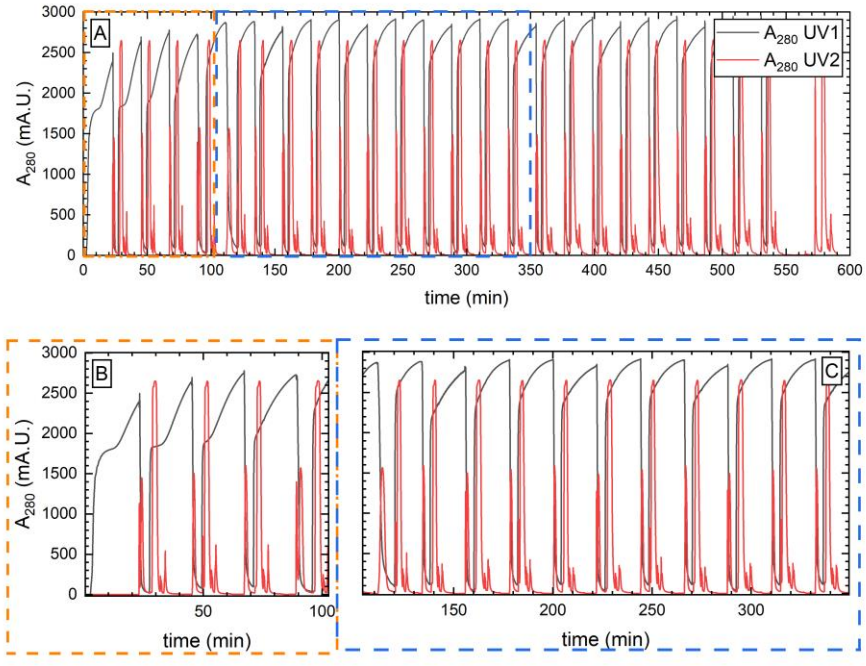

Figure 6.6 - Experimental run of the capture step with Harvest. A – Full length chromatogram; B – Zoom in on the start-up phase of the experiment; C – Zoom in on part of the cyclic operation of the continuous chromatography. In all graphs, black and red represent the absorbance values at 280 nm in UV1 and UV2, respectively.

Figure 6.6 B shows the startup phase and **Figure 6.6 C** shows the steady-state phase of the 3C-PCC operation. From **Figure 6.6 B** it is possible to see that the base UV signal is around 1800 mA.U. and from both **Figure 6.6 B** and **C** it is possible to see the BTC of the loading of the columns, even with the high baseline. The high baseline value made it impossible to calculate *%s*, since this KPI was estimated based on the chromatogram and sampling was only performed during the elution steps. Another difference from the pure mAb experiments is the presence of a peak in the UV2 during the washing phase, which corresponds to the components in solution that are being washed out and do not adsorb to the column that is receiving the wash from the column being washed. In **Figure 6.6 C** it is possible to see that the steady-state of the operation is reached, and that the UV signals during loading, washing, elution, and CIP are consistent over time.

From previous studies it was proven that adsorption behavior of the studied mAb does not change significantly between a pure mAb solution or mAb in harvest [17]. Based on this observation, it was expected that MSSpcc's KPIs would be comparable in the case of the harvest experiment. To assess if the KPIs of the harvest solution were comparable to those of the pure solution and the *in-silico* optimization, the KPIs were calculated and are shown in **Table 6.2**. The model's KPIs shown in **Table 6.2** for MSSpcc are the results that were obtained from the optimization at 5 g/L feed concentration, hence why these are different than what is shown in **Table 6.1** (which were obtained using the real concentration of the sample for the pure mAb MSSpcc trial). The feed concentration of mAb for the harvest trials could not be estimated, therefore it was assumed to be 5 g/L. The results in **Table 6.2** show a slight reduction in yield and productivity and a more pronounced reduction in CU, compared to the pure mAb experiments. The majority of mAbs adsorb to protein A ligands through the Fc-region [27]. If some other media components are present and causing some steric hindrance, it could be that this phenomenon would negatively interfere with the adsorption of mAbs to ProA ligands, justifying the reduction observed for CU. Nonetheless, the process showed that it could perform very similarly to the pure mAb process, and the obtained KPI values are very close to what the optimization had predicted. Besides the KPIs, the content of monomer, and High and Low Molecular Weight (HMW and LMW, respectively) species was determined **Table 6.2**. From this result we can see that the continuous capture step was able to purify the initial sample to great extent, with mAb content (monomer plus HMW species) representing more than 98.5% of the mixture.

6.3.4. Optimization PCC CEX

Similarly to what was done for the optimization of ProA, the optimization for the CEX step was achieved by estimating the Pareto fronts for Productivity and CU. Once again, the Yield was used as a constraint. In total, two different resins were used for the

optimization, and the optimization was performed only for the case of a continuous process (3C-PCC).

6.3.4.1. Resin selection

The variety of CEX resins available is even wider than the ProA resins. From a pool of 16 different resins (of which some were multimodal CEX resins), two were selected [17]. The selection was based on different criteria (binding capacity, operating stability, among others), and the two resins selected were SP Sepharose Fast Flow (SP Seph FF) and Capto™S ImpAct (CaptoS).

6.3.4.2. Different Concentrations tested

A total of four different concentrations were tested in the optimization of the 3C-PCC for the CEX step: 5, 10, 15, and 20 g/L. Since the capture step is both a purification and concentration step, it is logical that the concentration of the ProA eluates is higher than that of the feed, even considering a pH correction after VI. The results of the optimization for SP Seph FF and CaptoS are shown in **Figure 6.7**.

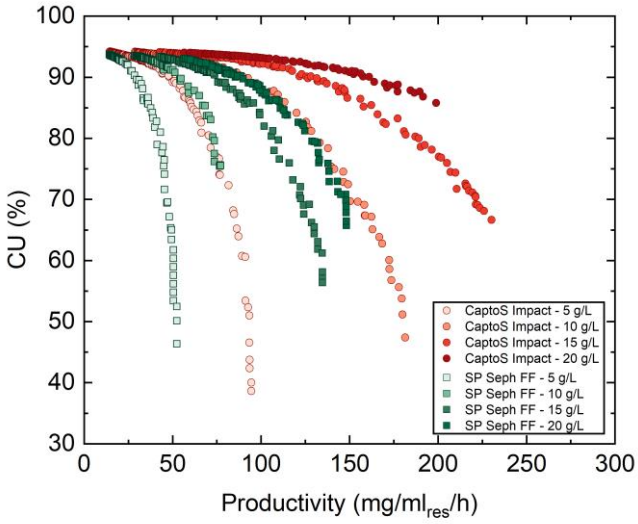

Figure 6.7 - Optimization plots of the two different CEX resins studied for the polishing step of mAb. Red and green represent CaptoS ImpAct and SP Seph FF, respectively. The optimization was done for continuous mode at 5, 10, 15, and 20 g/L feed concentration.

Comparing the Pareto fronts for both resins, it is possible to see that CaptoS shows better Pareto fronts, since for the same concentration, the productivity is in general much higher at the same CU. The CaptoS curves for 5 g/L and 10 g/L practically overlap with the SP Seph FF curves for 10 g/L and 20 g/L, highlighting the superior

performance of CaptoS. As mentioned for the ProA resins, the BTC profile influences greatly the Pareto front, sometimes significantly more than the binding capacity. From the 2 resins studied, SP Seph FF has a higher binding capacity compared to CaptoS (97 mg/ml_{res} VS 82 mg/ml_{res}) [17], but the BTC is flatter. Therefore, at the same flowrate it is expected that the sharper BTC profile of CaptoS will be advantageous in the interconnected loading phase, preventing losses in the second column. This is in line with what is advertised by Cytiva, since CaptoS was designed as a high-resolution resin.

The Pareto fronts for both resins in **Figure 6.7** also show that a higher feed concentration will lead to flatter Pareto curves, which is expected since to achieve the same productivity lower flow rates can be used and sharper BTC profiles will be obtained, consequently increasing CU [16]. The lower maximum productivity achieved for CaptoS for 20 g/L compared to 15 g/L is justified by the yield constraint. To increase productivity it is necessary to increase the flow rate and, at 20 g/L, the increase needed to achieve higher productivities would also lead to shallower BTCs, causing early breakthrough in the second column. Therefore, there is a limit productivity associated with each feed concentration, which for the 20 g/L solution and the operating conditions tested is around 200 $mg/ml_{res}/h$. The operating conditions (flow rate, column volume, etc.) also influence the maximum productivity value achievable for each feed concentration.

6.3.5. Continuous run CEX with eluates of Continuous Harvest run of MSSpcc

The 3C-PCC run with CEX resin was performed to mimic what could be implemented in a continuous end-to-end process. To this effect, the eluates of the ProA harvest run were mixed and the pH was corrected to 4.5, after enough time was allowed for the VI. The concentration of this pool was 12 g/L, which was diluted to 10 g/L to be directly compared to what was obtained from the optimization shown in **Figure 6.7**. CaptoS showed the best KPIs from the *in-silico* optimization, therefore it was selected as the CEX resin for this step.

When optimizing processes in sequence it is beneficial to do it by matching product throughput on each step rather than flow rates (provided that viral inactivation is accomplished by low pH hold in surge vessels). This will in turn mean that the resin volume used in the polishing steps could be lower than the one used in the capture step, adding another layer of optimization of the global process, with the resin volume also possibly being a design variable. Since CEX resins usually have higher DBC values than ProA resins, a lower resin volume with higher productivity could have the same product throughput than the capture step, facilitating the connection between the two processes. For the present work, the optimization was limited to the smallest volume of pre-packed columns available in the market (1 mL). Nonetheless, the goal of matching the

productivities of capture and CEX steps was still achieved, and the operating conditions associated with a process with a productivity of 100 $mg/ml_{res}/h$ were used for the experiment.

The resulting chromatogram is similar to what can be observed in **Figure 6.5**, but with different concentrations achieved (data not shown). This was expected since the sample obtained after the ProA step is already very pure The KPIs resulting from the CEX 3C-PCC are summarized in **Table 6.2**. Similarly to the harvest run, the *%s* could not be determined for the CEX 3C-PCC since the UV signal was outside of the calibration curve and there was no pooling during the loading step. The very high yield values are in accordance with what was observed during the runs, with virtually no breakthrough on the second column observed during the interconnected loading or peak observed in the CIP. Both experimental CU and productivity are in accordance with the optimization result, once again highlighting the usefulness and predictive ability of the used model. The percentage of monomer registered no major changes, with only a slight enrichment of monomer in the mixture being observed. The content of HMW and LMW species changed slightly after the CEX step, with a decrease in LMW and increase in HMW species. CEX is used as a polishing step to separate the monomer from remaining impurities, which can be aggregates, leached ProA, acidic proteins, genetic material, among others. Recombinant ProA has a pI lower than the mAb (4.7-4.8 [28]) and that is very close to the operating pH for the CEX run, which makes CEX a suitable step to remove leached ProA. Since ProA has a low Mw (45 kDa), the reduction of the LMW species could be a consequence of the removal of leached ProA from the mixture.

Table 6.2 - Comparison of the model and experimental Key Performance Indicators (KPIs) for the Harvest experiments, for MSSpcc and CaptoS Impact. The average percentage of Monomer, HMW, and LMW species in the eluate fractions are also shown, with the error representing the standard deviation of the eluates' values. Loading flow rate for each resin: MSSpcc – 0.72 ml/min; CaptoSImpact – 0.36 ml/min.

	MSSpcc		***CaptoS Impact***	
	Model	Experimental	Model	Experimental
Yield (%)	99.15	95.80 ± 5.42	99.56	99.30 ± 5.92
Productivity	101.80	94.88 ± 5.36	102.28	100.07 ± 5.97
CU (%)	90.00	84.53 ± 4.78	86.38	88.57 ± 5.28
% *s* (%)	89.50	-	83.73	-
Monomer (%)	-	97.39 ± 0.16	-	97.42 ± 0.04
HMW (%)	-	1.36 ± 0.19	-	1.46 ± 0.03
LMW (%)	-	1.25 ± 0.08	-	1.12 ± 0.03

6.3.6. Model Evaluation

The continuous model used in this work was used for the *in-silico* optimization of a ProA and CEX 3C-PCC steps. The model was then validated experimentally for the ProA step using a pure mAb solution for the three different ProA resins tested, with all resins showing experimental KPIs in accordance with the model's predictions. A 3C-PCC experiment with the best performing ProA resin was used to purify mAb from a harvest mixture, achieving results comparable with the pure mAb experiment and the model's predictions. The eluates from the 3C-PCC with harvest solution were used as feed for the CEX 3C-PCC, which served as the experimental validation of the CEX optimization. The experimental KPIs obtained were also in accordance with the model's predictions.

The continuous model was able to accurately predict chromatographic behavior for a 3C-PCC process. As can be seen in **Figure 6.5**, the model prediction of the chromatogram and experimental chromatogram have very similar profiles. The model also predicted a steady-state from the second cycle onwards (data not shown), which is in accordance with what is observed experimentally (**Figure 6.5 A** and **B**). The model was then used to optimize the 3C-PCC step, and the operating variables (flowrate and *%s*) corresponding to a productivity of 100 $mg/ml_{res}/h$ were selected for experimental validation, both for the ProA and CEX step. The results showed that the model could accurately predict the KPIs for the ProA (with pure mAb and harvest) and CEX 3C-PCC, with deviations lower than 6.8%, in the worst case. Therefore, the presented model provides a powerful tool for fast and accurate process optimization.

6.4. Conclusions

This work focused on the *in-silico* optimization of a continuous chromatography step for the capture and polishing of monoclonal antibodies. This approach focused on using a mechanistic model for the simulation of the chromatographic behavior and used as optimization objective two different KPIs: Productivity and Capacity Utilization. Since these cannot be optimized without penalizing the counterpart, Pareto fronts were generated and used to choose the best operating conditions according to the desired KPIs for each process.

Considering the recent advancements in USP, high feed concentrations of mAb were used for the optimization of the 3C-PCC capture step (2, 5, 7.5, and 10 g/L). Three different ProA resins were optimized: MSS, MSPrismA, and MSSpcc. The Pareto fronts of the three resins (**Figure 6.4**) show different profiles, and MSSpcc Pareto front has the flatter profile for all the tested resins. The sharper BTC profile this resin has compared to the other two allows to increase the flowrate without "flattening" the BTC excessively [17], thus allowing for a higher CU at the same productivity and reducing the

losses in the second column in the interconnected loading. The model's results were experimentally validated for all ProA resins with a pure mAb solution at 5 g/L, with operating variables chosen for a Productivity of approximately 100 mg/ml$_{res}$/h for all resins. Deviations of the KPIs (Productivity, CU, and *%s*) between model prediction and experimental values were marginal (only for *%s* there was a bigger deviation, discussed above). MSSpcc was then used for the continuous capture of mAb from a Harvest mixture, using the same experimental conditions as for the pure mAb. Once again, the KPIs were similar to what the model had predicted, thus proving that optimization results for ProA chromatography from pure mAb experiments can be achieved.

A 3C-PCC CEX was also optimized for two different resins (SP Seph FF and CaptoS) and four different concentration (5, 10, 15, and 20 g/L). Although SP Seph FF had higher binding capacity, the Pareto front for all feed concentrations of CaptoS had a less sharp slope, and thus performed better in the *in-silico* optimization. This highlights the importance of considering the BTC shape in continuous chromatography optimization, rather than only looking at binding capacity, since CaptoS had a lower binding capacity but a considerably sharper BTC profile than SP Seph FF. For experimental validation, a productivity of 100 mg/ml$_{res}$/h was also selected. Like for the ProA ligands, the results between model and experimental KPIs were marginal.

Although the model does not have an interconnected ProA and CEX, it could still be used to design a process where ProA and CEX are interconnected, with a VI step in between. The throughput of the processes (ProA, VI, and CEX) can be used as a decision variable for the interconnection of the steps, rather than the classic flow rate. If VI is performed in at least two different CSTR tanks, than the feed continuity of the CEX 3C-PCC can be ensured and a continuous output of material can be achieved. The experimental work described can be used to mimic a capture and polishing step for the purification of monoclonal antibodies from a harvest solution.

In conclusion, the presented model was able to predict continuous chromatographic behavior for capture and polishing steps of a mAb process. The model was validated experimentally for three different ProA resins using a pure sample, and the best performing resin was used for the purification of mAb from a harvest solution. Lastly, the CEX optimization was also validated experimentally, using as feed the pooled mAb from the harvest run after ProA purification (at a CEX feed concentration of 10 g/L). The sample obtained from the whole process, at an initial feed concentration of 5 g/L, is in a highly pure form (97.4% monomer, 1.5% HMW, 1.1% LMW) and the throughput of the process is approximately 100 mg/ml$_{res}$/h. Mechanistic models should be sufficiently accurate to provide a suitable process design, and the shift to the experimental space would benefit from having control mechanisms, where the next step would be to fine tune operating variables during processing [29]. This needs proper PAT

and control strategies and could help mitigate the effect of fouling and capacity loss while maintaining purity requirements.

6.5. Acknowledgements

The authors would like to acknowledge Joaquin Gomis-Fons for the valuable contributions in the development of the 3-Column Periodic Counter-Current Chromatography step in the ÄKTA Avant systems through the implementation of the Orbit software. This work has received funding from the European Union's Horizon 2020 research and innovation program under the Marie Skłodowska-Curie grant agreement No 812909 CODOBIO, within the Marie Skłodowska-Curie International Training Networks framework.

6.6. References

[1] G. Jagschies, E. Lindskog, K. Lacki, P.M. Galliher, Biopharmaceutical Processing: Development, Design, and Implementation of Manufacturing Processes, Elsevier2018. https://doi.org/10.1016/C2014-0-01092-1.

[2] A.L. Grilo, A. Mantalaris, The Increasingly Human and Profitable Monoclonal Antibody Market, Trends in Biotechnology 37(1) (2019) 9-16. https://doi.org/10.1016/j.tibtech.2018.05.014.

[3] B. Kiss, U. Gottschalk, M. Pohlscheidt, New bioprocessing strategies: development and manufacturing of recombinant antibodies and proteins, Springer2018.

[4] J. Pollock, G. Bolton, J. Coffman, S.V. Ho, D.G. Bracewell, S.S. Farid, Optimising the design and operation of semi-continuous affinity chromatography for clinical and commercial manufacture, Journal of Chromatography A 1284 (2013) 17-27. https://doi.org/10.1016/j.chroma.2013.01.082.

[5] D. Pfister, L. Nicoud, M. Morbidelli, Continuous biopharmaceutical processes: chromatography, bioconjugation, and protein stability, Cambridge University Press2018.

[6] D.E. Steinmeyer, E.L. McCormick, The art of antibody process development, Drug discovery today 13(13-14) (2008) 613-618. https://doi.org/10.1016/j.drudis.2008.04.005.

[7] A.M. Azevedo, P.A. Rosa, I.F. Ferreira, M.R. Aires-Barros, Chromatography-free recovery of biopharmaceuticals through aqueous two-phase processing, Trends in biotechnology 27(4) (2009) 240-247. https://doi.org/10.1016/j.tibtech.2009.01.004.

[8] A. Jungbauer, Continuous downstream processing of biopharmaceuticals, Trends in biotechnology 31(8) (2013) 479-492. https://doi.org/10.1016/j.tibtech.2013.05.011.

[9] A.C. Fisher, M.-H. Kamga, C. Agarabi, K. Brorson, S.L. Lee, S. Yoon, The current scientific and regulatory landscape in advancing integrated continuous biopharmaceutical manufacturing, Trends in biotechnology 37(3) (2019) 253-267. https://doi.org/10.1016/j.tibtech.2018.08.008.

[10] M.N. São Pedro, T.C. Silva, R. Patil, M. Ottens, White paper on high-throughput process development for integrated continuous biomanufacturing, Biotechnology and Bioengineering 118(9) (2021) 3275-3286. https://doi.org/10.1002/bit.27757.

[11] F. Steinebach, T. Müller-Späth, M. Morbidelli, Continuous counter-current chromatography for capture and polishing steps in biopharmaceutical production, Biotechnology Journal 11(9) (2016) 1126-1141. https://doi.org/10.1002/biot.201500354.

[12] T. Müller-Späth, L. Aumann, G. Ströhlein, H. Kornmann, P. Valax, L. Delegrange, E. Charbaut, G. Baer, A. Lamproye, M. Jöhnck, Two step capture and purification of IgG2 using multicolumn countercurrent solvent gradient purification (MCSGP), Biotechnology and Bioengineering 107(6) (2010) 974-984. https://doi.org/10.1002/bit.22887.

[13] B. Somasundaram, K. Pleitt, E. Shave, K. Baker, L.H. Lua, Progression of continuous downstream processing of monoclonal antibodies: Current trends and challenges, Biotechnology and Bioengineering 115(12) (2018) 2893-2907. https://doi.org/10.1002/bit.26812.

[14] A.T. Hanke, M. Ottens, Purifying biopharmaceuticals: knowledge-based chromatographic process development, Trends in Biotechnology 32(4) (2014) 210-20. https://doi.org/10.1016/j.tibtech.2014.02.001.

[15] C. Shi, Q.L. Zhang, B. Jiao, X.J. Chen, R. Chen, W. Gong, S.J. Yao, D.Q. Lin, Process development and optimization of continuous capture with three-column periodic counter-current chromatography, Biotechnology and Bioengineering 118(9) (2021) 3313-3322. https://doi.org/10.1002/bit.27689.

[16] J. Gomis-Fons, N. Andersson, B. Nilsson, Optimization study on periodic counter-current chromatography integrated in a monoclonal antibody downstream process, Journal of chromatography A 1621 (2020) 461055. https://doi.org/10.1016/j.chroma.2020.461055.

[17] Silva, T. C., Eppink, M., Ottens, M., Digital Twin in High Throughput Chromatographic Process Development for Monoclonal Antibodies, Continuous Chromatography of Biopharmaceuticals – Next Generation Process Development (2024).

[18] R. Godawat, K. Brower, S. Jain, K. Konstantinov, F. Riske, V. Warikoo, Periodic counter-current chromatography–design and operational considerations for integrated and continuous purification of proteins, Biotechnology Journal 7(12) (2012) 1496-1508. https://doi.org/10.1002/biot.201200068.

[19] P.V. Danckwerts, Continuous flow systems: distribution of residence times, Chemical Engineering Science 2(1) (1953) 1-13. https://doi.org/10.1016/0009-2509(53)80001-1.

[20] N. Andersson, A. Löfgren, M. Olofsson, A. Sellberg, B. Nilsson, P. Tiainen, Design and control of integrated chromatography column sequences, Biotechnology Progress 33(4) (2017) 923-930. https://doi.org/10.1002/btpr.2434.

[21] J. Gomis-Fons, A. Löfgren, N. Andersson, B. Nilsson, L. Berghard, S. Wood, Integration of a complete downstream process for the automated lab-scale production of a recombinant protein, Journal of biotechnology 301 (2019) 45-51. https://doi.org/10.1016/j.jbiotec.2019.05.013.

[22] H.D. Young, Statistical Treatment of Experimental Data, McGraw-Hill Book Company, Inc., USA, 1962.

[23] B.K. Nfor, D.S. Zuluaga, P.J. Verheijen, P.D. Verhaert, L.A. van der Wielen, Ottens, Marcel, Model-based rational strategy for chromatographic resin selection, Biotechnology Progress 27(6) (2011) 1629-1643. https://doi.org/10.1002/btpr.691.

[24] T. Doi, H. Kajihara, Y. Chuman, S. Kuwae, T. Kaminagayoshi, T. Omasa, Development of a scale-up strategy for Chinese hamster ovary cell culture processes using the k La ratio as a direct indicator of gas stripping conditions, Biotechnology Progress 36(5) (2020) e3000. https://doi.org/10.1002/btpr.3000.

[25] M.W. Handlogten, A. Lee-O'Brien, G. Roy, S.V. Levitskaya, R. Venkat, S. Singh, S. Ahuja, Intracellular response to process optimization and impact on productivity and product aggregates for a high-titer CHO cell process, Biotechnology and Bioengineering 115(1) (2018) 126-138. https://doi.org/10.1002/bit.26460.

[26] R. Hahn, P. Bauerhansl, K. Shimahara, C. Wizniewski, A. Tscheliessnig, A. Jungbauer, Comparison of protein A affinity sorbents: II. Mass transfer properties, Journal of Chromatography A 1093(1-2) (2005) 98-110. https://doi.org/10.1016/j.chroma.2005.07.050.

[27] K. Huse, H.-J. Böhme, G.H. Scholz, Purification of antibodies by affinity chromatography, Journal of biochemical and biophysical methods 51(3) (2002) 217-231. https://doi.org/10.1016/S0165-022X(02)00017-9.

[28] ThermoFisherScientific, Pierce™ Recombinant Protein A, 2023. https://www.thermofisher.com/order/catalog/product/77673. (Accessed 25/07/2023 2023).

[29] A.S. Rathore, S. Nikita, G. Thakur, S. Mishra, Artificial intelligence and machine learning applications in biopharmaceutical manufacturing, Trends in Biotechnology (2022). https://doi.org/10.1016/j.tibtech.2022.08.007.

6.7. Supplementary Information

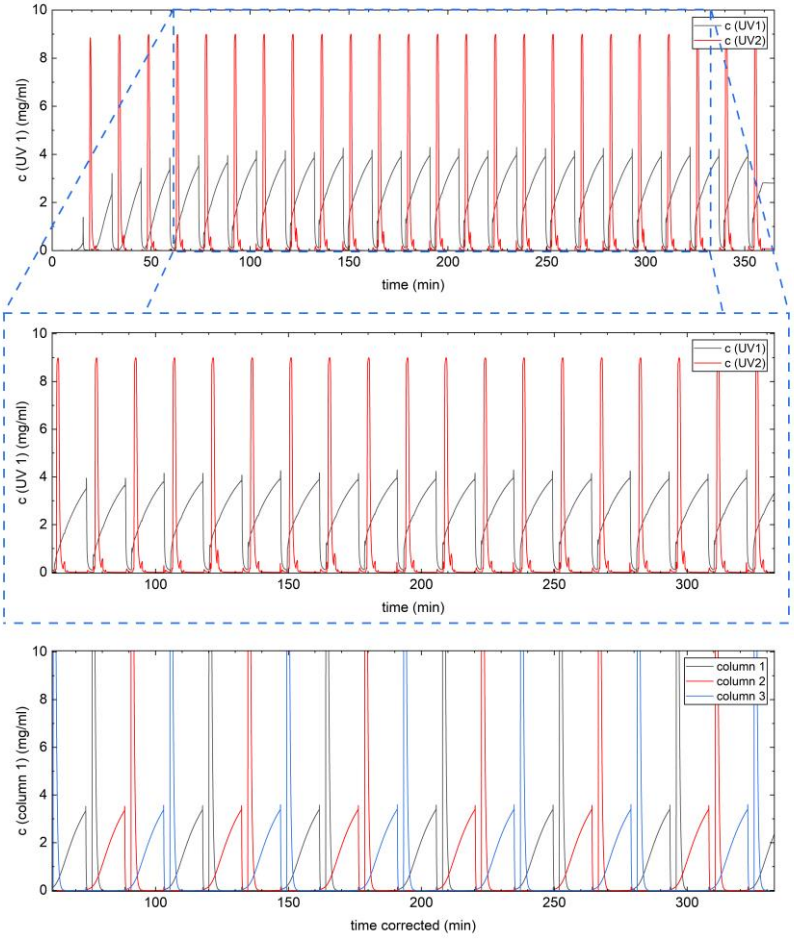

Figure SI 6.1 - Experimental validation of the continuous chromatography model for the capture step with a pure sample of mAb using MSS. The initial concentration is 5 g/L, and the loading flow rate is 0.70 ml/min. A – total chromatogram; B – Zoom in on the steady-state of the cyclic operation of the 3C-PCC; C – Model data for the same cyclic period as shown in B. In A and B, black and red represent the concentration observed in UV1 and UV2, respectively. In C, black, red, and blue represent the outlet concentrations observed for columns 1, 2, and 3, respectively.

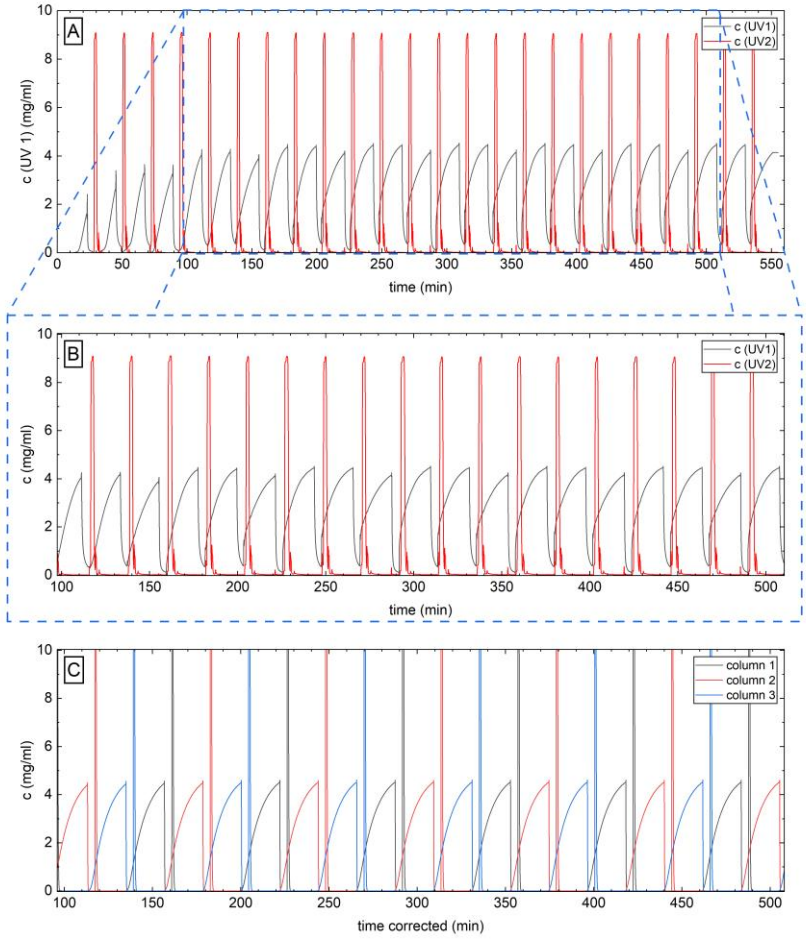

Figure SI 6.2 - Experimental validation of the continuous chromatography model for the capture step with a pure sample of mAb using MSSpcc. The initial concentration is 5 g/L, and the loading flow rate is 0.72 ml/min. A – total chromatogram; B – Zoom in on the steady-state of the cyclic operation of the 3C-PCC; C – Model data for the same cyclic period as shown in B. In A and B, black and red represent the concentration observed in UV1 and UV2, respectively. In C, black, red, and blue represent the outlet concentrations observed for columns 1, 2, and 3, respectively.

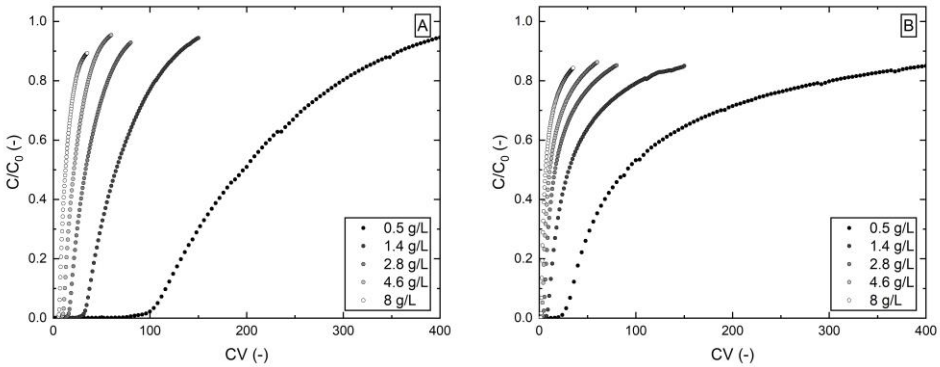

Figure SI 6.3 - Column experiments used for the calibration of the mechanistic model of CaptoS ImpAct (A) and SP Sepharose FF (B), at different initial concentrations and constant flow rate (F_v = 0.5 ml/min). Dots represent 100 data points from every experiment. In B and D, the line connecting the experimental data points is used to guide the reader's eye. C/C_0 – normalized concentration (concentration observed divided by inlet concentration). CV – column volumes.

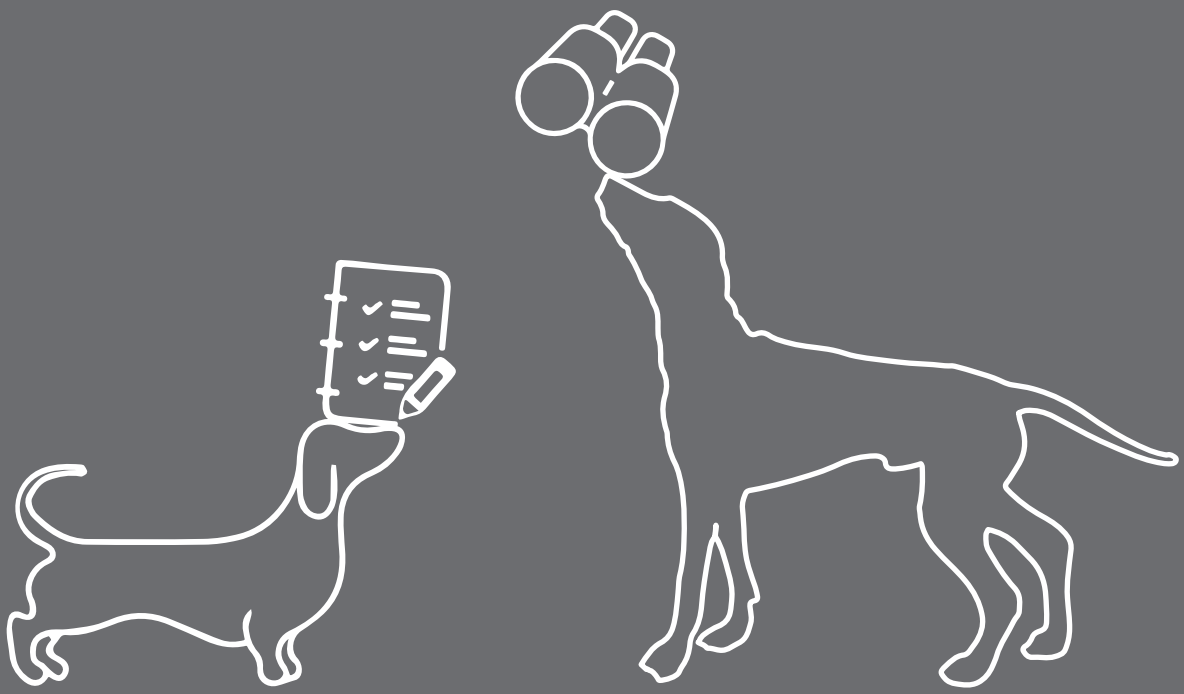

Chapter 7

Conclusions and Outlook

The biopharmaceuticals industry is dynamic and faces growing demand, especially for the monoclonal antibodies (mAbs) market. The emergence of biosimilars has helped to reduce costs for patients while platform processes are fast-tracking lab-to-production developments. Process development uses automated and miniaturized assays reliably and generates swift results, enabling manufacturers to develop and improve processes faster. A shift towards continuous biopharmaceutical production holds the promise to significantly enhance efficiency, quality, and sustainability.

This thesis covered process development of integrated continuous chromatography for the purification of mAbs, combining *in-silico* and experimental approaches. It investigated different (miniaturized) High-Throughput Screening (HTS) techniques for the generation of a database, that was subsequently used by a mechanistic model for the study of chromatographic behavior. Lastly, the validated mechanistic model was used for the *in-silico* optimization of continuous chromatography for capture and polishing of mAbs from a clarified cell culture supernatant (harvest).

A panel of experts in the field identified that major gaps in the transition to continuous manufacturing are the lack of suitable continuous scale-down models for a number of unit operations, and the accompanying development of Process Analytical Technologies (PAT) for process monitoring and control (Chapter 2). It was concluded that new technologies are needed for several unit operations (UO) and that a reduction of costs of current process development technologies is required. The inability/difficulty to operate these UOs continuously delays continuous process development. Additionally, process modelling and microfluidics were identified as promising tools to fill these gaps in process development for Integrated Continuous Biomanufacturing (ICB).

Nowadays, scale-down of process development heavily relies on miniaturizing and automating essays. The evolution of these process development tools has been summarized, together with the state-of-the-art for both Upstream Processing (USP) and Downstream Processing (DSP) (Chapter 3). While Liquid-Handling Stations (LHS) have been the standard for process development for many years, microfluidic devices offer unmatched versatility in design. Furthermore, microfluidics presents an interesting option to reduce process development costs, especially when access to microchip

manufacturing equipment is present. Current 3D printing technology will also help to widen the use of microfluidics in process development.

Chapter 4 presented a comparison of three different HTS methods for chromatographic process development: LHS, microfluidics, and Eppendorf tubes. These methods were used for the determination of protein adsorption isotherms. An in-house developed microchip achieved a 15-fold and up to 200-fold liquid and resin volume reductions, respectively compared to LHS. Cost considerations allowed to conclude that even though microfluidics is at a much lower technology readiness level (TRL), it could be a reliable alternative for process development, especially in the case of very expensive proteins or in early stages of process development when the amounts of protein availability are limited, leveraging on the miniaturization power of microfluidics.

Next to experimentation, High-Throughput Process Development (HTPD) uses modeling. The description of chromatographic behavior via mathematical models is only useful if the model used can accurately describe what happens experimentally. Mechanistic models should be as simple and as accurate as possible. A LHS-based HTS methodology was proposed to study adsorption equilibrium isotherms of mAbs to ProA resins in a harvest solution, to see the applicability of models developed with pure mAb experiments in a manufacturing scenario (Chapter 5). Lumped Kinetic Models (LKM) make use of lumped parameters to combine several physical and chemical phenomena in one parameter (*e.g.* intraparticle diffusion, film mass transfer coefficient, etc.). It was shown that relatively simple models such as LKMs can accurately describe protein adsorption behavior, reducing computational time while still achieving accurate results. Furthermore, the adsorption for the case of ProA with pure mAb is very similar to what would be expected from adsorption with the crude harvest solution.

Chapter 6 combined findings and methodologies from the previous chapters. The mechanistic model was adapted to continuous chromatography with three columns and was used to optimize a 3 Column Periodic Countercurrent Chromatography (3C-PCC) step. A range of high titer solutions was studied *in-silico* to prepare for future of mAb manufacturing. It was concluded that the batch process would always perform worse than the continuous process. The best performing ProA resin was then used to continuously capture a mAb from a harvest solution, with results comparable to model predictions and pure mAb experiments. Subsequent polishing of the 3C-PCC ProA eluates showed the applicability of the model for a CEX 3C-PCC. It was concluded that the shape of the Breakthrough Curves (BTC) are more important factors for the optimization of a continuous process, compared to resin binding capacity and affinity constants. It was shown that a model-based optimization was able to accurately optimize the continuous capture and polishing of a mAb from a high-titer harvest solution.

The work of this thesis demonstrates that it is possible to implement HTPD with state-of-the-art HTS equipment and common computer equipment, develop a continuous chromatography process, optimize it *in-silico*, and validate the process experimentally within 9 months. This is an optimistic time frame since the previous knowledge and effort is included. However, with experienced people this time frame is possible. This thesis shows how the combination of valuable tools can speed-up and help in the transition of the biopharmaceutical industry to Integrated Continuous Biomanufacturing. ICB will help in reducing production costs and selling prices of biotherapeutics. This will lead to a democratization of these molecules, which until now were only affordable to a minute slice of the population [1].

Process modelling can be extremely useful for the transition to ICB. Digital twins offer a platform for process development but also for process monitoring and control [2]. With accurate models in place, these can be used as predictive tools for the process during manufacturing and, therefore, be used to implement control strategies during production, prompting actions in a matter of seconds. The increased volumes of data need to be properly stored and treated, hence why developments in data science need to keep up with increased use of models in the industry [3].

Real time control is only possible if there are "enough eyes" looking at the process. Continuous manufacturing offers several advantages over classical batch manufacturing, but the true power of continuous manufacturing can only be unleashed if real-time control is possible. That is why better PAT tools will definitely be needed in the future to ease the transition to ICB, and parallel development of such tools with the use of mechanistic models in industry will improve the control strategies implemented. Regulatory agencies also welcome and support the co-development of continuous processes and PAT, allowing for the consistent delivery of products of the highest quality [4]. Furthermore, the current trend of miniaturization of process development is also "pressuring" analytics, as these are fundamental for the assays and need to follow the miniaturization trend [5].

Besides the development of PAT tools, another interesting topic for future research would be the development of feasible alternatives to packed-bed chromatography. Several technologies have been proposed throughout the past years [6], but their technology readiness level never reached the threshold needed for widespread implementation [7]. Both chromatographic and non-chromatographic methods should be studied, and recent studies in membrane chromatography showed that this technology can play an important role in the transition to continuous manufacturing [8]. This can be seen by the strong investment of resin manufacturers in ProA nanofiber technology (Cytiva – Fibro; Sartorius – Rapid A), that are less prone to fouling and offer higher productivity than the packed-bed counterpart, ultimately reducing the cost of

goods of the process [9]. Furthermore, studies on alternatives for protein A should also be done [10]. Although there has been extensive research on alternatives, the unprecedented level of specificity of protein A still keeps it at "the top of the food chain" for mAb manufacturing. A close collaboration between academia and industry could aid in the development of these technologies, helping to bring them from the bench-top to the shop floor. The novelty of ideas of academia mixed with the pragmatism of industry could help in the discovery and applicability of new technologies for manufacturing.

In conclusion, the use of HTPD for the development of continuous chromatography for the capture and polishing of a mAb has been presented. With the presented tools, methodologies and approach, process development of continuous chromatography will be accelerated and elicit a faster transition of the biopharmaceutical industry to continuous manufacturing.

7.1. References

[1] G. Jagschies, E. Lindskog, K. Lacki, P.M. Galliher, Biopharmaceutical Processing: Development, Design, and Implementation of Manufacturing Processes, Elsevier2018.https://doi.org/10.1016/C2014-0-01092-1.

[2] A.S. Rathore, S. Nikita, G. Thakur, N. Deore, Challenges in process control for continuous processing for production of monoclonal antibody products, Current Opinion in Chemical Engineering 31 (2021) 100671. https://doi.org/j.coche.2021.100671.

[3] A.L. Oliveira, Biotechnology, big data and artificial intelligence, Biotechnology Journal 14(8) (2019) 1800613. https://doi.org/10.1002/biot.201800613.

[4] A.C. Fisher, M.-H. Kamga, C. Agarabi, K. Brorson, S.L. Lee, S. Yoon, The current scientific and regulatory landscape in advancing integrated continuous biopharmaceutical manufacturing, Trends in biotechnology 37(3) (2019) 253-267. https://doi.org/10.1016/j.tibtech.2018.08.008.

[5] M.N. São Pedro, M.E. Klijn, M.H. Eppink, M. Ottens, Process analytical technique (PAT) miniaturization for monoclonal antibody aggregate detection in continuous downstream processing, Journal of Chemical Technology and Biotechnology 97(9) (2022) 2347-2364. https://doi.org/10.1002/jctb.6920.

[6] D. Burgstaller, A. Jungbauer, P. Satzer, Continuous integrated antibody precipitation with two-stage tangential flow microfiltration enables constant mass flow, Biotechnology and Bioengineering 116(5) (2019) 1053-1065. https://doi.org/10.1002/bit.26922.

[7] A.C.A. Roque, A.S. Pina, A.M. Azevedo, R. Aires-Barros, A. Jungbauer, G. Di Profio, J.Y. Heng, J. Haigh, M. Ottens, Anything but conventional chromatography approaches in bioseparation, Biotechnology Journal 15(8) (2020) 1900274. https://doi.org/10.1002/biot.201900274.

[8] F. Schmitz, T. Kruse, M. Minceva, M. Kampmann, Integrated double flow-through purification of monoclonal antibodies using membrane adsorbers and single-pass tangential flow filtration, Biochemical Engineering Journal 195 (2023) 108913. https://doi.org/10.1016/j.bej.2023.108913.

[9] R.R. Davis, F. Suber, I. Heller, B. Yang, J. Martinez, Improving mAb capture productivity on batch and continuous downstream processing using nanofiber PrismA adsorbents, Journal of Biotechnology 336 (2021) 50-55. https://doi.org/10.1016/j.jbiotec.2021.06.004.

[10] H.R. Reese, X. Xiao, C.C. Shanahan, W. Chu, G.A. Van Den Driessche, D. Fourches, R.G. Carbonell, C.K. Hall, S. Menegatti, Novel peptide ligands for antibody purification provide superior clearance of host cell protein impurities, Journal of Chromatography A 1625 (2020) 461237. https://doi.org/10.1016/j.chroma.2020.461237.

Acknowledgements

This journey of over 4 years couldn't have been completed without the help of a lot of people, whether related to work or outside of work, since that even when times looked dark and the results seemed to not come through, it was the time off that allowed for the frustrations to subside and keep going.

First, I would like to thank my supervisors for the guidance and support throughout the project.

Marcel, thank you for giving me the opportunity of doing the PhD. I really appreciate the freedom you gave me throughout the PhD and how you allowed me to pursue my ideas, even when you thought that it wouldn't yield results. Thank you for supporting my secondment at Byondis. Those three months were very enriching professionally and I was also able to produce great results that improved this thesis. Times were not always easy and against your own preference you agreed in letting me continue in the lab until the end of April 2023. Thank you for trusting me and supporting this decision, as I believe that it improved the contents of the thesis. I also appreciate that you take a mentorship role with your students, always introducing us to the "scary" (and of course knowledgeable) people in the field as experts, and you are always open to help us find a smooth transition from the PhD into industry or academia.

Michel, I would also like to thank you for the supervision throughout the PhD. You were always very enthusiastic and always supported our research decisions. I have deeply enjoyed the industry perspective that you brought to the table, because I feel that it helped me keep my feet on Earth when designing experiments. Thank you also for allowing me to do the secondment at Byondis, for arranging such a smooth start, and for the supervision and support provided during my time in Nijmegen.

I would also like to thank the students that have decided to join my project for their MSc thesis: **Lisa** and **Maria**. I have learned a lot from our discussions and the fresh perspective you brought to the table. Both of you showed incredible resilience, whether because you had to considerably change your scope due to the flooding and pandemic, or because the ÄKTA would not seem to cooperate.

Thank you to everyone involved in the CODOBIO consortium for all the input and feedback during the project meetings. I would like to thank especially **Alcântara**, **Madelène**, and **Nacho**, which made the meetings more fun and fruitful. Thank you also to **Madelène** for the incredible support in the Continuous Chromatography work.

Throughout the past 4 years I was part of the BPE group at TU Delft, where I had the pleasure to work with brilliant people and to forge strong friendships.

To my amazing paranymphs: **Mariana** and **Marijn**. **Mariana**, esta jornada de 4 anos não teria sido a mesma sem ti. Partilhar o escritório contigo foi uma bênção porque estavas sempre disposta a falar e a consolar-me quando as coisas não corriam bem, ou quando sabias que algo tinha acontecido (tu sabes sempre) e me sinalizavas para levantar e irmos para o *coffee-corner* para o *gossip*. Estiveste sempre lá para o que fosse preciso, *no questions asked*, fosse começar no laboratório com as galinhas ou ficar até tarde a limpar ÄKTAs, tudo foi mais divertido por te ter lá. Obrigado por todas as discussões científicas que tivemos e por me ajudares a elevar o meu trabalho (e mais importante de tudo, a "convenceres-me" a não usar *fluorescent dyes*). Obrigado também por, mais recentemente, todas as viagens de comboio de manhã para o trabalho: sei que falo demais, e sabes também que, se quiseres dormir, só tens de me dizer para me calar!

Marijn, when I saw you wearing metal bands t-shirts I was happy to see that someone shared a similar musical taste to mine, only to be disappointed when I realized you consider melodic death metal music and actually enjoy it (I'm sorry, I couldn't let this one by). You have also been there for me to discuss work and to comfort me when things were not going well. You have a very kind heart, which became kinder and kinder throughout the years. Thank you also for trying to explain MES to me every time I asked (I still don't understand much, to be honest) and together with **Oriol** you have made sure that the Red Lab is uninhabitable. Thank you also for helping us prepare for Graspop and for ensuring that we followed all the campsite rules (even though we were the only ones). If we had a burner, the tortillas with ragout and cucumber wouldn't have been the same!

Song, your help and support have been essential for my work and I owe part of this thesis to you (which is now the second I owe you, after the MSc thesis). You are an amazing technician, but you are an even better friend! You have been a great support on and off the lab, and I will always be grateful to you for helping me settle down in the Netherlands and wrapping my head around all the bureaucracy. You even went with me to different Makelaardij to help me find a house that allowed dogs! I lost count to the amount of equipment in which you trained me and of the hours you spent *troubleshooting* with me. You always found a way to make the sun shine when times were dark.

Marina a minha "velha conhecida" de BPE com quem convivi mais vezes nas primeiras duas semanas de doutoramento do que nos 2 anos que partilhámos no Técnico (ironias da vida)! Contagias toda a gente com a tua energia e riso, e estavas sempre pronta para nos ouvir e para dar um abracinho de consolação. Gostava que te visses mais vezes como todos nós te vemos: uma pessoa super inteligente, dedicada e carinhosa! Acredito que vais chegar alto (piada não intencional sobre a tua altura)!

Oriol, **Joan**, **Daniela**, and **David** I am fully aware that I am constantly bragging about my Spanish skills, but since this document will be publicly available, *por supuesto* that I cannot risk it and will proceed in English. **Oriol**, you too wore metal bands t-shirts but with much better taste! You are incredibly smart (let's not forget that you practically carried alone our NMST group on your shoulders), and I would like you to see that yourself. I am proud that we started the FACC-BPE and have made several successful events together! Your creativity in the emails is for sure unmatched! You are also a great friend which is always available to listen to us and who sticks for your friends through thick and thin. As Parkway Drive put it: *You've got one life, one shot, give it all you got*. I hope to receive pictures of your *cagatios* every Christmas forever.

Joan throughout these almost 5 years, I have always appreciated the way you ask questions in our philosophical discussions and how you really make me think about my ideas and the arguments to support them. To me, you have also been an example of hard work and perseverance, without taking life too seriously, which I think is an amazing trait. **Daniela**, you are the best cheerleader to your friends and I really enjoy the energy you bring to the room as soon as you walk in.

David, *señor*, I really enjoy spending time with you (especially when you invite over for *paella*!). You are the funny person of the group, because you can make our faces hurt almost every time we hang out. We share passions like dogs and cooking, but luckily for me you are also passionate about drawing and designing and have taken the challenge of producing the amazing piece of art that you made for my cover. You have been incredibly patient (e.g. for accepting that I did not want anything abstract) and have translated my ideas to paper much better than I expected. I cannot thank you enough for this! Thank you also to **Joan** and **Oriol** for the suggestions and contributions for the thesis cover!

Daphne, **Roxana**, and **Tim**, the "corner office" crew that had to put up with me dropping by with constant questions regarding one thing or another. **Daphne**, thank you for all the times you made yourself available to hear about my frustrations and for always helping me finding a way. Thank you also for all the sessions answering the modelling questions I had, and for helping me *troubleshooting* my code time and time again. Thank you also for making the teaching of TLS much more fun! I really liked working with you and learning from you. Final stretch for you! **Roxana**, thank you for all the *ad hoc* discussions in the lab and for the critical questions during these discussions and in meetings. You have made me see and think about possibilities that I couldn't before and have also made me stop sometimes and think before acting. **Tim**, we both share a great passion for our dogs and I feel like I know Guusje better than most dogs I see regularly. Thank you for always being a great sport (*cough cough* except in karting *cough cough*). You still owe me a karting race rematch!

To all my office mates, which have helped me throughout this journey: **Monica** for always being available to discuss science, **Bianca**, for always having kind words to say, **Robin**, for teaching me so much about history. To **Rizki** (**Zulhaj**) for putting up with me for two years. I know that sometimes I was loud, or asking too many questions, but you were always super patient with me and always kind. Thank you also for feeding the office in numerous occasions! The sweet snacks were always welcomed! To **Maarten**, our gentle giant. Several times I looked at you and it looked like you were mad but as soon as you heard your name being called, you "turned on" your smile (your focused face is a bit scary, by the way). I love your tendency to hug and lift people in parties, it is very altruistic of you to show everyone how you see the world! I loved having you training BJJ with me and throwing me around during the stand-up, it was super fun!

To the incredible BPE staff: **Adrie**, **Ludo**, **Cees**, **Christiaan**, **Stef**, and **Max**. **Kawieta**, I know that everyone knows how vital you are to the group and how welcome you make us feel when we first start. Thank you for taking care of all of us! **Marieke** thank you for all the scientific and non-scientific discussions throughout these years, it was always fun! Thank you also for being such a great and dedicated teacher, TLS is in great hands with you!

To the old BPE generation for welcoming me into the group: **Debby**, **Joana**, **Rita**, and **Marcelo** (obrigado por me "adoptares" quando ainda era aluno de mestrado e por sempre te interessares e quereres ajudar-me na minha investigação!). To **Chema**, for always showing me that a bit of chaos never hurts anyone (I'm still waiting for the recipe of the mushroom soup you cooked). To **Lars**, for all the endless discussions we had about monarchy. I am pretty sure that many lunch breaks were cut short because people were already fed up with the topic, but we both know we weren't! Thank you also for all the political discussions, I really enjoyed discussing these topics with you, and for always making yourself available to help with the modelling, even though I work in a field totally different from yours. To **Mona**, for all your advice and for cheering everyone up. To the new generation of BPE, with whom I shared few but good moments, please enjoy your time in this great group and cherish every moment: **Mariana**, **Miki**, **Rik**, **Brenda**, **Hector**, **Marika**, **Ramon**, **Tamara**, **Meryl**, and **Eduardo**.

Thank you to all the **DSP group** of Byondis. You welcomed me with arms wide opened and made my time in Byondis incredibly enriching. I am very thankful to everyone in the group, but especially to **Criss**, **Saskia**, **Sebastian**, and **Walter**. All of you made Nijmegen feel like home for the time I was there. Thank you for sharing time with me and for the great chats (in the lab and on the mats)!

Thank you to the **BJJ Delft family** for providing an outlet for many frustrating days during my PhD. To be able to train hard after a frustrating workday is a blessing and

helps the much-needed switch-off. Although we constantly overstretch each other's limbs and try to choke each other out, it all comes from a fond place, and I wouldn't want to do it with anyone else.

To all the **PDEngs** (now **EngDs**) that have been part of this journey. **Patricia** (the best programme coordinator), thank you for welcoming me as your own and for all the nice and kind words you always had whenever we met. To **Henrique**, **Rafa**, **Stella**, **Vaggelis**, **Daniela**, **Rita**, and **Carolina**, thank you for all the fun chats and fun dinners, nights out and Halloween parties. Thank you also for being the best cheerleading crew!

To **Sale**, **Andrea**, **Andy**, **Orlando**, and **Eva**, thank you for always making the time to be with us, for sharing your culture with us and for being the nice and kind people you all are! These past years wouldn't have been the same without **Sale's** competitiveness and football games we shared, without **Andrea's** *idiots* and discussions we had about chromatography, without **Andy's** cooking, without **Orlando's** and **Eva's** partying skills (and of course their amazing outfits)! It has been great seeing all of us grow up professionally and personally, and it is nice to have this **PDEng Kragna** (which I thought meant *family* until I asked a Serbian friend and he laughed at my face).

Está na altura de começar os agradecimentos em Português. Aos meu amigos que infelizmente nem sempre vejo quando vou a Portugal, mas que me perdoam sempre: **João**, **Sancho**, **Fernando**, **Faria**, e **Rui**. **João**, obrigado por teres sido o meu primeiro parceiro de estudo do Técnico (ainda não sei como fizemos MO) e por partilharmos muitas boleias e futeboladas! **Sancho**, obrigado por me iniciares no BJJ, uma paixão que dura há já 5 anos, e também por todas as futeboladas! **Fernando**, que maluco que foste (ou desperado!) por aceitares ir viver com 3 desconhecidos para Delft! Espero que tenha conseguido alegrar esse período da tua vida tanto quanto tu alegraste o meu, e que te mantenhas *totil* fiel a ti mesmo. **Faria**, obrigado por todas as discussões científicas não planeadas e por teres feito com que a experiência no laboratório do 8° piso muito mais divertida, tenho saudades das nossas discussões infinitas sobre tudo e sobre nada. **Rui**, obrigado por te teres disposto a ajudar-me a discutir coisas da minha tese de mestrado um dia antes da minha defesa, sem me conheceres; isto mostra duas coisas que te representam enquanto pessoa: 1 – disponibilidade para ajudar quem se mostra interessado e 2 – interesse por qualquer tipo de ciência.

Aos portugueses que fazem a Holanda um bocadinho mais portuguesa: **Domingos**, **Hugo**, **Parreira**, **Zé**, **Lenny**, **Ticha**, **Tiago**, **Pedro** e **Catarina**. Estar convosco é sempre diferente, mas há certas coisas que não mudam: o **Parreira** a chegar sempre atrasado (mas também a ser um bom amigo), o **Domingos** a tentar aldrabar alguém com as suas petas, os bolos espetaculares da **Ticha**, as infinitas fotos de gatos do **Tiago**, o **Hugo** a observar tudo e pela calada a fazer uma piada que mata toda a gente, a **Catarina** e o seu belo sotaque de Tondela, o **Pedro** e as discussões filosófico-científicas, e o **Zé**,

normalmente mais calado, a virar monstro competitivo nos jogos de tabuleiro. E claro há aquele que, em 2017, começou (sem saber) como massa agregadora deste grupo: **Lenny**. Obrigado por todos os churrascos, serões, idas ao parque, etc., e principalmente por todos os incríveis momentos ao longo destes quase 7 anos (ainda estou à espera do dia em que tens um cão chamado Carlos).

Ao melhor que a Jerónimo Martins me deu (além de decorar preçários): **Álvaro**, **Ahmad**, **Barra** e **Bernardo**. Os 8 meses que passámos juntos pareceram anos e fico feliz por termos conseguido manter-nos firmes mesmo depois de todos estes anos. A mais discussões políticas, *on-tours*, "Não há heróis", e idas a restaurantes portugueses na Holanda depois de aterrarem vindos de... Portugal. Fico feliz por ter podido enganar mais dois e agora poder contar com o **Álvaro** e a **Margarida** a apenas 70 km! São sempre bem-vindos para comer Francesinha lá em casa!

Aos melhores atletas e *dog-sitters*: **Francisca** e **Filipe**. Quem diria que um desafio engraçado, de correr 12 km, vai agora numa parvoíce em que já corremos 21.1 km e ainda queremos correr 42.2 km? E pelo meio, deu para partilharmos concertos, muitas oliebollen, *brunchs*, almoços e jantares (sem bacalhau e com pouco queijo), inúmeras corridas, treinos de Judo e BJJ e muitas outras coisas. Obrigado pelo entusiasmo e carinho com que sempre nos recebem e com que cuidam do Gu e da Caya sempre que precisamos. Eles adoram, e como diz o ditado: "o cão não engana".

Às Pombas que acompanharam este meu percurso e loucura académica, desde o nosso ingresso no Técnico, no fatídico ano de 2012 (fatídico porque depois de entrarmos no Técnico nunca mais fomos os mesmos): **Botas**, **Diva**, **Cavaco**, **Concha**, **Grilo**, **Joana**, **Lena**, **Lóia**, **Réu**, **Rita** e **Rodrigo**. Vocês têm sido, ano após ano, os melhores amigos que podia desejar e apesar de estarmos cada um para seu canto, conseguimos continuar a ver-nos, e 6 meses de distância parecem apenas 2 dias. Como verdadeiros amigos que são dizem quando estou errado, apoiam quando estou certo. A única coisa que tenho a apontar é que ninguém me tentou demover de fazer um doutoramento... Isso não se faz! Infelizmente não tenho orçamento para pagar o número de páginas que precisaria para escrever tudo o que queria sobre cada um, por isso vou escrever uma palavra que me vem à cabeça quando penso em vocês e o resto fica para interpretação vossa (e do leitor): **Botas** – Podcast; **Diva** – CrossFit; **Cavaco** – Política; **Concha** – Feitiço; **Grilo** – Piadas; **Joana** – *Down-under*; **Lena –** Luz-do-carro (palavra hifenizada para fins de cumprir com o desafio); **Lóia –** Chill; **Réu** – Legumes; **Rita** – Tampinhas; **Rodrigo** – Presidente.

À minha família do Norte, **Margarida**, **Paula** e **Rui**. Obrigado por me receberem a mim e à minha família sempre tão bem! **Paula** e **Rui** obrigado por constantemente se preocuparem com o nosso bem-estar e conforto e por serem parte do mesmo, e também por manterem um fluxo constante de Ferrero Rocher na vossa casa. **Margarida**, por favor não deixes de nos ligar de vez em quando a contar as peripécias da tua vida, porque

isso alegra sempre o nosso dia! Ao contrário do que dizem as más-línguas tu não és maluca, és divertida.

À minha família. **Avó** e **avô**, obrigado por se preocuparem sempre se eu chego bem e por me receberem sempre que vou a Portugal. Sei que muitas vezes as visitas parecem curtas, mas as boas conversas que temos para mim valem muito.

À **Inês**, **Gonçalo**, **Mia** e **Gustavo** que sempre me recebem de braços abertos quando vou a Portugal. **Inês**, sabes que para mim és e sempre serás um exemplo! Andaste muitas vezes a andar no limbo entre mãe e irmã (quando deveria ter sido só a segunda), e sei que isso também não foi fácil para ti. Sempre lutaste por mim e não vou esquecer da quantidade de barreiras que me ajudaste a quebrar nem das vezes que me apoiaste, mesmo nas decisões mais malucas. Tenho muito orgulho nas pessoas que nos tornámos e na família que criaste e estás a criar! Muito obrigado por tudo! **Gonçalo**, obrigado por teres sido a primeira pessoa a mostrar-me como funciona um laboratório de investigação, e por me levares contigo a fazer os mais diversos desportos (nem sei se me lembro de todos). Foste muitas vezes apanhado no olho do furacão mas sempre fizeste de tudo para nos apoiar. Quando voltar, prometo que vou fazer trilhos contigo! **Mia** e **Gustavo**, os reguilas preferidos do tio, vocês mostram sempre um entusiasmo enorme ao ver-me, e isso enche-me o coração!

Pai obrigado por me ajudares a vir fazer a tese de mestrado em 2017 a Delft, algo que acredito que possa ter, em parte, despoletado a cascata de acontecimentos que me levou a decidir fazer o doutoramento aqui em Delft. Obrigado por seres um pai carinhoso e que apoia incondicionalmente os filhos. Também foste forçado a mudar muito, mas asseguro-te que para melhor. Não me esqueço quando em Janeiro de 2013 eu cheguei à sala destroçado depois de saber que tinha chumbado a um exame e tu simplesmente me abraçaste e disseste que estava tudo bem. Nesse momento, tiraste uma pressão de cima de mim, que me ajudou a acabar o curso a tempo (ainda chumbei a muitas cadeiras pelo meio, mas com o teu apoio e ajuda tudo se fez!). Sei que nem sempre foi (nem fui) fácil, mas juntos conseguimos ultrapassar tudo. Obrigado por tudo!

Por último tenho de agradecer a dois cães e uma pessoa muito especiais para mim. **Gullit**, ensinaste-me muito mais do que eu te consegui ensinar e estes 10 anos foram cheios de aventuras. És o cão que, ao mesmo tempo, me faz querer ter mais cães e me faz não querer ter mais nenhum cão (Gusito fofo). **Caya**, um furacão com uma massa total de 5.5 kg, mas 5.5 toneladas de amor para dar. Foste a adição perfeita ao Gu e à nossa casa. Trouxeste a estrutura que estávamos a precisar mesmo a meio da pandemia, e muitas tardes regadas de muitos beijinhos (Cayazinha fofa).

Raquel, foste a primeira pessoa a quem liguei, da parte de trás da peixaria do Pingo Doce de Queijas, a dizer que me tinham aceitado no doutoramento (umas meras 5 semanas antes de começar). Desataste a chorar enquanto dizias que estavas muito feliz por mim. Obrigado pelo apoio incondicional. És a pessoa a quem conto tudo, para quem

mais gosto de cozinhar, a pessoa com quem mais gosto de estar e passear, a pessoa que procuro quando me sinto mais vulnerável. Aturaste-me nos meus momentos de maior frustração e sempre puxaste por mim. O teu poder de super-herói é conseguires fazer-me relaxar com apenas um abraço, abraços esses que me aquecem sempre o coração. Durante estes 4.5 anos mudámos de país, mudámos de casa, atravessámos uma pandemia, fizemos pão-de-ló sem batedeira (estava muito mau, por sinal), exercitámos juntos, fizemos uma corrida juntos, viajámos juntos, visitámos a Holanda de uma ponta à outra, mas aquele que continua a ser o nosso plano favorito é ir com os bichos à praia. Por tudo isto, e ao contrário do que sempre te disse para te chatear, este doutoramento também é teu!

List of publications

Silva, T. C., Eppink, M., & Ottens, M. (2022). Small, smaller, smallest: Miniaturization of chromatographic process development. Journal of Chromatography A, 1681, 463451. doi.org/10.1016/j.chroma.2022.463451.

São Pedro, M. N., **Silva, T. C**., Patil, R., & Ottens, M. (2021). White paper on high-throughput process development for integrated continuous biomanufacturing. Biotechnology and Bioengineering, 118(9), 3275-3286. doi.org/10.1002/bit.27757

Miao Yu, **Silva, T.C**., van Opstal, A., Romeijn, S., A. E., Hayley, Jiskoot, W., Witkamp, G. J., and Ottens, M. (2019). The investigation of protein diffusion via H-cell microfluidics. Biophysical journal, 116(4), 595-609. doi.org/10.1016/j.bpj.2019.01.014.

Faria, D. F., **Silva, T. P.**, Aires-Barros, M. R., & Azevedo, A. M. (2019). A Chronology of the Development of Aqueous Two-Phase Systems as a Viable Liquid-Liquid Extraction for Biological Products. doi:10.1016/B978-0-12-409547-2.14393-8.

Conference Contributions

Silva, T. C., Eppink, M., Ottens, M., *Microfluidic device for the determination of adsorption isotherms*, **ESBES 2021 — 13th European Symposium on Biochemical Engineering Sciences,** Online, May 2021, Poster Presentation.

Silva, T. C., Eppink, M., Ottens, M., *Microfluidics and Liquid-Handling Stations: comparison for chromatographic high-throughput process development*, **American Chemical Society 2021**, Online, August 2021, Oral Presentation.

Silva, T. C., Eppink, M., Ottens, M., *Miniaturization of chromatographic process development for fast results at minimal costs*, **International Symposium and Exhibition on the Purification of Proteins, Peptides and Polynucleotides (ISPPP) 2021,** Porto, November 2021, Flash Presentation.

Silva, T. C., Eppink, M., Ottens, M., *Chromatographic process development miniaturization: fast results with minimal costs*, **Netherlands Process Technology Symposium 2022**, Delft, April 2022, Poster Presentation.

Silva, T. C., Eppink, M., Ottens, M., *Miniaturization of chromatographic process development: achieving fast results with minimal costs*, **Integrated Continuous Biomanufacturing V**, Barcelona, October 2022, Poster Presentation.

Curriculum Vitae

Tiago Picanço Castanheira da Silva was born in Coimbra, Portugal on the 19th of December of 1994. In 2012, he started his Integrated Masters in Biological Engineering at Instituto Superior Técnico, University of Lisbon. During the BSc and MSc, an affinity with the engineering courses (both chemical and biological engineering) started to develop, leading to an increased interest in stem cell bioreactors and protein purification. With the help of a professor specialist on protein purification, he got in touch with prof. Marcel Ottens for the possibility of doing his master thesis at the Ottens' group. In February 2017, he joined TU Delft through the Erasmus program where he used microfluidics to study the diffusion coefficient of proteins and polyelectrolytes, under the supervision of Miao Yu and Marcel Ottens.

After finishing the MSc., Tiago decided to continue to explore the possibilities of microfluidics, this time on its application for screening of chromatographic resins, working for 6 months as a research fellow at iBB (*Instituto de Bioengenharia e Biociências*, Lisbon, Portugal) under the supervision of Ana Azevedo. After this work experience in research, he decided to explore a different career path in a more managerial landscape and joined the Operations Management Trainee program of Jerónimo Martins in September of 2018, one of the main food retailers in Portugal. There he had the opportunity to see the business and participate in it from the operations floor, which in his opinion is essential knowledge and experience for future managers.

Although a very fast paced and interesting job, he never disconnected from the purification field and after a few calls with a friend, he applied for a PhD position in the Ottens' group to work in continuous chromatography for monoclonal antibody purification. Therefore, in May 2019 he moved back to Delft and started a PhD position at Technische Universiteit Delft as part of the CODOBIO (Continuous Downstream Processing of Biologics) research project, an international training network (ITN) funded in the frame of Marie Sklodowska-Curie Actions. The project was focused on the use of High-Throughput Screening and High-Throughput Process Development for the development and optimization of continuous chromatography for the purification of monoclonal antibodies. The results of the work developed during these 4 years are presented in this thesis.

Following up on his affinity for Bioprocessing and Downstream processing, in September 2023 he joined Wacker B.V., Amsterdam, The Netherlands, as an MSAT (Manufacturing Science and Technology) Process Engineer.